

UNIVERSITY OF CALIFORNIA

Los Angeles

Economic and Distributed Model Predictive
Control of Nonlinear Systems

A dissertation submitted in partial satisfaction of the
requirements for the degree Doctor of Philosophy
in Electrical Engineering

by

Mohsen Heidarinejad

2012

*In Memory of My Grandfather, Aboutaleb,
Rest In Peace*

ABSTRACT OF THE DISSERTATION

Economic and Distributed Model Predictive
Control of Nonlinear Systems

by

Mohsen Heidarinejad

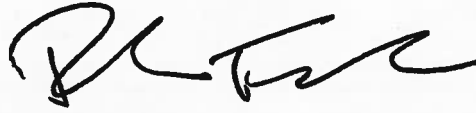
Doctor of Philosophy in Electrical Engineering
University of California, Los Angeles, 2012
Professor Panagiotis D. Christofides, Chair

Maximizing profit has been and will always be the primary purpose of optimal process operation. Within process control, the economic optimization considerations of a plant are usually addressed via a two-layer architecture. In general, this architecture includes: the upper layer that optimizes process operation set-points taking into account economic considerations using steady-state system models, and the lower layer (i.e., process control layer) whose primary objective is to employ feedback control systems to force the process to track the set-points. Optimizing closed-loop performance with respect to general economic considerations for nonlinear systems in a unified framework has recently become a subject of increasing theoretical interest and practical importance. In addition to a tighter integration of economics and control, advances in communication technologies have motivated augmentation of traditional point-to-point and wired local control systems with additional cheap and easy-to-install networked sensors and actuators and control systems. Networked distributed


control systems can substantially improve the efficiency, flexibility, robustness and fault tolerance of an industrial control system while reducing the installation, reconfiguration and maintenance expenses at the cost of coordination and design/redesign of different control systems in the new architecture.

This dissertation presents rigorous, yet practical, methods for the design of economic and distributed predictive control systems. Beginning with a review of recent results on the subject, the dissertation presents the design of Lyapunov-based economic model predictive control scheme for a broad class of nonlinear systems using state and output feedback. Then, the dissertation focuses on the development of an economic model predictive control method with guaranteed improvement in closed-loop performance compared to conventional Lyapunov-based model predictive control designs. Subsequently, the dissertation focuses on the design of a networked distributed model predictive control method for multirate uncertain systems subject to communication disruptions and measurement noise and distributed model predictive control method for switched systems to compute optimal manipulated input trajectories that achieve desired stability, performance and robustness specifications. The control methods are applied to nonlinear chemical process networks and their effectiveness and performance are evaluated through extensive computer simulations.

The dissertation of Mohsen Heidarinejad is approved.



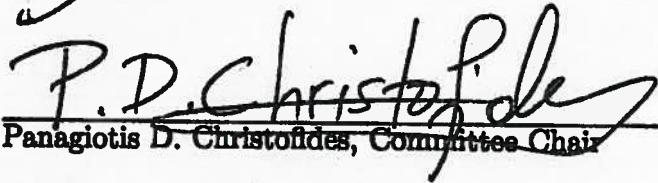
Paulo Tabuada



Mihaela van der Schaar



James F. Davis



Panagiotis D. Christofides, Committee Chair

University of California, Los Angeles

2012

Contents

1	Introduction	1
1.1	Background	1
1.1.1	Economic Model Predictive Control	1
1.1.2	Distributed Model Predictive Control	4
1.2	Objectives and Organization of the Dissertation	8
2	Economic Model Predictive Control of Nonlinear Process Systems Using Lyapunov Techniques	13
2.1	Preliminaries	14
2.1.1	Notation	14
2.1.2	Class of nonlinear systems	15
2.1.3	Lyapunov-based controller	15
2.2	Lyapunov-based economic MPC with synchronous measurement sampling	18
2.2.1	Implementation strategy	19
2.2.2	LEMPC formulation	20
2.2.3	Stability analysis	22

2.3	Lyapunov-based economic MPC with asynchronous and delayed measurements	28
2.3.1	LEMPC implementation strategy	29
2.3.2	LEMPC formulation	30
2.3.3	Stability analysis	32
2.4	Application to a chemical process example	37
2.4.1	Synchronous measurement sampling	39
2.4.2	Asynchronous measurements with delay	47
2.5	Conclusions	54
3	State Estimation-Based Economic Model Predictive Control of Non-linear Systems	55
3.1	Preliminaries	56
3.1.1	Notation	56
3.1.2	Class of Nonlinear Systems	57
3.1.3	Stabilizability assumption	59
3.1.4	State Estimation via High Gain Observer	60
3.2	State Estimation-Based Economic MPC	62
3.2.1	Implementation strategy	62
3.2.2	LEMPC formulation	64
3.3	Closed-loop Stability Analysis	66
3.4	Application To A Chemical Process Example	72
3.5	Conclusions	81

4	Algorithms for Improved Finite-Time Performance of Lyapunov-Based Economic Model Predictive Control of Nonlinear Systems	84
4.1	Preliminaries	85
4.1.1	Notation	85
4.1.2	Class of nonlinear systems	86
4.1.3	Stabilizability assumption	86
4.1.4	Lyapunov-based MPC	87
4.1.5	Lyapunov-based economic MPC	89
4.2	LEMPC Algorithm I: Nominal Operation	90
4.2.1	Implementation strategy	91
4.2.2	LEMPC formulation	92
4.2.3	Closed-loop stability and performance	94
4.3	LEMPC Algorithm II: Operation Under Disturbances	100
4.3.1	Implementation strategy	101
4.3.2	LEMPC formulation	103
4.3.3	Closed-loop stability and performance	105
4.4	Application To A Chemical Process Example	106
4.4.1	Nominal operation	108
4.4.2	Operation subject to bounded process disturbances	110
4.5	Conclusions	113
5	Handling Communication Disruptions in Distributed Model Predictive Control	116

5.1	Preliminaries	117
5.1.1	Notation	117
5.1.2	Problem formulation	118
5.1.3	Model of the communication channel	119
5.1.4	Lyapunov-based controller	120
5.2	DMPC with communication disruptions	121
5.3	DMPC Stability	128
5.4	Application to a chemical process	132
5.5	Conclusions	141
6	Multirate Distributed Model Predictive Control of Nonlinear Un-	
	certain Systems	143
6.1	Preliminaries	144
6.1.1	Notation and class of nonlinear systems	144
6.1.2	Modeling of measurements and communication	146
6.1.3	Lyapunov-based controller	148
6.2	Multirate DMPC	149
6.2.1	Multirate DMPC implementation strategy	149
6.2.2	Multirate DMPC formulation	152
6.2.3	Stability analysis	158
6.3	Application to a chemical process	172
6.4	Conclusions	180

7	Distributed Model Predictive Control of Switched Nonlinear Systems with Scheduled Mode Transitions	181
7.1	Preliminaries	183
7.1.1	Notation and class of switched nonlinear systems	183
7.1.2	Stabilizability assumptions on nonlinear switched system	185
7.1.3	Stability properties of $h_k(x)$	186
7.1.4	Centralized MPC of switched systems	189
7.2	DMPC of switched nonlinear systems	191
7.3	Stability analysis	195
7.4	Distributed optimization considerations	197
7.5	Application to a chemical process network	203
7.6	Conclusions	211
8	Conclusions and Future Research Directions	212
8.1	Summary	212
8.2	Future Research Work	215
	Bibliography	219

List of Figures

2.1	State trajectories of the process under the LEMPC design of Eq. 2.45 for initial condition $(C_A(0), T(0)) = (2\frac{kmol}{m^3}, 440K)$ without disturbances.	43
2.2	Manipulated input trajectories under the LEMPC design of Eq. 2.45 for initial condition $(C_A(0), T(0)) = (2\frac{kmol}{m^3}, 440K)$ without disturbances.	43
2.3	State trajectories of the process under the LEMPC design of Eq. 2.45 for initial condition $(C_A(0), T(0)) = (2\frac{kmol}{m^3}, 400K)$ without disturbances.	44
2.4	Manipulated input trajectories under the LEMPC design of Eq. 2.45 for initial condition $(C_A(0), T(0)) = (2\frac{kmol}{m^3}, 400K)$ without disturbances.	44
2.5	State trajectories of the process under the LEMPC design of Eq. 2.45 for initial condition $(C_A(0), T(0)) = (2\frac{kmol}{m^3}, 440K)$ subject to disturbances.	44
2.6	Manipulated input trajectories under the LEMPC design of Eq. 2.45 for initial condition $(C_A(0), T(0)) = (2\frac{kmol}{m^3}, 440K)$ subject to disturbances.	45
2.7	State trajectories of the process under the LEMPC design of Eq. 2.45 for initial condition $(C_A(0), T(0)) = (2\frac{kmol}{m^3}, 400K)$ subject to disturbances.	45
2.8	Manipulated input trajectories under the LEMPC design of Eq. 2.45 for initial condition $(C_A(0), T(0)) = (2\frac{kmol}{m^3}, 400K)$ subject to disturbances.	45
2.9	Disturbance realization for $\sigma_1 = 1 kmol/m^3$ and $\sigma_2 = 40 K$ with $ w_1 \leq 1 kmol/m^3$ and $ w_2 \leq 40 K$	46
2.10	Estimation of Ω_ρ and three closed-loop system trajectories for synchronous measurement case with disturbances.	46

2.11	Asynchronous measurement sampling times and their associated delay.	48
2.12	State trajectories of the process under the LEMPC design of Eq. 2.46 for initial condition $(C_A(0), T(0)) = (2\frac{kmol}{m^3}, 440K)$ subject to asynchronous and delayed measurements and disturbances.	49
2.13	Manipulated input trajectories under the LEMPC design of Eq. 2.46 for initial condition $(C_A(0), T(0)) = (2\frac{kmol}{m^3}, 440K)$ subject to asynchronous and delayed measurements and disturbances.	50
2.14	State trajectories of the process under the LEMPC design of Eq. 2.46 for initial condition $(C_A(0), T(0)) = (2\frac{kmol}{m^3}, 400K)$ subject to asynchronous and delayed measurements and disturbances.	50
2.15	Manipulated input trajectories under the LEMPC design of Eq. 2.46 for initial condition $(C_A(0), T(0)) = (2\frac{kmol}{m^3}, 400K)$ subject to asynchronous and delayed measurements and disturbances.	50
2.16	Estimation of Ω_ρ and three closed-loop system trajectories for asynchronous measurement case with disturbances.	51
2.17	State trajectories of the process under the LEMPC design of Eq. 2.46 for initial condition $(C_A(0), T(0)) = (2\frac{kmol}{m^3}, 400K)$ subject to asynchronous and delayed measurements and disturbances under enforcing the integral constraint over a two-hour period.	52
2.18	Manipulated input trajectories under the LEMPC design of Eq. 2.46 for initial condition $(C_A(0), T(0)) = (2\frac{kmol}{m^3}, 400K)$ subject to asynchronous and delayed measurements and disturbances under enforcing the integral constraint over a two-hour period.	52
2.19	State trajectories of the process under the LEMPC design of Eq. 2.46 for initial condition $(C_A(0), T(0)) = (2\frac{kmol}{m^3}, 400K)$ subject to asynchronous and delayed measurements and disturbances under enforcing the integral constraint over two consecutive one-hour periods.	53
2.20	Manipulated input trajectories under the LEMPC design of Eq. 2.46 for initial condition $(C_A(0), T(0)) = (2\frac{kmol}{m^3}, 400K)$ subject to asynchronous and delayed measurements and disturbances under enforcing the integral constraint over two consecutive one-hour periods.	53

3.1	Ω_ρ and state trajectories of the process under the LEMPC design of Eq. 3.35 with state feedback and initial state $(C_A(0), T(0)) = (1.3 \frac{kmol}{m^3}, 320K)$ for one period of operation with (solid line) and without (dash-dotted line) the constraint of Eq. 3.35e. The symbols \circ and \times denote the initial ($t = 0 \text{ hr}$) and final ($t = 1 \text{ hr}$) state of these closed-loop system trajectories, respectively.	78
3.2	State trajectories of the process under the LEMPC design of Eq. 3.35 with state feedback and initial state $(C_A(0), T(0)) = (1.3 \frac{kmol}{m^3}, 320K)$ for one period of operation with (solid line) and without (dash-dotted line) the constraint of Eq. 3.35e.	78
3.3	Manipulated input trajectory under the LEMPC design of Eq. 3.35 with state feedback and initial state $(C_A(0), T(0)) = (1.3 \frac{kmol}{m^3}, 320K)$ for one period of operation with (solid line) and without (dash-dotted line) the constraint of Eq. 3.35e.	79
3.4	Ω_ρ and state trajectories of the process under state estimation-based LEMPC and initial state $(C_A(0), T(0)) = (1.3 \frac{kmol}{m^3}, 320K)$ for one period of operation subject to the constraint of Eq. 3.35e. The symbols \circ and \times denote the initial ($t = 0 \text{ hr}$) and final ($t = 1 \text{ hr}$) state of this closed-loop system trajectories, respectively.	80
3.5	State trajectories of the process under state estimation-based LEMPC and initial state $(C_A(0), T(0)) = (1.3 \frac{kmol}{m^3}, 320K)$ for one period of operation subject to the constraint of Eq. 3.35e.	80
3.6	Manipulated input trajectory under under state estimation-based LEMPC and initial state $(C_A(0), T(0)) = (1.3 \frac{kmol}{m^3}, 320K)$ for one period of operation subject to the constraint of Eq. 3.35e.	81
3.7	Ω_ρ and state trajectories of the process under state estimation-based LEMPC and initial state $(C_A(0), T(0)) = (1.3 \frac{kmol}{m^3}, 320K)$ for one period of operation subject to the constraint of Eq. 3.35e and bounded measurement noise. The symbols \circ and \times denote the initial ($t = 0 \text{ hr}$) and final ($t = 1 \text{ hr}$) state of this closed-loop system trajectories, respectively.	82
3.8	State trajectories of the process under state estimation-based LEMPC and initial state $(C_A(0), T(0)) = (1.3 \frac{kmol}{m^3}, 320K)$ for one period of operation subject to the constraint of Eq. 3.35e and bounded measurement noise.	82

3.9	Manipulated input trajectory under under state estimation-based LEMPC and initial state $(C_A(0), T(0)) = (1.3 \frac{kmol}{m^3}, 320K)$ for one period of operation subject to the constraint of Eq. 3.35e and bounded measurement noise.	83
4.1	LEMPC architecture under nominal operation	92
4.2	LEMPC architecture subject to disturbances	102
4.3	Ω_ρ and state trajectories of the process under the LMPC design of Eq. 4.6 with initial state $(C_A(0), T(0)) = (1 \frac{kmol}{m^3}, 320K)$ for one period of operation. The symbols \circ and \times denote the initial ($t = 0 hr$) and final ($t = 1 hr$) state of these closed-loop system trajectories, respectively.	109
4.4	State trajectories of the process under the LMPC design of Eq. 4.6 with initial state $(C_A(0), T(0)) = (1 \frac{kmol}{m^3}, 320K)$ for one period of operation.	109
4.5	Manipulated input trajectory under the LMPC design of Eq. 4.6 with initial state $(C_A(0), T(0)) = (1 \frac{kmol}{m^3}, 320K)$ for one period of operation.	110
4.6	Ω_ρ and state trajectories of the process under the LEMPC design of Eq. 4.12 with initial state $(C_A(0), T(0)) = (1 \frac{kmol}{m^3}, 320K)$ for one period of operation. The symbols \circ and \times denote the initial ($t = 0 hr$) and final ($t = 1 hr$) state of these closed-loop system trajectories, respectively.	110
4.7	State trajectories of the process under the LEMPC design of Eq. 4.12 with initial state $(C_A(0), T(0)) = (1 \frac{kmol}{m^3}, 320K)$ for one period of operation.	111
4.8	Manipulated input trajectory under the LEMPC design of Eq. 4.12 with initial state $(C_A(0), T(0)) = (1 \frac{kmol}{m^3}, 320K)$ for one period of operation.	111
4.9	30 different initial states for evaluation of LEMPC and LMPC schemes from an economic cost function point of view.	112
4.10	Ω_ρ and state trajectories of the process under the LEMPC design of Eq. 4.37 with initial state $(C_A(0), T(0)) = (1 \frac{kmol}{m^3}, 320K)$ for one period of operation subject to bounded process disturbance. The symbols \circ and \times denote the initial ($t = 0 hr$) and final ($t = 1 hr$) state of these closed-loop system trajectories, respectively.	113

4.11	State trajectories of the process under the LEMPC design of Eq. 4.37 with initial state $(C_A(0), T(0)) = (1 \frac{kmol}{m^3}, 320K)$ for one period of operation subject to bounded process disturbance.	114
4.12	Manipulated input trajectory under the LEMPC design of Eq. 4.37 with initial state $(C_A(0), T(0)) = (1 \frac{kmol}{m^3}, 320K)$ for one period of operation subject to bounded process disturbance.	114
5.1	Bounded communication channel noise.	119
5.2	Distributed LMPC control architecture (F means solving a feasibility problem).	122
5.3	Two CSTRs and a flash tank with recycle stream.	133
5.4	Distributed LMPC control architecture for chemical process example (F means solving a feasibility problem).	138
5.5	State trajectories of the process under the proposed DMPC design.	139
6.1	Distributed LMPC control architecture (solid line denotes fast state sampling and/or point-to-point links; dashed line denotes slow state sampling and/or shared communication networks).	150
6.2	State trajectories of the process under the DMPC design of Eqs. 6.9-6.10 and 6.12-6.13 with noise.	177
6.3	Manipulated input trajectories under the DMPC design of Eqs. 6.9-6.10 and 6.12-6.13 with noise.	177
7.1	Two CSTRs and a flash tank with recycle stream.	204
7.2	Lyapunov function trajectory of the closed-loop system under the implementation of the Lyapunov-based controller (dashed-dotted line) in a sample-and-hold fashion and of the centralized MPC (solid line) at mode one.	208

7.3	Lyapunov function trajectory of the closed-loop system under the implementation of the Lyapunov-based controller (dashed-dotted line) in a sample-and-hold fashion and of the centralized MPC (solid line) at mode two.	208
7.4	Lyapunov function trajectory of the closed-loop system under the implementation of the Lyapunov-based controller (solid line) in a sample-and-hold fashion, centralized MPC of Eq. 7.12 (*) and DMPC of Eq. 7.15 (dashed-dotted line) for the given switching policy; the line composed of the (*) and the dashed-dotted line overlap. From $t = 0$ to 0.004 hr , the lines show $V_1(x)$ and from $t = 0.004 \text{ hr}$ to 0.1 hr , the lines show $V_2(x)$	209
7.5	State trajectories of the closed-loop system under the implementation of the DMPC system of Eq. 7.15.	210
7.6	Manipulated input trajectories computed by the DMPC of Eq. 7.15.	211

List of Tables

2.1	Parameter values	38
3.1	Parameter values	73
4.1	Parameter values	107
4.2	Economic closed-loop performance comparison	111
5.1	Process variables	135
5.2	Parameter values	136
5.3	Disturbance parameters.	136
5.4	Steady-state values for Q_{1s} , Q_{2s} and Q_{3s}	136
5.5	Steady-state values for x_s	136
5.6	Total performance cost ($*10^7$) along the closed-loop system trajectories.	140
5.7	Total performance cost ($*10^7$) along the closed-loop system trajectories for different data loss probabilities and $\sigma^2 = 0.01$	140
5.8	Total performance cost ($*10^7$) along the closed-loop system trajectories for different channel noise power values and $\alpha = 0.1$	141
6.1	Disturbance parameters.	173
6.2	Steady-state values for x_s	173

6.3	Communication noise parameters.	176
6.4	Total performance cost comparison along the closed-loop system trajectories in 10 different runs under: (1) the proposed multirate DMPC design; (2) a DMPC design with LMPCs formulated as in Eq. 6.9 evaluated only at time instants in which full system states are available and the inputs are implemented in open-loop fashion between two full system state measurements; (3) the proposed DMPC design but without communication between the distributed controllers and each controller estimating the full system states and the actions of the other controllers based on the process model and $h(x)$; (4) the DMPC design as in (2) but without communication between the distributed controllers and each controller estimating the full system states and actions of the other controllers based on the process model and $h(x)$; (5) $h(x)$ applied in sample-and-hold; (6) the centralized LMPC [79].	179
7.1	Steady-state values for x_{s_1}	206
7.2	Steady-state values for x_{s_2}	206

ACKNOWLEDGEMENTS

First and foremost, I would like to thank my advisor, Professor Panagiotis D. Christofides for his guidance and support throughout my PhD study at UCLA. His comments, knowledge on control theory, availability to discuss even during holidays, and insightful feedbacks and remarks completely inspired my work through line by line of this dissertation. I would like to thank Professor Paulo Tabuada, Professor Mihaela van der Schaar and Professor James F. Davis for agreeing to participate in my doctoral committee. I would like to thank my friends, Jinfeng Liu and Majid Zamani, for the long hours of discussions on research problems. I would like to thank all of my friends at Process Control and Applied Mathematic Laboratory at UCLA for good memories that we had together. Financial support from the National Science Foundation and from the UCLA Graduate Division is gratefully acknowledged. I would like to thank my parents in Iran for their encouragement and love. Last but not least, I would like to express my deepest gratitude to my wife, Mozhgan, for her unconditional love, encouragement, patience and support. Her contribution to my life is so great to fit on this page.

Chapter 2 is a version of M. Heidarinejad, J. Liu, and P. D. Christofides. Economic Model Predictive Control of Nonlinear Process Systems Using Lyapunov Techniques. *AICHE Journal*, 58:855–870, 2012.

Chapter 3 is a version of M. Heidarinejad, J. Liu, and P. D. Christofides. State Estimation-Based Economic Model Predictive Control of Nonlinear Systems. *Systems and Control Letters*, under revision.

Chapter 4 is a version of M. Heidarinejad, J. Liu, and P. D. Christofides. Algorithms for Improved Finite-Time Performance of Lyapunov-Based Economic Model Predictive Control of Nonlinear Systems. *Chemical Engineering Science*, submitted.

Chapter 5 is a version of M. Heidarinejad, J. Liu, D. Muñoz de la Peña, J. F. Davis, and P. D. Christofides. Handling Communication Disruptions in Distributed Model Predictive Control of Nonlinear Systems. *Journal of Process Control*, 21:173–181, 2011.

Chapter 6 is a version of M. Heidarinejad, J. Liu, D. Muñoz de la Peña, J. F. Davis, and P. D. Christofides. Multirate Lyapunov-Based Distributed Model Predictive Control of Nonlinear Uncertain Systems. *Journal of Process Control*, 21:1231–1242, 2011.

Chapter 7 is a version of M. Heidarinejad, J. Liu, and P. D. Christofides. Distributed Model Predictive Control of Switched Nonlinear Systems with Scheduled Mode Transitions. *IEEE Transactions on Automatic Control*, under revision.

VITA

- 2006 Bachelor of Science, Electrical Engineering
Department of Electrical Engineering
Sharif University of Technology, Tehran, Iran
- 2008 Master of Science, Electrical and Computer Engineering
Department of Electrical and Computer Engineering
University of Toronto, Toronto, Canada
- 2008–2012 PhD Student
Department of Electrical Engineering
University of California, Los Angeles
- 2009–2012 Teaching Assistant/Associate/Fellow
Department of Electrical Engineering
University of California, Los Angeles

PUBLICATIONS AND PRESENTATIONS

1. M. Heidarinejad, J. Liu, D. Muñoz de la Peña, J. F. Davis, and P. D. Christofides. Multirate Lyapunov-Based Distributed Model Predictive Control of Nonlinear Uncertain Systems. *Journal of Process Control*, 21:1231–1242, 2011.
2. M. Heidarinejad, J. Liu, D. Muñoz de la Peña, J. F. Davis, and P. D. Christofides. Handling Communication Disruptions in Distributed Model Predictive Control of Nonlinear Systems. *Journal of Process Control*, 21:173–181, 2011.
3. M. Heidarinejad, J. Liu, and P. D. Christofides. Economic Model Predictive Control of Nonlinear Process Systems Using Lyapunov Techniques. *AIChE Journal*, 58:855–870, 2012.
4. M. Heidarinejad, J. Liu, and P. D. Christofides. Distributed Model Predictive Control of Switched Nonlinear Systems with Scheduled Mode Transitions. *IEEE Transactions on Automatic Control*, under revision.
5. M. Heidarinejad, J. Liu, and P. D. Christofides. State Estimation-Based Economic Model Predictive Control of Nonlinear Systems. *Systems and Control Letters*, under revision.
6. M. Heidarinejad, J. Liu, and P. D. Christofides. Algorithms for Improved Finite-Time Performance of Lyapunov-Based Economic Model Predictive Control of Nonlinear Systems. *Chemical Engineering Science*, submitted.

7. X. Chen, M. Heidarinejad, J. Liu, D. Muñoz de la Peña, and P. D. Christofides. Model Predictive Control of Nonlinear Singularly Perturbed Systems: Application to a Large-Scale Process Network. *Journal of Process Control*, 21:1296–1305, 2011.
8. X. Chen, M. Heidarinejad, J. Liu, and P. D. Christofides. Composite Fast-Slow MPC Design for Nonlinear Singularly Perturbed Systems. *AIChE Journal*, 58:1801–1810, 2012.
9. X. Chen, M. Heidarinejad, J. Liu, and P. D. Christofides. Distributed Economic MPC: Application to a Nonlinear Chemical Process Network. *Journal of Process Control*, 22:689–699, 2012.
10. M. Heidarinejad, J. Liu, and P. D. Christofides. State Estimation-Based Economic Model Predictive Control of Nonlinear Systems. *submitted to the 51th IEEE Conference on Decision and Control*.
11. M. Heidarinejad, J. liu, and P. D. Christofides. Distributed Model Predictive Control of Switched Nonlinear Systems with Scheduled Mode Transitions. *Proceeding of the Amercian Control Conference*, in press, 2012.
12. M. Heidarinejad, J. Liu, and P. D. Christofides. Economic Model Predictive Control Using Lyapunov Techniques: Handling Asynchronous, Delayed Measurements and Distributed Implementation. *Proceedings of the 50th IEEE Conference on Decision and Control and European Control Conference*, pages 4646-4653, Orlando, Florida, 2011.
13. M. Heidarinejad, J. Liu, and P. D. Christofides. Lyapunov-based Economic Model Predictive Control of Nonlinear Systems. *Proceedings of the American Control Conference*, pages 5195-5200, San Francisco, California, 2011.
14. M. Heidarinejad, J. Liu, D. Muñoz de la Peña, J. F. Davis, and P. D. Christofides. Multirate Distributed Model Predictive Control of Nonlinear Systems. *Proceedings of the American Control Conference*, pages 5181-5188, San Francisco, California, 2011.
15. M. Heidarinejad, J. Liu, D. Muñoz de la Peña, and P. D. Christofides. Handling Communication Disruptions in Distributed Model Predictive Control of Nonlinear Systems. *Proceedings of 9th International Symposium on Dynamics and Control of Process Systems*, pages 282-287, Leuven, Belgium, 2010.
16. X. Chen, M. Heidarinejad, J. Liu, and P. D. Christofides. Composite Fast-Slow MPC Design for Nonlinear Singularly Perturbed Systems: Near-Optimality and Process Network Application. *submitted to the 51th IEEE Conference on Decision and Control*.

17. X. Chen, M. Heidarinejad, J. Liu, and P. D. Christofides. Composite Fast-slow MPC Design for Nonlinear Singularly Perturbed Systems. *Proceeding of the American Control Conference*, in press, 2012.
18. X. Chen, M. Heidarinejad, J. Liu, D. Muñoz de la Peña, and P. D. Christofides. Model Predictive Control of Nonlinear Singularly Perturbed Systems: Application to a Reactor-Separator Process Network. *Proceedings of the 50th IEEE Conference on Decision and Control and European Control Conference*, pages 8125-8132, Orlando, Florida, 2011.
19. M. Heidarinejad, J. Liu, D. Muñoz de la Peña, J. F. Davis, and P. D. Christofides. Multirate Distributed Model Predictive Control of Nonlinear Uncertain Systems. *AIChE Annual Meeting*, paper 740c, Salt Lake City, Utah, 2010.
20. M. Heidarinejad, J. Liu, and P. D. Christofides. Distributed Model Predictive Control of Switched Nonlinear Systems. *AIChE Annual Meeting*, paper 515c, Minneapolis, Minnesota, 2011.
21. M. Heidarinejad, J. Liu, and P. D. Christofides. Lyapunov-Based Economic Model Predictive Control of Nonlinear Systems: Handling Asynchronous, Delayed Measurements and Distributed Implementation. *AIChE Annual Meeting*, paper 473f, Minneapolis, Minnesota, 2011.
22. X. Chen, M. Heidarinejad, J. Liu, D. Muñoz de la Peña, and P. D. Christofides. Model Predictive Control of Nonlinear Singularly Perturbed Systems: Application to a Large-Scale Process Network. *AIChE Annual Meeting*, paper 214d, Minneapolis, Minnesota, 2011.
23. X. Chen, M. Heidarinejad, J. Liu, and P. D. Christofides. Economic Cost Function Design and Model Predictive Control of a Chemical Process Network. *AIChE Annual Meeting*, paper 772b, Minneapolis, Minnesota, 2011.
24. M. Heidarinejad, A. A. Yazdi, and K. N. Plataniotis, Algebraic Visual Cryptography Scheme For Color Images. *Proceedings of the 33rd IEEE International Conference on Acoustics, Speech, and Signal Processing*, pages 1761-1764, Las Vegas, Nevada, 2008.
25. M. Heidarinejad, and K. N. Plataniotis, A Second Generation Visual Secret Sharing Scheme For Color Images. *Proceedings of the 15th IEEE International Conference on Image Processing*, pages 481-484, San Diego, California, 2008.

Chapter 1

Introduction

1.1 Background

1.1.1 Economic Model Predictive Control

The development of optimal operation and control policies for chemical process systems aiming at optimizing process economics has always been an important research subject with major practical implications. Within process control, the economic optimization considerations of a plant are usually addressed via a two-layer architecture (e.g., [70] and the references therein). In general, this architecture includes: the upper layer that optimizes process operation set-points taking into account economic considerations using steady-state system models, and the lower layer (i.e., process control layer) whose primary objective is to employ feedback control systems to force the process to track the set-points. This two-layer approach usually limits process operation around a steady-state.

Model predictive control (MPC) is widely adopted in industry in the process control layer because of its ability to deal with large multivariable constrained control

problems and to account for optimization considerations [29, 72]. MPC takes advantage of a process model to predict the future evolution of the process at each sampling time according to the current state along a given prediction horizon. These predictions are incorporated in an optimization problem to obtain an optimal input trajectory by minimizing a meaningful performance index. To reduce the computational complexity of the optimization problem, MPC obtains the optimal input solution over the family of piecewise constant trajectories with fixed sampling time and finite prediction horizon. Once the optimization problem is solved, only the first manipulated input value is implemented, discarding the rest of the trajectory and repeating the optimization in the next sampling step (e.g., [85]). The key idea of a standard MPC is to choose control actions by repeatedly solving an on-line constrained optimization problem, which aims at minimizing a cost function that involves penalties on the state variables and on the control actions over a finite prediction horizon.

Typically, the cost function is in quadratic form including penalties on the deviations of the system state and control inputs from a desired steady-state. Because of the structure of the cost function, the control objective of a standard MPC is to drive the state of the closed-loop system to the desired steady-state. In MPC theory, the quadratic cost function is also widely used as a Lyapunov function to prove closed-loop stability (e.g., [72]). Even though in the standard MPC formulations, certain economic optimization considerations can be taken into account (e.g., optimal use of control action), general economic optimization considerations are usually not addressed. In order to account for general economic optimization considerations, the quadratic cost function used in standard MPC should be replaced by an economics-based cost function. Moreover, the standard MPC should be re-formulated in an appropriate way to guarantee closed-loop stability. Economic model predictive control framework deals with a reformulation of the conventional MPC quadratic cost

function in which an economic (not necessarily quadratic) cost function is used directly as the cost in MPC, and thus, it may, in general, lead to time-varying process operation policies (instead of steady-state operation), which directly optimize process economics.

Within process control, there have been several calls for the integration of MPC and economic optimization of processes (e.g., [2, 86, 48]). In the literature, two-stage MPC structures [6, 80, 78, 103], the so-called LP-MPC and QP-MPC, have been investigated in order to reduce the difference between the sampling rates of the steady-state optimization performed in the RTO layer and the lower layer linear MPC. There are also attempts to integrate steady-state RTO and linear MPC in a single level [22, 104]. In this type of approach, the economic optimization and control problems are solved simultaneously in a single optimization problem and an additional term is added into the MPC cost function to account for the economic considerations. There are also attempts to utilize a dynamic model in the RTO layer which interacts with lower layer linear MPC (e.g., [105]). This approach uses dynamical models in the RTO and re-calculates the optimal set-points for the linear MPC only if economic benefits are possible. Furthermore, there are efforts on the development of MPC accounting for general economic considerations in the cost function [28, 47, 24]. In [28], general ideas of a combined steady-state optimization and linear MPC scheme as well as a case study were reported. In [47], two economically oriented nonlinear MPC formulations were proposed for cyclic processes and nominal stability of the closed-loop system was established via Lyapunov techniques. In [24], MPC schemes using an economics-based cost function were proposed and the stability properties were established using a suitable Lyapunov function. The MPC schemes in [24] adopt a terminal constraint which requires that the closed-loop system state settles to a steady-state at the end of each optimal input trajectory calculation (i.e., end of the

prediction horizon). The work in [46] formulated a linear robust economic MPC by taking advantage of second-order cone programming. The work in [55] considered a cooperative distributed linear economic MPC scheme subject to convex economic objectives. Simultaneous consideration of economic and control performance has been studied in [69]. The use of economic MPC for the reduction of energy related costs has been considered in [65]. Economic performance of MPC for a simulated electric arc furnace has been considered in [100]. An implementation of an MPC architecture which deals with control and economic considerations has been considered in [83].

Despite the above recent progress, at this point, there is limited work to ensure improvement of closed-loop performance through time-varying operation via economic MPC with respect to operation under conventional MPC in the context of finite time operation. An important recent work has established improved economic MPC performance over steady-state operation for infinite-time operation [1]. Furthermore, even though a rigorous stability analysis is included in [24], it is difficult, in general, to characterize, a priori, the set of initial conditions starting from where feasibility and closed-loop stability of the proposed MPC scheme are guaranteed. Moreover, all economic MPC schemes including the ones above have been developed under the assumption of state feedback. State estimation in certain classes of nonlinear systems can be carried out within the framework of high-gain observers (e.g., [16, 23]), however, at this stage these estimation techniques have not been used in conjunction with economic MPC schemes.

1.1.2 Distributed Model Predictive Control

The chemical process industry is a major sector of the US and global economy. Hence, the development of optimal process control and operation methodologies for chemical

processes is a research subject of considerable importance. Advanced process control stands to benefit from the emergence of networked process control and operations, with the purpose of augmentation of traditional point-to-point local control systems with additional cheap, safe and easy-to-install networked sensors and actuators. Networked control systems (NCS) can substantially improve the efficiency, flexibility, robustness and fault tolerance of an industrial control system while reducing the installation, reconfiguration and maintenance expenses at the cost of coordination and design/redesign of different control systems in the new architecture [102, 82, 17]. Recent research efforts have led to important results on the design of networked control systems (e.g., [76, 77, 81, 64]), employing a centralized control paradigm where all manipulated inputs are evaluated by a single control system.

Model predictive control (MPC) is a natural framework for dealing with the design and coordination of distributed control systems because it can account for the influence of other control systems on the computation of the control action for a certain set of actuators. In a centralized MPC paradigm, all the manipulated inputs of a given control system are coupled in a single optimization problem to obtain the optimal input trajectory. In the case of large number of state variables and manipulated inputs for a given control system, the computational complexity of the centralized MPC may increase significantly and consequently degrade closed-loop system performance, especially in the case of employing a nonlinear model in MPC. Moreover, a centralized control system for large-scale systems may be difficult to organize and maintain and is vulnerable to potential process faults. Because in the evaluation of the control actions by MPC online optimization problems need to be solved, the evaluation time of the MPC is a very important concern. Specifically, the MPC evaluation time strongly depends on the number of manipulated inputs as well as the dimensionality of the process model. To overcome the above mentioned drawbacks

of centralized MPC, decentralized and/or distributed MPC can be utilized. While in a decentralized control architecture [91], individual controllers make their decisions based on local information, in a distributed framework, controllers communicate with each other to coordinate their actions. In distributed MPC (DMPC) the optimal trajectory is obtained through solving a number of distributed optimization problems with lower dimensionality compared to the centralized design.

Distributed MPC (DMPC) has attracted a lot of attention in the design of cooperative networked control systems. In a DMPC architecture, the manipulated inputs are computed by solving more than one control (optimization) problems in separate processors in a coordinated fashion. In the context of DMPC designs, a number of significant efforts have been recently made in the literature; please see [7, 87, 89, 19] for reviews of available results in this direction. Specifically, the stability of the closed-loop linear system by considering multiple communications between distributed predictive controllers and using system-wide control objective functions was guaranteed in [96]. In [92], a cooperative DMPC scheme was developed for linear systems with guaranteed stability of the closed-loop system and convergence of the cost to its corresponding, centralized optimal value. A distributed control method for weakly-coupled nonlinear systems subject to decoupled constraints was proposed in [25]. A DMPC scheme for linear systems coupled through the inputs, based on a game theoretic approach, was proposed in [66]. A robust DMPC formulation for decoupled linear systems was studied in [88]. A DMPC architecture for decoupled nonlinear systems coupled through cost functions was studied in [49]. A DMPC framework for a class of nonlinear discrete-time systems subject to no exchange of information between local controllers was proposed in [67]. Furthermore, in [93], a quasi-decentralized control framework was developed for multi-unit plants that achieves the desired closed-loop objectives with minimal cross communication between the controllers.

Two different DMPC architectures, namely, a sequential DMPC architecture and an iterative DMPC architecture, were designed for nonlinear systems in [61, 60], and the work were extended to account for asynchronous and delayed measurements [62]. Distributed MPCs were designed via Lyapunov-based MPC (LMPC) to coordinate their control actions using one-directional communication. Among the distributed LMPCs, one LMPC is responsible for closed-loop stability while the rest of the LMPCs communicate and cooperate with the stabilizing LMPC to improve the closed-loop performance. In [61], the communication between the distributed controllers was assumed to be perfect which is reasonable in applications where wired network communication links are utilized. Furthermore, the results in [61, 60, 62] were obtained under the assumptions of noise-free communication and availability of noise-free measurements of system states to all the distributed controllers at each sampling time.

Recently, wireless networks have received significant attention [95] and could play an increasingly important role in distributed control systems. In chemical process systems [17], there is an increasing trend toward developing industrial DMPC designs where individual MPCs operate through a shared wireless/wired communication network. However, the design of network-based DMPC system has to deal with the dynamics introduced by the communication network, which may include communication disruptions such as communication channel noise, data losses, bandwidth limitations, time-varying delays, and data quantization [79] which directly affect the closed-loop stability of NCS architectures. Thus, achieving closed-loop stability subject to communication disruptions in the context of DMPC is a subject of increasing importance. Motivated by this trend towards network-based control systems in a variety of engineering applications, significant efforts over the last ten years have led to results on analysis and design of networked control systems using centralized control architectures (e.g., [76, 81]).

1.2 Objectives and Organization of the Dissertation

Motivated by the lack of general economic and distributed control methods for process systems, the objectives of this dissertation are summarized as follows:

1. To develop economic model predictive control of nonlinear process systems using Lyapunov techniques taking into account asynchronous and time-varying delayed measurements.
2. To develop state estimation based economic model predictive control schemes of nonlinear systems.
3. To develop algorithms for improved finite-time performance of economic model predictive control of nonlinear systems.
4. To develop distributed model predictive control schemes subject to communication disruptions.
5. To develop multirate distributed model predictive control of nonlinear uncertain systems.
6. To develop distributed model predictive control of switched nonlinear systems with scheduled mode transitions.

The dissertation is organized as follows. In Chapter 2, we develop MPC designs which are capable of optimizing closed-loop performance with respect to general economic considerations for a broad class of nonlinear process systems. Specifically, in the proposed designs, the economic MPC optimizes a cost function which is related directly to desired economic considerations and is not necessarily dependent on a

steady-state — unlike conventional MPC designs. First, we consider nonlinear systems with synchronous measurement sampling and uncertain variables. The proposed economic MPC is designed via Lyapunov-based techniques and has two different operation modes. The first operation mode corresponds to the period in which the cost function should be optimized (e.g., normal production period); and in this operation mode, the MPC maintains the closed-loop system state within a pre-defined stability region and optimizes the cost function to its maximum extent. The second operation mode corresponds to operation in which the system is driven by the economic MPC to an appropriate steady-state. In this operation mode, suitable Lyapunov-based constraints are incorporated in the economic MPC design to guarantee that the closed-loop system state is always bounded in the pre-defined stability region and is ultimately bounded in a small region containing the origin. Subsequently, we extend the results to nonlinear systems subject to asynchronous and delayed measurements and uncertain variables. Under the assumptions that there exist an upper bound on the interval between two consecutive asynchronous measurements and an upper bound on the maximum measurement delay, an economic MPC design which takes explicitly into account asynchronous and delayed measurements and enforces closed-loop stability is proposed. All the proposed economic MPC designs are illustrated through a chemical process example and their performance and robustness are evaluated through simulations.

In Chapter 3, we focus on a class of nonlinear systems and design an estimator-based economic MPC system which is capable of optimizing closed-loop performance with respect to general economic considerations taken into account in the construction of the cost function. Working with the class of full-state feedback linearizable nonlinear systems, we use a high-gain observer to estimate the nonlinear system state using output measurements and a Lyapunov-based approach to design an economic MPC

system that uses the observer state estimates. We prove, using singular perturbation arguments, that the closed-loop system is practically stable provided the observer gain is sufficiently large. We use a chemical process example to demonstrate the ability of the state estimation-based economic MPC to achieve process time-varying operation that leads to a superior cost performance metric compared to steady-state operation using the same amount of reactant material.

In Chapter 4, we present algorithms for improved finite-time performance of Lyapunov-based economic model predictive control (LEMPC) of nonlinear systems. Unlike conventional LMPC schemes which typically utilize a quadratic cost function and regulate a process at a steady-state, LEMPC designs very often dictate time-varying operation to optimize an economic (typically non-quadratic) cost function. The LEMPC algorithms proposed here ensure improved performance, measured by the desired economic cost, over conventional LMPC by solving auxiliary LMPC problems and incorporating appropriate constraints, based on the LMPC solution, in their formulations at various sampling times. The proposed LEMPC schemes also take advantage of a predefined Lyapunov-based explicit feedback law to characterize their stability region while maintaining the closed-loop system state in an invariant set subject to bounded process disturbances. The LEMPC algorithms are demonstrated through a nonlinear chemical process example.

In Chapter 5, we study DMPC of nonlinear systems subject to communication disruptions - communication channel noise and data losses - between distributed controllers. Specifically, we focus on a DMPC architecture in which one of the distributed controllers is responsible for ensuring closed-loop stability while the rest of the distributed controllers communicate and cooperate with the stabilizing controller to further improve the closed-loop performance. To handle communication disruptions,

feasibility problems are incorporated in the DMPC architecture to determine if the data transmitted through the communication channel is reliable or not. Based on the results of the feasibility problems, the transmitted information is accepted or rejected by the stabilizing MPC. In order to ensure the stability of the closed-loop system under communication disruptions, each model predictive controller utilizes a stability constraint which is based on a suitable Lyapunov-based controller. The theoretical results are demonstrated through a nonlinear chemical process example.

In Chapter 6, we consider the design of a network-based DMPC system using multirate sampling for large-scale nonlinear uncertain systems composed of several coupled subsystems. Specifically, we assume that the states of each local subsystem can be divided into fast sampled states (which are available every sampling time) and slowly sampled states (which are available every several sampling times). The distributed model predictive controllers are connected through a shared communication network and cooperate in an iterative fashion at time instants in which full system state measurements (both fast and slow) are available, to guarantee closed-loop stability. When local subsystem fast sampled state information is only available, the distributed controllers operate in a decentralized fashion to improve closed-loop performance. In the proposed control architecture, the controllers are designed via LMPC techniques taking into account bounded measurement noise, process disturbances and communication noise. Sufficient conditions under which the state of the closed-loop system is ultimately bounded in an invariant region containing the origin are derived. The theoretical results are demonstrated through a nonlinear chemical process example.

In Chapter 7, we present a method for the design of distributed model predictive control systems for a class of switched nonlinear systems for which the mode tran-

sitions take place according to a prescribed switching schedule. Under appropriate stabilizability assumptions on the existence of a set of feedback controllers that can stabilize the closed-loop switched, nonlinear system, we design a cooperative, distributed model predictive control architecture using LMPC in which the distributed controllers carry out their calculations in parallel and communicate in an iterative fashion to compute their control actions. The proposed distributed model predictive control design is applied to a nonlinear chemical process network with scheduled mode transitions and its performance and computational efficiency properties in comparison to a centralized MPC architecture are evaluated through simulations.

Chapter 8 summarizes the main results of the dissertation and discusses future research possibilities in economic and distributed predictive control system design.

Chapter 2

Economic Model Predictive

Control of Nonlinear Process

Systems Using Lyapunov

Techniques

In this chapter, we develop Lyapunov-based economic MPC (LEMPC) designs which are capable of optimizing closed-loop performance with respect to general economic considerations for nonlinear systems. The design of the LEMPC is based on uniting receding horizon control with explicit Lyapunov-based nonlinear controller design techniques and allows for an explicit characterization of the stability region of the closed-loop system; such a characterization may be conservative in certain applications and it may be possible for the LEMPC to achieve closed-loop stability for initial conditions outside of the estimated stability region. In the proposed designs, the LEMPC schemes optimize a cost function which is related directly to certain

economic considerations and is not necessarily dependent on a steady-state — unlike conventional model predictive control (MPC) designs. First, we consider nonlinear systems with synchronous measurement sampling and uncertain variables. The proposed LEMPC is designed via Lyapunov-based techniques and has two different operation modes. The first operation mode corresponds to the period in which the cost function should be optimized (e.g., normal production period); and in this operation mode, the LEMPC maintains the closed-loop system state within a pre-defined stability region and optimizes the cost function to its maximum extent. The second operation mode corresponds to operation in which the system is driven by the LEMPC to an appropriate steady-state. In the LEMPC design, suitable Lyapunov-based constraints are incorporated to guarantee that the closed-loop system state is always bounded in the pre-defined stability region and is ultimately bounded in a small region containing the origin. Subsequently, we extend the results to nonlinear systems subject to asynchronous and delayed measurements and uncertain variables. Under the assumptions that there exist an upper bound on the interval between two consecutive asynchronous measurements and an upper bound on the maximum measurement delay, an LEMPC design which takes explicitly into account asynchronous and delayed measurements and enforces closed-loop stability is proposed. The theoretical results are illustrated through a chemical process example.

2.1 Preliminaries

2.1.1 Notation

The operator $\|\cdot\|$ is used to denote Euclidean norm of a vector, and a continuous function $\alpha : [0, a) \rightarrow [0, \infty)$ is said to belong to class \mathcal{K} if it is strictly increasing and

satisfies $\alpha(0) = 0$. The symbol Ω_r is used to denote the set $\Omega_r := \{x \in R^{n_x} : V(x) \leq r\}$ where V is a scalar function, and the operator ‘/’ denotes set subtraction, that is, $A/B := \{x \in R^{n_x} : x \in A, x \notin B\}$. The symbol $\text{diag}(v)$ denotes a matrix whose diagonal elements are the elements of vector v and all the other elements are zeros.

2.1.2 Class of nonlinear systems

We consider a class of nonlinear systems which can be described by the following state-space model:

$$\dot{x}(t) = f(x(t), u_1(t), \dots, u_m(t), w(t)) \quad (2.1)$$

where $x(t) \in R^{n_x}$ denotes the vector of state variables of the system and $u_i(t) \in R$, $i = 1, \dots, m$, and $w(t) \in R^{n_w}$ denote m control (manipulated) inputs and the disturbance vector, respectively. The m control inputs are restricted to be in m nonempty convex sets $U_i \subseteq R$, $i = 1, \dots, m$, which are defined as $U_i := \{u_i \in R : |u_i| \leq u_i^{\max}\}$ where u_i^{\max} , $i = 1, \dots, m$, are the magnitudes of the input constraints. The disturbance $w(t) \in R^{n_w}$ is bounded, i.e., $w(t) \in W$ where $W := \{w \in R^{n_w} \text{ s.t. } |w| \leq \theta, \theta > 0\}$. We assume that f is a locally Lipschitz vector function and that the origin is an equilibrium point of the unforced nominal system (i.e., the system of Eq. 2.1 with $u_i(t) \equiv 0$, $i = 1, \dots, m$ and $w(t) \equiv 0$ for all times) which implies that $f(0, 0, \dots, 0, 0) = 0$.

2.1.3 Lyapunov-based controller

We assume that there exists a Lyapunov-based controller $h(x) = [h_1(x) \cdots h_m(x)]^T$ which renders the origin of the nominal closed-loop system asymptotically stable with $u_i = h_i(x)$, $i = 1, \dots, m$, while satisfying the input constraints for all the

states x inside a given stability region. We note that this assumption is essentially equivalent to the assumption that the system is stabilizable or that the pair (A, B) in the case of linear systems is stabilizable. Using converse Lyapunov theorems [59, 18], this assumption implies that there exist class \mathcal{K} functions $\alpha_i(\cdot)$, $i = 1, 2, 3, 4$ and a continuously differentiable Lyapunov function $V(x)$ for the nominal closed-loop system, that satisfy the following inequalities:

$$\begin{aligned}
\alpha_1(|x|) &\leq V(x) \leq \alpha_2(|x|) \\
\frac{\partial V(x)}{\partial x} f(x, h_1(x), \dots, h_m(x), 0) &\leq -\alpha_3(|x|) \\
\left| \frac{\partial V(x)}{\partial x} \right| &\leq \alpha_4(|x|) \\
h_i(x) &\in U_i, \quad i = 1, \dots, m
\end{aligned} \tag{2.2}$$

for all $x \in O \subseteq R^{n_x}$ where O is an open neighborhood of the origin. We denote the region $\Omega_\rho \subseteq O$ as the stability region of the closed-loop system under the Lyapunov-based controller $h(x)$. Note that explicit stabilizing control laws that provide explicitly defined regions of attraction for the closed-loop system have been developed using Lyapunov techniques for specific classes of nonlinear systems, particularly input-affine nonlinear systems; the reader may refer to [51, 18, 58, 26] for results in this area including results on the design of bounded Lyapunov-based controllers by taking explicitly into account constraints for broad classes of nonlinear systems.

By continuity, the local Lipschitz property assumed for the vector field f and taking into account that the manipulated inputs u_i , $i = 1, \dots, m$ are bounded, there exists a positive constant M such that

$$|f(x, u_1, \dots, u_m, w)| \leq M \tag{2.3}$$

for all $x \in \Omega_\rho$ and $u_i \in U_i$, $i = 1, \dots, m$. In addition, by the continuous differentiable property of the Lyapunov function $V(x)$ and the Lipschitz property assumed for the vector field f , there exist positive constants L_x , L_w , L'_x and L'_w such that

$$\begin{aligned} |f(x, u_1, \dots, u_m, w) - f(x', u_1, \dots, u_m, 0)| &\leq L_x |x - x'| + L_w |w| \\ \left| \frac{\partial V(x)}{\partial x} f(x, u_1, \dots, u_m, w) - \frac{\partial V(x')}{\partial x} f(x', u_1, \dots, u_m, 0) \right| &\leq L'_x |x - x'| + L'_w |w| \end{aligned} \quad (2.4)$$

for all $x, x' \in \Omega_\rho$, $u_i \in U_i$, $i = 1, \dots, m$ and $w \in W$.

Remark 2.1. *We note that while there are currently no general methods for constructing Lyapunov functions for general nonlinear systems, for broad classes of nonlinear systems arising in the context of chemical process control applications, quadratic Lyapunov functions have been widely used and have been demonstrated to yield very good estimates of closed-loop stability regions [18]; please see also “Application to a chemical process example” section.*

Remark 2.2. *Note that in this chapter, we use the level set Ω_ρ of the Lyapunov function $V(x)$ to estimate the stability region (i.e., domain of attraction) of the closed-loop system under the controller $h(x)$. Specifically, an estimate of the domain of attraction of the closed-loop system is computed as follows: first, a controller (e.g., $h(x)$) is designed that makes the time-derivative of a Lyapunov function, $V(x)$, along the closed-loop system trajectory negative definite around the equilibrium point; then, an estimate of the set where \dot{V} is negative is computed, and finally, a level set (ideally the largest) of V (denoted by Ω_ρ in this chapter) embedded in the set where \dot{V} is negative, is computed. From this approach to calculate Ω_ρ , we can conclude that the set Ω_ρ is a guaranteed closed-loop stability set but it is possible that the controller $h(x)$ stabilizes the closed-loop system for initial conditions outside of the set Ω_ρ .*

2.2 Lyapunov-based economic MPC with synchronous measurement sampling

In this section, we design LEMPC for the system of Eq. 2.1 with synchronous measurement sampling. We assume that the state x of the system is sampled synchronously and the time instants at which we have state measurements are indicated by the time sequence $\{t_{k \geq 0}\}$ with $t_k = t_0 + k\Delta$, $k = 0, 1, \dots$ where t_0 is the initial time and Δ is the sampling time.

In the proposed design, the LEMPC maximizes a cost function which takes into account specific economic considerations and it has two operation modes. In the first operation mode, the LEMPC optimizes the economic cost function while maintaining the system state within the stability region Ω_ρ (i.e., $x(t) \in \Omega_\rho$); in the second operation mode, the LEMPC drives the state of the system to a desired steady-state. The economic MPC is designed via Lyapunov-based MPC techniques [74] to take advantage of the stability properties of the Lyapunov-based controller $h(x)$. Specifically, we assume that from the initial time t_0 up to a specific time t' , the LEMPC operates in the first operation mode to maximize the economic cost function; after the time t' , we assume that the LEMPC operates in the second operation mode and calculates the inputs in a way that the state of the closed-loop system is driven to a neighborhood of the desired steady-state (i.e., the origin $x = 0$). The proposed LEMPC provides more degrees of freedom in the economic optimal operation of the system and can eventually regulate the system state to a desired steady-state. For simplicity and without loss of generality in the rest of this chapter, we assume that the specific time t' is an integer multiple of the sampling time of the MPC, Δ .

2.2.1 Implementation strategy

From the initial time t_0 to t' , the LEMPC operates in the first operation mode. In the design of the LEMPC, one important issue we need to consider is the effect of the bounded disturbance w on the stability of the closed-loop system. In order to take the disturbance w into account explicitly, we consider a region $\Omega_{\tilde{\rho}}$, $\tilde{\rho} < \rho$. Specifically, when $x(t_k)$ is received at a sampling time t_k , if $x(t_k)$ is in the region $\Omega_{\tilde{\rho}}$, the LEMPC maximizes the cost function within the region $\Omega_{\tilde{\rho}}$; if $x(t_k)$ is in the region $\Omega_{\rho}/\Omega_{\tilde{\rho}}$, the LEMPC first drives the system state to the region $\Omega_{\tilde{\rho}}$ and then maximizes the cost function within $\Omega_{\tilde{\rho}}$. Note that the region $\Omega_{\tilde{\rho}}$ plays the role of a “safe” zone in which the LEMPC can maximize the cost function to its maximum extent while the effect of the disturbance w on the closed-loop stability is taken into account. Note also that the relation between $\tilde{\rho}$ and ρ is determined by the system property (i.e., the properties of the vector function f), the upper bound on the disturbance (i.e., θ) and the sampling time of the LEMPC. This relation will be characterized in Eq. 2.12 in Theorem 2.1.

After time t' , the system operates in the second operation mode. In this operation mode, the LEMPC calculates the inputs in a way that the Lyapunov function of the system continuously decreases to steer the state of the system to a neighborhood of the origin.

The implementation strategy of the proposed LEMPC with synchronous measurement sampling can be summarized as follows:

1. At a sampling time t_k , the controller receives the system state $x(t_k)$ from the sensors.
2. If $t_k < t'$, go to Step 3. Else, go to Step 4.

3. If $x(t_k) \in \Omega_{\tilde{\rho}}$, go to Step 3.1. Else, go to Step 3.2.
 - 3.1. The controller maximizes the economic cost function within $\Omega_{\tilde{\rho}}$. Go to Step 5.
 - 3.2. The controller drives the system state to the region $\Omega_{\tilde{\rho}}$. Go to Step 5.
4. The controller drives the system state to a small neighborhood of the desired steady-state.
5. Go to Step 1 ($k \leftarrow k + 1$).

2.2.2 LEMPC formulation

The optimization problem of the proposed LEMPC for the system of Eq. 2.1 with synchronous measurement sampling is as follows:

$$\max_{u_1, \dots, u_m \in S(\Delta)} \int_{t_k}^{t_{k+N}} L(\tilde{x}(\tau), u_1(\tau), \dots, u_m(\tau)) d\tau \quad (2.5a)$$

$$\text{s.t. } \dot{\tilde{x}}(t) = f(\tilde{x}(t), u_1(t), \dots, u_m(t), 0) \quad (2.5b)$$

$$u_i(t) \in U_i, \quad i = 1, \dots, m \quad (2.5c)$$

$$\tilde{x}(t_k) = x(t_k) \quad (2.5d)$$

$$V(\tilde{x}(t)) \leq \tilde{\rho}, \quad \forall t \in [t_k, t_{k+N}), \quad \text{if } t_k \leq t' \text{ and } V(x(t_k)) \leq \tilde{\rho} \quad (2.5e)$$

$$\begin{aligned} & \frac{\partial V(x(t_k))}{\partial x} f(x(t_k), u_1(t_k), \dots, u_m(t_k), 0) \\ & \leq \frac{\partial V(x(t_k))}{\partial x} f(x(t_k), h_1(x(t_k)), \dots, h_m(x(t_k)), 0), \\ & \text{if } t_k > t' \text{ or } \tilde{\rho} < V(x(t_k)) \leq \rho \end{aligned} \quad (2.5f)$$

where $S(\Delta)$ is the family of piece-wise constant functions with sampling period Δ , N is the prediction horizon of this LEMPC, $L(\tilde{x}(\tau), u_1(\tau), \dots, u_m(\tau))$ is the economic measure which defines the cost function, the state \tilde{x} is the predicted trajectory of the system with u_1, \dots, u_m computed by the LEMPC and $x(t_k)$ is the state measurement obtained at time t_k . The optimal solution to this optimization problem is denoted by $u_i^*(t|t_k)$, $i = 1, \dots, m$, which is defined for $t \in [t_k, t_{k+N})$.

In the optimization problem of Eq. 2.5, the constraint of Eqs. 2.5b is the nominal model of the system of Eq. 2.1 (i.e., $w(t) = 0$ for all t) and is used to predict the future evolution of the closed-loop system; the constraint of Eq. 2.5c defines the input constraints on all the inputs; the constraint of Eq. 2.5d defines the initial condition of the optimization problem; the constraint of Eq. 2.5e is only active when $x(t_k) \in \Omega_{\tilde{\rho}}$ in the first operation mode and is incorporated to ensure that the predicted state evolution of the closed-loop system is maintained in the region $\Omega_{\tilde{\rho}}$ (thus, the actual state of the closed-loop system is in the stability region Ω_{ρ}); the constraint of Eq. 2.5f is only active in the second operation mode or when $\tilde{\rho} < V(x(t_k)) \leq \rho$ in the first operation mode. This constraint is used to enforce that the Lyapunov function of the system decreases at least at the rate given by the Lyapunov-based controller $h(x)$ implemented in a sample-and-hold fashion.

The manipulated inputs of the proposed control design from time t_k to t_{k+1} ($k = 0, 1, 2, \dots$) are defined as follows:

$$u_i(t) = u_i^*(t|t_k), \quad i = 1, \dots, m, \quad \forall t \in [t_k, t_{k+1}). \quad (2.6)$$

2.2.3 Stability analysis

In this subsection, we present the stability properties of the proposed LEMPC of Eq. 2.5 for the system of Eq. 2.1 with synchronous measurement sampling. In order to proceed, we need the following two propositions.

Proposition 2.1 (c.f. [60]). *Consider the systems*

$$\begin{aligned}\dot{x}_a(t) &= f(x_a(t), u_1(t), \dots, u_m(t), w(t)) \\ \dot{x}_b(t) &= f(x_b(t), u_1(t), \dots, u_m(t), 0)\end{aligned}\tag{2.7}$$

with initial states $x_a(t_0) = x_b(t_0) \in \Omega_\rho$. There exists a \mathcal{K} function $f_W(\cdot)$ such that

$$|x_a(t) - x_b(t)| \leq f_W(t - t_0),\tag{2.8}$$

for all $x_a(t), x_b(t) \in \Omega_\rho$ and all $w(t) \in W$ with

$$f_W(\tau) = \frac{L_w \theta}{L_x} (e^{L_x \tau} - 1).\tag{2.9}$$

Proposition 2.1 provides an upper bound on the deviation of the state trajectory obtained using the nominal model, from the actual system state trajectory when the same control input trajectories are applied. Proposition 2.2 below bounds the difference between the magnitudes of the Lyapunov function of two different states in Ω_ρ .

Proposition 2.2 (c.f. [60]). *Consider the Lyapunov function $V(\cdot)$ of the system of Eq. 2.1. There exists a quadratic function $f_V(\cdot)$ such that*

$$V(x) \leq V(\hat{x}) + f_V(|x - \hat{x}|)\tag{2.10}$$

for all $x, \hat{x} \in \Omega_\rho$ with

$$f_V(s) = \alpha_4(\alpha_1^{-1}(\rho))s + M_v s^2 \quad (2.11)$$

where M_v is a positive constant.

Theorem 2.1 below provides sufficient conditions under which the LEMPC of Eq. 2.5 guarantees that the state of the closed-loop system of Eq. 2.1 is always bounded in Ω_ρ and is ultimately bounded in a small region containing the origin.

Theorem 2.1. *Consider the system of Eq. 2.1 in closed-loop under the LEMPC design of Eq. 2.5 based on a controller $h(x)$ that satisfies the conditions of Eq. 2.2. Let $\epsilon_w > 0$, $\Delta > 0$, $\rho > \tilde{\rho} > 0$ and $\rho > \rho_s > 0$ satisfy*

$$\tilde{\rho} \leq \rho - f_V(f_W(\Delta)) \quad (2.12)$$

and

$$-\alpha_3(\alpha_2^{-1}(\rho_s)) + L'_x M \Delta + L'_w \theta \leq -\epsilon_w / \Delta. \quad (2.13)$$

If $x(t_0) \in \Omega_\rho$, $\rho_s \leq \tilde{\rho}$, $\rho_{\min} \leq \rho$ and $N \geq 1$ where

$$\rho_{\min} = \max\{V(x(t + \Delta)) : V(x(t)) \leq \rho_s\}, \quad (2.14)$$

then the state $x(t)$ of the closed-loop system is always bounded in Ω_ρ and is ultimately bounded in $\Omega_{\rho_{\min}}$.

Proof 2.1. The proof consists of three parts. We first prove that the optimization problem of Eq. 2.5 is feasible for all states $x \in \Omega_\rho$. Subsequently, we prove that, in the first operation mode, under the LEMPC design of Eq. 2.5, the closed-loop state of the system of Eq. 2.1 is always bounded in Ω_ρ . Finally, we prove that, in the second

operation mode, under the LEMPC of Eq. 2.5, the closed-loop state of the system of Eq. 2.1 is ultimately bounded in ρ_{\min} .

Part 1: When $x(t)$ is maintained in Ω_ρ (which will be proved in Part 2), the feasibility of the LEMPC of Eq. 2.5 follows because input trajectories $u_i(t)$, $i = 1, \dots, m$, such that $u_i(t) = h_i(x(t_{k+j}))$, $\forall t \in [t_{k+j}, t_{k+j+1})$ with $j = 0, \dots, N - 1$ are feasible solutions to the optimization problem of Eq. 2.5 since such trajectories satisfy the input constraint of Eq. 2.5c and the Lyapunov-based constraints of Eqs. 2.5e and 2.5f. This is guaranteed by the closed-loop stability property of the Lyapunov-based controller $h(x)$; the reader may refer to [79] for more detailed discussion on the stability property of the Lyapunov-based controller $h(x)$.

Part 2: We assume that the LEMPC of Eq. 2.5 operates in the first operation mode. We prove that if $x(t_k) \in \Omega_{\tilde{\rho}}$, then $x(t_{k+1}) \in \Omega_\rho$; and if $x(t_k) \in \Omega_\rho/\Omega_{\tilde{\rho}}$, then $V(x(t_{k+1})) < V(x(t_k))$ and in finite steps, the state converges to $\Omega_{\tilde{\rho}}$ (i.e., $x(t_{k+j}) \in \Omega_{\tilde{\rho}}$ where j is a finite positive integer).

When $x(t_k) \in \Omega_{\tilde{\rho}}$, from the constraint of Eq. 2.5e, we obtain that $\tilde{x}(t_{k+1}) \in \Omega_{\tilde{\rho}}$. By Propositions 2.1 and 2.2, we have that

$$V(x(t_{k+1})) \leq V(\tilde{x}(t_{k+1})) + f_V(f_W(\Delta)). \quad (2.15)$$

Since $V(\tilde{x}(t_{k+1})) \leq \tilde{\rho}$, if the condition of Eq. 2.12 is satisfied, we can conclude that

$$x(t_{k+1}) \in \Omega_\rho.$$

When $x(t_k) \in \Omega_\rho/\Omega_{\tilde{\rho}}$, from the constraint of Eq. 2.5f and the condition of Eq. 2.2,

we can write

$$\begin{aligned} \frac{\partial V(x(t_k))}{\partial x} f(x(t_k), u_1^*(t_k), \dots, u_m^*(t_k), 0) &\leq \frac{\partial V(x(t_k))}{\partial x} f(x(t_k), h_1(x(t_k)), \dots, \\ &h_m(x(t_k)), 0) \\ &\leq -\alpha_3(|x(t_k)|) \end{aligned} \quad (2.16)$$

The time derivative of the Lyapunov function along the computed optimal trajectories u_1^*, \dots, u_m^* for $\forall \tau \in [t_k, t_{k+1})$ can be written as follows

$$\dot{V}(x(\tau)) = \frac{\partial V(x(\tau))}{\partial x} f(x(\tau), u_1^*(t_k), \dots, u_m^*(t_k), w(\tau)) \quad (2.17)$$

Adding and subtracting the term $\frac{\partial V(x(t_k))}{\partial x} f(x(t_k), u_1^*(t_k), \dots, u_m^*(t_k), 0)$ to/from the above equation and considering Eq. 2.16, we have

$$\begin{aligned} \dot{V}(x(\tau)) &\leq -\alpha_3(|x(t_k)|) + \frac{\partial V(x(\tau))}{\partial x} f(x(\tau), u_1^*(t_k), \dots, u_m^*(t_k), w(\tau)) \\ &\quad - \frac{\partial V(x(t_k))}{\partial x} f(x(t_k), u_1^*(t_k), \dots, u_m^*(t_k), 0) \end{aligned} \quad (2.18)$$

Due to the fact that the disturbance is bounded $|w| \leq \theta$ and the Lipschitz properties of Eq. 2.4, we can write

$$\dot{V}(x(\tau)) \leq -\alpha_3(|x(t_k)|) + L'_x |x(\tau) - x(t_k)| + L'_w \theta \quad (2.19)$$

Taking into account Eq. 2.3 and the continuity of $x(t)$, the following bound can be written for all $\tau \in [t_k, t_{k+1})$

$$|x(\tau) - x(t_k)| \leq M\Delta. \quad (2.20)$$

Since $x(t_k) \in \Omega_\rho/\Omega_{\bar{\rho}}$, it can be concluded that $x(t_k) \in \Omega_\rho/\Omega_{\rho_s}$. Thus, we can write

$$\dot{V}(x(\tau)) \leq -\alpha_3(\alpha_2^{-1}(\rho_s)) + L'_x M \Delta + L'_w \theta. \quad (2.21)$$

If the condition of Eq. 2.13 is satisfied, then there exists $\epsilon_w > 0$ such that the following inequality holds for $x(t_k) \in \Omega_\rho/\Omega_{\bar{\rho}}$:

$$\dot{V}(x(t)) \leq -\epsilon_w/\Delta, \quad \forall t = [t_k, t_{k+1}).$$

Integrating this bound on $t \in [t_k, t_{k+1})$, we obtain that:

$$\begin{aligned} V(x(t_{k+1})) &\leq V(x(t_k)) - \epsilon_w \\ V(x(t)) &\leq V(x(t_k)), \quad \forall t \in [t_k, t_{k+1}) \end{aligned} \quad (2.22)$$

for all $x(t_k) \in \Omega_\rho/\Omega_{\bar{\rho}}$. Using Eq. 2.22 recursively, it is proved that, if $x(t_k) \in \Omega_\rho/\Omega_{\bar{\rho}}$, the state converges to $\Omega_{\bar{\rho}}$ in a finite number of sampling times without leaving the stability region.

Part 3: We assume that the LEMPC of Eq. 2.5 operates in the second operation mode. We prove that if $x(t_k) \in \Omega_\rho$, then $V(x(t_{k+1})) \leq V(x(t_k))$ and the system state is ultimately bounded in an invariant set $\Omega_{\rho_{\min}}$. Following similar steps as in Part 2, we can derive that the inequality of Eq. 2.22 hold for all $x(t_k) \in \Omega_\rho/\Omega_{\rho_s}$. Using this result recursively, it is proved that, if $x(t_k) \in \Omega_\rho/\Omega_{\rho_s}$, the state converges to Ω_{ρ_s} in a finite number of sampling times without leaving the stability region. Once the state converges to $\Omega_{\rho_s} \subseteq \Omega_{\rho_{\min}}$, it remains inside $\Omega_{\rho_{\min}}$ for all times. This statement holds because of the definition of ρ_{\min} . This proves that the closed-loop system state under the LEMPC of Eq. 2.5 is ultimately bounded in $\Omega_{\rho_{\min}}$.

Remark 2.3. Note that the set Ω_ρ (i.e., $V \leq \rho$) is an invariant set for the nominal

closed-loop system and is also an invariant set for the closed-loop system subject to bounded disturbances w (i.e., $|w| \leq \theta$) under piece-wise continuous control action implementation when the conditions stated in Theorem 2.1 (as well as Theorem 2.2 presented in the next section) are satisfied. This can be interpreted as follows: \dot{V} is negative everywhere in Ω_ρ but the origin when there are no disturbances and the control actions are updated continuously; furthermore, the further away from the origin the more negative \dot{V} is. This implies that for sufficiently small disturbances (i.e., θ sufficiently small) and sufficiently small sampling time (i.e., Δ sufficiently small) \dot{V} of the uncertain closed-loop system will continue to be negative for all $x \in \Omega_\rho$ but in a small ball around the origin (i.e., $\Omega_{\rho_{\min}}$).

Remark 2.4. Note that the term “ultimately bounded” for the state of a nonlinear dynamic system (particularly of the closed-loop system in this chapter) means that after a sufficiently large time, t_q , the state of the closed-loop system enters a compact (closed and bounded) set including the origin (i.e., $\Omega_{\rho_{\min}}$ for the closed-loop system of Eq. 2.1 under the LEMPC of Eq. 2.5) and stays within this set for all times $t \geq t_q$ (i.e., $x(t) \in \Omega_{\rho_{\min}}$ for $t \geq t_q$).

Remark 2.5. Instead of requiring that the closed-loop system state settles to a steady-state at the end of the prediction horizon as in [24], in the proposed design, the LEMPC of Eq. 2.5 has two different operation modes. In the first operation mode, the LEMPC optimizes the economic cost function within the region $\Omega_{\hat{\rho}}$. When the proposed LEMPC is in the second operation mode, it drives the closed-loop system state to the steady-state. The LEMPC of Eq. 2.5 also possesses a stability region which can be explicitly characterized.

Remark 2.6. Note that in order to achieve optimal performance, in general, the prediction horizon of the LEMPC of Eq. 2.5 should be long enough to cover the period

in which the process operation should be optimized. However, long prediction horizon may not be practical for a real-time implementation of an MPC algorithm (especially when nonlinear systems with a large number of manipulated inputs are considered) because of the high computational burden. For certain applications, we may overcome this issue by driving part of the system states to certain economic optimal set-points and operating the rest of the system states in a time-varying manner to further maximize the economic cost function. This implies that we operate part of the system in the second operation mode and part of the system in the first operation mode simultaneously. Please see the example section for an application of this approach to a chemical process example.

2.3 Lyapunov-based economic MPC with asynchronous and delayed measurements

In this section, we consider the design of LEMPC for systems subject to asynchronous and delayed measurements. Specifically, we assume that the state of the system of Eq. 2.1, $x(t)$, is available at asynchronous time instants $\{t_{a \geq 0}\}$ which is a random increasing sequence and the interval between two consecutive time instants is not fixed. We also assume that there are delays involved in the measurements. In order to model delays in measurements, an auxiliary variable d_a is introduced to indicate the delay corresponding to the measurement received at time t_a , that is, at time t_a , the measurement $x(t_a - d_a)$ is received. In order to study the stability properties in a deterministic framework, we assume that there exists an upper bound T_m on the interval between two successive measurements (i.e., $\max_a \{t_{a+1} - t_a\} \leq T_m$) and an upper bound D on the delays (i.e., $d_a \leq D$). These assumptions are reasonable from

a process control perspective. Because the delays are time-varying, it is possible that at a time instant t_a , the controllers may receive a measurement $x(t_a - d_a)$ which does not provide new information (i.e., $t_a - d_a < t_{a-1} - d_{a-1}$) and the maximum amount of time the system might operate in open-loop following t_a is $D + T_m - d_a$. This upper bound will be used in the formulation of LEMPC for systems subject to asynchronous and delayed measurements. The reader may refer to [63] for more discussion on the modeling of asynchronous and delayed measurements.

2.3.1 LEMPC implementation strategy

At each asynchronous sampling time, when a delayed measurement is received, we propose to take advantage of the nominal system model of Eq. 2.1 and the manipulated inputs that have been applied to the system to estimate the current system state from the delayed measurement. Based on the estimate of the current system state, an MPC optimization problem is solved in order to decide the optimal future input trajectory that will be applied until the next new measurement is received. Similar to previous section, we introduce an LEMPC design which maximizes a cost function accounting for specific economic considerations. This LEMPC also has two operation modes.

From the initial time t_0 to t' , the LEMPC operates in the first operation mode. In this operation mode, the proposed LEMPC maximizes an economics-based cost function while maintaining the closed-loop system state in the stability region Ω_ρ . In order to account for the asynchronous and delayed measurement as well as the disturbance, we consider another region $\Omega_{\hat{\rho}}$ with $\hat{\rho} < \rho$. Specifically, when a delayed measurement is received at a sampling time, the current system state is estimated. If the estimated current state is in the region $\Omega_{\hat{\rho}}$, the LEMPC maximizes the cost

function within the region $\Omega_{\hat{\rho}}$; if the estimated current state is in the region $\Omega_{\rho}/\Omega_{\hat{\rho}}$, the LEMPC first drives the system state to the region $\Omega_{\hat{\rho}}$ and then maximizes the cost function within $\Omega_{\hat{\rho}}$. The relation between ρ and $\hat{\rho}$ will be characterized in Eq. 2.29 in Theorem 2.2.

After time t' , the system operates in the second operation mode. In this operation mode, the LEMPC calculates the inputs in a way that the Lyapunov function of the system continuously decreases to steer the state of the system to a neighborhood of the origin while taking into account asynchronous and delayed measurements.

The implementation strategy of the proposed LEMPC for systems subject to asynchronous and delayed measurements can be summarized as follows:

1. At a sampling time t_a , the controller receives the system state $x(t_a - d_a)$ from the sensors and estimates the current system state, $\tilde{x}(t_a)$.
2. If $t_a < t'$, go to Step 3. Else, go to Step 4.
3. If $\tilde{x}(t_a) \in \Omega_{\hat{\rho}}$, go to Step 3.1. Else, go to Step 3.2.
 - 3.1. The controller maximizes the economic cost function within $\Omega_{\hat{\rho}}$. Go to Step 5.
 - 3.2. The controller drives the system state to the region $\Omega_{\hat{\rho}}$. Go to Step 5.
4. The controller drives the system state to a small neighborhood of the origin.
5. Go to Step 1 ($a \leftarrow a + 1$).

2.3.2 LEMPC formulation

At a sampling time t_a , the MPC is evaluated to obtain the future input trajectories based on the received system state value $x(t_a - d_a)$. Specifically, the optimization

problem of the proposed LEMPC for systems subject to asynchronous and delayed measurements at t_a is as follows:

$$\max_{u_1, \dots, u_m \in S(\Delta)} \int_{t_a}^{t_a + N\Delta} L(\tilde{x}(\tau), u_1(\tau), \dots, u_m(\tau)) d\tau \quad (2.23a)$$

$$\text{s.t. } \dot{\tilde{x}}(t) = f(\tilde{x}(t), u_1(t), \dots, u_m(t), 0) \quad (2.23b)$$

$$u_i(t) = u_i^*(t), \quad i = 1, \dots, m, \quad t \in [t_a - d_a, t_a) \quad (2.23c)$$

$$u_i(t) \in U_i, \quad i = 1, \dots, m, \quad t \in [t_a, t_a + N\Delta) \quad (2.23d)$$

$$\tilde{x}(t_a - d_a) = x(t_a - d_a) \quad (2.23e)$$

$$\dot{\hat{x}}(t) = f(\hat{x}(t), h_1(\hat{x}(t_a + l\Delta)), \dots, h_m(\hat{x}(t_a + l\Delta)), 0),$$

$$\forall t \in [t_a + l\Delta, t_a + (l+1)\Delta), \quad l = 0, \dots, N-1 \quad (2.23f)$$

$$\hat{x}(t_a) = \tilde{x}(t_a) \quad (2.23g)$$

$$V(\tilde{x}(t)) \leq \hat{\rho}, \quad \forall t \in [t_a, t_a + N\Delta), \quad \text{if } t_a \leq t' \text{ and } V(\tilde{x}(t_k)) \leq \hat{\rho} \quad (2.23h)$$

$$V(\tilde{x}(t)) \leq V(\hat{x}(t)), \quad \forall t \in [t_a, t_a + N_{D_a}\Delta), \quad \text{if } t_a > t' \text{ or } \hat{\rho} < V(\tilde{x}(t_a)) \leq \rho \quad (2.23i)$$

where \tilde{x} is the predicted trajectory of the system with control inputs calculated by this LEMPC, $u_i^*(t)$ with $i = 1, \dots, m$ denotes the actual inputs that have been applied to the system, $x(t_a - d_a)$ is the received delayed measurement, \hat{x} is the predicted trajectory of the system with the control inputs determined by $h(x)$ implemented in a sample-and-hold fashion, and N_{D_a} is the smallest integer that satisfies $T_m + D - d_a \leq N_{D_a}\Delta$. The optimal solution to this optimization problem is denoted by $u_i^{a,*}(t|t_a)$, $i = 1, \dots, m$, which is defined for $t \in [t_a, t_a + N\Delta)$.

There are two types of calculations in the optimization problem of Eq. 2.23. The first type of calculation is to estimate the current state $\check{x}(t_a)$ based on the delayed measurement $x(t_a - d_a)$ and input values have been applied to the system from $t_a - d_a$ to t_a (constraints of Eqs. 2.23b, 2.23c and 2.23e). The second type of calculation is to evaluate the optimal input trajectory of u_i ($i = 1, \dots, m$) based on $\check{x}(t_a)$ while satisfying the input constraint of Eq. 2.23d and the stability constraints of Eqs. 2.23h and 2.23i. Note that the length of the constraint N_{D_a} depends on the current delay d_a , and thus, it may have different values at different time instants and has to be updated before solving the optimization problem of Eq. 2.23.

The manipulated inputs of the LEMPC of Eq. 2.23 for systems subject to asynchronous and delayed measurements are defined as follows:

$$u_j(t) = u_j^{a,*}(t|t_a), \quad \forall t \in [t_a, t_{a+i}] \quad (2.24)$$

for all t_a such that $t_a - d_a > \max_{l < a} t_l - d_l$ and for a given t_a , the variable i denotes the smallest integer that satisfies $t_{a+i} - d_{a+i} > t_a - d_a$ and $j = 1, \dots, m$.

2.3.3 Stability analysis

In this subsection, we present the stability properties of the proposed LEMPC of Eq. 2.23 in the presence of asynchronous and delayed measurements. In order to proceed, we need the following proposition.

Proposition 2.3 (c.f. [60, 79]). *Consider the nominal sampled trajectory $\hat{x}(t)$ of the system of Eq. 2.1 in closed-loop for a controller $h(x)$, which satisfies the condition of*

Eq. 2.2, obtained by solving recursively

$$\dot{\hat{x}}(t) = f(\hat{x}(t), h_1(\hat{x}(t_k)), \dots, h_m(\hat{x}(t_k)), 0), \quad t \in [t_k, t_{k+1}) \quad (2.25)$$

where $t_k = t_0 + k\Delta$, $k = 0, 1, \dots$. Let $\Delta, \epsilon_s > 0$ and $\rho > \rho_s > 0$ satisfy

$$-\alpha_3(\alpha_2^{-1}(\rho_s)) + L'_x M \Delta \leq -\epsilon_s / \Delta. \quad (2.26)$$

Then, if $\hat{x}(t_0) \in \Omega_\rho$ and $\rho_{\min} < \rho$ where ρ_{\min} is defined in Eq. 2.14, the following inequality holds

$$V(\hat{x}(t)) \leq V(\hat{x}(t_k)), \quad \forall t \in [t_k, t_{k+1}), \quad (2.27)$$

$$V(\hat{x}(t_k)) \leq \max\{V(\hat{x}(t_0)) - k\epsilon_s, \rho_{\min}\}. \quad (2.28)$$

Proposition 2.3 ensures that if the nominal system controlled by the Lyapunov-based controller $h(x)$ implemented in a sample-and-hold fashion and with open-loop state estimation starts in Ω_ρ , then it is ultimately bounded in $\Omega_{\rho_{\min}}$. Theorem 2.2 below provides sufficient conditions under which the LEMPC of Eq. 2.23 guarantees that the closed-loop system state is always bounded in Ω_ρ and is ultimately bounded in a small region containing the origin.

Theorem 2.2. *Consider the system of Eq. 2.1 in closed-loop under the LEMPC design of Eq. 2.23 based on a controller $h(x)$ that satisfies the condition of Eq. 2.2. Let $\epsilon_s > 0$, $\Delta > 0$, $\rho > \hat{\rho} > 0$ and $\rho > \rho_s > 0$ satisfy the condition of Eq. 2.26 and satisfy*

$$\hat{\rho} \leq \rho - f_V(f_W(N\Delta)) \quad (2.29)$$

and

$$-N_R\epsilon_s + f_V(f_W(N_D\Delta)) + f_V(f_W(D)) < 0 \quad (2.30)$$

where N_D is the smallest integer satisfying $N_D\Delta \geq T_m + D$ and N_R is the smallest integer satisfying $N_R\Delta \geq T_m$. If $N \geq N_D$, $\hat{\rho} \geq \rho_s$, $x(t_0) \in \Omega_\rho$, $d_0 = 0$, then the closed-loop state $x(t)$ of the system of Eq. 2.1 is always bounded in Ω_ρ and is ultimately bounded in $\Omega_{\rho_a} \subset \Omega_\rho$ where

$$\rho_a = \rho_{\min} + f_V(f_W(N_D\Delta)) + f_V(f_W(D)). \quad (2.31)$$

Proof 2.2. When $x(t)$ is maintained in the stability region Ω_ρ , the feasibility of the optimization problem of Eq. 2.23 can be proved following the same arguments as in Part 1 of the proof of Theorem 2.1. In the remainder of this proof, we focus on proving that $x(t)$ is always bounded in Ω_ρ and is ultimately bounded in Ω_{ρ_a} . The proof consists of two parts. In Part 1, we prove that $x(t)$ is always maintained in Ω_ρ in the first operation mode; and in Part 2, we prove that $x(t)$ is ultimately bounded in Ω_{ρ_a} in the second operation mode.

In this proof, we assume that $x(t_a - d_a)$ is received at t_a and the next asynchronous measurement containing new information is received at t_{a+i} with $t_{a+i} = t_a + T_m$ and $T_m = N\Delta$. This corresponds to the worst case scenario from feedback control point of view. When $x(t)$ is proved to be bounded in Ω_ρ and ultimately bounded in Ω_{ρ_a} for this worst case, the results are also guaranteed for the general case (i.e., $t_{a+i} \leq t_a + N\Delta$).

Part 1: We assume that the LEMPC of Eq. 2.23 operates in the first operation mode. We prove that if $\check{x}(t_a) \in \Omega_{\hat{\rho}}$, then $x(t_{a+i}) \in \Omega_\rho$; and if $\check{x}(t_a) \in \Omega_\rho/\Omega_{\hat{\rho}}$, then $V(x(t_{a+i})) < V(x(t_a))$ and in finite steps, the state converges to $\Omega_{\hat{\rho}}$.

When $\check{x}(t_a) \in \Omega_{\hat{\rho}}$, from the constraint of Eq. 2.23h, we obtain that $\check{x}(t_{a+i}) \in$

$\Omega_{\hat{\rho}}$. When $x(t) \in \Omega_{\rho}$ for all times (this point will be proved below), we can apply Propositions 2.1 and 2.2 to obtain the following inequality:

$$V(x(t_{a+i})) \leq V(\tilde{x}(t_{a+i})) + f_V(f_W(N\Delta)). \quad (2.32)$$

Since $V(\tilde{x}(t_{a+i})) \leq \hat{\rho}$, if the condition of Eq. 2.29 is satisfied, we can conclude that

$$x(t_{a+i}) \in \Omega_{\rho}. \quad (2.33)$$

When $\tilde{x}(t_a) \in \Omega_{\rho}/\Omega_{\hat{\rho}}$, from the condition of Eq. 2.23i, we can obtain that

$$V(\tilde{x}(t)) \leq V(\hat{x}(t)), \forall t \in [t_a, t_a + N_{Da}\Delta]. \quad (2.34)$$

By Proposition 2.3 and taking into account that $\hat{\rho} > \rho_s$, the following inequality can be obtained

$$V(\hat{x}(t_{a+i})) \leq \max\{V(\hat{x}(t_a)) - N_{Da}\epsilon_s, \rho_{\min}\}. \quad (2.35)$$

By Propositions 2.1 and 2.2, we can obtain the following inequalities

$$V(\tilde{x}(t_a)) \leq V(x(t_a)) + f_V(f_W(d_a)). \quad (2.36)$$

From the inequalities of Eqs. 2.32, 2.35 and 2.36, we can write that:

$$V(x(t_{a+i})) \leq \max\{V(x(t_a)) - N_{Da}\epsilon_s, \rho_{\min}\} + f_V(f_W(d_a)) + f_V(f_W(N_D\Delta)). \quad (2.37)$$

Note that in the derivation of the inequality of Eq. 2.37, we have taken into account that $N_D\Delta \geq T_m + D - d_a$ for all d_a .

In order to prove that the Lyapunov function is decreasing between t_a and t_{a+i} ,

the following inequality must hold

$$N_{D_a}\epsilon_s > f_V(f_W(N_D\Delta)) + f_V(f_W(d_a)) \quad (2.38)$$

for all possible $d_a \leq D$. Taking into account that $f_W(\cdot)$ and $f_V(\cdot)$ are strictly increasing functions of their arguments, that N_{D_a} is a decreasing function of the delay d_a and that if $d_a = D$ then $N_{D_a} = N_R$, if the condition of Eq. 2.30 is satisfied, then the condition of Eq. 2.38 holds for all possible d_a and there exist $\epsilon_w > 0$ such that the following inequality holds

$$V(x(t_{a+i})) \leq \max\{V(x(t_a)) - \epsilon_w, \rho_a\} \quad (2.39)$$

which implies that if $x(t_a) \in \Omega_\rho/\Omega_{\hat{\rho}}$, then $V(x(t_{a+i})) < V(x(t_a))$. This also implies that the state converges to $\Omega_{\hat{\rho}}$ in a finite number of sampling times without leaving the stability region.

Part 2: We assume that the LEMPC of Eq. 2.23 operates in the second operation mode. We prove that $x(t)$ is ultimately bounded in Ω_{ρ_a} . Following similar steps as in Part 1, we can again derive the condition of Eq. 2.39. Using this condition recursively, it is proved that, if $x(t_0) \in \Omega_\rho$, then the closed-loop trajectory of the system of Eq. 2.1 under the LEMPC of Eq. 2.23 stay in Ω_ρ and satisfy that

$$\limsup_{t \rightarrow \infty} V(x(t)) \leq \rho_a. \quad (2.40)$$

This proves the results stated in Theorem 2.2.

2.4 Application to a chemical process example

Consider a well-mixed, non-isothermal continuous stirred tank reactor (CSTR) where an irreversible second-order exothermic reaction $A \rightarrow B$ takes place [86]. A is the reactant and B is the product. The feed to the reactor consists of pure A at flow rate F , temperature T_0 and molar concentration C_{A0} . Due to the non-isothermal nature of the reactor, a jacket is used to remove/provide heat to the reactor. The dynamic equations describing the behavior of the system, obtained through material and energy balances under standard modeling assumptions, are given below:

$$\frac{dC_A}{dt} = \frac{F}{V}(C_{A0} - C_A) - k_0 e^{\frac{-E}{RT}} C_A^2 \quad (2.41a)$$

$$\frac{dT}{dt} = \frac{F}{V}(T_0 - T) + \frac{-\Delta H}{\sigma C_p} k_0 e^{\frac{-E}{RT}} C_A^2 + \frac{Q}{\sigma C_p V} \quad (2.41b)$$

where C_A denotes the concentration of the reactant A , T denotes the temperature of the reactor, Q denotes the rate of heat input/removal, V represents the volume of the reactor, ΔH , k_0 , and E denote the enthalpy, pre-exponential constant and activation energy of the reaction, respectively and C_p and σ denote the heat capacity and the density of the fluid in the reactor, respectively. The values of the process parameters used in the simulations are shown in Table 2.1. The process model of Eq. 2.41 is numerically simulated using an explicit Euler integration method with integration step $h_c = 10^{-4}$ hr.

The process model has one unstable steady state and one stable steady state in the operating range of interest. The control objective is to regulate the process in a region around the unstable steady-state (C_{As} , T_s) to maximize the production rate of B . There are two manipulated inputs. One of the inputs is the concentration of A in the inlet to the reactor, C_{A0} , and the other manipulated input is the external heat

Table 2.1: Parameter values

$T_0 = 300$	K	$F = 5$	$\frac{m^3}{hr}$
$V = 1.0$	m^3	$E = 5 \times 10^4$	$\frac{kJ}{kmol}$
$k_0 = 8.46 \times 10^6$	$\frac{1}{hr}$	$\Delta H = -1.15 \times 10^4$	$\frac{kJ}{kmol}$
$C_p = 0.231$	$\frac{kJ}{kgK}$	$R = 8.314$	$\frac{kJ}{kmolK}$
$\sigma = 1000$	$\frac{kg}{m^3}$	$C_{As} = 2$	$\frac{kmol}{m^3}$
$T_s = 400$	K	$C_{A0s} = 4$	$\frac{kmol}{m^3}$
$Q_s = 0$	$\frac{KJ}{hr}$		

input/removal, Q . The steady-state input values associated with the steady-state are denoted by C_{A0s} and Q_s , respectively.

The process model of Eq. 2.41 belongs to the following class of nonlinear systems:

$$\dot{x}(t) = f(x(t)) + g_1(x(t))u_1(t) + g_2(x(t))u_2(t) + w(t)$$

where $x^T = [C_A - C_{As} \ T - T_s]$ is the state, $u_1 = C_{A0} - C_{A0s}$ and $u_2 = Q - Q_s$ are the inputs, $f = [f_1 \ f_2]^T$ and $g_i = [g_{i1} \ g_{i2}]^T$ ($i = 1, 2$) are vector functions. The inputs are subject to constraints as follows: $|u_1| \leq 3.5 \text{ kmol}/m^3$ and $|u_2| \leq 5 \times 10^5 \text{ KJ}/hr$. $w = [w_1 \ w_2]^T$ is the bounded disturbance vector (Gaussian white noise with variances $\sigma_1 = 1 \text{ kmol}/m^3$ and $\sigma_2 = 40 \text{ K}$) with $|w_1| \leq 1 \text{ kmol}/m^3$ and $|w_2| \leq 40 \text{ K}$.

The economic measure that we consider in this example is as follows [86]:

$$L(x, u_1, u_2) = \frac{1}{t_f} \int_0^{t_f} k_0 e^{-\frac{E}{RT(\tau)}} C_A^2(\tau) d\tau \quad (2.42)$$

where $t_f = 1 \text{ hr}$ is the final time of the simulation. This economic objective function is to maximize the average production rate over process operation for $t_f = 1 \text{ hr}$. We also consider that there is limitation on the amount of material which can be used

over the period t_f . Specifically, the control input trajectory of u_1 should satisfy the following constraint:

$$\frac{1}{t_f} \int_0^{t_f} u_1(\tau) d\tau = 1 \text{ kmol}/m^3. \quad (2.43)$$

This constraint means that the average amount of u_1 during one period is fixed. For the sake of simplicity and without loss of generality, we will refer to Eq. 2.43 as the integral constraint. It has been clarified in [86] (see also [54, 90, 99, 98]) that by periodic operation through switching between upper and lower bound the average production rate can be improved owing to the second-order dependence of the reaction rate on reactant concentration. In other words, since the amount of reactant material over one period of operation is fixed and the reaction is of second-order, to get the maximum reaction rate over one period, all of the material should be fed at the beginning of the process operation period. Since this policy is not practically implementable given the presence of constraints on C_{A_0} value, periodic operation is the best practical choice to maximize the average production rate over one period subject to input constraints; please see simulations below.

In the first set of simulations, we assume that the state feedback information is available at synchronous time instants while in the second set of simulations we assume that the controller receives asynchronous and delayed measurements.

2.4.1 Synchronous measurement sampling

We will design an LEMPC following Eq. 2.5 to manipulate the two control inputs. We assume that the full system state x is measured and sent to the LEMPC at synchronous time instants $t_k = k\Delta$, $k = 0, 1, \dots$, with $\Delta = 0.01 \text{ hr} = 36 \text{ sec}$. The LEMPC horizon is $N = 10$. For the computation of the stability region, we consider a quadratic Lyapunov function $V(x) = x^T P x$ with $P = \text{diag}([796.17 \ 0.5])$. To estimate

the stability region Ω_ρ , we evaluate \dot{V} by assuming that u_1 is equally distributed over t_f (i.e., $u_1(\tau) = 1$, $0 \leq \tau \leq t_f$) and utilize feedback linearization for u_2 subject to input constraint u_2^{max} and bounded disturbance ($|w_1| \leq 1 \text{ kmol/m}^3$ and $|w_2| \leq 40 \text{ K}$).

Since the LEMPC is evaluated at discrete-time instants during the closed-loop simulation, the integral constraint is enforced as follows:

$$\sum_{i=0}^{M-1} u_1(t_i) = \frac{t_f}{\Delta} \quad (2.44)$$

where $M = 100$.

To ensure that the integral constraint is satisfied through the period t_f , at every sampling time in which the LEMPC obtains the optimal control input trajectory, it utilizes the previously computed inputs u_1 to constrain the first step value of the control input trajectory u_1 at the current sampling time. Based on the cost function formulation, for maximization purposes, it is expected that C_A and T should be increased which results in the fact that at the beginning of the closed-loop simulation u_1 should rise to its maximum value and after a while it will go down to its lowest value to satisfy the integral constraint. We assume that the decrease of the Lyapunov function starts from the beginning of the simulation (i.e., $t' = 0$) for part of the system state (i.e., temperature). To maximize the production rate, we pick a temperature set-point near the boundary of the stability region ($T = 430 \text{ K}$), considering the constraints on the control input Q . Due to the fact that the first differential equation (C_A) in Eq 2.41 is input-to-state-stable (ISS) with respect to T , and the contractive constraint of Eq. 2.45g (see Eq. 2.45) ensures that the temperature converges to the set-point, the stability of the closed-loop system is guaranteed in the operating range of interest. To this end, we define $V_T(t_k) = (T(t_k) - 430)^2$. The LEMPC formulation

for the chemical process example in question has the following form:

$$\max_{u_1, u_2 \in \mathcal{S}(\Delta)} \frac{1}{N\Delta} \int_{t_k}^{t_{k+N}} [k_0 e^{-\frac{E}{RT(\tau)}} C_A^2(\tau)] d\tau \quad (2.45a)$$

$$\dot{\tilde{x}}(t) = f(\tilde{x}(t)) + \sum_{i=1}^2 g_i(\tilde{x}(t)) u_i(t) \quad (2.45b)$$

$$u_1(t) \in g_\zeta, \forall t \in [t_k, t_{k+1}) \quad (2.45c)$$

$$\tilde{x}(t_k) = x(t_k) \quad (2.45d)$$

$$\tilde{x}(t) \in \Omega_{\tilde{\rho}} \quad (2.45e)$$

$$u_i(t) \in U_i \quad (2.45f)$$

$$\frac{dV_T(t_k)}{dT} (f_2(x(t_k)) + g_{22}(x(t_k))u_2(t_k)) \leq -\gamma V_T(t_k) \quad (2.45g)$$

where $x(t_k)$ is the measurement of the process state at sampling time t_k , $\gamma = 9.53$ and the constraint of Eq. 2.45c implies that the first step value of u_1 should be chosen to satisfy the integral constraint where the explicit expression of g_ζ can be computed based on Eq. 2.44 and the magnitude constraint on u_1 . Also, the constraint of Eq. 2.45g enforces the Lyapunov function, based on the temperature, to decrease from the beginning of the simulation. The simulations were carried out using Java programming language in a Pentium 3.20 GHz computer. The optimization problems were solved using the open source interior point optimizer Ipopt [97].

The purpose of the following set of simulations is to demonstrate that: I) the proposed LEMPC design stabilizes the closed-loop system for different initial conditions; II) the proposed LEMPC design maximizes the economic measure $L(x, u_1, u_2)$; III) the proposed LEMPC design achieves practical closed-loop stability under different

initial conditions; and IV) the proposed LEMPC design affords a higher cost function value compared to the steady-state operation. We consider two different scenarios in terms of the existence of process disturbance.

Figures 2.1 and 2.2 depict the state and manipulated input profiles, respectively, without process disturbances starting from the initial condition $(2\frac{kmol}{m^3}, 440K)$. Figures 2.3 and 2.4 depict the state and manipulated input profiles, respectively, without process disturbances starting from the initial condition $(2\frac{kmol}{m^3}, 400K)$. These simulations demonstrate that in the absence of disturbances the LEMPC of Eq. 2.45 drives the closed-loop system temperature at the desired steady-state, 430 K. Figures 2.5-2.8 show the corresponding state and manipulated input profiles starting from the two initial conditions under bounded process disturbances (Gaussian white noise with variances $\sigma_1 = 1 kmol/m^3$ and $\sigma_2 = 40 K$) with $|w_1| \leq 1 kmol/m^3$ and $|w_2| \leq 40 K$. Figure 2.9 shows a possible realization of the process disturbance. As expected, in all scenarios, u_1 goes up to its allowable maximum value to increase reactant concentration as much as possible early on (given the second-order reaction rate) and after a while it drops to its minimum value to satisfy the integral constraint $(\frac{1}{t_f} \int_0^{t_f} u_1(\tau) d\tau = 1)$. On the other hand, the temperature rises as fast as possible when the temperature initial condition is below 430 K to maximize the reaction rate, and it decreases as slow as possible when the initial temperature is above 430 K to maintain the maximum possible reaction rate while satisfying the stability constraint; in both cases, the temperature finally settles at $T = 430 K$ and the LEMPC design of Eq. 2.45 achieves practical stability. Figure 2.10 shows Ω_ρ with $\rho = 2500$ and three closed-loop system trajectories which start at $(2\frac{kmol}{m^3}, 400K)$ (inside of Ω_ρ ; solid line), $(2\frac{kmol}{m^3}, 440K)$ (inside of Ω_ρ ; dotted line) and $(1\frac{kmol}{m^3}, 500K)$ (outside of Ω_ρ ; dashed line), respectively. This set of simulations demonstrates that in this case it is possible to achieve closed-loop stability even for initial conditions outside Ω_ρ , demonstrating

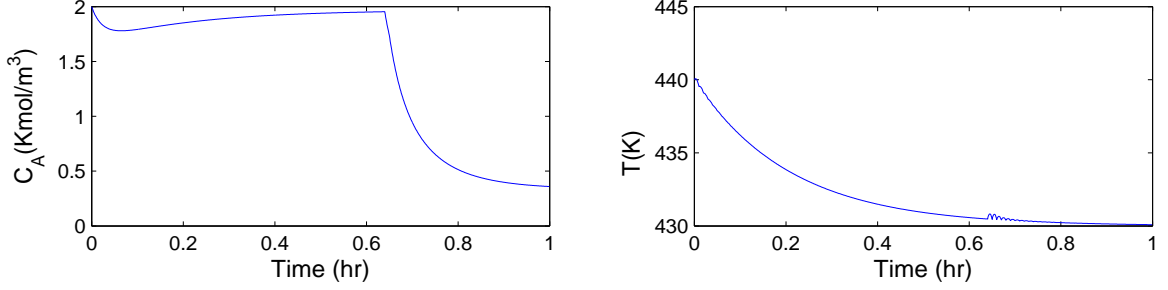


Figure 2.1: State trajectories of the process under the LEMPC design of Eq. 2.45 for initial condition $(C_A(0), T(0)) = (2 \frac{\text{kmol}}{\text{m}^3}, 440\text{K})$ without disturbances.

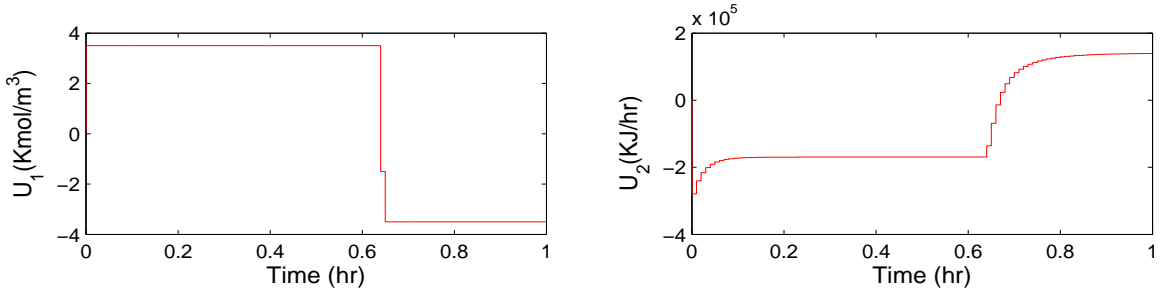


Figure 2.2: Manipulated input trajectories under the LEMPC design of Eq. 2.45 for initial condition $(C_A(0), T(0)) = (2 \frac{\text{kmol}}{\text{m}^3}, 440\text{K})$ without disturbances.

that in the present example the computed Ω_ρ estimate is a rather conservative one.

Also, we have carried out a set of simulations to confirm that the application of the LEMPC design with the integral constraint on u_1 improves the economic objective function compared to the case that the system operates at a steady-state satisfying the integral constraint. It should be mentioned that this comparison is performed under the case that there is no process disturbance. This steady-state is computed by assuming that the reactant material amount is equally distributed in the interval $[0, t_f]$. To carry out this comparison, we have computed the total cost of each scenario based on the index of the following form:

$$J = \frac{1}{t_M} \sum_{i=0}^M [k_0 e^{-\frac{E}{RT(t_i)}} C_A^2(t_i)]$$

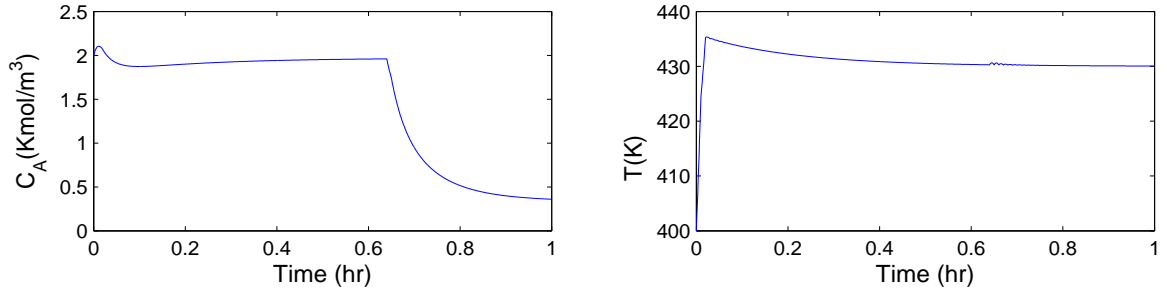


Figure 2.3: State trajectories of the process under the LEMPC design of Eq. 2.45 for initial condition $(C_A(0), T(0)) = (2 \frac{kmol}{m^3}, 400K)$ without disturbances.

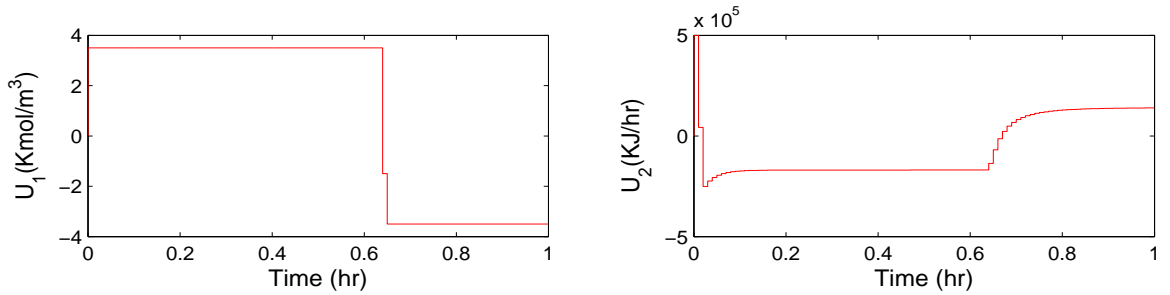


Figure 2.4: Manipulated input trajectories under the LEMPC design of Eq. 2.45 for initial condition $(C_A(0), T(0)) = (2 \frac{kmol}{m^3}, 400K)$ without disturbances.

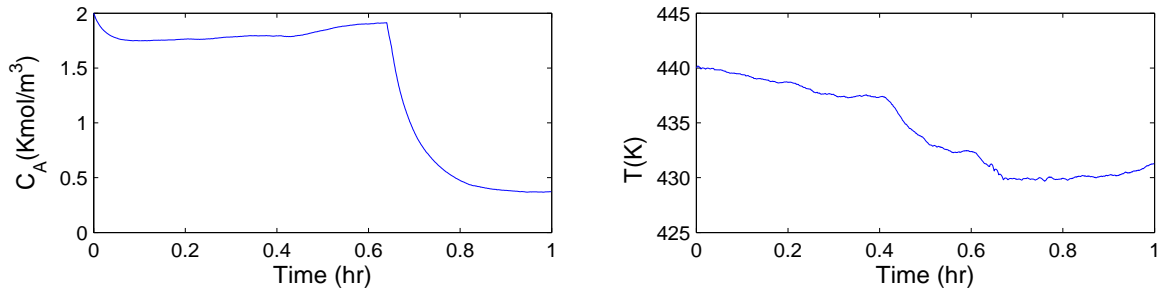


Figure 2.5: State trajectories of the process under the LEMPC design of Eq. 2.45 for initial condition $(C_A(0), T(0)) = (2 \frac{kmol}{m^3}, 440K)$ subject to disturbances.

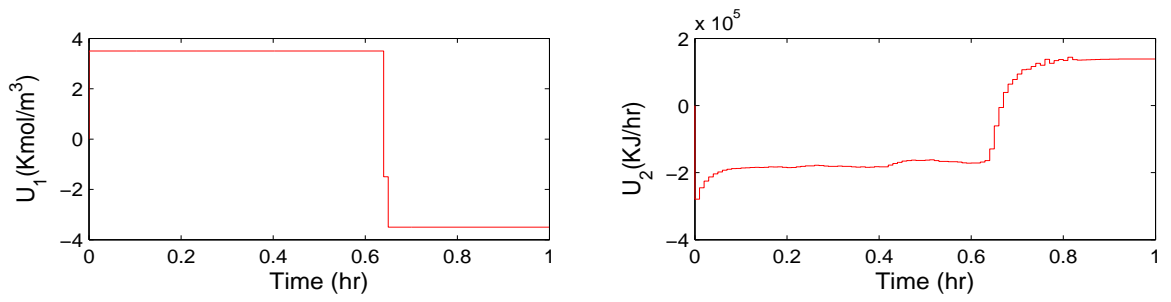


Figure 2.6: Manipulated input trajectories under the LEMPC design of Eq. 2.45 for initial condition $(C_A(0), T(0)) = (2 \frac{kmol}{m^3}, 440K)$ subject to disturbances.

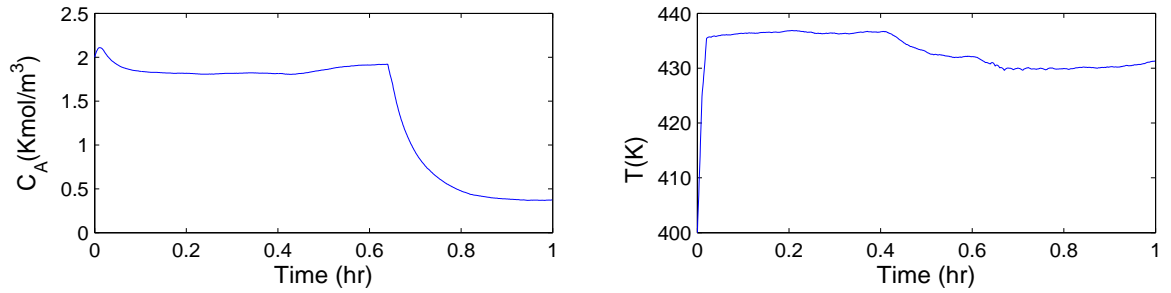


Figure 2.7: State trajectories of the process under the LEMPC design of Eq. 2.45 for initial condition $(C_A(0), T(0)) = (2 \frac{kmol}{m^3}, 400K)$ subject to disturbances.

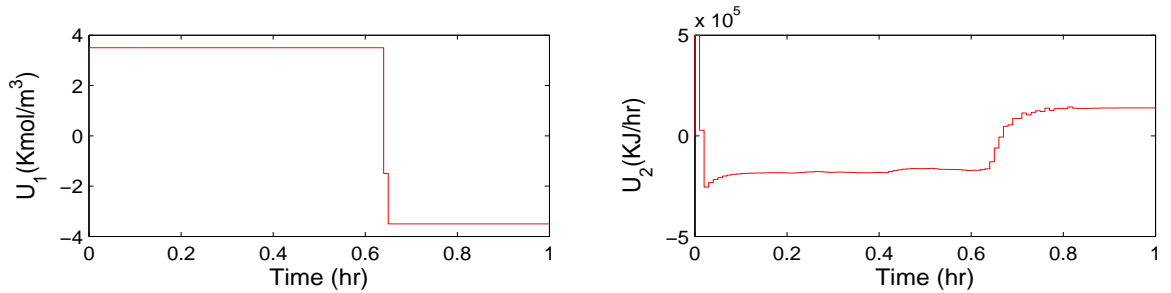


Figure 2.8: Manipulated input trajectories under the LEMPC design of Eq. 2.45 for initial condition $(C_A(0), T(0)) = (2 \frac{kmol}{m^3}, 400K)$ subject to disturbances.

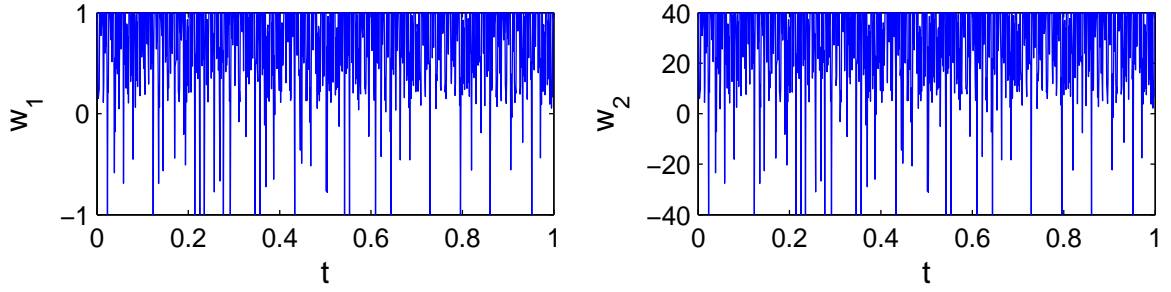


Figure 2.9: Disturbance realization for $\sigma_1 = 1 \text{ kmol/m}^3$ and $\sigma_2 = 40 \text{ K}$ with $|w_1| \leq 1 \text{ kmol/m}^3$ and $|w_2| \leq 40 \text{ K}$

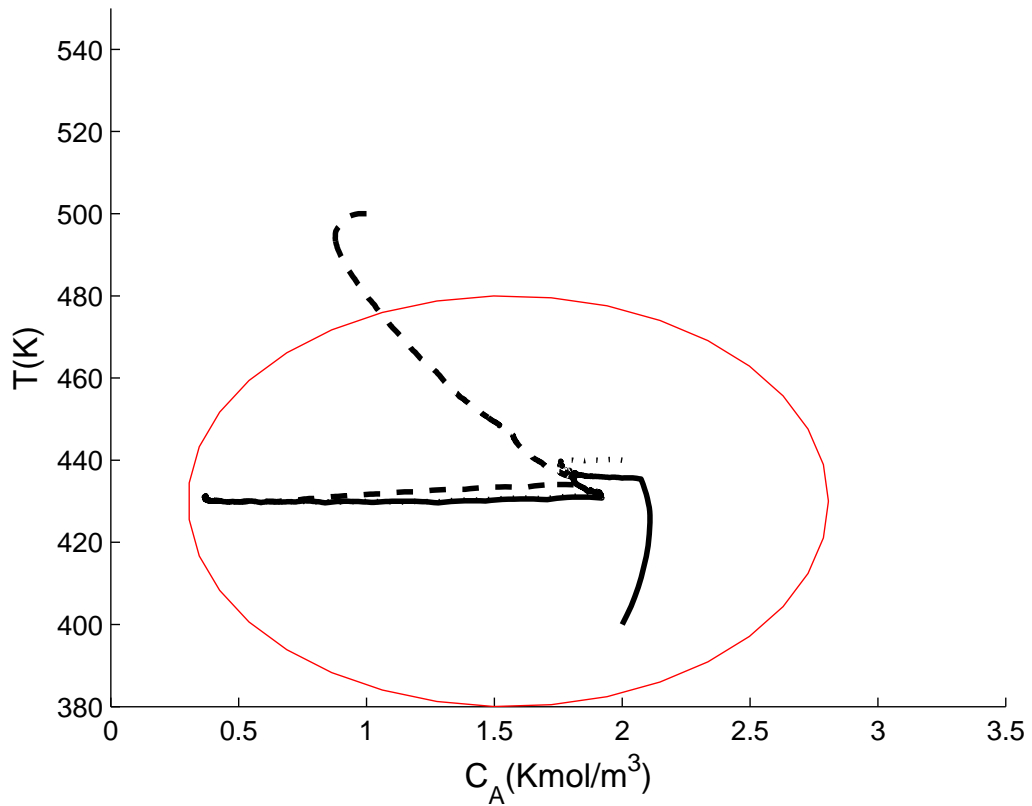


Figure 2.10: Estimation of Ω_ρ and three closed-loop system trajectories for synchronous measurement case with disturbances.

where $t_0 = 0 \text{ hr}$, $t_M = 1 \text{ hr}$ and $M = 100$. To be consistent in comparison we set u_1 to a constant value over the simulation such that it satisfies the integral constraint while letting u_2 be computed by the controller. By comparing the cost function values, we find that in the proposed LEMPC design via time-varying operation (starting from $(C_A, T) = (2 \frac{\text{kmol}}{\text{m}^3}, 400\text{K})$), the cost function achieves a higher value (19299.47) compared to the case of steady-state operation (17722.07) (i.e., equal in time distribution of the reactant). Also, by starting from $(C_A, T) = (2 \frac{\text{kmol}}{\text{m}^3}, 440\text{K})$, the cost function achieves a higher value (19459.67) compared to the case of steady-state operation (17852.85).

2.4.2 Asynchronous measurements with delay

For this set of simulations, it is assumed that the state measurements of the process are available asynchronously at time instants $\{t_{a \geq 0}\}$ with an upper bound $T_m = 6\Delta$ on the maximum interval between two successive asynchronous state measurements, where Δ is the controller and sensor sampling time and is chosen to be $\Delta = 0.01 \text{ hr} = 36 \text{ sec}$. To model the time sequence $\{t_{a \geq 0}\}$, we use an upper bounded Poisson process. The Poisson process is defined by the number of events per unit time W . The interval between two successive concentration sampling times (events of the Poisson process) is given by $\Delta_a = \min\{-\ln\chi/W, T_m\}$, where χ is a random variable with uniform probability distribution between 0 and 1. This generation ensures that $\max_a \{t_{a+1} - t_a\} \leq T_m$. In this example, W is chosen to be $W = 25$. A gaussian random process is used to generate the associated delay sequence $\{d_{a \geq 0}\}$ with $d_a \leq D$ while $D = 3\Delta$. Figure 2.11 shows the asynchronous time instants when measurements are available and the corresponding delay size associated with each measurement.

The LEMPC formulation for the chemical process example in question subject to

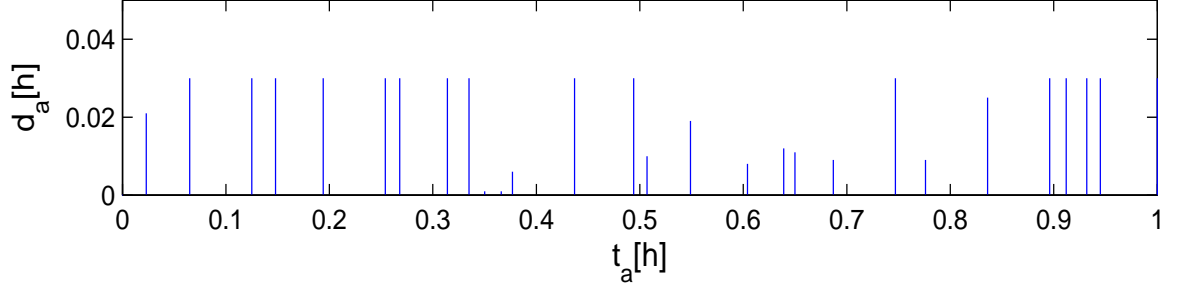


Figure 2.11: Asynchronous measurement sampling times and their associated delay.

asynchronous and delayed state measurements has the following form:

$$\max_{u_1, u_2 \in S(\Delta)} \frac{1}{N\Delta} \int_{t_a}^{t_a + N\Delta} [k_0 e^{-\frac{E}{RT(\tau)}} C_A^2(\tau)] d\tau \quad (2.46a)$$

$$\dot{\tilde{x}}(t) = f(\tilde{x}(t)) + \sum_{i=1}^2 g_i(\tilde{x}(t)) u_i^*(t), \quad \forall t \in [t_a - d_a, t_a) \quad (2.46b)$$

$$\dot{\tilde{x}}(t) = f(\tilde{x}(t)) + \sum_{i=1}^2 g_i(\tilde{x}(t)) u_i(t), \quad \forall t \in [t_a, t_a + N\Delta) \quad (2.46c)$$

$$u_1(t) \in g_\zeta, \quad \forall t \in [t_a, t_a + N\Delta) \quad (2.46d)$$

$$\tilde{x}(t_a - d_a) = x(t_a - d_a) \quad (2.46e)$$

$$\tilde{x}(t) \in \Omega_{\hat{\rho}} \quad (2.46f)$$

$$u_i(t) \in U_i \quad (2.46g)$$

$$V_T(t_a + (l+1)\Delta) \leq \beta V_T(t_a + l\Delta) \quad l = 0, \dots, N_{Da} \quad (2.46h)$$

where $x(t_a)$ is the measurement of the process state at sampling time t_a and $\beta = 1/1.1 = 0.909$. The constraint of Eq. 2.46h forces the Lyapunov function, based on the temperature, to decrease for N_{Da} sampling times.

Figures 2.12 and 2.13 show the state and manipulated input profiles, respectively,

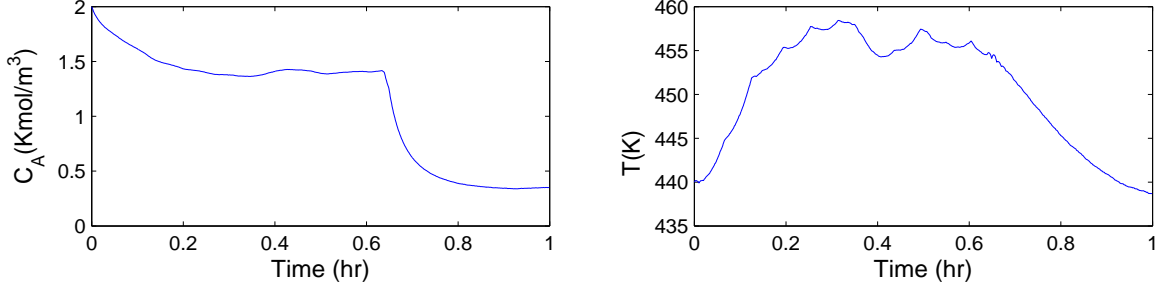


Figure 2.12: State trajectories of the process under the LEMPC design of Eq. 2.46 for initial condition $(C_A(0), T(0)) = (2\frac{kmol}{m^3}, 440K)$ subject to asynchronous and delayed measurements and disturbances.

starting from the initial condition $(2\frac{kmol}{m^3}, 440K)$ under bounded process disturbances (the same to the ones used in the case of synchronous measurement sampling). Figures 2.14 and 2.15 show the corresponding state and manipulated input profiles, respectively, starting from the initial condition $(2\frac{kmol}{m^3}, 400K)$, respectively. From these figures, we can see similar results as in the case of synchronous measurement sampling, such as, u_1 goes up to its allowable maximum value to increase the reactant concentration as much as possible early on and the temperature rises as fast as possible when the temperature initial condition is below $430 K$ to maximize the reaction rate and it decreases as slow as possible when the initial temperature is above $430 K$ to maintain the maximum possible reaction rate. From these figures, we can also see that the practical stability of the closed-loop system is ensured in the presence of asynchronous and delayed measurements. This is because in the design of the LEMPC of Eq. 2.46, asynchronous and delayed measurements are taken explicitly into account. Similar to the synchronous measurement case, Figure 2.16 shows Ω_ρ with $\rho = 2500$ and three closed-loop system trajectories which start at $(2\frac{kmol}{m^3}, 400K)$ (inside of Ω_ρ ; solid line), $(2\frac{kmol}{m^3}, 440K)$ (inside of Ω_ρ ; dotted line) and $(1\frac{kmol}{m^3}, 500K)$ (outside of Ω_ρ ; dashed line), respectively.

Finally, we have also carried out two sets of simulations in which: a) the integral

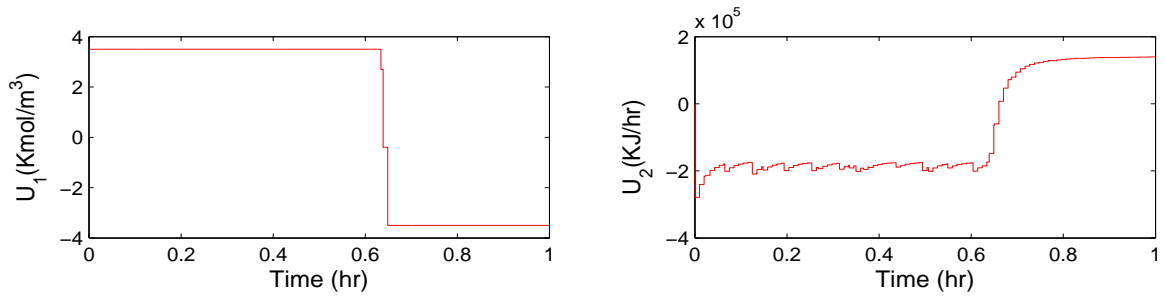


Figure 2.13: Manipulated input trajectories under the LEMPC design of Eq. 2.46 for initial condition $(C_A(0), T(0)) = (2 \frac{kmol}{m^3}, 440K)$ subject to asynchronous and delayed measurements and disturbances.

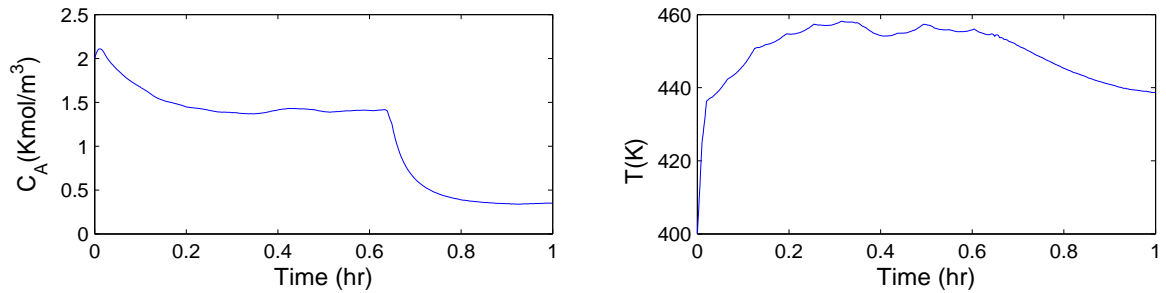


Figure 2.14: State trajectories of the process under the LEMPC design of Eq. 2.46 for initial condition $(C_A(0), T(0)) = (2 \frac{kmol}{m^3}, 400K)$ subject to asynchronous and delayed measurements and disturbances.

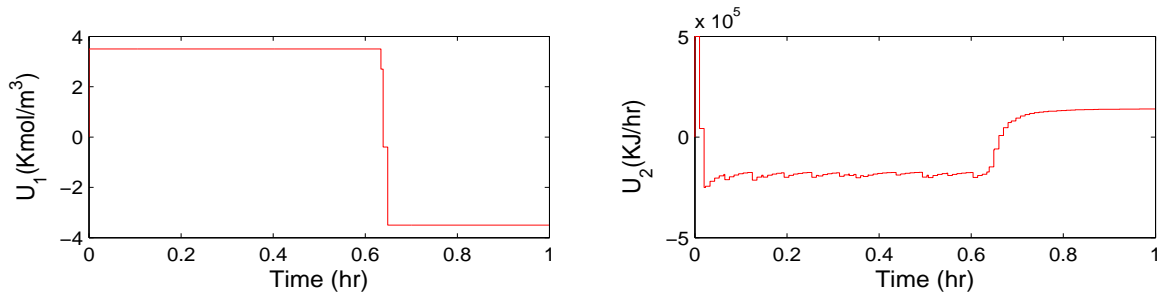


Figure 2.15: Manipulated input trajectories under the LEMPC design of Eq. 2.46 for initial condition $(C_A(0), T(0)) = (2 \frac{kmol}{m^3}, 400K)$ subject to asynchronous and delayed measurements and disturbances.

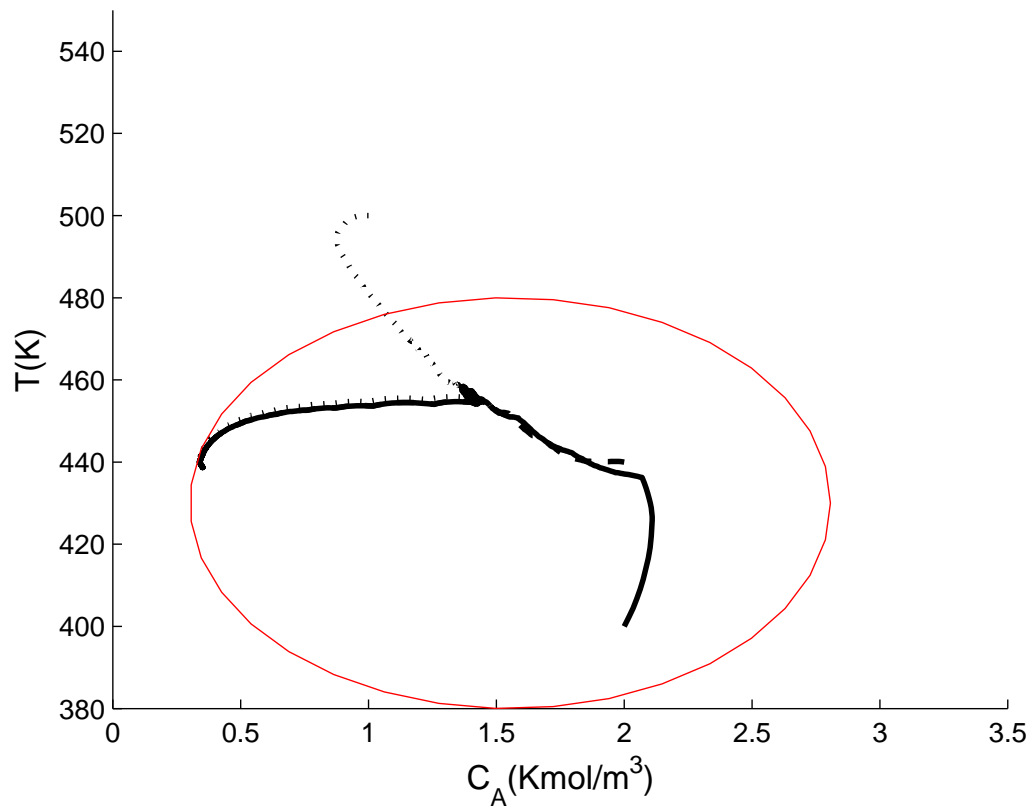


Figure 2.16: Estimation of Ω_ρ and three closed-loop system trajectories for asynchronous measurement case with disturbances.

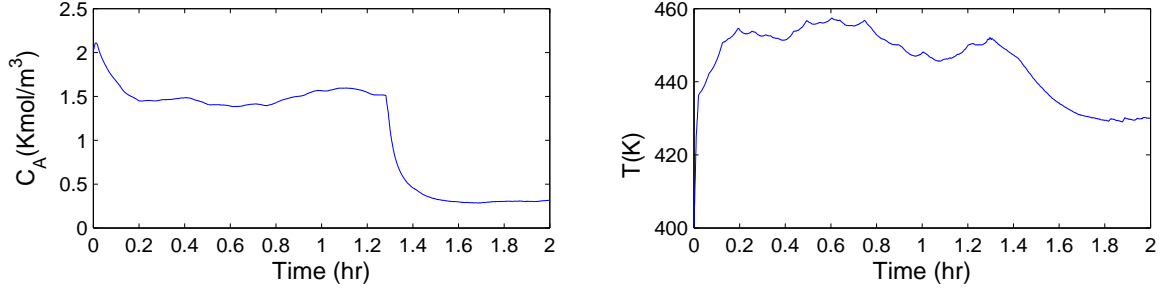


Figure 2.17: State trajectories of the process under the LEMPC design of Eq. 2.46 for initial condition $(C_A(0), T(0)) = (2 \frac{kmol}{m^3}, 400K)$ subject to asynchronous and delayed measurements and disturbances under enforcing the integral constraint over a two-hour period.

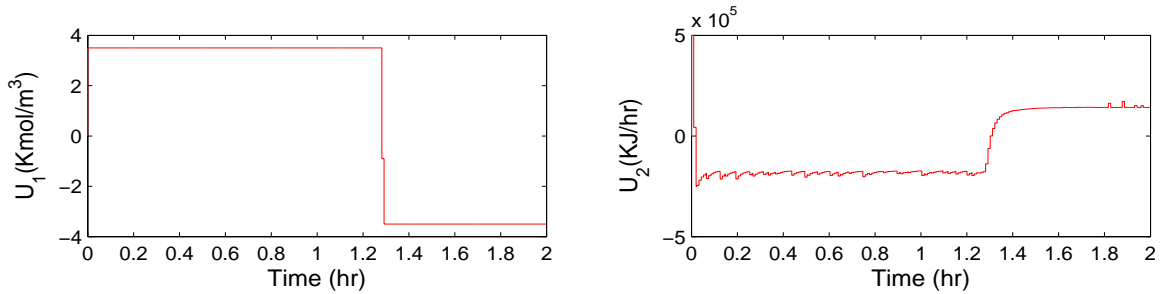


Figure 2.18: Manipulated input trajectories under the LEMPC design of Eq. 2.46 for initial condition $(C_A(0), T(0)) = (2 \frac{kmol}{m^3}, 400K)$ subject to asynchronous and delayed measurements and disturbances under enforcing the integral constraint over a two-hour period.

constraint is enforced over a time period of two hours, and b) the integral constraint is enforced over two consecutive one-hour periods. Figures 2.17 and 2.18 depict the state and input trajectories of the closed-loop system in case (a) and Figures 2.19 and 2.20 depict the state and input trajectories in case (b). These figures illustrate that the periodic operation of the plant under the proposed LEMPC can be readily achieved for different operating scenarios.

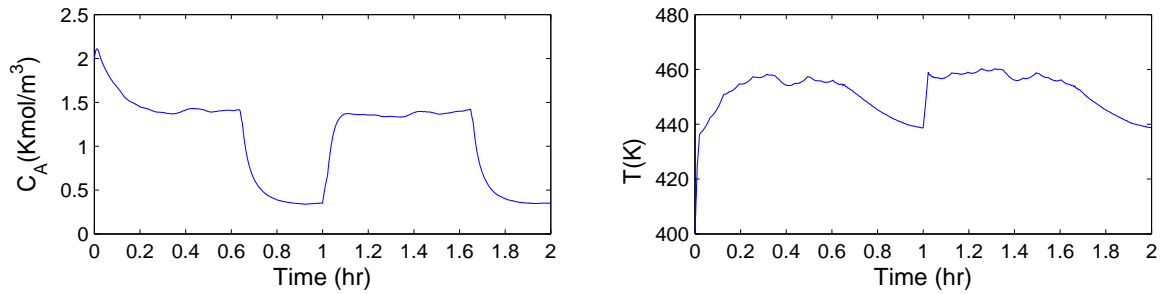


Figure 2.19: State trajectories of the process under the LEMPC design of Eq. 2.46 for initial condition $(C_A(0), T(0)) = (2\frac{kmol}{m^3}, 400K)$ subject to asynchronous and delayed measurements and disturbances under enforcing the integral constraint over two consecutive one-hour periods.

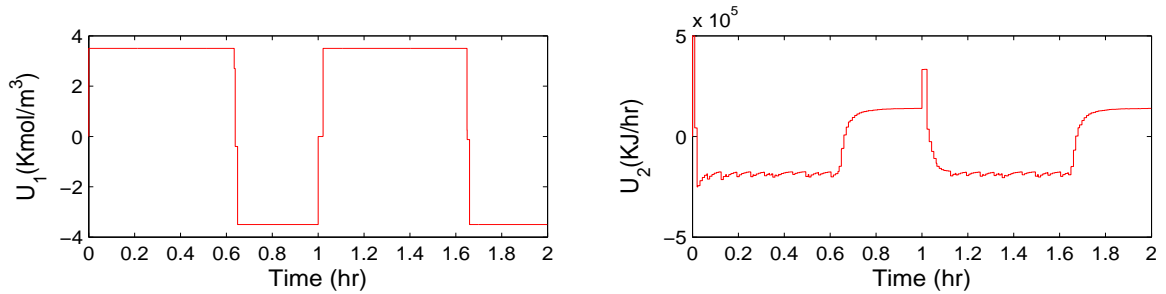


Figure 2.20: Manipulated input trajectories under the LEMPC design of Eq. 2.46 for initial condition $(C_A(0), T(0)) = (2\frac{kmol}{m^3}, 400K)$ subject to asynchronous and delayed measurements and disturbances under enforcing the integral constraint over two consecutive one-hour periods.

2.5 Conclusions

In this chapter, we developed LEMPC designs which are capable of optimizing closed-loop performance with respect to general economic considerations for nonlinear systems. First, we considered nonlinear systems with synchronous measurement sampling and uncertain variables, and designed an LEMPC via Lyapunov-based techniques. The proposed LEMPC design has two different operation modes. The first operation mode corresponds to the period in which the cost function should be optimized; and in this operation mode, the LEMPC maintains the closed-loop system state within the stability region and optimizes the cost function to its maximum extent. The second operation mode corresponds to operation in which the system is driven by the LEMPC to an appropriate steady-state. Subsequently, we extended the results to nonlinear systems subject to asynchronous and delayed measurements and uncertain variables. In both LEMPC designs, suitable constraints were incorporated to guarantee that the closed-loop system state is always bounded in the stability region and is ultimately bounded in small regions containing the origin. The theoretical results were illustrated through a chemical process example.

Chapter 3

State Estimation-Based Economic Model Predictive Control of Nonlinear Systems

In this chapter, we focus on a class of nonlinear systems and design an estimator-based economic model predictive control (EMPC) system. Working with the class of full-state feedback linearizable nonlinear systems, we use a high-gain observer to estimate the nonlinear system state using output measurements and a Lyapunov-based approach to design an EMPC system that uses the observer state estimates. We prove, using singular perturbation arguments, that the closed-loop system is practically stable provided the observer gain is sufficiently large. We use a chemical process example to demonstrate the ability of the state-estimation based EMPC to achieve process time-varying operation that leads to a superior cost performance metric compared to steady-state operation. In the example, the high-gain observer is used to obtain estimates of the reactant concentration from temperature measurements; a

meaningful case in process control practice.

3.1 Preliminaries

3.1.1 Notation

The notation $|\cdot|$ is used to denote the Euclidean norm of a vector. A continuous function $\alpha : [0, a) \rightarrow [0, \infty)$ is said to belong to class \mathcal{K} if it is strictly increasing and satisfies $\alpha(0) = 0$. A continuous function $\beta : [0, a) \times [0, \infty) \rightarrow [0, \infty)$ is said to belong to class \mathcal{KL} if, for each fixed s , the mapping $\beta(r, s)$ belongs to class \mathcal{K} , and for each fixed r , the mapping $\beta(r, s)$ is decreasing with respect to s and $\beta(r, s) \rightarrow 0$ as $s \rightarrow \infty$. The symbol Ω_r is used to denote the set $\Omega_r := \{x \in R^{n_x} : V(x) \leq r\}$ where V is a sufficiently smooth, positive definite scalar function and $r > 0$, and the operator $'/'$ denotes set subtraction, that is, $A/B := \{x \in R^{n_x} : x \in A, x \notin B\}$. The notation $L_f^k h(\cdot)$ denotes the standard k -th order Lie derivative of a scalar function $h(\cdot)$ with respect to the vector function $f(\cdot)$. The notation $L_g L_f h(\cdot)$ denotes the mixed Lie derivative of a scalar function $h(\cdot)$, with respect to vector functions $f(\cdot)$ and $g(\cdot)$. The symbol $diag(v)$ denotes a matrix whose diagonal elements are the elements of vector v and all the other elements are zeros. $sat(\cdot)$ denotes the standard saturation function. I_n and 0_n are the identity matrix and a vector of zeros of dimension n , respectively. Also, the ball B_δ with radius $\delta > 0$ is defined as $B_\delta = \{x \in R^{n_x} : |x| \leq \delta\}$.

3.1.2 Class of Nonlinear Systems

We consider single-input single-output nonlinear systems described by the following state-space model:

$$\begin{aligned}\dot{x} &= f(x) + g(x)u \\ y &= h(x)\end{aligned}\tag{3.1}$$

where $x \in R^{n_x}$ denotes the vector of state variables of the system, $x(t_0) = x(0) = x_0$, $u \in R$ is the manipulated input and $y \in R$ is the measured output. The manipulated input is restricted to be in a nonempty convex set $U \subseteq R$, which is defined as $U := \{u \in R : |u| \leq u^{\max}\}$ where u^{\max} is the magnitude of the input constraint. We assume that f , g and h are sufficiently smooth functions and that the origin is an equilibrium point of the unforced nominal system (i.e., system of Eq. 3.1 with $u(t) \equiv 0$) which implies that $f(0) = 0$. Without loss of generality, in this chapter we focus on single input, single output systems; however, the proposed approach can be extended to multi-input multi-output systems in a conceptually straightforward manner. We assume that the output measurement y of the system is continuously available at all times. We also assume that the system in Eq. 3.1 is full-state feedback linearizable. Thus, the relative degree of the output with respect to the input is n . Assumption 3.1 below states this requirement.

Assumption 3.1. *There exists a set of coordinates*

$$z = \begin{bmatrix} z_1 \\ z_2 \\ \vdots \\ z_n \end{bmatrix} = T(x) = \begin{bmatrix} h(x) \\ L_f h(x) \\ \vdots \\ L_f^{n-1} h(x) \end{bmatrix}\tag{3.2}$$

such that the system of Eq. 3.1 can be written as:

$$\begin{aligned}
\dot{z}_1 &= z_2 \\
&\vdots \\
\dot{z}_{n-1} &= z_n \\
\dot{z}_n &= L_f^n h(T^{-1}(z)) + L_g L_f^{n-1} h(T^{-1}(z))u \\
y &= z_1
\end{aligned}$$

where $L_g L_f^{n-1} h(x) \neq 0$ for all $x \in R^{n_x}$.

Using Assumption 3.1, the system of Eq. 3.1 can be rewritten in the following compact form:

$$\begin{aligned}
\dot{z} &= Az + B[L_f^n h(T^{-1}(z)) + L_g L_f^{n-1} h(T^{-1}(z))u] \\
y &= Cz
\end{aligned}$$

where

$$A = \begin{bmatrix} 0_{n-1} & I_{n-1} \\ 0 & 0_{n-1}^T \end{bmatrix}, \quad B = \begin{bmatrix} 0_{n-1} \\ 1 \end{bmatrix}, \quad C = \begin{bmatrix} 1 \\ 0_{n-1} \end{bmatrix}^T$$

Remark 3.1. We note that Assumption 3.1 imposes certain practical restrictions on the applicability of the method, however, this should be balanced with the nature of the results achieved by the output feedback controller (please see Theorem 3.1 below) in the sense that for a sufficiently large observer gain, the closed-loop system under the output feedback controller approaches the closed-loop stability region and performance of the state feedback controller (essentially a nonlinear separation-principle that is achieved because of Assumption 3.1 and the use of a high-gain observer). This is an assumption imposed in all previous works that use high-gain observers for state estimation, starting from the early work of Khalil and co-workers [50]. With respect

to practical restrictions, our example demonstrates that the method is applicable to a class of chemical reactor models. We note that the requirement of full state linearizability can be relaxed by allowing for inverse dynamics (case where the relative degree, r , is smaller than the system dimension n ; i.e., input/output linearizable systems) at the expense of having an additional observer to estimate the state of the inverse dynamics; please see [26] for a detailed development of this case.

3.1.3 Stabilizability assumption

We assume that there exists a state feedback controller $u = k(x)$, which renders the origin of the closed-loop system asymptotically stable while satisfying the input constraints for all the states x inside a given stability region. Using converse Lyapunov theorems [18, 59], this assumption implies that there exist class \mathcal{K} functions $\alpha_i(\cdot)$, $i = 1, 2, 3, 4$ and a continuously differentiable Lyapunov function $V(x)$ for the closed-loop system, that satisfy the following inequalities:

$$\begin{aligned} \alpha_1(|x|) &\leq V(x) \leq \alpha_2(|x|) \\ \frac{\partial V(x)}{\partial x}(f(x) + g(x)k(x)) &\leq -\alpha_3(|x|) \\ \left| \frac{\partial V(x)}{\partial x} \right| &\leq \alpha_4(|x|) \\ k(x) &\in U \end{aligned} \tag{3.3}$$

for all $x \in D \subseteq R^{n_x}$ where D is an open neighborhood of the origin. We denote the region $\Omega_\rho \subseteq D$ as the stability region of the closed-loop system under the controller $k(x)$. Using the smoothness assumed for the f and g , and taking into account that the manipulated input u is bounded, there exists a positive constant M such that

$$|f(x) + g(x)u| \leq M \tag{3.4}$$

for all $x \in \Omega_\rho$ and $u \in U$. In addition, by the continuous differentiable property of the Lyapunov function $V(x)$ and the smoothness of f and g , there exist positive constants $L_x, L_u, C_x, C_{g'}$ and C_g such that

$$\begin{aligned}
\left| \frac{\partial V}{\partial x} f(x) - \frac{\partial V}{\partial x} f(x') \right| &\leq L_x |x - x'| \\
\left| \frac{\partial V}{\partial x} g(x) - \frac{\partial V}{\partial x} g(x') \right| &\leq L_u |x - x'| \\
|f(x) - f(x')| &\leq C_x |x - x'| \\
|g(x) - g(x')| &\leq C_{g'} |x - x'| \\
\left| \frac{\partial V}{\partial x} g(x) \right| &\leq C_g
\end{aligned} \tag{3.5}$$

for all $x, x' \in \Omega_\rho$ and $u \in U$.

3.1.4 State Estimation via High Gain Observer

The state estimation-based EMPC takes advantage of a high-gain observer ([50, 68]), which obtains estimates of the output derivatives up to order $n - 1$ and consequently, provides estimates of the transformed system state z , to obtain the estimated state of the system \hat{x} through the inverse transformation $T^{-1}(\cdot)$. Proposition 3.1 below defines the high-gain observer equations and establishes precise conditions under which the combination of the high-gain observer and of the controller $k(x)$ together with appropriate saturation functions to eliminate wrong estimates enforce asymptotic stability of the origin in the closed-loop system for sufficiently large observer gain. The proof of the proposition follows from the results in [26, 23].

Proposition 3.1. *Consider the nonlinear system of Eq. 3.1 for which Assumption 3.1 holds. Also, assume that there exists a $k(x)$ for which Eq. 3.3 holds and it enforces local exponential stability of the origin in the closed-loop system. Consider the nonlinear*

system of Eq. 3.1 under the output feedback controller

$$u = k(\hat{x}) \quad (3.6)$$

where

$$\hat{x} = T^{-1}(\text{sat}(\hat{z})) \quad (3.7)$$

and

$$\dot{\hat{z}} = A\hat{z} + L(y - C\hat{z}) \quad (3.8)$$

with

$$L = \begin{bmatrix} a_1 & a_2 & \cdots & a_n \\ \epsilon & \epsilon^2 & \cdots & \epsilon^n \end{bmatrix}^T,$$

and the parameters a_i are chosen such that the roots of

$$s^n + a_1 s^{n-1} + \dots + a_{n-1} s + a_n = 0 \quad (3.9)$$

are in the open left-half of the complex plane. Then given δ , there exists ϵ^* such that if $\epsilon \in (0, \epsilon^*]$, $|\hat{z}(0)| \leq z_m$, $x(0) \in \Omega_\delta$ with z_m being the maximum of the vector \hat{z} for $|\hat{z}| \leq \beta_z(\delta_z, 0)$ where β_z is a class \mathcal{KL} function and $\delta_z = \max\{|T(x)|, x \in \Omega_\delta\}$; the origin of the closed-loop system is asymptotically stable. This stability property implies that given $\epsilon \in (0, \epsilon^*]$ and some positive constant $e_m > 0$ there exists positive real constant $t_b > 0$ such that if $x(0) \in \Omega_\delta$ and $|\hat{z}(0)| \leq z_m$, then $|x(t) - \hat{x}(t)| \leq e_m$ for all $t \geq t_b$.

Remark 3.2. Note that in Proposition 3.1, saturation function, $\text{sat}(\cdot)$, is used to eliminate the peaking phenomenon associated with the high-gain observer, see for example [50]. Note also that it is considered that the estimated state \hat{x} has converged to the actual state x , when the estimation error $|x - \hat{x}|$ is less or equal than a given

bound e_m . The time needed to converge, is given by t_b which is proportional to the observer gain $1/\epsilon$. During this transient, the value of the Lyapunov function $V(x)$ may increase. Finally, we note that for nonlinear MPC designs, computational complexity of the state estimation scheme is very critical. A high-gain observer, as adopted in this chapter, can be solved very fast and it could be more suitable in the context of output feedback control. Other state observers (e.g., moving horizon estimation) may also be used to estimate the system state but the closed-loop stability for this case needs to be studied carefully.

3.2 State Estimation-Based Economic MPC

In this section, we consider the design of an estimation-based Lyapunov-based EMPC (LEMPC) for nonlinear systems (see also [38, 37]). We assume that the output measurements are continuously available. Also, LEMPC is evaluated at synchronous time instants $\{t_{k \geq 0}\}$ with $t_k = t_0 + k\Delta$, $k = 0, 1, \dots$ where $t_0 = 0$ is the first time that LEMPC is evaluated while the high gain observer has converged and Δ is the LEMPC sampling time.

3.2.1 Implementation strategy

The high gain observer of Eq. 3.8 receives output measurements (i.e., y) and provides estimated system states (i.e., \hat{x}) continuously. At each sampling time t_k , the LEMPC obtains the estimated system state $\hat{x}(t_k)$ from the observer. Based on $\hat{x}(t_k)$, the LEMPC takes advantage of the nominal system model to predict the future evolution of the system over a finite prediction horizon while maximizing a cost function that accounts for specific economic considerations.

The two-mode operation architecture in Chapter 2 (see also [34, 33, 32, 10]) is adopted in the design of the LEMPC. Specifically, we assume that from the time t_0 up to a specific time t' where without loss of generality t' is assumed to be a multiple of LEMPC sampling time, the LEMPC operates in the first operation mode to maximize the economic cost function while maintaining the closed-loop system state in the stability region Ω_ρ . In this operation mode, in order to account for the high gain observer effect, we consider another region Ω_{ρ_e} with $\rho_e < \rho$. If the estimated current state is in the region Ω_{ρ_e} , the LEMPC maximizes the cost function within the region Ω_{ρ_e} ; if the estimated current state is in the region $\Omega_\rho/\Omega_{\rho_e}$, the LEMPC first drives the system state to the region Ω_{ρ_e} and then maximizes the cost function within Ω_{ρ_e} .

After time t' , the LEMPC operates in the second operation mode and calculates the inputs in a way that the state of the closed-loop system is driven to a neighborhood of the desired steady-state through the knowledge of the Lyapunov-based controller $k(x)$.

The above described implementation strategy of the proposed LEMPC can be summarized as follows:

1. Based on the output measurements $y(t)$, the high gain observer estimates continuously the system state $\hat{x}(t)$. The LEMPC gets an sample of the estimated system state at t_k from the observer.
2. If $t_k < t'$, go to Step 3. Else, go to Step 4.
3. If $\hat{x}(t_k) \in \Omega_{\rho_e}$, go to Step 3.1. Else, go to Step 3.2.
 - 3.1. The controller maximizes the economic cost function within Ω_{ρ_e} . Go to Step 5.

- 3.2. The controller drives the system state to the region Ω_{ρ_e} and then maximizes the economic cost function within Ω_{ρ_e} . Go to Step 5.
4. The controller drives the system state to a small neighborhood of the origin.
5. Go to Step 1 ($k \leftarrow k + 1$).

Remark 3.3. *The two-mode operation in the design and implementation of the proposed output feedback LEMPC is adopted in order to reconcile two objectives: 1) time-varying operation (off steady-state operation) of the process that optimizes a given economic cost function, ensuring boundedness for the closed-loop system state within a well-defined stability region (mode 1), and 2) eventual convergence of the closed-loop system state to an economically optimal steady-state (mode 2). We note that it is not necessary to adopt a two-mode operation strategy and it is possible to operate the process under mode 1 for arbitrary large period of time (i.e., t' can be made arbitrarily large). The operation in mode 2, where the state of the closed-loop system state converges eventually to a steady-state (potentially economically optimal) is very often dictated by practical considerations which require time-invariant operation at steady-state to minimize wear and tear on the control actuators. Possible reasons for picking t' (i.e., duration of operation in mode 1) in practice may include acceptable time to operate the process in time-varying fashion given actuator specifications and economic considerations.*

3.2.2 LEMPC formulation

The LEMPC is evaluated to obtain the future input trajectories based on estimated state $\hat{x}(t_k)$ provided by the high gain observer. Specifically, the optimization problem

of the proposed LEMPC is as follows:

$$\max_{u \in S(\Delta)} \int_{t_k}^{t_{k+N}} L(\tilde{x}(\tau), u(\tau)) d\tau \quad (3.10a)$$

$$\text{s.t. } \dot{\tilde{x}}(\tau) = f(\tilde{x}(\tau)) + g(\tilde{x}(\tau))u(\tau) \quad (3.10b)$$

$$u(\tau) \in U, \tau \in [t_k, t_{k+N}) \quad (3.10c)$$

$$\tilde{x}(t_k) = \hat{x}(t_k) \quad (3.10d)$$

$$V(\tilde{x}(t)) \leq \rho_e, \forall t \in [t_k, t_{k+N}), \text{ if } t_k \leq t' \text{ and } V(\hat{x}(t_k)) \leq \rho_e \quad (3.10e)$$

$$L_g V(\hat{x}(t_k))u(0) \leq L_g V(\hat{x}(t_k))k(\hat{x}(t_k)),$$

$$\text{if } t_k > t' \text{ or } \rho_e < V(\hat{x}(t_k)) \leq \rho \quad (3.10f)$$

where \tilde{x} is the predicted trajectory of the system with control inputs calculated by this LEMPC and $S(\Delta)$ is the family of piecewise continuous functions with period Δ which allows to obtain an optimization problem to be solved at each sampling time with a finite number decision variables. The constraint of Eq. 3.10b is the system model used to predict the future evolution of the system subject to the input constraint of Eq. 3.10c. The constraint of Eq. 3.10e is associated with the operation mode 1 which restricts the predicted system state to be in the set Ω_{ρ_e} while the constraint of Eq. 3.10f is associated with the operation mode 2 and the operation mode 1 when the estimated system state is out of the predefined set Ω_{ρ_e} . This constraint makes sure that the amount of reduction of the Lyapunov function value when the first step of LEMPC input is applied is at least at the level achieved by applying $k(x)$. The optimal solution to this optimization problem is denoted by $u^*(t|t_k)$, which is defined for $t \in [t_k, t_{k+N})$. The manipulated inputs of the LEMPC of Eq. 3.10 are defined as

follows:

$$u(t) = u^*(t|t_k), \forall t \in [t_k, t_{k+1}) \quad (3.11)$$

3.3 Closed-loop Stability Analysis

To state our main closed-loop stability result, we need the following proposition.

Proposition 3.2 (c.f. [34]). *Consider the system of Eq. 3.1 in closed-loop under the LEMPC of Eq. 3.10 with state feedback (i.e, $\tilde{x}(t_k) = x(t_k)$) based on a controller $k(\cdot)$ that satisfies the conditions of Eq. 3.3. Let $\epsilon_w > 0$, $\Delta > 0$ and $\rho > \rho_s > 0$ satisfy the following constraint:*

$$-\alpha_3(\alpha_2^{-1}(\rho_s)) + L_x M \Delta \leq -\epsilon_w / \Delta. \quad (3.12)$$

If $x(0) \in \Omega_\rho$, then $x(t) \in \Omega_\rho, \forall t \geq 0$. Furthermore, there exists a class \mathcal{KL} function β and a class \mathcal{K} function γ such that

$$|x(t)| \leq \beta(|x(t^*)|, t - t^*) + \gamma(\rho^*) \quad (3.13)$$

with $\rho^ = \max\{V(x(t + \Delta)) : V(x(t)) \leq \rho_s\}, \forall x(t^*) \in B_\delta \subset \Omega_\rho$ and $\forall t \geq t^* > t'$ where t^* is chosen such that $x(t^*) \in B_\delta$.*

Theorem 3.1 below provides sufficient conditions under which the state estimation-based LEMPC of Eq. 3.10 with the high-gain observer of Eq. 3.8 guarantees that the state of the closed-loop system of Eq. 3.1 is always bounded and is ultimately bounded in a small region containing the origin. To state Theorem 3.1, we need the following definitions:

$$e_i = \frac{1}{\epsilon^{n-i}}(y^{(i-1)} - \hat{z}_i), \quad i = 1, \dots, n, \quad (3.14)$$

$$e = [e_1 \ e_2 \ \dots \ e_n]^T \quad (3.15)$$

and

$$A^* = \begin{bmatrix} -a_1 & 1 & 0 & \cdots & 0 & 0 \\ \vdots & \vdots & \vdots & \ddots & \vdots & \vdots \\ -a_{n-1} & 0 & 0 & \cdots & 0 & 1 \\ -a_n & 0 & 0 & \cdots & 0 & 0 \end{bmatrix}, \quad b = \begin{bmatrix} 0 \\ \vdots \\ 0 \\ 1 \end{bmatrix} \quad (3.16)$$

where $y^{(i-1)}$ is the $(i-1)$ -th derivative of the output measurement y and \hat{z}_i is the i -th component of \hat{z} .

Theorem 3.1. *Consider the system of Eq. 3.1 in closed-loop with u computed by the state estimation-based LEMPC of Eqs. 3.7, 3.8 and 3.10 based on a feedback controller $k(\cdot)$ that satisfies the conditions of Eq. 3.3. Let Assumption 3.1, Eq. 3.12 and Eqs. 3.14-3.16 hold and choose the parameters a_i ($i = 1, \dots, n$) such that the roots of Eq. 3.9 are in the open left-half of the complex plane. Then there exist a class \mathcal{KL} function β , a class \mathcal{K} function γ , a pair of positive real numbers (δ_x, d_x) , $0 < \rho_e < \rho$, $\epsilon^* > 0$ and $\Delta^* > 0$ such that if $\max\{|x(0)|, |e(0)|\} \leq \delta_x$, $\epsilon \in (0, \epsilon^*]$, $\Delta \in (0, \Delta^*]$,*

$$-\alpha_3(\alpha_1^{-1}(\rho_s)) + (M\Delta + e_m)(L_x + L_u u^{\max}) < 0 \quad (3.17)$$

and

$$\rho_e \leq \rho - \alpha_4(\alpha_1^{-1}(\rho))M \max\{t_b(\epsilon), \Delta\} \quad (3.18)$$

with t_b defined in Proposition 3.1, then $x(t) \in \Omega_\rho \forall t \geq 0$. Furthermore, $\forall t \geq t^* > t'$, the following bound holds:

$$|x(t)| \leq \beta(|x(t^*)|, t - t^*) + \gamma(\rho^*) + d_x \quad (3.19)$$

Proof 3.1. When $u = u^*$ is obtained from the state estimation-based LEMPC of Eqs. 3.7, 3.8 and 3.10, the closed-loop system takes the following singularly perturbed

form:

$$\begin{aligned}\dot{x} &= f(x) + g(x)u^*(\hat{x}) \\ \epsilon \dot{e} &= A^*e + \epsilon bL_f^n h(T^{-1}(z)) + \epsilon bL_g L_f^{n-1} h(T^{-1}(z))u^*(\hat{x})\end{aligned}\tag{3.20}$$

First, we compute the reduced-order slow and fast closed-loop subsystems related to Eq. 3.20 and prove the closed-loop stability of the slow and fast subsystems.

Setting $\epsilon = 0$ in Eq. 3.20, we obtain the corresponding slow subsystem as follows:

$$\dot{x} = f(x) + g(x)u^*(\hat{x})\tag{3.21a}$$

$$A^*e = 0\tag{3.21b}$$

Taking into account the fact that A^* is non-singular and $e = [0 \ 0 \ \dots \ 0]^T$ is the unique solution of Eq. 3.21b, we can obtain $\hat{z}_i = y^{(i-1)}$, $i = 1, \dots, n$ and $x(t) = \hat{x}(t)$. This means that the closed-loop slow subsystem is reduced to the one studied in Proposition 3.2 under state feedback. According to Proposition 3.2, if $x(0) \in B_\delta \subset \Omega_\rho$, then $x(t) \in \Omega_\rho$, $\forall t \geq 0$ and $\forall t \geq t^* > t'$, the following bound holds:

$$|x(t)| \leq \beta(|x(t^*)|, t - t^*) + \gamma(\rho^*)\tag{3.22}$$

where ρ^* and t^* have been defined in Proposition 3.2.

Introducing the fast time scale $\bar{\tau} = \frac{t}{\epsilon}$ and setting $\epsilon = 0$, the closed-loop fast subsystem can be represented as follows:

$$\frac{de}{d\bar{\tau}} = A^*e\tag{3.23}$$

Since A^* is Hurwitz, the closed-loop fast subsystem is also stable. Moreover, there

exist $k_e \geq 1$ and $a_e > 0$ such that:

$$|e(\bar{\tau})| \leq k_e |e(0)| e^{-a_e \bar{\tau}}, \quad \forall \bar{\tau} \geq 0. \quad (3.24)$$

Next, we consider $t \in (0, \max\{\Delta, t_b\}]$ and $t \geq \max\{\Delta, t_b\}$ separately and prove that if conditions stated in Theorem 3.1 are satisfied, the boundedness of the state is ensured. Note that t_b decreases as ϵ decreases.

When $x(0) \in B_{\delta_x} \subset \Omega_{\rho_e} \subset \Omega_{\rho}$, and $\delta_x < \delta$, considering the closed-loop system state trajectory:

$$\dot{x}(t) = f(x(t)) + g(x(t))u^*(\hat{x}(0)), \quad \forall t \in (0, \max\{\Delta, t_b\}]$$

and using Eqs. 3.4 and 3.3, we can obtain that for all $t \in (0, \max\{\Delta, t_b\}]$:

$$\begin{aligned} V(x(t)) &= V(x(0)) + \int_0^t \dot{V}(x(\tau)) d\tau \\ &= V(x(0)) + \int_0^t \frac{\partial V(x(\tau))}{\partial x} \dot{x}(\tau) d\tau \\ &\leq \rho_e + M \max\{\Delta, t_b(\epsilon)\} \alpha_4(\alpha_1^{-1}(\rho)) \end{aligned} \quad (3.25)$$

Since t_b decreases as ϵ decreases, there exist Δ_1 and ϵ_1 such that if $\Delta \in (0, \Delta_1]$ and $\epsilon \in (0, \epsilon_1]$, Eq. 3.18 holds and thus,

$$V(x(t)) < \rho, \quad \forall t \in (0, \max\{\Delta, t_b\}]. \quad (3.26)$$

For $t \geq \max\{\Delta, t_b\}$, we have that $|x(t) - \hat{x}(t)| \leq e_m$ (this follows from Proposition 3.1 and e_m decreases as ϵ decreases), and we can write the time derivative of the Lyapunov function along the closed-loop system state of Eq. 3.1 under the state estimation-based LEMPC of Eqs. 3.7, 3.8 and 3.10 for all $t \in [t_k, t_{k+1})$ (assuming without loss of

generality that $t_k = \max\{\Delta, t_b\}$) as follows

$$\dot{V}(x(t)) = \frac{\partial V(x(t))}{\partial x}(f(x(t)) + g(x(t))u^*(\hat{x}(t_k))) \quad (3.27)$$

Adding and subtracting the term $\frac{\partial V(\hat{x}(t_k))}{\partial x}(f(\hat{x}(t_k)) + g(x(t_k))u^*(\hat{x}(t_k)))$ to/from the above inequality and taking advantage of Eqs. 3.3 and 3.10f, we can obtain

$$\begin{aligned} \dot{V}(x(t)) \leq & -\alpha_3(\alpha_1^{-1}(\rho_s)) + \frac{\partial V(x)}{\partial x}(f(x(t)) - f(\hat{x}(t_k))) \\ & + u^*(\hat{x}(t_k))(g(x(t)) - g(\hat{x}(t_k))) \end{aligned} \quad (3.28)$$

Using the smoothness properties of $V(\cdot), f(\cdot), g(\cdot)$ and Eq. 3.5, we can obtain

$$\dot{V}(x(t)) \leq -\alpha_3(\alpha_1^{-1}(\rho_s)) + (L_x + L_u u^{\max})|x(t) - \hat{x}(t_k)| \quad (3.29)$$

By taking advantage of $|x(t) - \hat{x}(t_k)| \leq |x(t) - x(t_k)| + |x(t_k) - \hat{x}(t_k)| \leq M\Delta + e_m$ (using Eq. 3.4) and the fact that the estimation error is bounded by e_m for $t \geq \max\{\Delta, t_b\}$, we have

$$\dot{V}(x(t)) \leq -\alpha_3(\alpha_1^{-1}(\rho_s)) + (L_x + L_u u^{\max})(M\Delta + e_m) \quad (3.30)$$

Picking ϵ_2 and Δ_2 such that $\forall \epsilon \in (0, \epsilon_2]$ and $\forall \Delta \in (0, \Delta_2]$, Eq. 3.17 is satisfied, the closed-loop system state $x(t)$ is bounded in Ω_ρ , $\forall t \geq \max\{\Delta, t_b\}$. Finally, using similar arguments to the proof of Theorem 1 in [16], we have that there exist class \mathcal{KL} function β , positive real numbers (δ_x, d_x) (note that the existence of $\delta_x < \delta$ such that $|x(0)| \leq \delta_x$ follows from the smoothness of $V(x)$), and $0 < \epsilon^* < \min\{\epsilon_1, \epsilon_2\}$ and $0 < \Delta^* < \min\{\Delta_1, \Delta_2\}$ such that if $\max\{|x(0)|, |e(0)|\} \leq \delta_x$, $\epsilon \in (0, \epsilon^*]$ and $\Delta \in (0, \Delta^*]$, then, the bound of Eq.3.19 holds for all $t \geq 0$.

Remark 3.4. *It needs to be clarified that under state feedback LEMPC, the closed-loop*

system state is always bounded in Ω_ρ for both mode 1 and mode 2 operation; however, for mode 2 operation, after time t^* the closed-loop system state enters the ball B_δ , and the closed-loop system state can be bounded by Eq. 3.22. On the other hand, in state estimation-based LEMPC, the closed-loop system state is always bounded in Ω_ρ , if the initial system state belongs in $B_{\delta_x} \subset \Omega_{\rho_e} \subset \Omega_\rho$.

Remark 3.5. *In this chapter, we consider that there is no measurement noise in the process output and assume that the full system model is available. We can consider a smaller stability region, say $\Omega_{\bar{\rho}}$, which takes into account the effect of measurement noise as well as a lower observer gain to deal better with measurement noise. Please refer to Chapter 6 of [19] (see also [10]) for a detailed discussion on how to determine the stability region Ω_ρ in the presence of measurement noise and to the example Section for an evaluation of the closed-loop performance of the proposed output feedback controller under measurement noise.*

Remark 3.6. *If the initial condition $x(t_0)$ (and the following $\hat{x}(t_k)$ estimate) is outside of the stability region Ω_ρ , we can not take advantage of the stability properties of the nonlinear controller $k(x)$. However, since Ω_ρ is an estimate of the stability region, it is possible to achieve closed-loop stability under the proposed LEMPC design for states outside of Ω_ρ . In the case that $x(t_k)$ is outside of Ω_ρ , the proposed LEMPC mode 1 can be made feasible by removing the constraint of Eq. 3.10f at the expense of losing closed-loop stability guarantees.*

Remark 3.7. *The major motivation for taking advantage of the nonlinear controller $k(x)$ arises from the need for formulating an a priori feasible economic MPC problem for a well-defined set of initial conditions. The control action of $k(x)$ is always a feasible candidate for the proposed LEMPC design (even though the LEMPC via optimization is free to choose a different control action) and the LEMPC can take*

advantage of $k(x)$ to characterize its own corresponding stability region. In addition, the closed-loop system state is always bounded in the invariant stability region of $k(x)$.

3.4 Application To A Chemical Process Example

Consider a well-mixed, non-isothermal continuous stirred tank reactor (CSTR) where an irreversible, second-order, endothermic reaction $A \rightarrow B$ takes place, where A is the reactant and B is the desired product. The feed to the reactor consists of pure A at flow rate F , temperature T_0 and molar concentration C_{A0} . Due to the non-isothermal nature of the reactor, a jacket is used to provide heat to the reactor. The dynamic equations describing the behavior of the reactor, obtained through material and energy balances under standard modeling assumptions, are given below:

$$\frac{dC_A}{dt} = \frac{F}{V}(C_{A0} - C_A) - k_0 e^{\frac{-E}{RT}} C_A^2 \quad (3.31a)$$

$$\frac{dT}{dt} = \frac{F}{V}(T_0 - T) + \frac{-\Delta H}{\sigma C_p} k_0 e^{\frac{-E}{RT}} C_A^2 + \frac{Q_s}{\sigma C_p V} \quad (3.31b)$$

where C_A denotes the concentration of the reactant A , T denotes the temperature of the reactor, Q_s denotes the steady-state rate of heat supply to the reactor, V represents the volume of the reactor, ΔH , k_0 , and E denote the enthalpy, pre-exponential constant and activation energy of the reaction, respectively, and C_p and σ denote the heat capacity and the density of the fluid in the reactor, respectively. The values of the process parameters used in the simulations are shown in Table 3.1. The process model of Eq. 3.31 is numerically simulated using an explicit Euler integration method with integration step $h_c = 10^{-3}$ hr.

The process model has one stable steady-state in the operating range of interest.

Table 3.1: Parameter values

$T_0 = 300$	K	$F = 5$	$\frac{m^3}{hr}$
$V = 1.0$	m^3	$E = 5 \times 10^3$	$\frac{kJ}{kmol}$
$k_0 = 13.93$	$\frac{1}{hr}$	$\Delta H = 1.15 \times 10^4$	$\frac{kJ}{kmol}$
$C_p = 0.231$	$\frac{kJ}{kgK}$	$R = 8.314$	$\frac{kJ}{kmolK}$
$\sigma = 1000$	$\frac{kg}{m^3}$	$C_{As} = 2$	$\frac{kmol}{m^3}$
$T_s = 350$	K	$C_{A0s} = 4$	$\frac{kmol}{m^3}$
$Q_s = 1.73 \times 10^5$	$\frac{KJ}{hr}$		

The control objective is to economically optimize the process in a region around the stable steady-state (C_{As}, T_s) to maximize the average production rate of B through manipulation of the concentration of A in the inlet to the reactor, C_{A0} . The steady-state input value associated with the steady-state point is denoted by C_{A0s} . The process model of Eq. 3.31 belongs to the following class of nonlinear systems:

$$\dot{x}(t) = f(x(t)) + g(x(t))u(t)$$

where $x^T = [x_1 \ x_2] = [C_A - C_{As} \ T - T_s]$ is the state, $u = C_{A0} - C_{A0s}$ is the input, $f = [f_1 \ f_2]^T$ and $g_i = [g_{i1} \ g_{i2}]^T$ ($i = 1, 2$) are vector functions. The input is subject to constraint as follows: $|u| \leq 3.5 kmol/m^3$. There is an economic measure considered in this example as follows [86]:

$$L(x, u) = \frac{1}{t_f} \int_0^{t_f} k_0 e^{-\frac{E}{RT(\tau)}} C_A^2(\tau) d\tau \quad (3.32)$$

where $t_f = 1 hr$ is the time duration of the reactor operation. This economic objective function highlights the maximization of the average production rate over process operation for $t_f = 1 hr$. We also consider that there is a limitation on the amount

of reactant material which can be used over the operation period t_f . The average amount of the manipulated input trajectory u during one period of operation is fixed. Specifically, u should satisfy the following constraint:

$$\frac{1}{t_f} \int_0^{t_f} u(\tau) d\tau = 1 \text{ kmol}/m^3. \quad (3.33)$$

For the sake of simplicity, we will refer to Eq. 3.33 as the material constraint. It should be emphasized that due to the second-order dependence of the reaction rate on the reactant concentration, the production rate can be improved through switching between upper and lower bounds of the manipulated input [86], as opposed to steady-state operation via steady in time distribution of the reactant in the feed. In this section we will design an estimation-based LEMPC to manipulate the C_{A0} subject to the material constraint. In the first set of simulations, we assume that state feedback information is available at synchronous time instants while in the second set of simulations we take advantage of a high-gain observer to estimate the reactant concentration from temperature measurements.

In terms of the Lyapunov-based controller, we use a proportional controller (P controller) in the form $u = -\gamma_1 x_1 - \gamma_2 x_2$ subject to input constraints and the quadratic Lyapunov function $V(x) = x^T P x$ where $\gamma_1 = 1.6$, $\gamma_2 = 0.01$, $P = \text{diag}([110.11, 0.12])$ and $\rho = 430$. It should be emphasized that Ω_ρ has been estimated through evaluation of \dot{V} when we apply the proportional controller. We assume that the full system state $x = [x_1 \ x_2]^T$ is measured and sent to the LEMPC at synchronous time instants $t_k = k\Delta$, $k = 0, 1, \dots$, with $\Delta = 0.01 \text{ hr} = 36 \text{ sec}$ in the first set of simulations while for output feedback LEMPC only temperature (x_2) is available to LEMPC and a high-gain observer is utilized to estimate the reactant concentration from temperature measurements. Considering the material constraint which needs

to be satisfied through one period of process operation, a decreasing LEMPC horizon sequence N_0, \dots, N_{99} where $N_i = 100 - i$ and $i = 0, \dots, 99$ is utilized at the different sampling times. At each sampling time t_k , LEMPC with horizon N_k takes into account the leftover amount of reactant material and adjusts its horizon to predict future system state up to time $t_f = 1 \text{ hr}$ to maximize the average production rate. Since the LEMPC is evaluated at discrete-time instants during the closed-loop simulation, the material constraint is enforced as follows:

$$\sum_{i=0}^{M-1} u(t_i) = \frac{t_f}{\Delta} \quad (3.34)$$

where $M = 100$. As LEMPC proceeds at different sampling times, this constraint is adjusted according to the optimal manipulated input at previous sampling times. Specifically, the state feedback LEMPC formulation for the chemical process example in question has the following form:

$$\max_{u \in S(\Delta)} \frac{1}{N_k \Delta} \int_{t_k}^{t_k + N_k} [k_0 e^{-\frac{E}{RT(\tau)}} C_A^2(\tau)] d\tau \quad (3.35a)$$

$$\dot{\tilde{x}}(t) = f(\tilde{x}(t)) + g(\tilde{x}(t))u(t) \quad t \in [t_k, t_k + N_k] \quad (3.35b)$$

$$\sum_{i=k}^{k+N_k-1} u(t_i | t_k) = \zeta_k \quad (3.35c)$$

$$\tilde{x}(t_k) = x(t_k) \quad (3.35d)$$

$$V(\tilde{x}(t)) \leq \rho \quad t \in [t_k, t_k + N_k] \quad (3.35e)$$

$$u(t) \in U \quad t \in [t_k, t_k + N_k] \quad (3.35f)$$

where $x(t_k)$ is the process state measurement at sampling time t_k and the predicted

system state along the LEMPC horizon is restricted in the invariant set Ω_ρ through enforcement of the constraint of Eq. 3.35e subject to the manipulated input constraint of Eq. 3.35f. The constraint of Eq. 3.35c implies that the optimal values of u along the prediction horizon should be chosen to satisfy the material constraint where the explicit expression of ζ_k can be computed based on Eq.3.34 and the optimal manipulated input values prior to sampling time t_k . In other words, this constraint indicates the amount of the remaining reactant material at each sampling time. Thus, it ensures that the material constraint is enforced through one period of process operation. In terms of the initial guess for solving the optimization problem of Eq. 3.35, at the first sampling time we take advantage of the Lyapunov-based controller while for the subsequent sampling times, a shifted version of the optimal solution of the previous sampling time is utilized. The simulations were carried out using Java programming language in a Pentium 3.20 GHz computer and the optimization problems were solved using the open source interior point optimizer Ipopt [97]. The purpose of the following set of simulations is to demonstrate that: I) the proposed LEMPC design subject to state and output feedback restricts the system state in an invariant set; II) the proposed LEMPC design maximizes the economic measure of Eq. 3.35a; and III) the proposed LEMPC design achieves a higher objective function value compared to steady-state operation with equal distribution in time of the reactant material. We have also performed simulations for the case that the constraint of Eq. 3.35e is not included in the LEMPC design of Eq. 3.35. In this case, the process state is not constrained to be in a specific invariant set.

Figures 3.1-3.3 illustrate the process state profile in state space (temperature T versus concentration C_A) considering the stability region Ω_ρ , the time evolution of process state and the manipulated input profile for the LEMPC formulation of Eq. 3.35 with and without the state constraint of Eq. 3.35e, respectively. In both

cases the initial process state is $(1.3 \frac{kmol}{m^3}, 320 K)$. For both cases, the material constraint is satisfied while in the unconstrained state case, there is more freedom to compute the optimal input trajectory to maximize the average production rate. It needs to be emphasized that the process state trajectory under the LEMPC design of Eq. 3.35 subject to the constraint of Eq. 3.35e never leaves the invariant level set Ω_ρ when this constraint is enforced. We have also compared the time-varying operation through LEMPC of Eq. 3.35 to steady-state operation where the reactant material is uniformly distributed in the feed to the reactor over the process operation time (1 hr), from a closed-loop performance point of view. To carry out this comparison, we have computed the total cost of each operating scenario based on an index of the following form:

$$J = \frac{1}{t_M} \sum_{i=0}^M [k_0 e^{-\frac{E}{RT(t_i)}} C_A^2(t_i)]$$

where $t_0 = 0$ hr, $t_M = 1$ hr and $M = 100$. To be consistent in comparison, both of the simulations have been initialized from the steady-state point $(2 \frac{kmol}{m^3}, 350K)$. We find that through time-varying LEMPC operation, there is approximately 7% improvement with respect to steady-state operation. Specifically, in the case of LEMPC operation with $\rho = 430$ the cost is 13.48, in the case of LEMPC operation with $\rho = \infty$ (LEMPC of Eq. 3.35 without the state constraint of Eq. 3.35e) the cost is 13.55 and in the case of steady-state operation the cost is 12.66.

We have also performed closed-loop simulation with the state estimation-based LEMPC. For this set of simulation the high-gain observer parameters are $\epsilon = 0.01$, $a_1 = a_2 = 1$, $\rho_e = 400$ and $z_m = 1685$; the high-gain observer is of the form of Eq. 3.8 with $n = 2$. In this case, the LEMPC formulation at each sampling time is initialized by the estimated system state $\hat{x}(t_k)$ while the output (temperature) measurement is continuously available to the high-gain observer. To ensure that the actual system

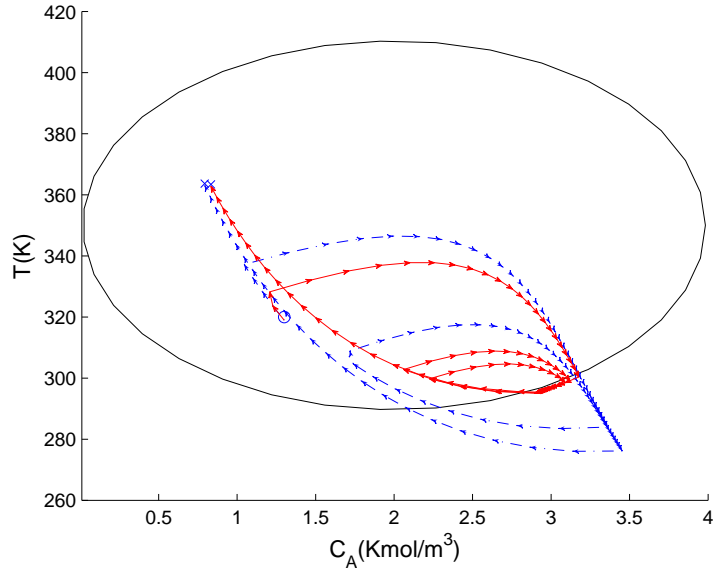


Figure 3.1: Ω_ρ and state trajectories of the process under the LEMPC design of Eq. 3.35 with state feedback and initial state $(C_A(0), T(0)) = (1.3 \frac{\text{kmol}}{\text{m}^3}, 320\text{K})$ for one period of operation with (solid line) and without (dash-dotted line) the constraint of Eq. 3.35e. The symbols \circ and \times denote the initial ($t = 0 \text{ hr}$) and final ($t = 1 \text{ hr}$) state of these closed-loop system trajectories, respectively.

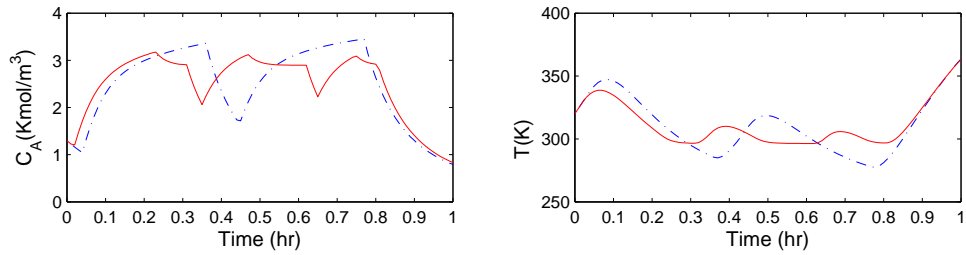


Figure 3.2: State trajectories of the process under the LEMPC design of Eq. 3.35 with state feedback and initial state $(C_A(0), T(0)) = (1.3 \frac{\text{kmol}}{\text{m}^3}, 320\text{K})$ for one period of operation with (solid line) and without (dash-dotted line) the constraint of Eq. 3.35e.

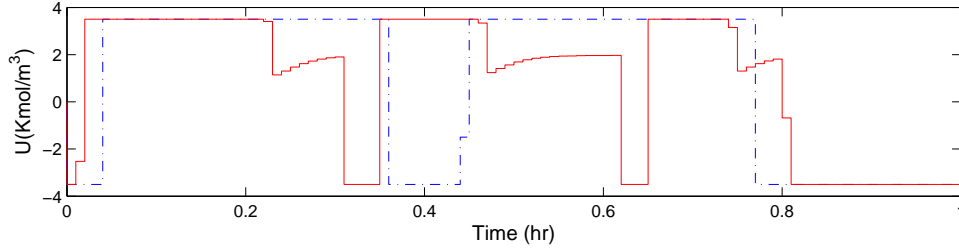


Figure 3.3: Manipulated input trajectory under the LEMPC design of Eq. 3.35 with state feedback and initial state $(C_A(0), T(0)) = (1.3 \frac{\text{kmol}}{\text{m}^3}, 320\text{K})$ for one period of operation with (solid line) and without (dash-dotted line) the constraint of Eq. 3.35e.

state is restricted in Ω_ρ , we set $\rho_e = 400$. Figures 3.4-3.6 illustrate the process state profile in state space (temperature T versus concentration C_A) considering the stability region Ω_ρ , the time evolution of process states and the manipulated input profile for the LEMPC formulation of Eq. 3.35 using high-gain observer and with the state constraint of Eq. 3.35e, respectively. Similar to the state feedback case, the initial process state is $(1.3 \frac{\text{kmol}}{\text{m}^3}, 320 \text{ K})$. Through LEMPC implementation, the material constraint is satisfied while the closed-loop system state is restricted inside the stability region Ω_ρ . The cost is 12.98 which is above the one for steady-state operation (12.66).

Also, we performed a set of simulations to compare LEMPC with the Lyapunov-based controller from an economic closed-loop performance point of view for operation over two consecutive one hour periods. To be consistent in this comparison in the sense that both the LEMPC and the Lyapunov-based controller use the same, available amount of reactant material, we start the simulation in both cases from the same initial condition $(2.44 \frac{\text{kmol}}{\text{m}^3}, 321.96 \text{ K})$, which corresponds to the steady-state of the process when the available reactant material is uniformly distributed over each period of operation. The objective of the Lyapunov-based controller is to keep the system state at this steady-state, while the output feedback LEMPC leads to

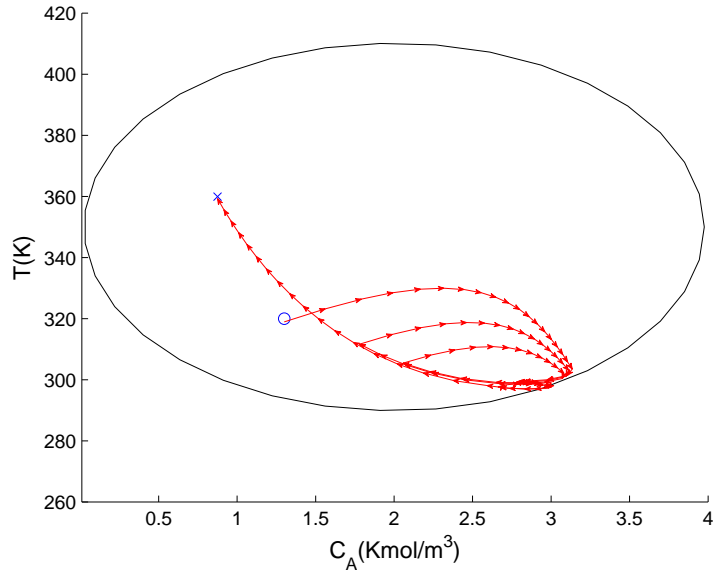


Figure 3.4: Ω_ρ and state trajectories of the process under state estimation-based LEMPC and initial state $(C_A(0), T(0)) = (1.3 \frac{\text{kmol}}{\text{m}^3}, 320\text{K})$ for one period of operation subject to the constraint of Eq. 3.35e. The symbols \circ and \times denote the initial ($t = 0 \text{ hr}$) and final ($t = 1 \text{ hr}$) state of this closed-loop system trajectories, respectively.

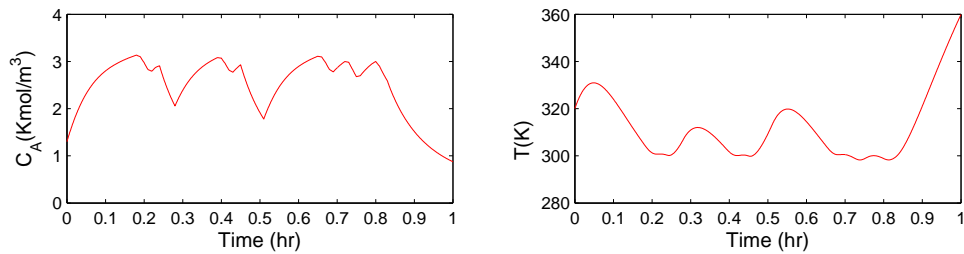


Figure 3.5: State trajectories of the process under state estimation-based LEMPC and initial state $(C_A(0), T(0)) = (1.3 \frac{\text{kmol}}{\text{m}^3}, 320\text{K})$ for one period of operation subject to the constraint of Eq. 3.35e.

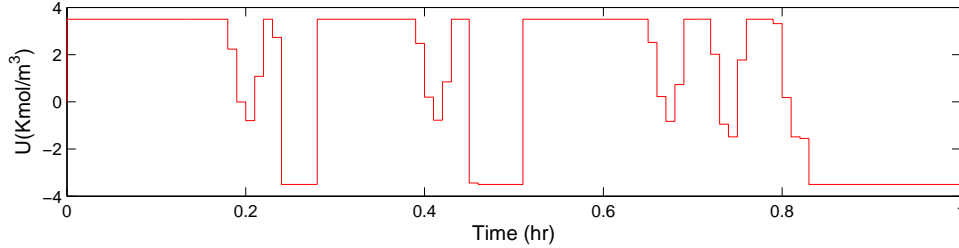


Figure 3.6: Manipulated input trajectory under under state estimation-based LEMPC and initial state $(C_A(0), T(0)) = (1.3 \frac{\text{kmol}}{\text{m}^3}, 320\text{K})$ for one period of operation subject to the constraint of Eq. 3.35e.

time-varying operation that optimizes directly the economic cost. The corresponding economic costs for this two-hour operation are 26.50 for the LEMPC and 25.61 for the Lyapunov-based controller.

Finally, we performed a set of simulations to highlight the effect of bounded measurement noise. Figures 3.7-3.9 display the closed-loop system state and manipulated input of the state-estimation-based LEMPC subject to bounded output (temperature) measurement noise whose absolute value is bounded by 1 K. As it can be seen in Figures 3.7-3.9, the controller can tolerate the effect of measurement noise; in this case, ρ_e was reduced to 370 to improve the robustness margin of the controller to measurement noise. Economic closed-loop performance in this case is 12.95.

3.5 Conclusions

In this chapter, we designed an estimator-based EMPC for the class of full-state feedback linearizable nonlinear systems. A high-gain observer is used to estimate the nonlinear system state using output measurements and a Lyapunov-based approach is adopted to design the EMPC that uses the observer state estimates. It was proved, using singular perturbation arguments, that the closed-loop system is

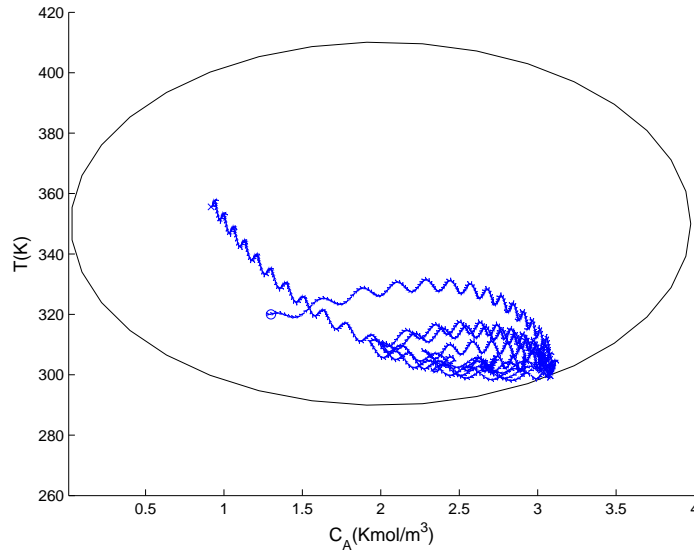


Figure 3.7: Ω_ρ and state trajectories of the process under state estimation-based LEMPC and initial state $(C_A(0), T(0)) = (1.3 \frac{\text{kmol}}{\text{m}^3}, 320\text{K})$ for one period of operation subject to the constraint of Eq. 3.35e and bounded measurement noise. The symbols \circ and \times denote the initial ($t = 0 \text{ hr}$) and final ($t = 1 \text{ hr}$) state of this closed-loop system trajectories, respectively.

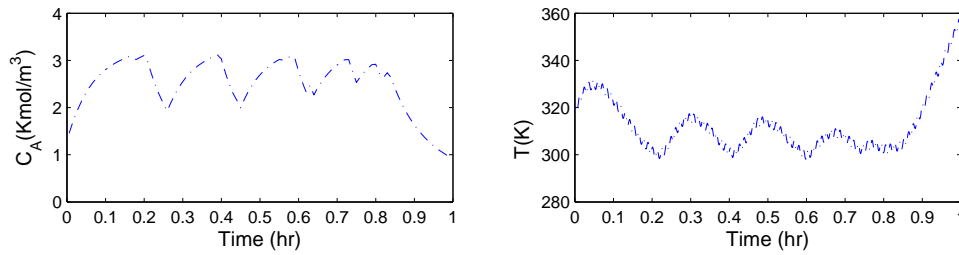


Figure 3.8: State trajectories of the process under state estimation-based LEMPC and initial state $(C_A(0), T(0)) = (1.3 \frac{\text{kmol}}{\text{m}^3}, 320\text{K})$ for one period of operation subject to the constraint of Eq. 3.35e and bounded measurement noise.

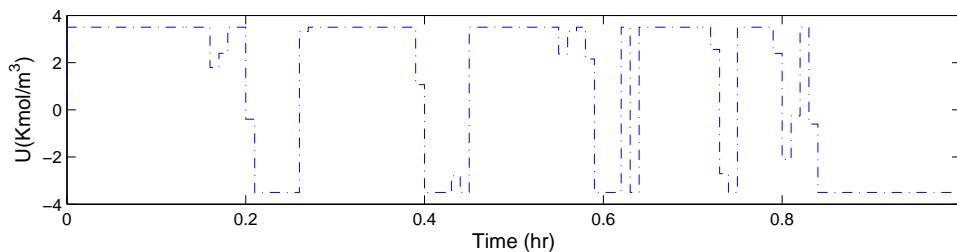


Figure 3.9: Manipulated input trajectory under under state estimation-based LEMPC and initial state $(C_A(0), T(0)) = (1.3 \frac{\text{kmol}}{\text{m}^3}, 320\text{K})$ for one period of operation subject to the constraint of Eq. 3.35e and bounded measurement noise.

practically stable provided the observer gain is sufficiently large. A chemical process example was used to demonstrate the ability of the state estimation-based economic MPC to achieve time-varying process operation that leads to a superior cost performance metric compared to steady-state operation using the same amount of reactant material.

Chapter 4

Algorithms for Improved Finite-Time Performance of Lyapunov-Based Economic Model Predictive Control of Nonlinear Systems

In Chapter 2, we presented a two-mode Lyapunov-based economic MPC (LEMPC) design for nonlinear systems which is also capable of handling asynchronous and delayed measurements and extended it in the context of distributed MPC [10]. Despite the above recent progress, at this point, there is limited work to ensure improvement of closed-loop performance through time-varying operation via economic MPC with respect to operation under conventional MPC in the context of finite time operation. An important recent work has established improved economic MPC

performance over steady-state operation for infinite-time operation [1]. Motivated by the lack of available methodologies to guarantee performance of economic MPC for finite-time operation, this chapter presents two Lyapunov-based economic model predictive control (LEMPC) algorithms for nonlinear systems which are capable of optimizing closed-loop performance with respect to a general objective function that may directly address economic considerations. The LEMPC algorithms proposed in this chapter ensure improved performance, measured by the desired economic cost, over conventional LMPC by solving auxiliary LMPC problems and incorporating appropriate constraints in their formulations at various sampling times. The proposed LEMPC schemes may dictate time-varying process operation, take advantage of a predefined Lyapunov-based explicit feedback law to characterize their stability region while maintaining the closed-loop system state in an invariant set subject to bounded process disturbances. The LEMPC algorithms are demonstrated through a nonlinear chemical process example and their superiority with respect to conventional LMPC schemes is demonstrated for a broad set of initial conditions.

4.1 Preliminaries

4.1.1 Notation

The notation $|\cdot|$ is used to denote the Euclidean norm of a vector. A continuous function $\alpha : [0, a) \rightarrow [0, \infty)$ is said to belong to class \mathcal{K} if it is strictly increasing and satisfies $\alpha(0) = 0$. The symbol Ω_r is used to denote the set $\Omega_r := \{x \in R^{n_x} : V(x) \leq r\}$ where V is a continuously differentiable, positive definite scalar function and $r > 0$, and the operator ‘/’ denotes set subtraction, that is, $A/B := \{x \in R^{n_x} : x \in A, x \notin B\}$. The symbol $diag(v)$ denotes a matrix whose diagonal elements are

the elements of vector v and all the other elements are zeros.

4.1.2 Class of nonlinear systems

We consider a class of nonlinear systems which can be described by the following state-space model:

$$\dot{x}(t) = f(x(t), u(t), w(t)) \quad (4.1)$$

where $x \in R^{n_x}$ denotes the vector of state variables of the system, and $u \in R$ and $w \in R^{n_w}$ denote the control (manipulated) input and the disturbance vector, respectively. The control input is restricted to be in a nonempty convex set $U \subseteq R$, which is defined as $U := \{u \in R : |u| \leq u^{\max}\}$ where u^{\max} is the magnitude of the input constraint. The disturbance $w \in R^{n_w}$ is bounded, i.e., $w \in W$ where $W := \{w \in R^{n_w} \text{ s.t. } |w| \leq \theta, \theta > 0\}$. We assume that f is a locally Lipschitz vector function and that the origin is an equilibrium point of the unforced nominal system (i.e., the system of Eq. 4.1 with $u(t) \equiv 0$ and $w(t) \equiv 0$ for all times) which implies that $f(0, 0, 0) = 0$. We assume that the state x of the system is sampled synchronously and the time instants at which we have state measurements are indicated by the time sequence $\{t_{k \geq 0}\}$ with $t_k = t_0 + k\Delta$, $k = 0, 1, \dots$ where t_0 is the initial time and Δ is the sampling time.

4.1.3 Stabilizability assumption

We assume that there exists a Lyapunov-based controller $u = h(x)$ which satisfies the input constraints for all the states x inside a given stability region and makes the origin of the closed-loop system asymptotically stable. Using converse Lyapunov theorems [18, 59], this assumption implies that there exist class \mathcal{K} functions $\alpha_i(\cdot)$, $i = 1, 2, 3, 4$

and a continuously differentiable Lyapunov function $V(x)$, that satisfy the following inequalities:

$$\begin{aligned}
\alpha_1(|x|) &\leq V(x) \leq \alpha_2(|x|) \\
\frac{\partial V(x)}{\partial x} f(x, h(x), 0) &\leq -\alpha_3(|x|) \\
\left| \frac{\partial V(x)}{\partial x} \right| &\leq \alpha_4(|x|) \\
h(x) &\in U, \quad i = 1, \dots, m
\end{aligned} \tag{4.2}$$

for all $x \in D \subseteq R^{n_x}$ where D is an open neighborhood of the origin. We represent the region $\Omega_\rho \subseteq D$ as the stability region of the closed-loop system under the controller $h(x)$. Using the Lipschitz property assumed for the f , and taking into account that the manipulated input u and the disturbance vector w are bounded, there exists a positive constant M such that

$$|f(x, u, w)| \leq M \tag{4.3}$$

for all $x \in \Omega_\rho$, $u \in U$ and $w \in W$. In addition, by the continuous differentiable property of the Lyapunov function $V(x)$ and the Lipschitz property assumed for the vector field f , there exist positive constants L_x , L_w , L'_x and L'_w such that

$$\begin{aligned}
|f(x, u, w) - f(x', u, 0)| &\leq L_x |x - x'| + L_w |w| \\
\left| \frac{\partial V(x)}{\partial x} f(x, u, w) - \frac{\partial V(x')}{\partial x} f(x', u, 0) \right| &\leq L'_x |x - x'| + L'_w |w|
\end{aligned} \tag{4.4}$$

for all $x, x' \in \Omega_\rho$, $u \in U$ and $w \in W$.

4.1.4 Lyapunov-based MPC

The Lyapunov-based MPC (LMPC) design [73] inherits the closed-loop stability properties of the Lyapunov-based controller $h(\cdot)$ when it is applied in a sample and hold

fashion. Specifically, using a conventional quadratic cost function

$$L_s(x(t), u(t)) = x^T(t)Qx(t) + u^T(t)Ru(t) \quad (4.5)$$

and the LMPC at sampling time t_k is formulated as follows

$$\min_{u \in S(\Delta)} \int_{t_k}^{t_{k+N}} L_s(\tilde{x}(\tau), u(\tau)) d\tau \quad (4.6a)$$

$$\text{s.t. } \dot{\tilde{x}}(\tau) = f(\tilde{x}(\tau), u(\tau), 0) \quad (4.6b)$$

$$u(\tau) \in U, \tau \in [t_k, t_{k+N}) \quad (4.6c)$$

$$\tilde{x}(t_k) = x(t_k) \quad (4.6d)$$

$$\frac{\partial V(x(t_k))}{\partial x} f(x(t_k), u(t_k), 0) \leq \frac{\partial V(x(t_k))}{\partial x} f(x(t_k), h(x(t_k)), 0) \quad (4.6e)$$

where \tilde{x} is the predicted state trajectory of the system with control input calculated by this LMPC, $S(\Delta)$ is the set of piecewise constant functions with period Δ , N is the finite prediction horizon and Q and R are positive definite weighting matrices. Eq. 4.6b utilizes a nominal system model to predict the future evolution of the system state with initialization by sampled state feedback at time t_k (Eq. 4.6d) and Eq. 4.6c denotes the constraint on the manipulated input. The Lyapunov-based constraint of Eq. 4.6e guarantees that the amount of reduction in the Lyapunov function when we apply the input computed by the LMPC at t_k is at least at the level when the Lyapunov-based controller $h(x(t_k))$ is applied in a sample and hold fashion (i.e, through two consecutive sampling times t_k and t_{k+1} , the manipulated input is fixed). Thus, the LMPC inherits the closed-stability properties of $h(\cdot)$. For a detailed closed-loop stability analysis, please refer to [19].

4.1.5 Lyapunov-based economic MPC

Lyapunov-based economic MPC (LEMPC) includes an economic cost function $L_e(x(t), u(t))$ in its formulation which may directly address economic considerations and it does not necessarily take its optimum value at the steady-state point corresponding to the LMPC formulation of Eq. 4.6 (taken to be the origin in this chapter for simplicity). This LEMPC characteristic requires reformulation of the conventional LMPC to address possibly time-varying operation instead of steady-state operation achieved by the LMPC of Eq. 4.6; however, the closed-loop stability region needs to be precisely characterized. In Chapter 2, we proposed an LEMPC scheme through taking advantage of the Lyapunov-based controller $h(x)$. Specifically, the LEMPC was formulated as follows:

$$\max_{u \in S(\Delta)} \int_{t_k}^{t_{k+N}} L_e(\tilde{x}(\tau), u(\tau)) d\tau \quad (4.7a)$$

$$\text{s.t. } \dot{\tilde{x}}(\tau) = f(\tilde{x}(\tau), u(\tau), 0) \quad (4.7b)$$

$$u(\tau) \in U, \tau \in [t_k, t_{k+N}) \quad (4.7c)$$

$$\tilde{x}(t_k) = x(t_k) \quad (4.7d)$$

$$V(\tilde{x}(t)) \leq \rho, \forall t \in [t_k, t_{k+N}) \quad (4.7e)$$

Eq. 4.7b uses a nominal system model to predict the future evolution of the system state initialized at $x(t_k)$ (Eq. 4.7d) and Eq. 4.7c denotes the constraint on the manipulated input. The constraint of Eq. 4.7e maintains the predicted system state along the prediction horizon in the invariant set Ω_ρ , and within this set, the LEMPC addresses economic considerations by optimizing the economic cost function of Eq. 4.7a. Please

refer to Chapter 2 for a detailed description and analysis of the LEMPC formulation of Eq. 4.7.

4.2 LEMPC Algorithm I: Nominal Operation

In this section, we consider the design of Lyapunov-based economic MPC (LEMPC) for nonlinear systems under nominal operation (i.e., $w(t) \equiv 0$). When there is an economic cost function which directly addresses economic considerations of the system (e.g., $L_e(x(t), u(t))$), steady-state operation may not yield optimal economic closed-loop performance. We propose a finite prediction horizon LEMPC formulation which leads to improvement in economic closed-loop performance compared to a conventional steady-state LMPC operation. The proposed scheme at the first stage solves an auxiliary LMPC problem and then through different sampling times, it incorporates the solution of this LMPC problem to the LEMPC formulation (see also [36]). Specifically, we define the manipulated input of the LMPC design of Eq. 4.6 which is only evaluated at sampling time t_0 as follows:

$$u_{LMPC}(t) = u^*(t|t_0), \quad \forall t \in [t_0, t_N]. \quad (4.8)$$

For simplicity, we assume that $\Delta = \frac{t_N - t_0}{N}$. Subsequently, let the state trajectory $x_{LMPC}(t)$ be defined as follows:

$$\dot{x}_{LMPC}(t) = f(x_{LMPC}(t), u_{LMPC}(t), 0), \quad \forall t \in [t_0, t_N] \quad (4.9)$$

which is the closed-loop system state trajectory when the manipulated input obtained through the LMPC of Eq. 4.6 is applied. Also, we define

$$\bar{u}_{LMPC} = \int_{t_0}^{t_N} u_{LMPC}(\tau) d\tau \quad (4.10)$$

as the overall amount of control action utilized by the LMPC of Eq. 4.6 over a finite prediction horizon N . Subsequently, let us define

$$c_{LMPC} = \int_{t_0}^{t_N} L_e(x_{LMPC}(\tau), u_{LMPC}(\tau)) d\tau \quad (4.11)$$

as the overall value of the corresponding economic cost function when we apply the LMPC solution obtained at sampling time t_0 over the period $[t_0, t_N)$. The purpose of the LEMPC design discussed below is to obtain an optimal manipulated input trajectory which uses the same amount of control action obtained by the LMPC of Eq. 4.6, while improving the economic cost function value over the process operation period $[t_0, t_N)$.

4.2.1 Implementation strategy

At time t_0 , first the LMPC obtains its manipulated input trajectory over $[t_0, t_N)$ based on state feedback $x(t_0)$. After computing the amount of control action and economic cost over time $[t_0, t_N)$ induced by the LMPC state and manipulated input trajectories using Eqs. 4.10 and 4.11, respectively, the LEMPC obtains its optimal manipulated input in a receding horizon manner. At each sampling time t_k , based on $x(t_k)$, the LEMPC takes advantage of the nominal system model to predict the future state of the system over a finite prediction horizon while maximizing an economic cost function. A schematic diagram of the proposed LEMPC design is depicted in Fig. 4.1.

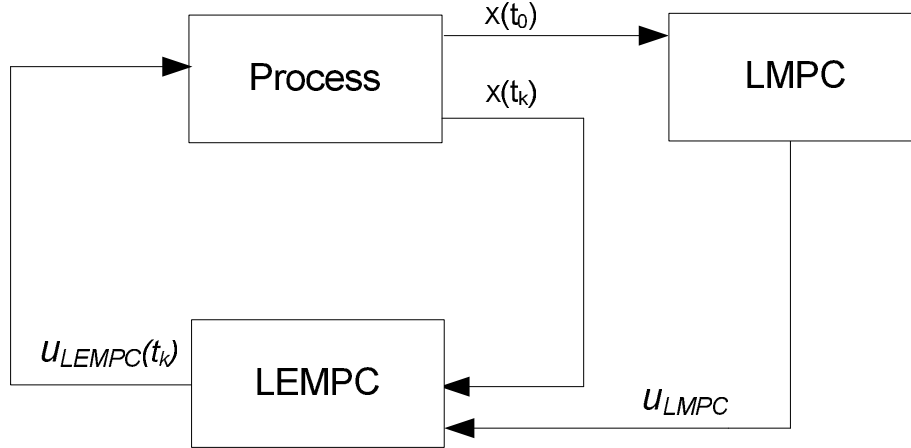


Figure 4.1: LEMPC architecture under nominal operation

The implementation strategy of the proposed LEMPC can be summarized as follows:

1. At time t_0 , an auxiliary LMPC optimization problem of Eq. 4.6 is solved based on state measurement $x(t_0)$.
2. The amount of control action used by the LMPC and its corresponding economic cost over $[t_0, t_N)$ are computed using Eqs. 4.10 and 4.11, respectively.
3. The LEMPC receives state feedback $x(t_k)$ ($k = 0, \dots, N - 1$) and solves an optimization problem with prediction horizon $N_k = N - k$.
4. The LEMPC sends the first step of its optimal solution to the control actuators.
5. Go to Step 3 ($k \leftarrow k + 1$).

4.2.2 LEMPC formulation

The LEMPC is evaluated to obtain the future input trajectories based on state feedback $x(t_k)$ at sampling time t_k . Specifically, the optimization problem of the proposed

LEMPC under nominal operation is as follows:

$$\max_{u \in \mathcal{S}(\Delta)} \int_{t_k}^{t_N} L_e(\tilde{x}(\tau), u(\tau)) d\tau \quad (4.12a)$$

$$\text{s.t. } \dot{\tilde{x}}(\tau) = f(\tilde{x}(\tau), u(\tau), 0) \quad (4.12b)$$

$$u(\tau) \in U, \tau \in [t_k, t_N) \quad (4.12c)$$

$$\tilde{x}(t_k) = x(t_k) \quad (4.12d)$$

$$V(\tilde{x}(t)) \leq \rho, \forall t \in [t_k, t_N) \quad (4.12e)$$

$$\int_{t_k}^{t_N} u(\tau) d\tau = \bar{u}_{LMPC} - \bar{u}_k \quad (4.12f)$$

$$\int_{t_k}^{t_N} L_e(\tilde{x}(\tau), u(\tau)) d\tau \geq c_{LMPC} - c_k \quad (4.12g)$$

The constraint of Eq. 4.12b is the nominal system model used to predict the future evolution of the system state subject to the input constraint of Eq. 4.12c. The constraint of Eq. 4.12e restricts the predicted system state to be in the set Ω_ρ . The constraint of Eq. 4.12f ensures that the same amount of control action is used by both the LMPC of Eq. 4.6 and the LEMPC of Eq. 4.12 in the time interval $[t_0, t_N)$. The constraint of Eq. 4.12g guarantees that the economic cost function value over the time interval $[t_0, t_N)$ is at least at the level achieved when we use the state and manipulated input trajectory obtained through the LMPC of Eq. 4.6 considering the optimal manipulated inputs obtained by the LEMPC at previous sampling times (see also Eqs. 4.14-4.15 below). It should be mentioned that through this implementation strategy, LEMPC utilizes a decreasing sequence of finite prediction horizons $N_k = N - k$ ($k = 0, \dots, N - 1$) where N is the horizon of LMPC optimization

problem which is solved at sampling time t_0 and its solution is incorporated at the LEMPC formulation. The optimal solution to this optimization problem is denoted by $u^*(t|t_k)$, which is defined for $t \in [t_k, t_N)$. The manipulated input of the LEMPC of Eq. 4.12 is defined as follows:

$$u_{LEMPC}(t) = u^*(t|t_k), \quad \forall t \in [t_k, t_N) \quad (4.13)$$

Based on the LEMPC solution, we have

$$\bar{u}_k = \int_{t_0}^{t_k} u_{LEMPC}(\tau) d\tau \quad (4.14)$$

and

$$c_k = \int_{t_0}^{t_k} L_e(\tilde{x}(\tau), u_{LEMPC}(\tau)) d\tau \quad (4.15)$$

which are incorporated in the LEMPC of Eq. 4.12 to account for the optimal manipulated input obtained at previous sampling times t_j where $j = 0, 1, \dots, k - 1$.

Remark 4.1. *It should be emphasized that both the LMPC of Eq. 4.6 and the LEMPC of Eq. 4.12 use the same amount of control action through the enforcement of the constraint of Eq. 4.12f; however, we can formulate the LEMPC in a slightly different manner by replacing the equality constraint of Eq. 4.12f with an inequality to ensure that the LEMPC uses less or equal amount of control action compared to the LMPC.*

4.2.3 Closed-loop stability and performance

Theorem 4.1 below provides sufficient conditions under which the LEMPC of Eq. 4.12 guarantees that the state of the closed-loop system of Eq. 4.1 is always bounded in an invariant set and it yields a closed-loop economic cost that is as good or superior

to the one of the LMPC for finite-time operation over $[t_0, t_N)$.

Theorem 4.1. *Consider the system of Eq. 4.1 in closed-loop under the LEMPC of Eq. 4.12 based on a controller $h(x)$ that satisfies the conditions of Eq. 4.2. Let $\epsilon_w > 0$, $\Delta > 0$ and $\rho > \rho_s > 0$ satisfy*

$$-\alpha_3(\alpha_2^{-1}(\rho_s)) + L'_x M \Delta \leq -\epsilon_w / \Delta. \quad (4.16)$$

If $x(t_0) \in \Omega_\rho$, then the state $x(t)$ of the closed-loop system is bounded in $\Omega_\rho \forall t \in [t_0, t_N)$ and

$$\int_{t_0}^{t_N} L_e(x_{LEMPC}(\tau), u_{LEMPC}(\tau)) d\tau \geq \int_{t_0}^{t_N} L_e(x_{LMPC}(\tau), u_{LMPC}(\tau)) d\tau \quad (4.17)$$

Proof 4.1. For the optimization problem of the LMPC of Eq. 4.6, $u(\tau) = h(\tilde{x}(\tau))$, $\forall \tau \in [t_0, t_N)$ is a feasible solution. For the LEMPC optimization problem of Eq. 4.12, at sampling time t_0 , the solution of the LMPC of Eq. 4.6 ($u_{LMPC}(\tau)$, $\forall \tau \in [t_0, t_N)$) is also a feasible solution. This solution satisfies the input constraint of Eq. 4.7c through the stabilizability assumption of Eq. 4.2 and the Lyapunov-based stability constraint of Eq. 4.6e. At sampling time t_k where $k > 0$, the last $N_{k-1} - 1$ steps of the optimal solution of the LEMPC at sampling time t_{k-1} (i.e., $u^*(t|t_{k-1})$, $\forall t \in [t_k, t_N)$) is a feasible solution to the LEMPC of Eq. 4.12 due to the fact that there is no process disturbance. Furthermore, through the enforcement of the constraint of Eq. 4.12d, the closed-loop system state is bounded within Ω_ρ .

To be consistent in the comparison from an economic closed-loop performance point of view between the LMPC of Eq. 4.6 and the LEMPC of Eq. 4.12, we chose a decreasing sequence of prediction horizons to ensure that both formulations have been evaluated over time interval $[t_0, t_N)$. Considering the constraint of Eq. 4.12g at

sampling time t_{N-1} , we can write

$$\int_{t_{N-1}}^{t_N} L_e(\tilde{x}(\tau), u(\tau))d\tau \geq c_{LMPC} - c_{N-1} \quad (4.18)$$

Replacing c_{LMPC} and c_{N-1} using Eqs. 4.11, 4.15 in Eq. 4.18, we can obtain

$$\int_{t_0}^{t_N} L_e(x_{LEMPC}(\tau), u_{LEMPC}(\tau))d\tau \geq \int_{t_0}^{t_N} L_e(x_{LMPC}(\tau), u_{LMPC}(\tau))d\tau \quad (4.19)$$

where the state trajectory $x_{LEMPC}(t)$ is defined as follows:

$$\dot{x}_{LEMPC}(t) = f(x_{LEMPC}(t), u_{LEMPC}(t), 0), \forall t \in [t_0, t_N) \quad (4.20)$$

Considering the constraint of Eq. 4.12f at sampling time t_{N-1} , we can write

$$\int_{t_{N-1}}^{t_N} u(\tau)d\tau = \bar{u}_{LMPC} - \bar{u}_{N-1} \quad (4.21)$$

Using Eqs. 4.10, 4.14 and 4.21, we can obtain

$$\int_{t_0}^{t_N} u_{LEMPC}(\tau)d\tau = \int_{t_0}^{t_N} u_{LMPC}d\tau \quad (4.22)$$

Eqs. 4.19 and 4.22 highlight the fact that the LEMPC through time-varying operation yields a closed-loop economic cost that is as good or superior to the one of the LMPC for finite-time operation over $[t_0, t_N)$ while both of them utilize the same amount of control action over $[t_0, t_N)$.

Remark 4.2. *It should be emphasized that the LEMPC architecture proposed in Chapter 2 employs a two-mode operation where at the first mode it deals with addressing economic considerations by maintaining the system state in an invariant set and at*

the second mode it focuses on convergence to a small invariant set around a steady-state by incorporating an appropriate Lyapunov-based constraint. Since in this chapter, we focus on economic closed-loop performance, we only described the proposed LEMPC designs in the context of mode one operation in Chapter 2 by evaluating both the LMPC and the LEMPC over a finite-time operation interval $[t_0, t_N)$. Note that, depending on the application and certain specifications, the LEMPC of Eq. 4.12 can operate at mode 2 after time t_N to achieve practical closed-loop stability (i.e., ultimate convergence of the closed-loop state to a small invariant set including the origin). We deal with applying the LEMPC in the interval $[t_N, t_f)$ where t_f denotes the final time of LEMPC evaluation and the time the closed-loop system state enters a small invariant set around the origin. In a similar manner, first the LMPC is evaluated at sampling time t_N and the corresponding input and economic cost based constraints (Eqs. 4.12f and 4.12g) are obtained and are incorporated in the formulation of the LEMPC at mode 2 at subsequent sampling times t_k where $k \geq N$. In terms of the LEMPC formulation at mode 2, it includes the Lyapunov-based constraint of Eq. 4.6e to address closed-loop stability instead of the constraint of Eq. 4.12e which deals with maintaining the closed-loop system state in an invariant set for economic optimization purposes. Specifically, at sampling time t_N the auxiliary LMPC problem is as follows

$$\min_{u \in \mathcal{S}(\Delta)} \int_{t_N}^{t_f} L_s(\tilde{x}(\tau), u(\tau)) d\tau \quad (4.23a)$$

$$s.t. \dot{\tilde{x}}(\tau) = f(\tilde{x}(\tau), u(\tau), 0) \quad (4.23b)$$

$$u(\tau) \in U, \tau \in [t_N, t_f) \quad (4.23c)$$

$$\tilde{x}(t_N) = x(t_N) \quad (4.23d)$$

$$\frac{\partial V(x(t_N))}{\partial x} f(x(t_N), u(t_N), 0) \leq \frac{\partial V(x(t_N))}{\partial x} f(x(t_N), h(x(t_N)), 0) \quad (4.23e)$$

From the solution of this problem, we can obtain

$$u_{LMPC}(t) = u^*(t|t_0), \quad \forall t \in [t_N, t_f] \quad (4.24)$$

$$\dot{x}_{LMPC}(t) = f(x_{LMPC}(t), u_{LMPC}(t), 0), \quad \forall t \in [t_N, t_f] \quad (4.25)$$

$$\bar{u}_{LMPC} = \int_{t_N}^{t_f} u_{LMPC}(\tau) d\tau \quad (4.26)$$

and

$$c_{LMPC} = \int_{t_N}^{t_f} L_e(x_{LMPC}(\tau), u_{LMPC}(\tau)) d\tau \quad (4.27)$$

Also, a decreasing sequence of finite prediction horizon $N_k = \frac{t_f - t_k}{\Delta}$ is used in the LEMPC formulation to make sure that at each sampling time $t_k \in [t_N, t_f)$, the prediction horizon considers the operation time interval $[t_k, t_f)$. Specifically, for a specific sampling time t_k where $k \geq N$, the LEMPC at mode 2 is formulated as follows

$$\max_{u \in S(\Delta)} \int_{t_k}^{t_f} L_e(\tilde{x}(\tau), u(\tau)) d\tau \quad (4.28a)$$

$$s.t. \quad \dot{\tilde{x}}(\tau) = f(\tilde{x}(\tau), u(\tau), 0) \quad (4.28b)$$

$$u(\tau) \in U, \quad \tau \in [t_k, t_f) \quad (4.28c)$$

$$\tilde{x}(t_k) = x(t_k) \quad (4.28d)$$

$$\int_{t_k}^{t_f} u(\tau) d\tau = \bar{u}_{LMPC} - \bar{u}_k \quad (4.28e)$$

$$\int_{t_k}^{t_f} L_e(\tilde{x}(\tau), u(\tau)) d\tau \geq c_{LMPC} - c_k \quad (4.28f)$$

$$\frac{\partial V(x(t_k))}{\partial x} f(x(t_k), u(t_k), 0) \leq \frac{\partial V(x(t_k))}{\partial x} f(x(t_k), h(x(t_k)), 0) \quad (4.28g)$$

Eq. 4.28b uses the nominal system model to predict the future state of closed-loop system initialized by $x(t_k)$ (Eq. 4.28d) and Eq. 4.28c denotes the constraint on the manipulated input. The Lyapunov-based constraint of Eq. 4.28g guarantees that the amount of reduction in the Lyapunov function value when we apply the input computed by the LEMPC at mode 2 is at least at the level when the Lyapunov-based controller $h(x(t_k))$ is applied in a sample and hold fashion. The constraint of Eq. 4.28e ensures that the same amount of control action is used by both the LMPC of Eq. 4.23 and the LEMPC of Eq. 4.28 for operation in the time interval $[t_N, t_f)$ while the constraint of Eq. 4.28f guarantees that the economic cost function value over the time interval $[t_N, t_f)$ is at least at the level achieved when we apply the state and manipulated input trajectories obtained through the LMPC of Eq. 4.23 considering the control actions utilized by the LEMPC at previous sampling times. The optimal solution to this optimization problem is denoted by $u^*(t|t_k)$, which is defined for $t \in [t_k, t_f)$. The manipulated input of the LEMPC of Eq. 4.28 is defined as follows:

$$u_{LEMPC}(t) = u^*(t|t_k), \forall t \in [t_k, t_f) \quad (4.29)$$

Based on this manipulated input, the following parameters can be computed

$$\bar{u}_k = \int_{t_N}^{t_k} u_{LEMPC}(\tau) d\tau \quad (4.30)$$

and

$$c_k = \int_{t_N}^{t_k} L_e(\tilde{x}(\tau), u_{LEMPC}(\tau)) d\tau \quad (4.31)$$

which are incorporated in the LEMPC of Eq. 4.28 to account for the optimal manip-

ulated input obtained at previous sampling times t_j where $j = N, N + 1, \dots, k - 1$.

4.3 LEMPC Algorithm II: Operation Under Disturbances

In this section, we consider the design of an LEMPC scheme for nonlinear systems subject to bounded process disturbances (i.e., $w(t) \neq 0$). The proposed scheme at each sampling time solves an auxiliary LMPC problem and then incorporates the LMPC solution to the LEMPC formulation as constraints. The manipulated input of the LMPC design of Eq. 4.6 from time t_k to t_N is defined as follows:

$$u_{LMPC}(t) = u^*(t|t_k), \forall t \in [t_k, t_N). \quad (4.32)$$

Let the state trajectory $x_{LMPC}(t)$ be defined as follows:

$$\dot{x}_{LMPC}(t) = f(x_{LMPC}(t), u_{LMPC}(t), 0), \forall t \in [t_k, t_N) \quad (4.33)$$

which is the system state trajectory when the manipulated input is obtained through the LMPC of Eq. 4.6. Also, we define

$$\bar{u}_{LMPC} = \int_{t_k}^{t_N} u_{LMPC}(\tau) d\tau \quad (4.34)$$

as the amount of control action utilized by the LMPC of Eq. 4.6 over a finite prediction horizon N_k where $N_k = N - k$ and $k = 0, 1, \dots, N - 1$. Subsequently, let us define

$$c_{LMPC}^1 = \int_{t_k}^{t_{k+1}} L_e(x_{LMPC}(\tau), u_{LMPC}(\tau)) d\tau \quad (4.35)$$

and

$$c_{LMPC}^2 = \int_{t_k}^{t_N} L_e(x_{LMPC}(\tau), u_{LMPC}(\tau)) d\tau \quad (4.36)$$

as the value of the economic cost function induced by the LMPC over the first prediction step and the entire prediction horizon, respectively. The purpose of the LEMPC design is to obtain an optimal manipulated input trajectory which uses the same amount of control action as the LMPC of Eq. 4.6 at each sampling time while it ensures that at each sampling time t_k , it achieves a better economic cost value compared to the LMPC over the operation periods $[t_k, t_{k+1})$ and $[t_k, t_N)$, respectively.

4.3.1 Implementation strategy

The proposed control scheme solves an auxiliary LMPC optimization problem of Eq. 4.6 at each sampling time t_k . After computing the amount of control action over the time interval $[t_k, t_N)$ and the economic cost function values over time intervals $[t_k, t_{k+1})$ and $[t_k, t_N)$ using the LMPC state and manipulated input trajectories of Eqs. 4.34-4.36, respectively, the LEMPC obtains its optimal manipulated input trajectory in a receding horizon manner. Specifically, at each sampling time t_k , using $x(t_k)$, the LEMPC takes advantage of the nominal system model to predict the future state of the system over a finite prediction horizon while maximizing a cost function that addresses specific economic considerations and maintaining the closed-loop system state in the stability region Ω_ρ . In order to account for the bounded process disturbance effect, we consider another region Ω_{ρ_e} with $\rho_e < \rho$. If the state measurement $x(t_k)$ is in the region Ω_{ρ_e} , the LEMPC maximizes the cost function within the region Ω_{ρ_e} ; if the state measurement is in the region $\Omega_\rho/\Omega_{\rho_e}$, the LEMPC first drives the system state to the region Ω_{ρ_e} and then maximizes the cost function within Ω_{ρ_e} . A schematic diagram of the proposed LEMPC design is depicted in Fig. 4.2.

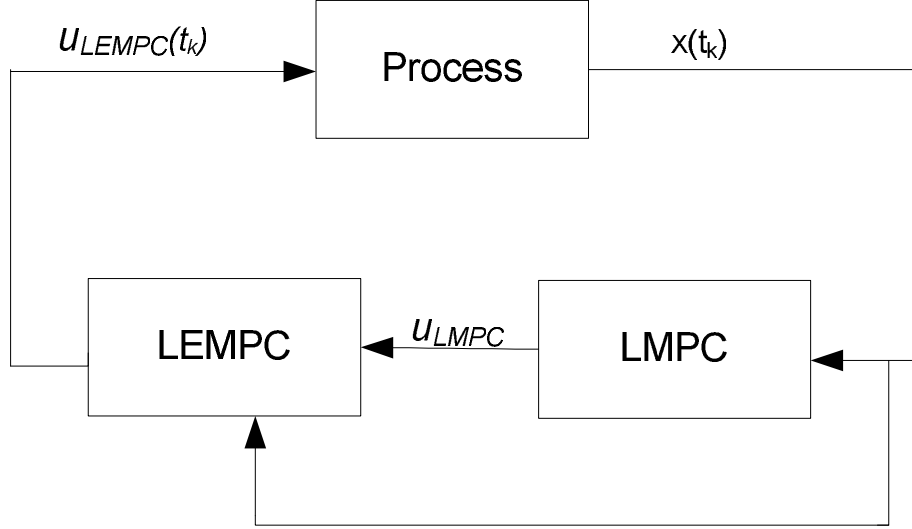


Figure 4.2: LEMPC architecture subject to disturbances

Specifically, the implementation strategy of the proposed LEMPC can be summarized as follows:

1. At time t_k with $t_k \in [t_0, t_N)$, an auxiliary LMPC optimization problem of Eq. 4.6 is solved based on state measurement $x(t_k)$ for $t \in [t_k, t_N)$.
2. The amount of control action used by the LMPC and its corresponding economic cost are computed using Eqs. 4.34-4.36.
3. The LEMPC receives $x(t_k)$ and solves its optimization problem with prediction horizon $N - k$.
4. If $x(t_k) \in \Omega_{\rho_e}$, go to Step 4.1. Else, go to Step 4.2.
 - 4.1. The controller maximizes the economic cost function within Ω_{ρ_e} . Go to Step 5.
 - 4.2. The controller drives the system state to the region Ω_{ρ_e} and then maximizes the economic cost function within Ω_{ρ_e} . Go to Step 5.

5. Go to Step 1 ($k \leftarrow k + 1$).

4.3.2 LEMPC formulation

The optimization problem of the proposed LEMPC at sampling time t_k is as follows:

$$\max_{u \in S(\Delta)} \int_{t_k}^{t_N} L_e(\tilde{x}(\tau), u(\tau)) d\tau \quad (4.37a)$$

$$\text{s.t. } \dot{\tilde{x}}(\tau) = f(\tilde{x}(\tau), u(\tau), 0) \quad (4.37b)$$

$$u(\tau) \in U, \tau \in [t_k, t_N) \quad (4.37c)$$

$$\tilde{x}(t_k) = x(t_k) \quad (4.37d)$$

$$V(\tilde{x}(t)) \leq \rho_e, \forall t \in [t_k, t_N),$$

$$\text{if } V(x(t_k)) \leq \rho_e \quad (4.37e)$$

$$\int_{t_k}^{t_N} u(\tau) d\tau = \bar{u}_{LMPC} \quad (4.37f)$$

$$\int_{t_k}^{t_{k+1}} L_e(x(\tau), u(\tau)) d\tau \geq c_{LMPC}^1 \quad (4.37g)$$

$$\int_{t_k}^{t_N} L_e(x(\tau), u(\tau)) d\tau \geq c_{LMPC}^2 \quad (4.37h)$$

$$\frac{\partial V(x(t_k))}{\partial x} f(x(t_k), u(t_k), 0) \leq \frac{\partial V(x(t_k))}{\partial x} f(x(t_k), h(x(t_k)), 0),$$

$$\text{if } \rho_e < V(x(t_k)) \leq \rho \quad (4.37i)$$

The constraint of Eq. 4.37b is the system model used to predict the future evolution of the system state subject to the input constraint of Eq. 4.37c. The constraint of Eq. 4.37e restricts the predicted system state to be in the set Ω_{ρ_e} . The constraint of Eq. 4.37i guarantees that the reduction rate of the Lyapunov function value when the first step of the LEMPC input is applied is at least at the level achieved by applying the Lyapunov-based controller $h(x)$ when it is applied in a sample and hold fashion and $\rho_e < V(x(t_k)) \leq \rho$. The constraint of Eq. 4.37f makes sure that the same amount of control action is used by both the LMPC of Eq. 4.6 and the LEMPC of Eq. 4.37 while the constraints of Eqs. 4.37g-4.37h guarantee that the economic cost function value over the time intervals $[t_k, t_{k+1})$ and $[t_k, t_N)$ is at least at the level achieved when we apply the state and manipulated input trajectories obtained through the LMPC of Eq. 4.6 over the time intervals $[t_k, t_{k+1})$ and $[t_k, t_N)$, respectively. It should be mentioned that a decreasing sequence of finite prediction horizons $N_k = N - k$ where $k = 0, \dots, N - 1$ is incorporated in the LMPC and LEMPC formulations at sampling time $t_k \in [t_0, t_N)$. The optimal solution to this optimization problem is denoted by $u^*(t|t_k)$ and is defined for $t \in [t_k, t_N)$. The manipulated input of the LEMPC of Eq. 4.37 is defined as follows:

$$u_{LEMPC}(t) = u^*(t|t_k), \forall t \in [t_k, t_N) \quad (4.38)$$

Remark 4.3. *The main difference of the proposed LEMPC algorithms of Eqs. 4.12 and 4.37 arises from the existence of bounded process disturbance. The LEMPC of Eq. 4.12 takes only advantage of the solution of the auxiliary LMPC problem at time t_0 through a decreasing sequence of finite prediction horizons, while the LEMPC of Eq. 4.37, utilizes the solution of the LMPC at each sampling time t_k .*

4.3.3 Closed-loop stability and performance

Corollary 4.1 below provides sufficient conditions under which the LEMPC of Eq. 4.37 guarantees that the state of the closed-loop system of Eq. 4.1 is always bounded in Ω_ρ and at each sampling time the LEMPC yields a closed-loop economic cost that is as good or superior to the one of the LMPC over the interval $[t_k, t_{k+1})$.

Corollary 4.1. *Consider the system of Eq. 4.1 in closed-loop under the LEMPC design of Eq. 4.37 based on a controller $h(x)$ that satisfies the conditions of Eq. 4.2. Let $\epsilon_w > 0$, $\Delta > 0$, $\rho > \rho_e > 0$ and $\rho > \rho_s > 0$ satisfy*

$$\rho_e \leq \rho - f_V(f_W(\Delta)) \quad (4.39)$$

and

$$-\alpha_3(\alpha_2^{-1}(\rho_s)) + L'_x M \Delta + L'_w \theta \leq -\epsilon_w / \Delta. \quad (4.40)$$

If $x(t_0) \in \Omega_\rho$ and $\rho_s \leq \rho_e$, then the state $x(t)$ of the closed-loop system is bounded in Ω_ρ for $\forall t \in [t_0, t_N)$ and at each sampling time t_k

$$\int_{t_k}^{t_{k+1}} L_e(x_{LEMPC}(\tau), u_{LEMPC}(\tau)) d\tau \geq \int_{t_k}^{t_{k+1}} L_e(x_{LMPC}(\tau), u_{LMPC}(\tau)) d\tau \quad (4.41)$$

Proof 4.2. Since the proof of this corollary follows similar arguments to the one of the proof of Theorem 4.1, we provide a sketch of the proof. From a feasibility point of view, at sampling time t_k , the LMPC solution $u_{LMPC}(\tau)$, $\forall \tau \in [t_k, t_{k+N}]$ is a feasible solution for the LEMPC of Eq. 4.37. For a detailed proof regarding boundedness of the closed-loop system state, please refer to Chapter 2. Through enforcing the constraints of Eqs. 4.37g and 4.37h at each sampling time t_k , the LEMPC of Eq. 4.37 ensures that it obtains an input trajectory that optimizes the economic cost function

over the first step and the entire prediction horizon, respectively, while, both the LMPC and LEMPC designs use the same amount of control action over the entire prediction horizon by enforcing the constraint of Eq. 4.37f at each sampling time.

4.4 Application To A Chemical Process Example

Consider a well-mixed, non-isothermal continuous stirred tank reactor (CSTR) where an irreversible, second-order, endothermic reaction $A \rightarrow B$ takes place, where A is the reactant and B is the desired product. The feed to the reactor consists of pure A at flow rate F , temperature T_0 and molar concentration C_{A0} . Due to the non-isothermal nature of the reactor, a jacket is used to provide heat to the reactor. The dynamic equations describing the behavior of the reactor, obtained through material and energy balances under standard modeling assumptions, are given below:

$$\frac{dC_A}{dt} = \frac{F}{V}(C_{A0} - C_A) - k_0 e^{\frac{-E}{RT}} C_A^2 \quad (4.42a)$$

$$\frac{dT}{dt} = \frac{F}{V}(T_0 - T) + \frac{-\Delta H}{\sigma C_p} k_0 e^{\frac{-E}{RT}} C_A^2 + \frac{Q}{\sigma C_p V} \quad (4.42b)$$

where C_A denotes the concentration of the reactant A , T denotes the temperature of the reactor, Q denotes the rate of heat supply to the reactor, V represents the volume of the reactor, ΔH , k_0 and E denote the enthalpy, pre-exponential constant and activation energy of the reaction, respectively, and C_p and σ denote the heat capacity and the density of the fluid in the reactor, respectively. The values of the process parameters used in the simulations are shown in Table 4.1. The process model of Eq. 4.42 is numerically simulated using an explicit Euler integration method with integration step $h_c = 10^{-4}$ hr.

Table 4.1: Parameter values

$T_0 = 300$	K	$F = 5$	$\frac{m^3}{hr}$
$V = 1.0$	m^3	$E = 5 \times 10^3$	$\frac{kJ}{kmol}$
$k_0 = 13.93$	$\frac{1}{hr}$	$\Delta H = 1.15 \times 10^4$	$\frac{kJ}{kmol}$
$C_p = 0.231$	$\frac{kJ}{kgK}$	$R = 8.314$	$\frac{kJ}{kmolK}$
$\sigma = 1000$	$\frac{kg}{m^3}$	$C_{As} = 2$	$\frac{kmol}{m^3}$
$T_s = 350$	K	$C_{A0s} = 4$	$\frac{kmol}{m^3}$
$Q = 1.73 \times 10^5$	$\frac{KJ}{hr}$		

The process model has one stable steady-state in the operating range of interest. The control objective is to optimize the process operation in a region around the stable steady-state (C_{As}, T_s) to maximize the average production rate of B through manipulation of the concentration of A in the inlet to the reactor, C_{A0} . The steady-state input value associated with the steady-state point is denoted by C_{A0s} . The process model of Eq. 4.42 belongs to the following class of nonlinear systems:

$$\dot{x}(t) = f(x(t)) + g(x(t))u(t)$$

where $x^T = [x_1 \ x_2] = [C_A - C_{As} \ T - T_s]$ is the state, $u = C_{A0} - C_{A0s}$ is the input, and $f = [f_1 \ f_2]^T$ and $g = [g_1 \ g_2]^T$ are vector functions. The input is subject to constraints as follows: $|u| \leq 3.5 kmol/m^3$. The economic measure considered in this example is as follows [86]:

$$L_e(x, u) = \frac{1}{t_N} \int_0^{t_N} k_0 e^{-\frac{E}{RT(\tau)}} C_A^2(\tau) d\tau \quad (4.43)$$

where $t_N = 1 \text{ hr}$ is the time duration of the reactor operation. This economic objective function highlights the maximization of the average production rate over process operation for $t_N = 1 \text{ hr}$ (of course, different, yet finite, values of t_N can be chosen.). According to the proposed LEMPC schemes, under mode one operation, auxiliary

LMPC problems are solved to obtain constraints on the amount of reactant material (control action) which can be used by the LEMPC control schemes. For the sake of simplicity, we will refer to these type of constraint as the material constraint. We consider both nominal and subject to bounded disturbance operations.

In terms of the Lyapunov-based controller, we use a proportional controller (P controller) in the form $u = -\gamma_1 x_1 - \gamma_2 x_2$ subject to input constraints and the quadratic Lyapunov function $V(x) = x^T P x$ where $\gamma_1 = 1.6$, $\gamma_2 = 0.01$, $P = \text{diag}([110.11 \ 0.12])$ and $\rho = 430$. It should be emphasized that Ω_ρ has been estimated through evaluation of \dot{V} when we apply the proportional controller. We assume that the full system state $x = [x_1 \ x_2]^T$ is measured and sent to the LEMPC at synchronous time instants $t_k = k\Delta$, $k = 0, 1, \dots$, with $\Delta = 0.01 \text{ hr} = 36 \text{ sec}$.

4.4.1 Nominal operation

An LMPC optimization problem which is only solved at sampling time $t_0 = 0$ is formulated with prediction horizon $N = 100$ ($t_N = 1 \text{ hr}$) and weighting matrix $Q = \text{diag}([1 \ 0.01])$ and $R = 1$. Figures 4.3-4.5 display the closed-loop state and manipulated input profiles for the LMPC of Eq. 4.6 which leads to steady-state operation. The LMPC scheme steers the closed-loop system state to the steady-state. However, this steady-state operation may not be optimal from the standpoint of the cost of Eq. 4.43. It should be emphasized that this LMPC formulation is only evaluated at time t_0 .

Considering the material constraint which needs to be satisfied through each period of process operation, a decreasing LEMPC horizon sequence N_0, \dots, N_{99} where $N_i = 100 - i$ and $i = 0, \dots, 99$ is utilized at the different sampling times. Figures 4.6-4.8 represent the closed-loop state and the manipulated input for the LEMPC of

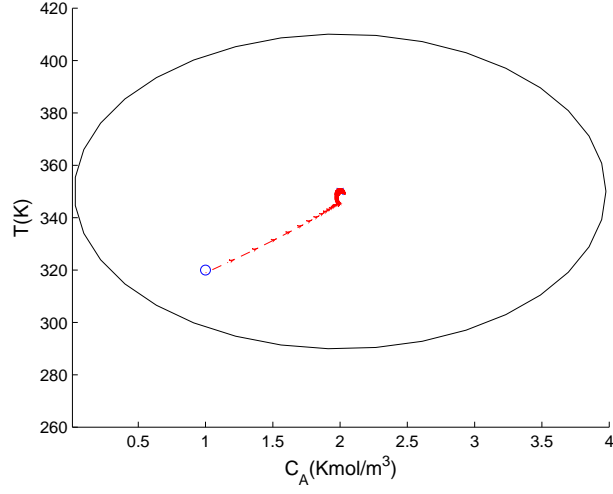


Figure 4.3: Ω_ρ and state trajectories of the process under the LMPC design of Eq. 4.6 with initial state $(C_A(0), T(0)) = (1 \frac{\text{kmol}}{\text{m}^3}, 320\text{K})$ for one period of operation. The symbols \circ and \times denote the initial ($t = 0 \text{ hr}$) and final ($t = 1 \text{ hr}$) state of these closed-loop system trajectories, respectively.

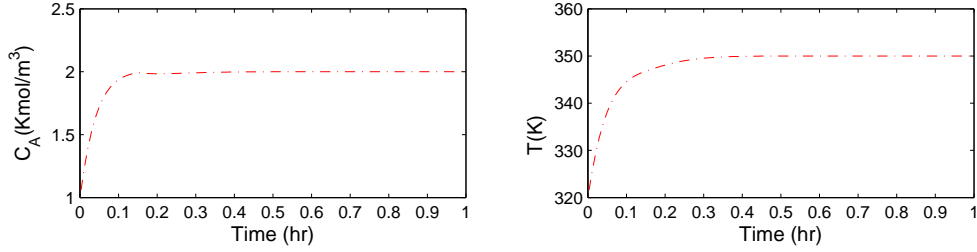


Figure 4.4: State trajectories of the process under the LMPC design of Eq. 4.6 with initial state $(C_A(0), T(0)) = (1 \frac{\text{kmol}}{\text{m}^3}, 320\text{K})$ for one period of operation.

Eq. 4.12 which dictates a time-varying operation to achieve optimal economic closed-loop performance. Table 4.2 shows the evaluation of LEMPC and LMPC from an economic cost function point of view for 30 different initial states within Ω_ρ as illustrated in Figure 4.9. To carry out this comparison, we have computed the total cost of each operating scenario based on an index of the following form:

$$J = \frac{1}{t_{100}} \sum_{i=0}^{100} [k_0 e^{-\frac{E}{RT(t_i)}} C_A^2(t_i)] \quad (4.44)$$

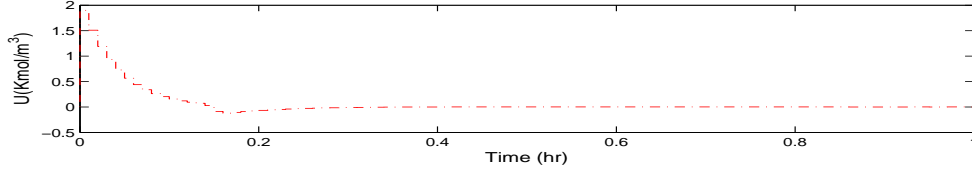


Figure 4.5: Manipulated input trajectory under the LMPC design of Eq. 4.6 with initial state $(C_A(0), T(0)) = (1 \frac{\text{kmol}}{\text{m}^3}, 320\text{K})$ for one period of operation.

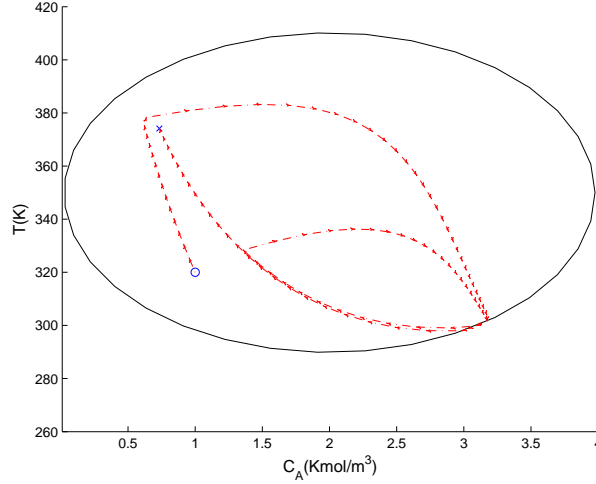


Figure 4.6: Ω_ρ and state trajectories of the process under the LEMPC design of Eq. 4.12 with initial state $(C_A(0), T(0)) = (1 \frac{\text{kmol}}{\text{m}^3}, 320\text{K})$ for one period of operation. The symbols \circ and \times denote the initial ($t = 0 \text{ hr}$) and final ($t = 1 \text{ hr}$) state of these closed-loop system trajectories, respectively.

where $t_0 = 0 \text{ hr}$ and $t_{100} = 1 \text{ hr}$. It has been confirmed by these sets of simulations that the LEMPC through time-varying process operation improves the economic closed-loop performance by 10 % on average against steady-state operation by LMPC.

4.4.2 Operation subject to bounded process disturbances

Considering the material constraint which needs to be satisfied through each period of process operation, a decreasing finite prediction horizon sequence N_0, \dots, N_{99} where

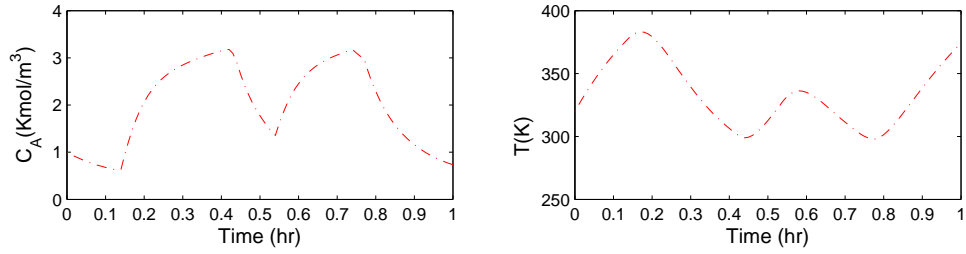


Figure 4.7: State trajectories of the process under the LEMPC design of Eq. 4.12 with initial state $(C_A(0), T(0)) = (1 \frac{\text{kmol}}{\text{m}^3}, 320\text{K})$ for one period of operation.

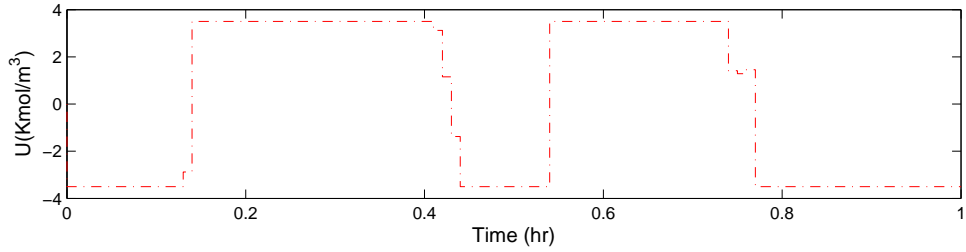


Figure 4.8: Manipulated input trajectory under the LEMPC design of Eq. 4.12 with initial state $(C_A(0), T(0)) = (1 \frac{\text{kmol}}{\text{m}^3}, 320\text{K})$ for one period of operation.

Table 4.2: Economic closed-loop performance comparison

	LEMPC	LMPC		LEMPC	LMPC		LEMPC	LMPC
1	10.43	9.53	11	11.31	10.35	21	10.85	9.94
2	11.35	10.37	12	10.60	9.67	22	10.55	9.57
3	11.12	10.17	13	10.57	9.67	23	10.46	9.56
4	10.53	9.58	14	10.99	10.05	24	11.61	10.61
5	10.94	10	15	10.59	9.64	25	10.47	9.55
6	10.36	9.44	16	10.64	9.68	26	11.53	10.54
7	11.55	10.59	17	11.50	10.53	27	10.52	9.56
8	10.70	9.73	18	10.79	9.81	28	11.06	10.11
9	11.09	10.14	19	10.68	9.77	29	11.48	10.49
10	10.84	9.94	20	10.61	9.71	30	11.36	10.40

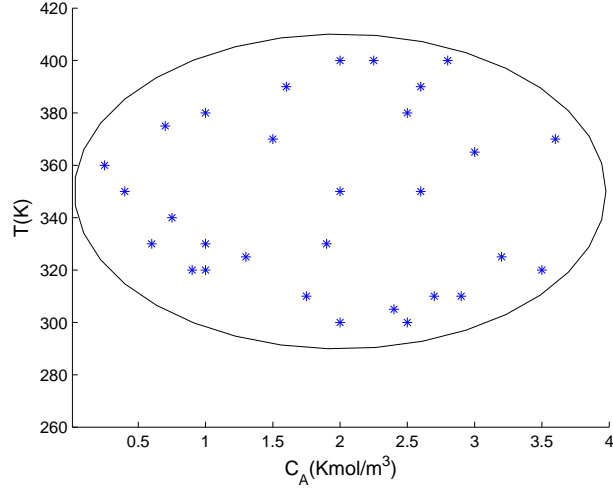


Figure 4.9: 30 different initial states for evaluation of LEMPC and LMPC schemes from an economic cost function point of view.

$N_i = 100 - i$ and $i = 0, \dots, 99$ is utilized at different sampling times. At each sampling time t_k , after solving an auxiliary LMPC problem with prediction horizon N_k , the LEMPC with prediction horizon N_k takes into account the control action and cost constraints and adjusts its finite prediction horizon to predict the future system evolution up to time $t_N = 1 \text{ hr}$ to maximize the cost of Eq. 4.44. Since the LEMPC is evaluated at discrete-time instants during the closed-loop simulation, the material constraint is enforced as follows:

$$\sum_{i=0}^{N_k-1} u_{LEMPC}(t_i) = \sum_{i=0}^{N_k-1} u_{LMPC}(t_i) \quad (4.45)$$

The above equation indicates that the same amount of reactant material at each sampling time is used to solve both the LMPC and the LEMPC optimization problems. For the purpose of simulations, we set $\rho_e = 400$. Also, bounded process disturbances have been added to the right hand side of the dynamic model of Eq. 4.42 which have been sampled from a gaussian distribution. The absolute values of process distur-

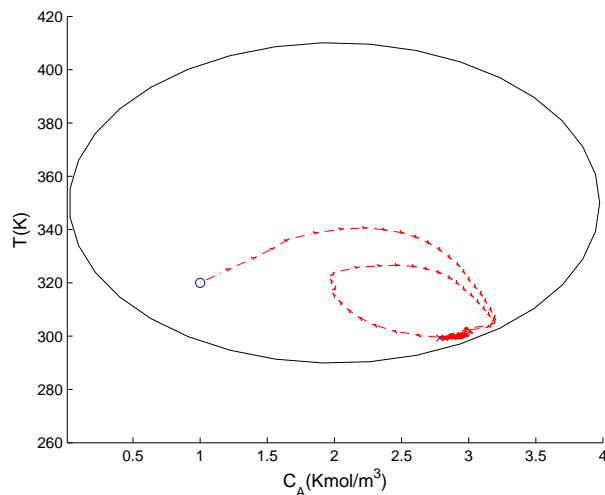


Figure 4.10: Ω_ρ and state trajectories of the process under the LEMPC design of Eq. 4.37 with initial state $(C_A(0), T(0)) = (1 \frac{\text{kmol}}{\text{m}^3}, 320\text{K})$ for one period of operation subject to bounded process disturbance. The symbols \circ and \times denote the initial ($t = 0 \text{ hr}$) and final ($t = 1 \text{ hr}$) state of these closed-loop system trajectories, respectively.

bances are bounded by 2 and 50 for the first and the second equation, respectively. Specifically, the LMPC formulation of Eq. 4.6 at sampling time t_k for the chemical process example is first solved. Having the solution of the LMPC at sampling time t_k , the LEMPC of Eq. 4.37 is then solved. Figures 4.10-4.12 display the closed-loop system state and the manipulated input with initial state $(C_A(0), T(0)) = (1 \frac{\text{kmol}}{\text{m}^3}, 320\text{K})$ for one period of operation subject to bounded process disturbances. Through time-varying operation, LEMPC achieves 15.12 in economic cost function of Eq. 4.44 while the LMPC yields 13.91.

4.5 Conclusions

This chapter focused on the design of LEMPC algorithms for a class of nonlinear systems which are capable of optimizing closed-loop performance with respect to a general objective function that may directly address economic considerations. Under

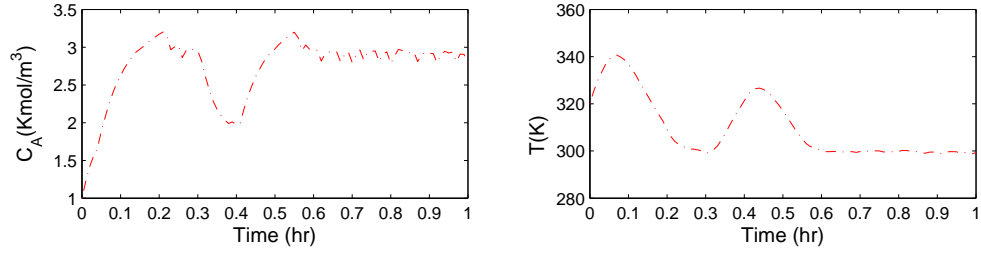


Figure 4.11: State trajectories of the process under the LEMPC design of Eq. 4.37 with initial state $(C_A(0), T(0)) = (1 \frac{\text{kmol}}{\text{m}^3}, 320\text{K})$ for one period of operation subject to bounded process disturbance.

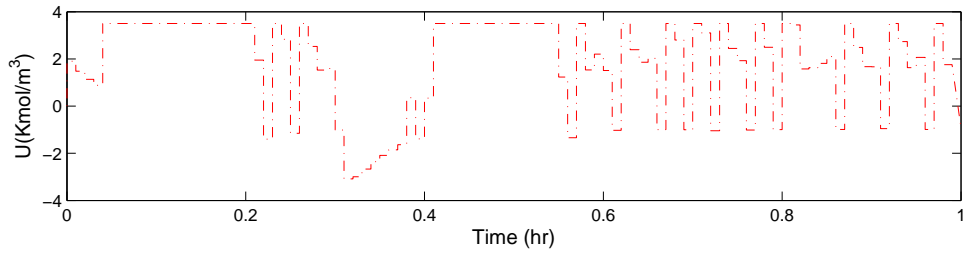


Figure 4.12: Manipulated input trajectory under the LEMPC design of Eq. 4.37 with initial state $(C_A(0), T(0)) = (1 \frac{\text{kmol}}{\text{m}^3}, 320\text{K})$ for one period of operation subject to bounded process disturbance.

appropriate stabilizability assumptions, the proposed LEMPC designs very often dictate time-varying operation to optimize an economic (typically non-quadratic) cost function in contrast to conventional LMPC designs which typically include a quadratic objective function and regulate a process at a steady-state. The proposed LEMPC algorithms took advantage of the solution of auxiliary LMPC problems at different sampling times to incorporate appropriate economic cost and control action-based constraints in the LEMPC formulations and ensure improved performance, measured by the desired economic cost, with respect to conventional LMPC. A chemical process example was used to demonstrate the proposed LEMPC algorithms.

Chapter 5

Handling Communication

Disruptions in Distributed Model

Predictive Control

In this chapter, we consider distributed MPC (DMPC) of nonlinear systems subject to communication disruptions between the distributed controllers. Specifically, we focus on the design of DMPC architectures that take explicitly into account communication channel noise and data losses between the distributed controllers. In the proposed DMPC architecture, one of the distributed controllers is responsible for ensuring closed-loop stability while the rest of the distributed controllers communicate and cooperate with the stabilizing controller to further improve the closed-loop performance. The communication between the distributed controllers is prone to communication noise and data losses. We employ a specific channel model to consider a number of realistic data transmission scenarios. In order to determine if the data transmitted through the communication channel is reliable or not, feasibility

problems are incorporated in the DMPC architecture and based on the result of these feasibility problems, the transmitted information is accepted or rejected by the stabilizing MPC. In order to ensure the stability of the closed-loop system under communication disruptions, each model predictive controller utilizes a stability constraint which is based on a suitable Lyapunov-based controller. The proposed DMPC system possesses an explicit characterization of the stability region of the closed-loop system and guarantees that the closed-loop system is ultimately bounded in an invariant set which contains the origin. The theoretical results are illustrated using a nonlinear chemical process example.

5.1 Preliminaries

5.1.1 Notation

The operator $|\cdot|$ is used to denote the Euclidean norm of a vector. A continuous function $\alpha : [0, a) \rightarrow [0, \infty)$ is said to belong to class \mathcal{K} if it is strictly increasing and satisfies $\alpha(0) = 0$. The symbol Ω_r is used to denote the set $\Omega_r := \{x \in R^{n_x} : V(x) \leq r\}$ where V is a scalar positive definite, continuous differentiable function and $V(0) = 0$, and the operator ‘\’ denotes set subtraction, that is, $A \setminus B := \{x \in R^{n_x} : x \in A, x \notin B\}$. The symbol $\text{diag}(v)$ denotes a square diagonal matrix whose diagonal elements are the elements of vector v .

5.1.2 Problem formulation

We consider nonlinear process systems described by the following state-space model:

$$\dot{x}(t) = f(x(t)) + \sum_{i=1}^m g_i(x(t))u_i(t) + k(x(t))w(t) \quad (5.1)$$

where $x(t) \in R^{n_x}$ denotes the vector of process state variables, $u_i(t) \in R^{m_{u_i}}$, $i = 1, \dots, m$, are m sets of control (manipulated) inputs and $w(t) \in R^{n_w}$ denotes the vector of disturbance variables which is assumed to be bounded, that is, $w(t) \in W$ where

$$W := \{w \in R^{n_w} : |w| \leq \theta_w, \theta_w > 0\}.$$

The m sets of inputs are restricted to be in m nonempty convex sets $U_i \subseteq R^{m_{u_i}}$, $i = 1, \dots, m$, which are defined as follows:

$$U_i := \{u_i \in R^{m_{u_i}} : |u_i| \leq u_i^{\max}\}, i = 1, \dots, m$$

where u_i^{\max} , $i = 1, \dots, m$, are the magnitudes of the input constraints. We will design m distributed controllers to compute the m sets of control inputs, respectively.

We assume that f , g_i , $i = 1, \dots, m$, and k are locally Lipschitz vector, matrix and matrix functions, respectively and that the origin is an equilibrium of the unforced nominal system (i.e., system of Eq. 5.1 with $u_i(t) = 0$, $i = 1, \dots, m$, $w(t) = 0$ for all t) which implies that $f(0) = 0$. We also assume that the state x of the system is sampled synchronously and the time instants at which we have state measurement samplings are indicated by the time sequence $\{t_{k \geq 0}\}$ with $t_k = t_0 + k\Delta$, $k = 0, 1, \dots$ where t_0 is the initial time and Δ is the sampling time.

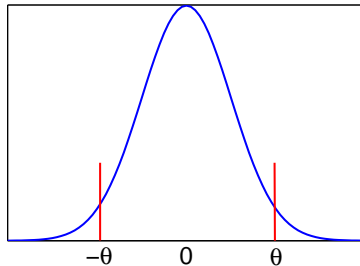


Figure 5.1: Bounded communication channel noise.

5.1.3 Model of the communication channel

We consider data losses and noise in communication between the m distributed controllers. For a given input $r \in R^{m_u}$ to the communication channel, the output $\tilde{r} \in R^{m_u}$ is characterized as

$$\tilde{r} = lr + n \quad (5.2)$$

where l is a Bernoulli random variable with parameter α and $n \in R^{m_u}$ is a vector whose elements are white gaussian noise with zero mean and the same variance σ^2 . The random variable l is used to model data losses in the communication channel. The white noise, n , is used to model channel noise, quantization error or any other error to the transmitted signal, and it is independent of the data losses in a probabilistic sense. If the receiver determines that a successful transmission is made, then $l = 1$, otherwise $l = 0$. Furthermore, in order to obtain deterministic stability results, we assume that, when a successful transmission is made, the noise, n , attached to the input signal, r , is bounded by θ (that is $|n| \leq \theta$) as shown in Fig. 5.1. Both assumptions are meaningful from a practical standpoint; please see the example in Section 5.4. We assume that the capacity of the communication channel [20] is high enough so that we can transmit data through it with a high rate.

Remark 5.1. *Note that there are a variety of approaches to detect whether data loss*

has happened at the receiver side of a communication channel. One common approach is to measure the power of the received signal and compare it with a pre-configured signal transmission power level. If the power of the received signal is much smaller than the pre-configured signal transmission power level, then data loss is declared; and if the power of the received signal is close to the pre-configured signal transmission power level, then transmission is assumed to be successful.

5.1.4 Lyapunov-based controller

We assume that there exists a Lyapunov-based controller $h(x)$ which renders the origin of the nominal closed-loop system asymptotically stable with $u_1 = h(x)$ and $u_i = 0$ ($i = 2, \dots, m$), while satisfying the input constraint on u_1 for all the states x inside a given stability region. We note that this assumption is essentially equivalent to the assumption that the process is stabilizable or that the pair (A, B) in the case of linear systems is stabilizable. Using converse Lyapunov theorems [71, 59, 18], this assumption implies that there exist functions $\alpha_i(\cdot)$, $i = 1, 2, 3, 4$ of class \mathcal{K} and a continuously differentiable Lyapunov function $V(x)$ for the nominal closed-loop system, that satisfy the following inequalities:

$$\begin{aligned}
 \alpha_1(|x|) &\leq V(x) \leq \alpha_2(|x|) \\
 \frac{\partial V(x)}{\partial x}(f(x) + g_1(x)h(x)) &\leq -\alpha_3(|x|) \\
 \left| \frac{\partial V(x)}{\partial x} \right| &\leq \alpha_4(|x|) \\
 h(x) &\in U_1
 \end{aligned} \tag{5.3}$$

for all $x \in D \subseteq R^{n_x}$ where D is an open neighborhood of the origin. We denote the region Ω_ρ as the stability region of the closed-loop system under the control inputs $u_1 = h(x)$ and $u_i = 0$ ($i = 2, \dots, m$). By continuity, the local Lipschitz property

assumed for the functions $f(x), g_i(x)$ where $i = 1, \dots, m$ and $k(x)$ and the fact that the manipulated inputs u_i belong to the convex sets U_i , it can be concluded that there exists a positive constant M such that

$$|f(x(t)) + \sum_{i=1}^m g_i(x(t))u_i(t) + k(x(t))w(t)| \leq M \quad (5.4)$$

for all $x \in \Omega_\rho$, $u_i \in U_i$ and $w \in W$. In addition, by the continuous differentiable property of the Lyapunov function V and the Lipschitz property assumed for the functions $f(x), g_i(x)$ and $k(x)$, there exist positive constants L_x, L_{ui} , and L_w such that

$$\begin{aligned} \left| \frac{\partial V(x)}{\partial x} f(x) - \frac{\partial V(x')}{\partial x} f(x') \right| &\leq L_x |x - x'| \\ \left| \frac{\partial V(x)}{\partial x} g_i(x) - \frac{\partial V(x')}{\partial x} g_i(x') \right| &\leq L_{ui} |x - x'|, i = 1, \dots, m \\ \left| \frac{\partial V(x)}{\partial x} k(x) \right| &\leq L_w \end{aligned} \quad (5.5)$$

for all $x, x' \in \Omega_\rho$, $u_i \in U_i$ and $w \in W$. These constants will be employed in the proof of the stability of the closed-loop system (Theorem 5.1 in Section 5.3).

Remark 5.2. *Note that while there are currently no general methods for constructing Lyapunov functions for general nonlinear systems, for broad classes of nonlinear systems arising in the context of chemical process control applications, quadratic Lyapunov functions are widely used and provide very good estimates of closed-loop stability regions; please see example in Section 5.4.*

5.2 DMPC with communication disruptions

In our previous work [61], a DMPC architecture with flawless communication between controllers was introduced. In practice, however, there is communication disruption including channel noise and data loss between distributed controllers. The objective of

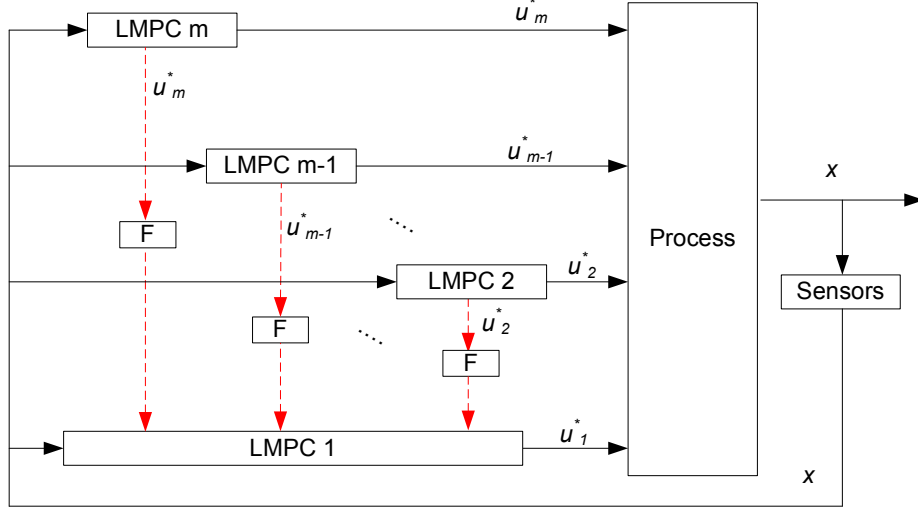


Figure 5.2: Distributed LMPC control architecture (F means solving a feasibility problem).

this chapter (see also [41, 40]) is to propose a DMPC framework which deals with communication disruptions while maintaining closed-loop stability and improving closed-loop performance. In the sequel, we design m LMPCs to calculate the m sets of control inputs, respectively, and refer to the controller calculate u_i ($i = 1, \dots, m$) as LMPC i . In the proposed methodology, LMPC 1 is responsible for the stability of the closed-loop while the rest of LMPCs (i.e., LMPC 2 to LMPC m) communicate and cooperate with LMPC 1 to improve the closed-loop performance. The proposed DMPC design inherits the closed-loop stability from the Lyapunov-based controller $h(\cdot)$. A schematic diagram of the proposed DMPC design for systems subject to communication disruptions between distributed controllers is depicted in Fig. 5.2.

We propose to use the following implementation strategy:

1. All LMPCs receive the sensor measurements $x(t_k)$ at sampling time t_k .
2. For $i = 2, \dots, m$

2.1. LMPC i evaluates the optimal input trajectory of u_i based on $x(t_k)$ and

sends the first step input values of u_i to its corresponding actuators.

2.2. LMPC i sends the entire optimal input trajectory of u_i to LMPC 1 through a communication channel.

3. LMPC 1 solves a feasibility problem for each input trajectory it received to determine if the trajectory should be accepted or rejected.

5. LMPC 1 evaluates the future input trajectory of u_1 based on $x(t_k)$ and the results of the feasibility problems for the trajectories it received from LMPC i with $i = 2, \dots, m$.

6. LMPC 1 sends the first step input value of u_1 to its corresponding actuators.

In the sequel, we describe the design of LMPC j ($j = 2, \dots, m$) and its corresponding feasibility problem and the design of LMPC 1.

Upon receiving the sensor measurement $x(t_k)$, LMPC j obtains its optimal input trajectory by solving the following optimization problem:

$$\min_{u_j \in \mathcal{S}(\Delta)} \int_0^{N\Delta} [\tilde{x}^j(\tau)^T Q_c \tilde{x}^j(\tau) + \sum_{i=1}^m u_i^T(\tau) R_{ci} u_i(\tau)] d\tau \quad (5.6a)$$

$$\dot{\tilde{x}}^j(\tau) = f(\tilde{x}^j(\tau)) + \sum_{i=1}^m g_i(\tilde{x}^j(\tau)) u_i(\tau) \quad (5.6b)$$

$$u_1(\tau) = h(\tilde{x}^j(q\Delta)), \quad \forall \tau \in [q\Delta, (q+1)\Delta) \quad (5.6c)$$

$$u_i(\tau) = 0, \quad \forall 2 \leq i \leq m \ \& \ i \neq j \quad (5.6d)$$

$$\tilde{x}^j(0) = x(t_k) \quad (5.6e)$$

$$u_j(\tau) \in U_j \quad (5.6f)$$

$$\frac{\partial V(x(t_k))}{\partial x} g_j(x(t_k)) u_j(0) \leq 0 \quad (5.6g)$$

where $S(\Delta)$ is the family of piece-wise constant functions with sampling period Δ , Q_c and R_{ci} ($i = 1, \dots, m$) are positive definite weight matrices that define the cost, $q = 0, \dots, N - 1$, $x(t_k)$ is the state measurement obtained at t_k , \tilde{x}^j is the predicted trajectory of the nominal system for the input trajectory computed by the LMPC j , and N is the prediction horizon. We note that in order to simplify the notation, $\frac{\partial V(x(t_k))}{\partial x}$ is used to denote $\frac{\partial V(x(t))}{\partial x}|_{t=t_k}$. In the prediction of the future evolution of the system by LMPC j , it is assumed that LMPC 1 applies the explicit Lyapunov-based controller $h(\cdot)$ while the rest of the controllers apply zero. While this LMPC formulation intends to improve the closed-loop performance, Eq. 5.6g ensures that the implemented control action contributes to further decrease of the value of the derivative of the Lyapunov function.

Let $u_j^*(\tau|t_k)$ denote the optimal solution of the optimization problem of Eq. 5.6. LMPC j sends the first step value of $u_j^*(\tau|t_k)$ to its actuators and transmits the whole optimal trajectory through the communication channel to LMPC 1. LMPC 1 receives a corrupted version of $u_j^*(\tau|t_k)$ which can be formulated as:

$$\tilde{u}_j(\tau|t_k) = l u_j^*(\tau|t_k) + n$$

If data losses occur during the transmission of the control input trajectory from LMPC j to LMPC 1, LMPC 1 assumes that LMPC j applies a zero input (i.e., $u_j = 0$). Note that in this chapter, we do not consider explicitly the step of determining whether data losses occur or not in the transmission of input trajectories. Please see Remark 5.1 on approaches of determining transmission data losses.

When a transmission of the input trajectory $u_j^*(\tau|t_k)$ is successful, LMPC 1 re-

ceives $\tilde{u}_j(\tau|t_k)$ which is a noise-corrupted version of $u_j^*(\tau|t_k)$. To determine the reliability of the received information, LMPC 1 solves a feasibility problem. Based on the result of the feasibility problem, LMPC 1 determines if the received information should be accepted or rejected. The feasibility problem for the information received from LMPC j is as follows:

$$\text{find } z \in S(\Delta)$$

$$\tilde{u}_j(\tau|t_k) - \theta \leq z(\tau) \leq \tilde{u}_j(\tau|t_k) + \theta \quad (5.7a)$$

$$z(\tau) \in U_j \quad (5.7b)$$

$$\frac{\partial V(x(t_k))}{\partial x} g_j(x(t_k)) z(0) > 0 \quad (5.7c)$$

According to the bounded noise value and the received signal from the communication channel, LMPC 1 considers all the possibilities of noise effect on the optimal trajectory of LMPC j (i.e., constraint of Eq. 5.7a) and checks whether in these cases LMPC j satisfies the constraint of Eq. 5.7c. Note that when the optimization problem of Eq. 5.7 is not feasible, it is guaranteed that the original signal $u_j^*(\tau|t_k)$ after transmission through the channel still satisfies the stability constraint of Eq. 5.6g. The feasibility of this problem is used to test whether there exists any possible value of the noise that could (due to corruption) end up making the implemented control action cause an increase in the Lyapunov function derivative, i.e., that $\frac{\partial V(x(t_k))}{\partial x} g_j(x(t_k)) u_j(0) > 0$. If the problem is infeasible, it is guaranteed that the noise cannot make the control action destabilizing, and hence, the control action is accepted. On the other hand, if the problem is feasible, it opens up the possibility of the noise rendering the control action destabilizing, and hence, it is discarded. We also note that there is no

requirement that θ is sufficient small, however, larger values of θ increase the range of $z(\tau)$ and influence the feasibility of the problem of Eq. 5.7.

If the optimization problem of Eq. 5.7 is not feasible, then the trajectory information received by LMPC 1 (i.e., $\tilde{u}_j(\tau|t_k)$) is used in the evaluation of LMPC 1; and if the optimization problem of Eq. 5.7 is feasible, then $\tilde{u}_j(\tau|t_k)$ is discarded and a zero trajectory for u_j will be used in the evaluation of LMPC 1. If we define the trajectory of u_j that is used in the evaluation of LMPC 1 as $\tilde{u}_j^*(\tau|t_k)$, then it is defined as follows:

$$\tilde{u}_j^*(\tau|t_k) = \begin{cases} \tilde{u}_j(\tau|t_k) & \text{if (5.7) is not feasible and there} \\ & \text{is no data loss} \\ \mathbf{0} & \text{if (5.7) is feasible or there exists} \\ & \text{data loss} \end{cases}$$

where $\mathbf{0} \in R^{m_{u_j}}$. Note that when data loss in the communication channel occurs, a zero trajectory of u_j is also used in the evaluation of LMPC 1. Note also that the above strategy on the use of the corrupted communication information is just one of many possible options to handle communication disruptions in the DMPC architecture.

Employing \tilde{u}_j^* where $j = 2, \dots, m$, LMPC 1 obtains its optimal trajectory according to the following optimization problem:

$$\min_{u_1 \in S(\Delta)} \int_0^{N\Delta} [\tilde{x}^1(\tau)^T Q_c \tilde{x}^1(\tau) + \sum_{i=1}^m u_i^T(\tau) R_{ci} u_i(\tau)] d\tau$$

$$\dot{\tilde{x}}^1(\tau) = f(\tilde{x}^1(\tau)) + \sum_{i=1}^m g_i(\tilde{x}^1(\tau)) u_i(\tau) \quad (5.8a)$$

$$u_1(\tau) \in U_1 \quad (5.8b)$$

$$u_j(\tau) = \tilde{u}_j^*(\tau|t_k), \quad j = 2, \dots, m \quad (5.8c)$$

$$\tilde{x}(0) = x(t_k) \quad (5.8d)$$

$$\frac{\partial V(x(t_k))}{\partial x} g_1(x(t_k)) u_1(0) \leq \frac{\partial V(x(t_k))}{\partial x} g_1(x(t_k)) h(x(t_k)) \quad (5.8e)$$

In this formulation, LMPC 1 takes advantage of the knowledge of $m - 1$ feasibility problems (i.e., \tilde{u}_j^* , $j = 2, \dots, m$) and the Lyapunov-based controller $h(\cdot)$ to predict the future evolution of the system \tilde{x}^1 . Let $u_1^*(\tau|t_k)$ denote the optimal solution of the optimization problem of Eq. 5.6.

Based on the solutions of the m LMPC optimization problems, the manipulated inputs of the proposed DMPC design are defined as follows:

$$u_i(t) = u_i^*(t - t_k|t_k), \quad \forall t \in [t_k, t_{k+1}) \quad i = 1, \dots, m. \quad (5.9)$$

Remark 5.3. *It should be mentioned that the white gaussian noise considered in this chapter is the accumulation of thermal effects and quantization errors. We did not consider the effects of multi-path transmission, terrain blocking, interference, etc. Further, in this chapter, we assume that when packet loss happens, all of the information we want to transmit is lost; however, without loss of generality, we can extend the results in this chapter to the case in which data loss happens only in some packets of information following a similar methodology like Eq. 5.7 to deal with this issue. The interested reader may refer to [20] and [84] for more details on communication channel modeling.*

5.3 DMPC Stability

As it will be proved in Theorem 5.1 below, the proposed DMPC framework takes advantage of the constraints of Eqs. 5.6g and 5.8e to compute the optimal trajectories u_1, \dots, u_m such that the Lyapunov function value $V(x(t_k))$ is a decreasing sequence with a lower bound and achieves the closed-loop stability of the system.

Theorem 5.1. *Consider the system of Eq. 5.1 in closed-loop under the DMPC design of Eqs. 5.6-5.9 based on a controller $u_1 = h(x)$ that satisfies the conditions of Eq. 5.3. Let $\epsilon_w > 0$, $\Delta > 0$ and $\rho > \rho_s > 0$ satisfy the following constraint:*

$$-\alpha_3(\alpha_2^{-1}(\rho_s)) + (L_x + \sum_{i=1}^m L_{u_i} u_i^{\max})M\Delta + L_w\theta_w \leq -\epsilon_w/\Delta. \quad (5.10)$$

If $x(t_0) \in \Omega_\rho$ and if $\rho^ \leq \rho$ where $\rho^* = \max\{V(x(t + \Delta)) : V(x(t)) \leq \rho_s\}$, then the state $x(t)$ of the closed-loop system is ultimately bounded in Ω_{ρ^*} .*

Proof 5.1. The proof consists of two parts. We first prove that the optimization problems of Eqs. 5.6 and 5.8 are feasible for all states $x \in \Omega_\rho$. Subsequently, we prove that, under the DMPC design of Eqs. 5.6-5.9, the state of the system of Eq. 5.1 is ultimately bounded in a region that contains the origin.

Part 1: First, we consider the feasibility of LMPC j ($j = 2, \dots, m$) and then focus on the feasibility of LMPC 1. All input trajectories of $u_j(\tau)$ such that $u_j(\tau) = 0$, $\forall \tau \in [0, N\Delta)$ satisfy all the constraints (including the input constraint of Eq. 5.6f and the constraint of Eq. 5.6g) of LMPC j , thus the feasibility of LMPC j is obtained. The feasibility of LMPC 1 follows because all input trajectories $u_1(\tau)$ such that $u_1(\tau) = h(x(t_k))$, $\forall \tau \in [0, \Delta)$ and $u_1(\tau) = 0$, $\forall \tau \in [\Delta, N\Delta)$ are feasible solutions to the optimization problem of LMPC 1 since all such trajectories satisfy the input constraint of Eq. 5.8b and the constraint of Eq. 5.8e; this is guaranteed by the assumed property

of the Lyapunov-based controller $h(\cdot)$.

Part 2: Considering the inequalities of Eq. 5.3, addition of inequalities of Eqs. 5.6g and 5.8e for $j = 2, \dots, m$ implies that if $x(t_k) \in \Omega_\rho$, the following inequality holds:

$$\begin{aligned} \frac{\partial V(x(t_k))}{\partial x}(f(x(t_k)) + \sum_{i=1}^m g_i(x(t_k))u_i^*(0|t_k)) &\leq \frac{\partial V(x(t_k))}{\partial x}(f(x(t_k)) + g_1(x(t_k))h(x(t_k))) \\ &\leq -\alpha_3(|x(t_k)|). \end{aligned} \quad (5.11)$$

The time derivative of the Lyapunov function along the actual state trajectory $x(t)$ of system of Eq. 5.1 in $t \in [t_k, t_{k+1})$ is given by:

$$\dot{V}(x(t)) = \frac{\partial V(x)}{\partial x}(f(x(t)) + \sum_{i=1}^m g_i(x(t))u_i^*(0|t_k) + k(x(t))w(t)). \quad (5.12)$$

Adding and subtracting $\frac{\partial V(x(t_k))}{\partial x}(f(x(t_k)) + \sum_{i=1}^m g_i(x(t_k))u_i^*(0|t_k))$ to the right-hand-side of Eq. 5.12 and taking Eq. 5.11 into account, we obtain the following inequality:

$$\begin{aligned} \dot{V}(x(t)) &\leq -\alpha_3(|x(t_k)|) + \frac{\partial V(x)}{\partial x}(f(x(t)) + \sum_{i=1}^m g_i(x(t))u_i^*(0|t_k) + k(x(t))w(t)) \\ &\quad - \frac{\partial V(x(t_k))}{\partial x}(f(x(t_k)) + \sum_{i=1}^m g_i(x(t_k))u_i^*(0|t_k)). \end{aligned} \quad (5.13)$$

From Eq. 5.5 and the inequality of Eq. 5.13, the following inequality is obtained for all $x(t_k) \in \Omega_\rho \setminus \Omega_{\rho_s}$:

$$\dot{V}(x(t)) \leq -\alpha_3(\alpha_2^{-1}(\rho_s)) + L_w|w(t)| + (L_x + \sum_{i=1}^m L_{u_i}u_i^*(0|t_k))|x(t) - x(t_k)|. \quad (5.14)$$

Taking into account Eq. 5.4 and the continuity of $x(t)$, the following bound can be written for all $t \in [t_k, t_{k+1})$, $|x(t) - x(t_k)| \leq M\Delta$. Using this expression, we obtain the following bound on the time derivative of the Lyapunov function for $t \in [t_k, t_{k+1})$,

for all initial states $x(t_k) \in \Omega_\rho \setminus \Omega_{\rho_s}$:

$$\dot{V}(x(t)) \leq -\alpha_3(\alpha_2^{-1}(\rho_s)) + (L_x + \sum_{i=1}^m L_{u_i} u_i^{max})M\Delta + L_w\theta_w.$$

If the condition of Eq. 5.10 is satisfied, then there exists $\epsilon_w > 0$ such that the following inequality holds for $x(t_k) \in \Omega_\rho \setminus \Omega_{\rho_s}$:

$$\dot{V}(x(t)) \leq -\epsilon_w/\Delta, \quad \forall t \in [t_k, t_{k+1}).$$

Integrating this bound on $t \in [t_k, t_{k+1})$, we obtain that:

$$\begin{aligned} V(x(t_{k+1})) &\leq V(x(t_k)) - \epsilon_w \\ V(x(t)) &\leq V(x(t_k)), \quad \forall t \in [t_k, t_{k+1}) \end{aligned} \tag{5.15}$$

for all $x(t_k) \in \Omega_\rho \setminus \Omega_{\rho_s}$. Using Eq. 5.15 recursively, it is proved that, if $x(t_0) \in \Omega_\rho \setminus \Omega_{\rho_s}$, the state converges to Ω_{ρ_s} in a finite number of sampling times without leaving the stability region. Once the state converges to $\Omega_{\rho_s} \subseteq \Omega_{\rho^*}$, it remains inside Ω_{ρ^*} for all times. This statement holds because of the definition of ρ^* . This proves that the closed-loop system under the distributed LMPC design is ultimately bounded in Ω_{ρ^*} .

Remark 5.4. *The condition of Eq. 5.10 guarantees that if the state of the closed-loop system at a sampling time t_k is outside the level set $V(x(t_k)) = \rho_s$ but inside the level set $V(x(t_k)) = \rho$, the derivative of the Lyapunov function of the state of the closed-loop system is negative under the proposed design.*

Remark 5.5. *For nonlinear systems under continuous control implementation, a sufficient condition for invariance is that the Lyapunov function is decreasing on the boundary of a set. For systems with continuous-time dynamics and sample-and-hold control implementation, this condition is not sufficient because the derivative may*

become positive during the sampling period and the system may leave the set before a new sample is obtained. Based on Theorem 5.1, ρ^* is the maximum value that the Lyapunov function can achieve in a time period of length Δ when $x(t_k) \in \Omega_{\rho_s}$. Ω_{ρ^*} defines an invariant set for the state $x(t)$ under sample-and-hold implementation of the control action.

Remark 5.6. Note that the closed-loop stability is guaranteed by the constraints of Eqs. 5.6g and 5.8e. The use of the corrupted input trajectory information of u_j (i.e., \tilde{u}_j) where $j = 2, \dots, m$ does not affect the feasibility of the optimization problems of Eqs. 5.6 and 5.8 as well as the stability of the closed-loop system; however, it does affect the closed-loop system performance. This is the reason for the introduction of the feasibility problem of Eq. 5.7 which is used to decide whether the corrupted information can be used to improve the closed-loop performance.

Remark 5.7. We have partitioned Ω_ρ into two regions ($\Omega_\rho \setminus \Omega_{\rho_s}$ and Ω_{ρ_s}). When $x(t_k) \in \Omega_\rho$, it follows that either $x(t_k) \in \Omega_\rho \setminus \Omega_{\rho_s}$ or $x(t_k) \in \Omega_{\rho_s}$. As we stated and proved in Theorem 5.1, according to definition of ρ^* , once the state converges to $\Omega_{\rho_s} \subseteq \Omega_{\rho^*}$, it remains inside Ω_{ρ^*} for all times. If $x(t_k) \in \Omega_\rho \setminus \Omega_{\rho_s}$ and the condition in Eq 5.10 is satisfied, the state converges to Ω_{ρ_s} in a finite number of sampling times without leaving the stability region. In both cases, the state will be bounded in Ω_{ρ^*} .

Remark 5.8. In this chapter, we deal with communication disruptions and do not address issues arising due to faults in the control actuators or in the control system (e.g., [75, 15]). Also, we assume that all the distributed controllers have access to the full system state. In Chapter 6, we will address the scenario in which each controller has access only to partial state information and utilizes an observer to estimate the full system state subject to bounded process noise (disturbance). It should be mentioned that due to the effect of disturbances and model errors, the controllers should

be updated at every several sampling time with full system state information in order to provide deterministic closed-loop stability properties.

5.4 Application to a chemical process

The process considered in this study is a three vessel, reactor-separator system consisting of two continuously stirred tank reactors (CSTRs) and a flash tank separator shown in Fig. 5.3 [15]. A feed stream to the first CSTR F_{10} contains the reactant A which is converted into the desired product B . The desired product B can then further react into an undesired side-product C . The effluent of the first CSTR along with additional fresh feed F_{20} makes up the inlet to the second CSTR. The reactions $A \rightarrow B$ and $B \rightarrow C$ (referred to as 1 and 2, respectively) take place in the two CSTRs in series before the effluent from CSTR 2 is fed to a flash tank. The overhead vapor from the flash tank is condensed and recycled to the first CSTR, and the bottom product stream is removed. A small portion of the overhead is purged before being recycled to the first CSTR. All the three vessels are assumed to have static holdup. The dynamic equations describing the behavior of the system, obtained through material and energy balances under standard modeling assumptions, are given below:

$$\frac{dT_1}{dt} = \frac{F_{10}}{V_1}(T_{10} - T_1) + \frac{F_r}{V_1}(T_3 - T_1) + \frac{-\Delta H_1}{\rho C_p} k_1 e^{\frac{-E_1}{RT_1}} C_{A1} + \frac{-\Delta H_2}{\rho C_p} k_2 e^{\frac{-E_2}{RT_1}} C_{A1} + \frac{Q_1}{\rho C_p V_1} \quad (5.16a)$$

$$\frac{dC_{A1}}{dt} = \frac{F_{10}}{V_1}(C_{A10} - C_{A1}) + \frac{F_r}{V_1}(C_{Ar} - C_{A1}) - k_1 e^{\frac{-E_1}{RT_1}} C_{A1} - k_2 e^{\frac{-E_2}{RT_1}} C_{A1} \quad (5.16b)$$

$$\frac{dC_{B1}}{dt} = \frac{-F_{10}}{V_1} C_{B1} + \frac{F_r}{V_1}(C_{Br} - C_{B1}) + k_1 e^{\frac{-E_1}{RT_1}} C_{A1} \quad (5.16c)$$

$$\frac{dC_{C1}}{dt} = \frac{-F_{10}}{V_1} C_{C1} + \frac{F_r}{V_1}(C_{Cr} - C_{C1}) + k_2 e^{\frac{-E_2}{RT_1}} C_{A1} \quad (5.16d)$$

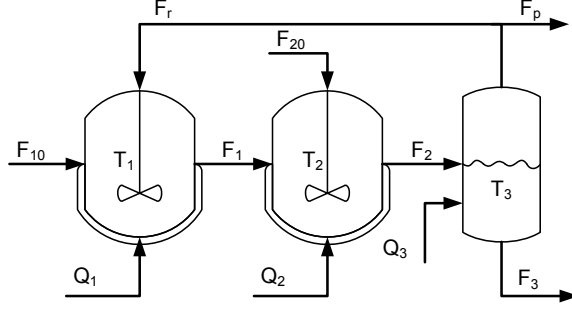


Figure 5.3: Two CSTRs and a flash tank with recycle stream.

$$\begin{aligned} \frac{dT_2}{dt} = & \frac{F_1}{V_2}(T_1 - T_2) + \frac{(F_{20} + \Delta F_{20})}{V_2}(T_{20} - T_2) + \frac{-\Delta H_1}{\rho C_p} k_1 e^{\frac{-E_1}{RT_2}} C_{A2} + \frac{-\Delta H_2}{\rho C_p} k_2 e^{\frac{-E_2}{RT_2}} C_{A2} \\ & + \frac{Q_2}{\rho C_p V_2} \end{aligned} \quad (5.16e)$$

$$\frac{dC_{A2}}{dt} = \frac{F_1}{V_2}(C_{A1} - C_{A2}) + \frac{(F_{20} + \Delta F_{20})}{V_2}(C_{A20} - C_{A2}) - k_1 e^{\frac{-E_1}{RT_2}} C_{A2} - k_2 e^{\frac{-E_2}{RT_2}} C_{A2} \quad (5.16f)$$

$$\frac{dC_{B2}}{dt} = \frac{F_1}{V_2}(C_{B1} - C_{B2}) - \frac{(F_{20} + \Delta F_{20})}{V_2} C_{B2} + k_1 e^{\frac{-E_1}{RT_2}} C_{A2} \quad (5.16g)$$

$$\frac{dC_{C2}}{dt} = \frac{F_1}{V_2}(C_{C1} - C_{C2}) - \frac{(F_{20} + \Delta F_{20})}{V_2} C_{C2} + k_2 e^{\frac{-E_2}{RT_2}} C_{A2} \quad (5.16h)$$

$$\frac{dT_3}{dt} = \frac{F_2}{V_3}(T_2 - T_3) - \frac{H_{vap} F_r}{\rho C_p V_3} + \frac{Q_3}{\rho C_p V_3} \quad (5.16i)$$

$$\frac{dC_{A3}}{dt} = \frac{F_2}{V_3}(C_{A2} - C_{A3}) - \frac{F_r}{V_3}(C_{Ar} - C_{A3}) \quad (5.16j)$$

$$\frac{dC_{B3}}{dt} = \frac{F_2}{V_3}(C_{B2} - C_{B3}) - \frac{F_r}{V_3}(C_{Br} - C_{B3}) \quad (5.16k)$$

$$\frac{dC_{C3}}{dt} = \frac{F_2}{V_3}(C_{C2} - C_{C3}) - \frac{F_r}{V_3}(C_{Cr} - C_{C3}) \quad (5.16l)$$

Each of the tanks has an external heat input/removal actuator. The model of the flash tank separator is derived under the assumption that the relative volatility for

each of the species remains constant within the operating temperature range of the flash tank. This assumption allows calculating the mass fractions in the overhead based upon the mass fractions in the liquid portion of the vessel. It has also been assumed that there is a negligible amount of reaction taking place in the separator. The following algebraic equations model the composition of the overhead stream relative to the composition of the liquid holdup in the flash tank:

$$\begin{aligned}
 C_{Ar} &= \frac{\alpha_A C_{A3}}{K}, \quad C_{Br} = \frac{\alpha_B C_{B3}}{K}, \quad C_{Cr} = \frac{\alpha_C C_{C3}}{K} \\
 K &= \alpha_A C_{A3} \frac{MW_A}{\rho} + \alpha_B C_{B3} \frac{MW_B}{\rho} + \alpha_C C_{C3} \frac{MW_C}{\rho} + \alpha_D x_D \rho
 \end{aligned} \tag{5.17}$$

where x_D is the mass fraction of the solvent in the flash tank liquid holdup and is found from a mass balance. The definitions for the variables used in Eqs. 5.16-5.17 can be found in Table 5.1, with the parameter values given in Table 5.2.

The system of Eqs. 5.16-5.17 is numerically simulated using a standard Euler integration method. Process noise was added to the right-hand side of each equation in the process of Eq. 5.16 to simulate disturbances/model uncertainty and it is generated as autocorrelated noise of the form $w_k = \phi w_{k-1} + \xi_k$ where $k = 0, 1, \dots$ is the discrete time step of 0.001 *hr*, ξ_k is generated by a normally distributed random variable with standard deviation σ_p , and ϕ is the autocorrelation factor and w_k is bounded by θ_p , that is $|w_k| \leq \theta_p$. Table 5.3 contains the parameters used in generating the process noise.

We assume that the state measurements which include the temperatures and species concentrations in the three vessels are available synchronously and continuously at time instants $\{t_{k \geq 0}\}$ with $t_k = t_0 + k\Delta$, $k = 0, 1, \dots$ where t_0 is the initial time and Δ is the sampling time. For the simulations carried out in this section, we pick the initial time to be $t_0 = 0$ and the sampling time to be $\Delta = 0.01 \text{ hr} = 36 \text{ sec}$.

Table 5.1: Process variables

C_{A1}, C_{A2}, C_{A3}	concentrations of A in vessels 1, 2, 3
C_{B1}, C_{B2}, C_{B3}	concentrations of B in vessels 1, 2, 3
C_{C1}, C_{C2}, C_{C3}	concentrations of C in vessels 1, 2, 3
C_{Ar}, C_{Br}, C_{Cr}	concentrations of A, B, C in the recycle
T_1, T_2, T_3	temperatures in vessels 1, 2, 3
T_{10}, T_{20}	feed stream temperatures to vessels 1, 2
F_1, F_2, F_3	effluent flow rates from vessels 1, 2, 3
F_{10}, F_{20}	feed stream flow rates to vessels 1, 2
C_{A10}, C_{A20}	concentrations of A in the feed stream to vessels 1, 2
F_r	recycle flow rate
V_1, V_2, V_3	volumes of vessels 1, 2, 3
u_1, u_2, u_3, u_4	manipulated inputs
E_1, E_2	activation energy for reactions 1, 2
k_1, k_2	pre-exponential values for reactions 1, 2
$\Delta H_1, \Delta H_2$	heats of reaction for reactions 1, 2
H_{vap}	heat of vaporization
$\alpha_A, \alpha_B, \alpha_C, \alpha_D$	relative volatilities of A, B, C, D
MW_A, MW_B, MW_C	molecular weights of $A, B,$ and C
Q_1, Q_2, Q_3	heat inputs into vessels 1, 2, 3
C_p, R, ρ	heat capacity, gas constant and solution density

Table 5.2: Parameter values

$T_{10} = 300, T_{20} = 300$	K
$F_{10} = 5, F_{20} = 5, F_r = 1.9$	$\frac{m^3}{hr}$
$C_{A10} = 4, C_{A20} = 3$	$\frac{kmol}{m^3}$
$V_1 = 1.0, V_2 = 0.5, V_3 = 1.0$	m^3
$E_1 = 5E4, E_2 = 5.5E4$	$\frac{kJ}{kmol}$
$k_1 = 3E6, k_2 = 3E6$	$\frac{1}{hr}$
$\Delta H_1 = -5E4, \Delta H_2 = -5.3E4$	$\frac{kJ}{kmol}$
$H_{vap} = 5$	$\frac{kJ}{kmol}$
$C_p = 0.231$	$\frac{kJ}{kgK}$
$R = 8.314$	$\frac{kJ}{kmolK}$
$\rho = 1000$	$\frac{kg}{m^3}$
$\alpha_A = 2, \alpha_B = 1, \alpha_C = 1.5, \alpha_D = 3$	unitless
$MW_A = 50, MW_B = 50, MW_C = 50$	$\frac{kg}{kmol}$

Table 5.3: Disturbance parameters.

	σ_p	ϕ	θ_p		σ_p	ϕ	θ_p		σ_p	ϕ	θ_p
C_{A1}	0.1	0.7	0.09	C_{A2}	0.1	0.7	0.09	C_{A3}	0.1	0.7	0.09
C_{B1}	0.02	0.7	0.01	C_{B2}	0.1	0.7	0.03	C_{B3}	0.1	0.7	0.02
C_{C1}	0.02	0.7	0.01	C_{C2}	0.1	0.7	0.01	C_{C3}	0.02	0.7	0.01
T_1	10	0.7	1.17	T_2	10	0.7	1.35	T_3	10	0.7	1.35

Table 5.4: Steady-state values for Q_{1s} , Q_{2s} and Q_{3s} .

Q_{1s}	0 [KJ/hr]	Q_{2s}	0 [KJ/hr]	Q_{3s}	0 [KJ/hr]
----------	-----------	----------	-----------	----------	-----------

Table 5.5: Steady-state values for x_s .

C_{A1s}	3.31 [kmol/m ³]	C_{A2s}	2.75 [kmol/m ³]	C_{A3s}	2.88 [kmol/m ³]
C_{B1s}	0.17 [kmol/m ³]	C_{B2s}	0.45 [kmol/m ³]	C_{B3s}	0.50 [kmol/m ³]
C_{C1s}	0.04 [kmol/m ³]	C_{C2s}	0.11 [kmol/m ³]	C_{C3s}	0.12 [kmol/m ³]
T_{1s}	369.53 [K]	T_{2s}	435.25 [K]	T_{3s}	435.25 [K]

The first set of manipulated inputs is the heat injected to or removed from the three vessels, that is $u_1 = [Q_1 - Q_{1s} \ Q_2 - Q_{2s} \ Q_3 - Q_{3s}]^T$; the second set of manipulated inputs is the deviated inlet flow rate to vessel 2, that is $u_2 = \Delta F_{20} = F_{20} - F_{20s}$. The open-loop system has one unstable and two stable steady states. The control objective is to regulate the system to the unstable steady-state x_s corresponding to the operating point defined by Q_{1s} , Q_{2s} , Q_{3s} and F_{20s} . The steady-state values for u_1 and u_2 are zero. Taking this control objective into account, the process model belongs to the following class of nonlinear systems: $\dot{x}(t) = f(x(t)) + g_1(x(t))u_1(t) + g_2(x(t))u_2(t) + w(t)$ where $x^T = [x_1 \ x_2 \ x_3 \ x_4 \ x_5 \ x_6 \ x_7 \ x_8 \ x_9 \ x_{10} \ x_{11} \ x_{12}] = [T_1 - T_{1s} \ C_{A1} - C_{A1s} \ C_{B1} - C_{B1s} \ C_{C1} - C_{C1s} \ T_2 - T_{2s} \ C_{A2} - C_{A2s} \ C_{B2} - C_{B2s} \ C_{C2} - C_{C2s} \ T_3 - T_{3s} \ C_{A3} - C_{A3s} \ C_{B3} - C_{B3s} \ C_{C3} - C_{C3s}]$ is the state, $u_1^T = [u_{11} \ u_{12} \ u_{13}] = [Q_1 - Q_{1s} \ Q_2 - Q_{2s} \ Q_3 - Q_{3s}]$ and $u_2 = \Delta F_{20} = F_{20} - F_{20s}$ are the manipulated inputs which are deviation variables and are subject to the constraints $|u_{1i}| \leq 10^4 \text{ KJ/hr}$ ($i = 1, 2, 3$) and $|u_2| \leq 5 \text{ m}^3/\text{hr}$, and w is a bounded noise.

We consider a quadratic Lyapunov function $V(x) = x^T P x$ with $P = \text{diag}([10 \ 10^4 \ 10^4 \ 10^4 \ 10 \ 10^4 \ 10^4 \ 10^4 \ 10^4 \ 10^4 \ 10^4 \ 10^4])$ and design the controller $h(x)$ as three PI controllers with proportional gains $K_{p1} = K_{p2} = K_{p3} = 8000$ and integral time constants $\tau_{I1} = \tau_{I2} = \tau_{I3} = 10$ based on the measurements of T_1 , T_2 and T_3 , respectively. The values of the weights in P have been chosen in a way such that the Lyapunov-based controller $h(x)$ satisfies the input constraints, stabilizes the closed-loop system and provides good closed-loop performance. Note that, in the absence of process and measurement noise, this design of $h(x)$ manipulating $u_1^T = [Q_1 \ Q_2 \ Q_3]$ can stabilize the closed-loop system asymptotically without the help of u_2 . Based on $h(x)$ and $V(x)$, we design LMPC 1 to determine u_1 and LMPC 2 to determine u_2 following the forms given in Eqs. 5.6 and 5.8, respectively. In the design of the LMPC controllers, the weighting matrices are chosen to be

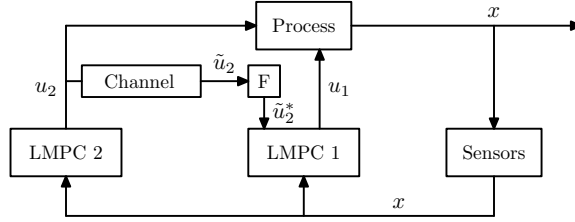


Figure 5.4: Distributed LMPC control architecture for chemical process example (F means solving a feasibility problem).

$Q_c = \text{diag}([10 \ 10^4 \ 10^4 \ 10^4 \ 9 \ 10^4 \ 10^4 \ 10^4 \ 10 \ 10^4 \ 10^4 \ 10^4])$, $R_1 = \text{diag}([(5 \ 5 \ 5) \cdot 10^{-4}])$ and $R_2 = 10^4$. The prediction horizon for the optimization problem is $N = 5$ with a time step of $\Delta = 0.01 \text{ hr}$. The initial condition which is utilized to carry out the simulations is $x(0)^T = [362.14 \ 3.1191 \ 0.13 \ 0.01 \ 348.21 \ 2.01 \ 0.16 \ 0.01 \ 462.55 \ 2.31 \ 0.26 \ 0.01]$. We set the communication channel noise power (σ^2), the data loss probability α and the noise bound θ to 0.01, 0.1 and 0.25, respectively. Figure 5.4 depicts the proposed control design for the chemical process example which is composed of two LMPCs.

The state trajectory of the process under the proposed DMPC design from the initial state are shown in Fig. 5.5. These figures show that the proposed control design drive the temperatures and the concentrations in the closed-loop system close to the desired steady-state and achieves closed-loop stability.

To emphasize the importance of solving the feasibility problem in LMPC 1 during obtaining its optimal input trajectory, we have carried out a set of simulations to compare the proposed design with our previous control scheme [61] in which LMPC 1 incorporates the received channel signal in its optimization problem without any pre-processing. In other words, in this case LMPC 1 ignores the fact that whether communication channel noise and data loss effects violate the feasibility constraints of LMPC 2 optimization problem. We have carried out a number of simulations to compare the proposed DMPC design with our previous DMPC design with the same

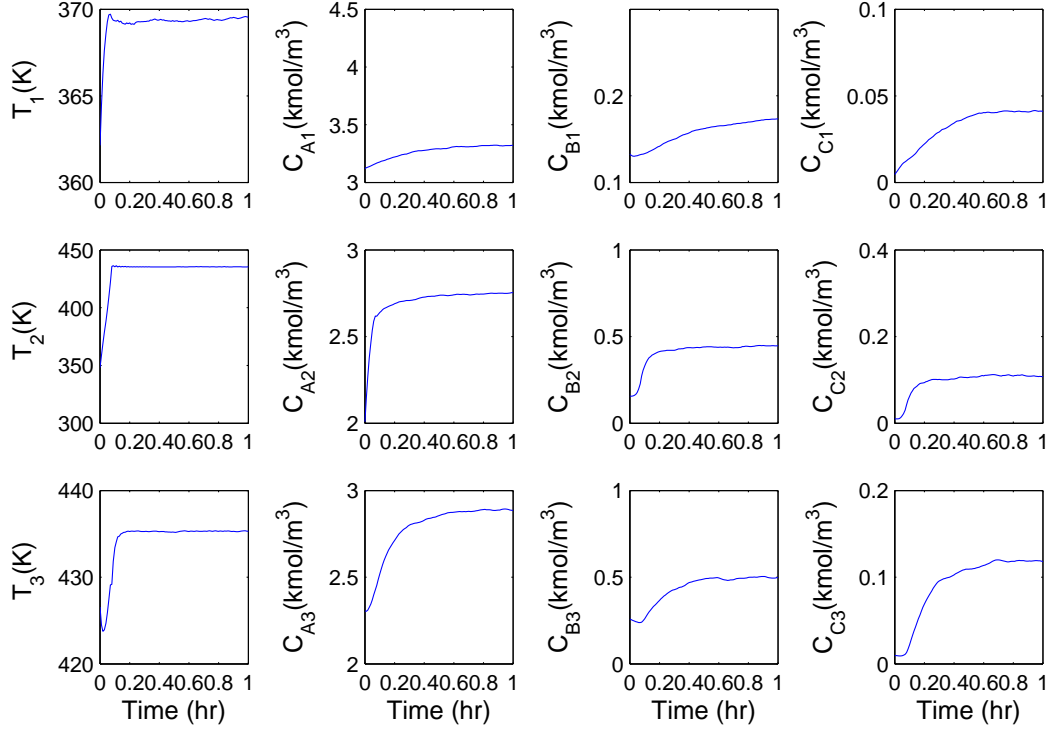


Figure 5.5: State trajectories of the process under the proposed DMPC design.

parameters and initial condition from a performance index point of view. Table 5.6 shows the total cost computed for 10 different closed-loop simulations under the proposed DMPC design and our previous control scheme. To carry out this comparison, we have computed the total cost of each simulation with different operating conditions (different initial states and process disturbances) based on the index of the following form:

$$J = \sum_{i=0}^G x(t_i)^T Q_c x(t_i) + u_1(t_i)^T R_{c1} u_1(t_i) + u_2(t_i)^T R_{c2} u_2(t_i)$$

where t_0 is the initial time of the simulations and $t_G = 1 \text{ hr}$ is the final time of the simulations. As we can see in Table 5.6, the proposed distributed LMPC design has a cost lower than the previous DMPC design in all 10 simulations. This illustrates that in this example, the proposed distributed LMPC design improves our previous design from a closed-loop performance point of view.

Table 5.6: Total performance cost ($\times 10^7$) along the closed-loop system trajectories.

sim.	Prop.	Prev.	sim.	Prop.	Prev.
1	5.486	5.488	6	2.549	2.559
2	2.497	2.519	7	1.691	1.697
3	1.771	1.785	8	6.688	6.695
4	1.203	1.215	9	6.632	6.633
5	3.163	3.181	10	2.498	2.515

Table 5.7: Total performance cost ($\times 10^7$) along the closed-loop system trajectories for different data loss probabilities and $\sigma^2 = 0.01$.

α	Prop.	Prev.	α	Prop.	Prev.
0.05	6.803	6.900	0.30	6.808	6.901
0.10	6.779	6.908	0.35	6.818	6.906
0.15	6.821	6.897	0.40	6.779	6.901
0.20	6.821	6.905	0.45	6.793	6.893
0.25	6.801	6.899	0.50	6.744	6.895

Finally, we have carried out a set of simulations to evaluate the performance of the proposed DMPC design over the one in [61] from a closed-loop performance index point of view under different communication channel noise powers and data loss probabilities. Tables 5.7 and 5.8 show the total cost computed for 10 different data loss probabilities and noise powers compared to our previous DMPC design, respectively. As it can be seen from these tables, the proposed DMPC design is superior from a closed-loop performance point of view for different noise power and data loss probability values. It should be mentioned that the number of feasible and infeasible solutions of the optimization problem of Eq. 5.7 depends on the bound on the communication channel noise; as this bound increases, the number of feasible solutions increases. For the simulation results corresponding to Fig. 5.5, LMPC 1 utilizes the received signal about 8% of the total number of transmissions.

Table 5.8: Total performance cost ($\times 10^7$) along the closed-loop system trajectories for different channel noise power values and $\alpha = 0.1$.

σ^2	Prop.	Prev.	σ^2	Prop.	Prev.
0.005	6.787	6.907	0.030	6.802	6.899
0.010	6.762	6.894	0.035	6.809	6.894
0.015	6.820	6.895	0.040	6.769	6.939
0.020	6.744	6.898	0.045	6.835	6.909
0.025	6.841	6.893	0.050	6.756	6.892

Remark 5.9. *Note that the DMPC design in [61] can still guarantee the closed-loop system stability in the presence of communication disruptions; however, the closed-loop performance may be degraded. In this chapter, we propose a practical approach to deal with communication disruptions to improve the closed-loop performance while maintaining the stability properties of the closed-loop system. In all simulations, the proposed DMPC design accounting for disruptions yields reduced performance costs compared to the previous DMPC design, even though this benefit cannot be proved to hold in general.*

5.5 Conclusions

In this chapter, we proposed a DMPC design for nonlinear systems taking into account explicitly communication disruptions (i.e., data losses and channel noise) between the distributed controllers. In the proposed DMPC architecture, one of the distributed controllers is responsible for ensuring closed-loop stability while the rest of the distributed controllers communicate and cooperate with the stabilizing controller to further improve the closed-loop performance. To determine if the data transmitted through the communication channel is reliable or not, feasibility problems were incorporated in the DMPC design and based on the result of these feasibility problems, the

transmitted information was accepted or rejected by the stabilizing MPC. In order to ensure the stability of the closed-loop system under communication disruptions, each distributed controller utilized a stability constraint which is based on a suitable Lyapunov-based controller. The proposed DMPC system possesses an explicit characterization of the closed-loop system stability region and guarantees that the closed-loop system is ultimately bounded in an invariant set which contains the origin. The theoretical results were demonstrated through a nonlinear chemical process example.

Chapter 6

Multirate Distributed Model Predictive Control of Nonlinear Uncertain Systems

In the chapter, we consider the design of a network-based DMPC system using multi-rate sampling for large-scale nonlinear uncertain systems composed of several coupled subsystems. This problem formulation is important in the context of large-scale networks of heterogeneous components that involve variables that exhibit dynamics and are sampled in significantly different time-scales, for example, energy/water networks as well as chemical process networks. Specifically, we assume that the states of each local subsystem can be divided into fast sampled states and slowly sampled states. Furthermore, we assume that there is a distributed controller associated with each subsystem and the distributed controllers are connected through a shared communication network. We propose to design the distributed controllers via Lyapunov-based MPC (LMPC) and coordinate their actions in an iterative fashion to guarantee closed-

loop stability when full system state measurements (both fast and slow) are available. The transmitted information over the shared communication network is subject to communication channel noise. When only fast sampled states are available, the distributed controllers operate in a decentralized fashion to improve closed-loop performance. Sufficient conditions under which the state of the closed-loop system is ultimately bounded in an invariant region containing the origin are derived. The theoretical results are demonstrated through a nonlinear chemical process example.

6.1 Preliminaries

6.1.1 Notation and class of nonlinear systems

The operator $|\cdot|$ is used to denote Euclidean norm of a vector while $|\cdot|_Q$ refers to the square of the weighted Euclidean norm, defined by $|x|_Q = x^T Q x$. A continuous function $\alpha : [0, a) \rightarrow [0, \infty)$ is said to belong to class \mathcal{K} if it is strictly increasing and satisfies $\alpha(0) = 0$. The symbol Ω_r is used to denote the set $\Omega_r := \{x \in R^{n_x} : V(x) \leq r\}$ where V is a scalar positive definite, continuous differentiable function and $V(0) = 0$, and the operator $'/'$ denotes set subtraction, that is, $A/B := \{x \in R^{n_x} : x \in A, x \notin B\}$. The symbol $\text{diag}(v)$ denotes a square diagonal matrix whose diagonal elements are the elements of vector v . We consider a class of nonlinear systems composed of m interconnected subsystems where each of the subsystems can be described by the following state-space model:

$$\dot{x}_i(t) = f_i(x) + g_{si}(x)u_i(t) + k_i(x)w_i(t) \quad (6.1)$$

where $i = 1, \dots, m$, $x_i(t) \in R^{n_{x_i}}$ denotes the vector of state variables of subsystem i , $u_i(t) \in R^{n_{u_i}}$ and $w_i(t) \in R^{n_w}$ denote the set of control (manipulated) inputs and disturbances associated with subsystem i , respectively. The variable $x \in R^{n_x}$ denotes the state of the entire nonlinear system which is composed of the states of the m subsystems, that is $x = [x_1^T \cdots x_i^T \cdots x_m^T]^T \in R^{n_x}$. The dynamics of x can be described as follows:

$$\dot{x}(t) = f(x) + \sum_{i=1}^m g_i(x)u_i(t) + k(x)w(t) \quad (6.2)$$

where $f = [f_1^T \cdots f_i^T \cdots f_m^T]^T$, $g_i = [\mathbf{0}^T \cdots g_{si}^T \cdots \mathbf{0}^T]^T$ with $\mathbf{0}$ being the zero matrix of appropriate dimensions, k is a matrix composed of k_i ($i = 1, \dots, m$) and zeros whose explicit expression is omitted for brevity, and

$w = [w_1^T \cdots w_i^T \cdots w_m^T]^T$ is assumed to be bounded, that is, $w(t) \in W$ with $W := \{w \in R^{n_w} : |w| \leq \theta, \theta > 0\}$. The m sets of inputs are restricted to be in m nonempty convex sets $U_i \subseteq R^{n_{u_i}}$, $i = 1, \dots, m$, which are defined as $U_i := \{u_i \in R^{n_{u_i}} : |u_i| \leq u_i^{\max}\}$ where u_i^{\max} , $i = 1, \dots, m$, is the magnitude of the constraint on the inputs of the i -th subsystem. We will design m controllers to compute the m sets of control inputs u_i , $i = 1, \dots, m$, respectively. We will refer to the controller computing u_i as controller i . We assume that f , g_i , $i = 1, \dots, m$, and k are locally Lipschitz vector functions and that the origin is an equilibrium point of the unforced nominal system (i.e., system of Eq. 6.2 with $u_i(t) = 0$, $i = 1, \dots, m$, $w(t) = 0$ for all t) which implies that $f(0) = 0$.

6.1.2 Modeling of measurements and communication

We assume that the states of each of the m subsystems, x_i ($i = 1, \dots, m$), are divided into two parts: $x_{f,i}$, states that can be measured at each sampling time (e.g., temperatures and pressures) and $x_{s,i}$, states which are sampled at a relatively slow rate (e.g., species concentrations). Specifically, we assume that $x_{f,i}$, are available at synchronous time instants $t_p = t_0 + p\Delta$, $p = 0, 1, \dots$, where t_0 is the initial time and Δ is the sampling time; and assume that $x_{s,i}$, are available every T sampling times (i.e., $x_{s,i}$, are available at t_k with $k = 0, T, 2T, \dots$). Note that, in order to simplify the development, we assume that the slowly sampled states of different subsystems are all available at the same time instants. This modeling of measurements is relevant to systems involving heterogeneous measurements which have different sampling rates; please see the example in Section 6.3. We also assume that for each subsystem its local sensors, actuators and controller are connected using point-to-point links, which implies that $x_{f,i}$ and $x_{s,i}$ are available without delay to controller i once they are measured and that the controllers for different subsystems are connected through a shared communication network and communicate when the full (fast and slow) system state is available. We consider measurement noise and communication network noise. Specifically, we consider measurement noise caused by the lack of complete accuracy of measurement sensors. This type of noise is defined as the difference between the reading value of a state from a sensor and the true value of the state. We assume that the sensor reading values of states $x_{f,i}$ and $x_{s,i}$ are $\tilde{x}_{f,i}^s$ and $\tilde{x}_{s,i}^s$, respectively; and $\tilde{x}_{f,i}^s$ and $\tilde{x}_{s,i}^s$ are modeled as follows: $\tilde{x}_{f,i}^s = x_{f,i} + n_{x_{f,i}}^s$, $\tilde{x}_{s,i}^s = x_{s,i} + n_{x_{s,i}}^s$ where $n_{x_{f,i}}^s$ and $n_{x_{s,i}}^s$ are the measurement noise terms associated with $x_{f,i}$ and $x_{s,i}$, respectively. The measurement noise is assumed to be bounded; that is, $|n_{x_{f,i}}^s| \leq \theta_{x_{f,i}}^s$ and $|n_{x_{s,i}}^s| \leq \theta_{x_{s,i}}^s$ with $\theta_{x_{f,i}}^s$ and $\theta_{x_{s,i}}^s$ being positive real numbers. It should be mentioned

that this assumption on the type of measurement noise is meaningful from a practical standpoint due to the limit on the accuracy of the measurement sensors and the fact that measurement noise is usually modeled as a percentage of the actual value.

At t_k with $k = 0, T, 2T, \dots$, when fast and slowly sampled states are available to each controller, the distributed controllers exchange information which is subject to communication channel noise. Specifically, we assume that controller i sends $\tilde{x}_i^s = [\tilde{x}_{f,i}^{s,T} \ \tilde{x}_{s,i}^{s,T}]^T$ as well as its control input trajectory u_i to the other controllers; and the values received by controller j ($j \neq i$), \tilde{x}_i^j and \tilde{u}_i^j , are modeled as follows: $\tilde{x}_i^j = \tilde{x}_i^s + n_{x_i}^{c,j}$, $\tilde{u}_i^j = u_i + n_{u_i}^j$ where $n_{x_i}^{c,j}$ and $n_{u_i}^j$ are the communication noise terms. The communication noise terms are also assumed to be bounded; that is, $|n_{x_i}^{c,j}| \leq \theta_{x_i}^{c,j}$ and $|n_{u_i}^j| \leq \theta_{u_i}$ with $\theta_{x_i}^{c,j}$ and θ_{u_i} being positive real numbers. According to the above modeling, at time t_k with $k = 0, T, 2T, \dots$ when fast and slowly sampled states are available, the state information received by controller i ($i = 1, \dots, m$) is described as follows:

$$\tilde{x}^i(t_k) = [\tilde{x}_1^i, \dots, \tilde{x}_{i-1}^i, \tilde{x}_i^s, \tilde{x}_{i+1}^i, \dots, \tilde{x}_m^i] = x(t_k) + n_x^i \quad (6.3)$$

where $n_x^i \in R^{n_x}$ denotes combined communication and measurement noise and $|n_x^i| \leq \theta_x^i$ with θ_x^i being a suitable composition of $\theta_{x_{f,i}}^s$, $\theta_{x_{s,i}}^s$ and $\theta_{x_j}^{c,i}$ ($j \neq i$). This class of systems is relevant to the case of large-scale chemical processes that are controlled by distributed control systems that exchange information over a shared communication network through which it is not cost-effective to communicate at every sampling time. Instead, in order to achieve closed-loop stability and good closed-loop performance, the controllers communicate every several sampling times. Please see Fig. 6.1 for a schematic of such type of DMPC system with the local controllers designed via Lyapunov-based MPC techniques.

6.1.3 Lyapunov-based controller

We assume that there exists a locally Lipschitz Lyapunov-based controller $h(x) = [h_1^T(x) \cdots h_m^T(x)]^T$ such that when the m control inputs are determined as $u_i = h_i(x)$, $i = 1, \dots, m$, the origin of the nominal interconnected closed-loop system is asymptotically stable and the input constraints are satisfied for all x inside a compact set. This assumption implies that there exist a continuously differentiable Lyapunov function $V(x)$ for the nominal closed-loop system, a class \mathcal{K} function $\alpha_1(\cdot)$ which bounds the value of the Lyapunov function from above and a class \mathcal{K} function $\alpha_2(\cdot)$ which bounds the time derivative of the Lyapunov function from above [59, 18]. Specifically, from this assumption, we have the following inequalities:

$$\begin{aligned} V(x) &\leq \alpha_1(|x|), \quad h_i(x) \in U_i, \quad i = 1, \dots, m \\ \frac{\partial V(x)}{\partial x} \left(f(x) + \sum_{i=1}^m g_i(x)h_i(x) \right) &\leq -\alpha_2(|x|) \end{aligned} \quad (6.4)$$

for all $x \in \Omega_\rho$ where Ω_ρ denotes the stability region of the closed-loop system under $h(x)$. The set Ω_ρ is usually chosen to be a level set of $V(x)$.

Since the manipulated inputs u_i , $i = 1, \dots, m$, and the disturbance w are bounded in closed sets and the vector fields f , g_i , $i = 1, \dots, m$, k are locally Lipschitz, we can have the following inequality for all the states within the stability region (i.e., $x \in \Omega_\rho$):

$$\left| f(x) + \sum_{i=1}^m g_i(x)u_i + k(x)w \right| \leq M \quad (6.5)$$

where M is a positive constant. Moreover, if we take into account the continuous differentiable property of the Lyapunov function $V(x)$, we can write the following

inequalities:

$$\begin{aligned}
\left| \frac{\partial V(x)}{\partial x} f(x) - \frac{\partial V(x')}{\partial x} f(x') \right| &\leq L_x |x - x'| \\
|f(x) - f(x')| &\leq C_x |x - x'| \\
\left| \frac{\partial V(x)}{\partial x} g_i(x) - \frac{\partial V(x')}{\partial x} g_i(x') \right| &\leq L_{u_i} |x - x'| \\
\left| \frac{\partial V(x)}{\partial x} k(x) \right| &\leq L_w, \quad \left| \frac{\partial V(x)}{\partial x} g_i(x) \right| \leq C_{g_i} \\
|h_i(x) - h_i(x')| &\leq C_{h_i} |x - x'|, \quad |g_i(x)| \leq M_{g_i} \\
|g_i(x) - g_i(x')| &\leq C_{u_i} |x - x'|, \quad |k(x)| \leq M_w
\end{aligned} \tag{6.6}$$

with $L_x, L_{u_i}, C_x, C_{h_i}, C_{u_i}, C_{g_i}, M_{g_i}, M_w$ $i = 1, \dots, m$, and L_w being positive constants for all $x, x' \in \Omega_\rho$, $u_i \in U_i$, $i = 1, \dots, m$, and $w \in W$. Note that the inequalities of Eqs. 6.4-6.6 are derived from the basic assumptions (i.e., Lipschitz vector fields and existence of stabilizing Lyapunov-based controller) used in this chapter. The various constants involved in the upper bounds are not assumed to be arbitrarily small.

Remark 6.1. *The construction of Lyapunov functions can be carried out in a number of ways using techniques like, for example, sum-of-squares methods. For broad classes of nonlinear systems arising in the context of chemical process control applications, quadratic Lyapunov functions are widely used and provide very good estimates of closed-loop stability regions; please see example in Section 6.3.*

6.2 Multirate DMPC

6.2.1 Multirate DMPC implementation strategy

In this chapter, the m controllers manipulating the m sets of inputs will be designed through LMPC techniques (see also [43, 42]). For the LMPC associated with controller i , $i = 1, \dots, m$, we will refer to it as LMPC i . A schematic of the control

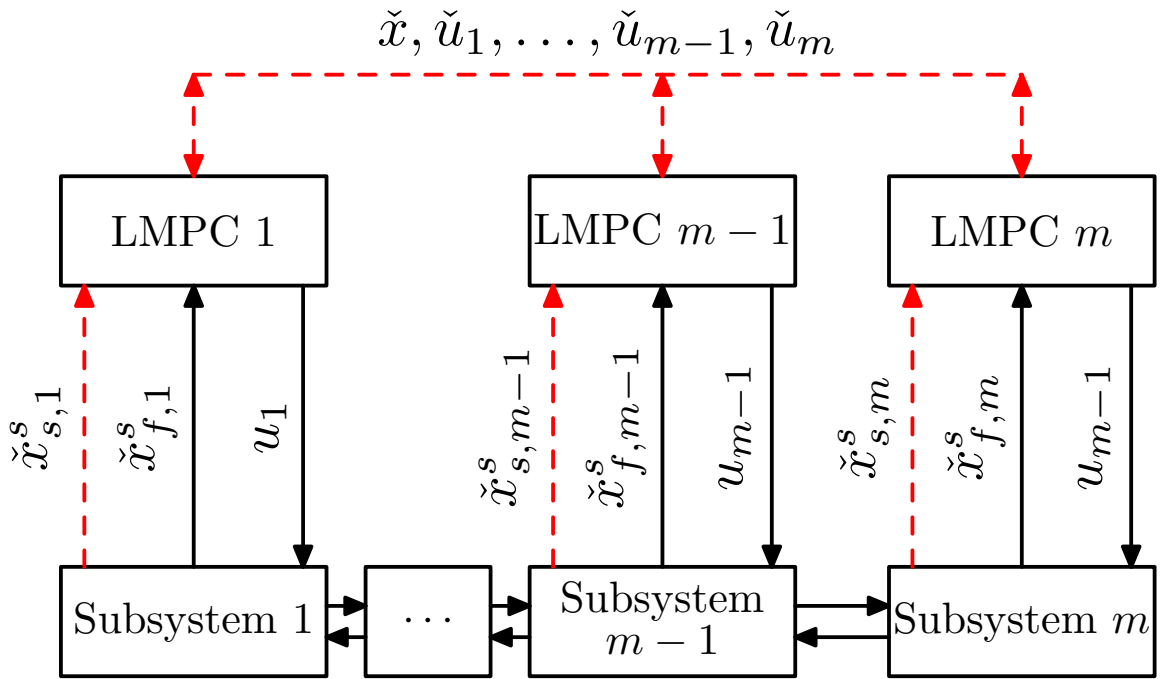


Figure 6.1: Distributed LMPC control architecture (solid line denotes fast state sampling and/or point-to-point links; dashed line denotes slow state sampling and/or shared communication networks).

system is shown in Fig. 6.1. At a sampling time in which slowly and fast sampled states are available, the distributed controllers coordinate their actions and predict future input trajectories which, if applied until the next instant that both slowly and fast sampled states are available, guarantee closed-loop stability. At a sampling time in which only fast sampled states are available, each distributed controller tries to further optimize the input trajectories calculated at the last instant in which the controllers communicated, within a constrained set of values to improve the closed-loop performance with the help of the available fast sampled states of its subsystem.

The proposed implementation strategy of the DMPC architecture at time instants in which fast and slowly sampled states are available is as follows:

1. At t_k with $k = 0, T, 2T, \dots$, all the controllers first broadcast their local subsystem states to the other controllers and then evaluate their future input trajectories in an iterative fashion with initial input guesses generated by $h(\cdot)$.
2. At iteration c ($c \geq 1$)
 - 2.1. Each controller evaluates its own future input trajectory based on $\tilde{x}^i(t_k)$ (noisy version of $x(t_k)$) and the last received control input trajectories (initial input guesses generated by $h(\cdot)$ when $c = 1$).
 - 2.2. All the distributed controllers exchange their latest future input trajectories. Based on the input information, each controller calculates and stores the corresponding value of the cost.
 - 2.3. If a termination condition is satisfied, each controller sends its entire future input trajectory corresponding to the smallest value of the cost to its actuators; if the termination condition is not satisfied, go to step 2.1 ($c \leftarrow c + 1$).

The proposed implementation strategy of the DMPC architecture at time instants when only local fast sampled states are available is as follows:

1. Controller i , $i = 1, \dots, m$, receives its local fast sampled states, $\tilde{x}_{f,i}^s$.
2. Each controller i estimates the current full system state and evaluates its future input trajectory and sends the first step input value to its actuators.

6.2.2 Multirate DMPC formulation

Before presenting the design of the LMPCs, we define a nominal sampled trajectory for each subsystem $x_h^i(\tau|t_k)$, $k = 0, T, 2T, \dots$, which will be employed in the construction of the stability constraint of LMPC i ($i = 1, \dots, m$). This nominal sampled trajectory is obtained by integrating recursively, for $t \in [t_k, t_{k+T})$ and $k = 0, T, 2T, \dots$, the following equation:

$$\begin{aligned} \dot{x}_h^i(\tau|t_k) &= f(x_h^i(\tau|t_k)) + \sum_{i=1}^m g_i(x_h^i(\tau|t_k)) h_i(x_h^i(l\Delta|t_k)), \\ \forall \tau &\in [l\Delta, (l+1)\Delta) \end{aligned} \quad (6.7)$$

with initial condition $x_h^i(0|t_k) = \tilde{x}^i(t_k)$ where $l = 0, \dots, T-1$, $\tilde{x}^i(t_k)$ is the system state received by controller i at t_k . Based on this sampled trajectory, we define the following input trajectories:

$$u_{h,j}^i(\tau|t_k) = h_j(x_h^i(l\Delta|t_k)), \forall \tau \in [l\Delta, (l+1)\Delta) \quad (6.8)$$

where $j = 1, \dots, m$. This sampled trajectory, $x_h^i(\tau|t_k)$, will be used in the LMPC i formulation.

At time t_k , $k = 0, T, 2T, \dots$, the LMPCs are evaluated in an iterative fashion to

obtain the future input trajectories. Specifically, the optimization problem of LMPC j at iteration c is as follows:

$$\min_{u_j \in S(\Delta)} \int_0^{N\Delta} \left[|\tilde{x}^j(\tau)|_{Q_c} + \sum_{i=1}^m |u_i(\tau)|_{R_{ci}} \right] d\tau \quad (6.9a)$$

$$\text{s.t. } \dot{\tilde{x}}^j(\tau) = f(\tilde{x}^j(\tau)) + \sum_{i=1}^m g_i(\tilde{x}^j(\tau))u_i \quad (6.9b)$$

$$u_i(\tau) = \check{u}_i^{*,c-1}(\tau|t_k), \quad \forall i \neq j \quad (6.9c)$$

$$|u_j(\tau) - u_j^{*,c-1}(\tau|t_k)| \leq \Delta u_j, \quad \forall \tau \in [0, T\Delta] \quad (6.9d)$$

$$u_j(\tau) \in U_j \quad (6.9e)$$

$$\tilde{x}^j(0) = \check{x}^j(t_k) \quad (6.9f)$$

$$\begin{aligned} & \frac{\partial V(\tilde{x}^j(\tau))}{\partial x} \left(\frac{1}{m} f(\tilde{x}^j(\tau)) + g_j(\tilde{x}^j(\tau))u_j(\tau) \right) \\ & \leq \frac{\partial V(x_h^j(\tau|t_k))}{\partial x} \left(\frac{1}{m} f(x_h^j(\tau|t_k)) + g_j(x_h^j(\tau|t_k))u_{h,j}^j(\tau|t_k) \right), \\ & \forall \tau \in [0, T\Delta] \end{aligned} \quad (6.9g)$$

where $S(\Delta)$ is the family of piece-wise constant functions with sampling period Δ , N is the prediction horizon, Q_c and R_{ci} , $i = 1, \dots, m$, are positive definite weight matrices, the state \tilde{x}^j is the predicted trajectory of the nominal system with u_j computed by the LMPC of Eq. 6.9 and all the other inputs are received from the other controllers (i.e., $\check{u}_i^{*,c-1}(\tau|t_k)$ which is a noisy version of $u_i^{*,c-1}(\tau|t_k)$). The optimal solution to this optimization problem is denoted by $u_j^{*,c}(\tau|t_k)$ which is defined for $\tau \in [0, N\Delta)$. Accordingly, we define the final optimal input trajectory of LMPC j (that is, the

optimal trajectories computed at the last iteration) as $u_j^{*,f}(\tau|t_k)$ which is also defined for $\tau \in [0, N\Delta)$. Note that for the first iteration of each distributed LMPC, the input trajectories defined in Eq. 6.8 are used as the initial input trajectory guesses; that is, $u_i^{*,0} = u_{h,i}^j$ with $i = 1, \dots, m$.

The constraint of Eq. 6.9d imposes a limit on the input change between two consecutive iterations. Note that this constraint does not restrict the input to be in a small region and as the iteration number increases, the final optimal input could be quite different from the initial guess. This constraint is enforced to make sure that the predicted future evolutions of the system state in the distributed controllers are close enough so that their actions are coordinated and they work together to improve the closed-loop performance. For LMPC j (i.e., u_j), the magnitude of input change between two consecutive iterations is restricted to be smaller than a positive constant Δu_j . The constraint of Eq. 6.9g is used to guarantee the closed-loop stability. The manipulated inputs of the proposed control design for $t \in [t_k, t_{k+1})$ ($k = 0, T, 2T, \dots$) are defined as follows:

$$u_i(t) = u_i^{*,f}(t - t_k|t_k), i = 1, \dots, m. \quad (6.10)$$

For the iterations in the design of Eq. 6.9, the number of iterations c may be restricted to be smaller than a maximum iteration number c_{\max} (i.e., $c \leq c_{\max}$) or/and the iterations may be terminated when a maximum computational time is reached. In order to improve the performance, between two slow sampling times, each controller uses the available local fast sampled measurements to adjust its control input based on the calculated optimal input trajectory for the current time obtained at the last time instant in which fast and slowly sampled states were available. In order to guarantee closed-loop stability, the maximum deviation of the adjusted inputs from the optimal

input trajectory at each time step is bounded. Between two slow sampling times, each controller estimates the current full system state using an observer based on the system model and the available information. Specifically, the observer for controller i takes the following form for $t \in [t_{l-1}, t_l]$:

$$\begin{aligned} \dot{\hat{x}}^i(t) = & f(\hat{x}^i(t)) + \sum_{j=1}^{m, j \neq i} g_j(\hat{x}^i(t)) \check{u}_j^{*,i}(t - t_k | t_k) \\ & + g_i(\hat{x}^i(t)) u_i^*(t) \end{aligned} \quad (6.11)$$

with initial condition $\hat{x}^i(t_{l-1}) = x_e^i(t_{l-1})$ where \hat{x}^i is the state of this observer, $\check{u}_j^{*,i}(\tau | t_k)$ is the optimal input trajectory of LMPC j ($j = 1, \dots, m, j \neq i$) received by LMPC i , $u_i^*(t)$ is the actual input that has been applied to subsystem i , and $x_e^i(t_{l-1})$ is the full state estimate obtained at t_{l-1} . The state estimate $x_e^i(t_l)$, $l \neq 0, T, 2T, \dots$, is a combination of the state of the observer of Eq. 6.11 and of the available local state information $\check{x}_{f,i}^s(t_l)$ as follows: $x_e^i(t_l) = [\hat{x}_1^i(t_l)^T \dots \check{x}_i(t_l)^T \dots \hat{x}_m^i(t_l)^T]^T$ where $\check{x}_i(t_l)^T = [\check{x}_{f,i}^{s,T} \hat{x}_{s,i}^T]$. The optimization problem of LMPC j for a time instant t_l , $l \neq 0, T, 2T, \dots$ is as follows:

$$\min_{u_j \in S(\Delta)} \int_0^{N\Delta} \left[|\tilde{x}^j(\tau)|_{Q_c} + \sum_{i=1}^m |u_i(\tau)|_{R_{ci}} \right] d\tau \quad (6.12a)$$

$$\text{s.t. } \dot{\tilde{x}}^j(\tau) = f(\tilde{x}^j(\tau)) + \sum_{i=1}^m g_i(\tilde{x}^j(\tau)) u_i \quad (6.12b)$$

$$u_i(\tau) = \check{u}_i^{*,j}(t_l - t_k + \tau | t_k), \forall i \neq j,$$

$$\tau \in [0, t_k + N\Delta - t_l] \quad (6.12c)$$

$$u_i(\tau) = h_i(\tilde{x}^j(\tau)), \forall i \neq j,$$

$$\tau \in [t_k + N\Delta - t_l, N\Delta) \quad (6.12d)$$

$$\left| u_j(\tau) - u_j^{*,f}(t_l - t_k + \tau | t_k) \right| \leq \Delta u_j,$$

$$\tau \in [0, t_k + N\Delta - t_l) \quad (6.12e)$$

$$u_j(\tau) \in U_j \quad (6.12f)$$

$$\tilde{x}^j(0) = x_e^j(t_l) \quad (6.12g)$$

where t_k is the last time instant in which both fast and slowly sampled states are available, the state \tilde{x}^j is the predicted trajectory of the nominal system with u_j computed by the LMPC of Eq. 6.12 and all the other inputs are determined by the constraints of Eqs. 6.12c and 6.12d. In this optimization problem, the input u_j is restricted to be within a bounded region around the reference input trajectories given by $u_i^{*,f}(\tau | t_k)$ and $h(x)$. The optimal solution to this optimization problem is denoted by $u_j^{*,l}(\tau | t_l)$ which is defined for $\tau \in [0, N\Delta)$. The manipulated inputs of the control design of Eq. 6.12 for $t \in [t_l, t_{l+1})$ ($l \neq 0, T, 2T, \dots$) are defined as follows:

$$u_i(t) = u_i^{*,l}(t - t_l | t_l), \quad i = 1, \dots, m. \quad (6.13)$$

In the design of Eqs. 6.9-6.10 and 6.12-6.13, the closed-loop stability of the system of Eq. 6.2 is guaranteed by the design of Eqs. 6.9-6.10 at each sampling time t_k , $k = 0, T, 2T, \dots$, when the full state measurements are available. The design of Eqs. 6.12-6.13 takes advantage of the predicted input trajectories $u_i^{*,f}$, $i = 1, \dots, m$, at sampling times t_k , $k = 0, T, 2T, \dots$, and the additional available fast-sampling state measurements to adjust the predicted inputs, $u_i^{*,f}$, to improve the closed-loop performance.

Remark 6.2. Note that in the case of linear systems and flawless communication, at each iteration, the input given by LMPC j of Eq. 6.9 may be defined as a convex combination of the current optimal input trajectory and the previous one; for example,

$$u_j^c(\tau|t_k) = \sum_{i=1}^{m, i \neq j} w_i u_j^{c-1}(\tau|t_k) + w_j u_j^{*,c}(\tau|t_k) \quad (6.14)$$

where $\sum_{i=1}^m w_i = 1$ with $0 < w_i < 1$, $u_j^{*,c}$ is the current solution given by the optimization problem of Eq. 6.9 and u_j^{c-1} is the convex combination of the solutions obtained at iteration $c - 1$. By doing this, it is possible to prove that the optimal cost of the distributed LMPC of Eq. 6.9 converges to its optimal value [3, 92]. We also note that in this case, the constraint of Eq. 6.9d can be removed and the stability of the proposed DMPC architecture is still ensured. Please see Corollary 6.1 below. We further note that for nonlinear systems it is not possible to prove the convergence of the optimal cost of the distributed optimization problem of Eq. 6.9 to the cost of the centralized LMPC [73] because the distributed LMPC does not solve the centralized LMPC in a distributed fashion due to the way the Lyapunov-based constraint of the centralized LMPC is broken down into constraints imposed on the individual LMPCs (i.e., Eq. 6.9g).

Remark 6.3. Note that when there is no measurement noise or communication noise, the implementation strategy at t_k ($k = 0, T, 2T, \dots$) guarantees that at each sampling time the optimal cost of the distributed optimization of Eq. 6.9 is upper bounded by the cost of the Lyapunov-based controller $h(\cdot)$.

6.2.3 Stability analysis

The stability of the closed-loop system is achieved due to the constraints of Eq. 6.9g incorporated in each LMPC. The stability property is presented in Theorem 6.1 below. To prove this theorem, we need the following definitions and propositions. Specifically, we first define the stability region of the closed-loop system under Lyapunov-based control, and certain state trajectories of the closed-loop system accounting for the effect of noise. Subsequently, we state four propositions that bound the discrepancy between various closed-loop system solutions for finite-time under Lyapunov-based control that will be used to state the conditions and prove the closed-loop stability result under multirate DMPC of Theorem 6.1.

Definition 6.1. *We define Ω_{ρ_n} as follows:*

$$\rho_n = \max \{V(x) : (x + n) \in \Omega_\rho, |n| \leq \theta_x\} \quad (6.15)$$

where $\theta_x = \max_{1 \leq i \leq m} \{\theta_x^i\}$ defines the upper bound on the noise n . The region Ω_{ρ_n} will be used as the stability region of the system under the Lyapunov-based controller $h(x)$ in the presence of measurement noise, process disturbances and communication noise.

Definition 6.2. *The closed-loop state trajectory of the nominal system for $t \in [t_k, t_{k+1})$ under $h(x)$ based on actual system state, $x(t_k)$, and applied in sample and hold fashion is denoted by $x_{h,2}(t)$ which is obtained by integrating, for $t \in [t_k, t_{k+1})$, the following equation:*

$$\dot{x}_{h,2}(t) = f(x_{h,2}(t)) + \sum_{i=1}^m g_i(x_{h,2}(t))h_i(x_{h,2}(t_k)) \quad (6.16)$$

where $x_{h,2}(t_k) \in \Omega_{\rho_n}$.

Definition 6.3. *The closed-loop state trajectory of the nominal system for $t \in [t_k, t_{k+1})$ under $h(x)$ based on noisy system states and applied in sample and hold fashion is*

denoted by $x_h(t)$ which is obtained by integrating, for $t \in [t_k, t_{k+1})$, the following equation:

$$\dot{x}_h(t) = f(x_h(t)) + \sum_{i=1}^m g_i(x_h(t))h_i(\check{x}_h(t_k)) \quad (6.17)$$

where $x_h(t_k) \in \Omega_{\rho_n}$, $\check{x}_h(t_k) = x_{h,2}(t_k) + n(t_k)$, $|n| \leq \theta_x$.

Proposition 6.1 below bounds the difference between the state trajectories starting from two different initial conditions in Ω_{ρ_n} (which is in the stability region Ω_ρ of the control law $h(x)$) under noise with control inputs generated by $h(x)$.

Proposition 6.1. *Consider the systems:*

$$\begin{aligned} \dot{x}_a(t) &= f(x_a(t)) + \sum_{i=1}^m g_i(x_a(t))h_i(\check{x}_a(0)) \\ \dot{x}_b(t) &= f(x_b(t)) + \sum_{i=1}^m g_i(x_b(t))h_i(\check{x}_b(0)) \end{aligned}$$

where the initial states $x_a(0), x_b(0) \in \Omega_{\rho_n}$, $|x_a(0) - x_b(0)| \leq \theta_{ab}$, $|x_a(0) - \check{x}_a(0)| \leq \theta_a$ and $|x_b(0) - \check{x}_b(0)| \leq \theta_b$. If $0 < \rho_n < \rho$, then there exists a function $f_E(\cdot, \cdot, \cdot, \cdot)$ such that $|x_a(t) - x_b(t)| \leq f_E(\theta_{ab}, \theta_a, \theta_b, t)$ for all $x_a(t), x_b(t) \in \Omega_{\rho_n}$ with $f_E(\theta_{ab}, \theta_a, \theta_b, t) = (\theta_{ab} + \frac{L_2}{L_1})e^{L_1 t} - \frac{L_2}{L_1}$ where $L_1, L_2, \theta_{ab}, \theta_a$ and θ_b are positive real numbers.

Proof 6.1. If we define $e(t) = x_a(t) - x_b(t)$, then the derivative of $e(t)$ can be calculated as $\dot{e}(t) = \dot{x}_a - \dot{x}_b$. Adding/subtracting $\sum_{i=1}^m g_i(x_a(t))h_i(\check{x}_b(0))$ to/from the expression of $\dot{e}(t)$ and using the conditions defined in Eq. 6.6 obtained by the local Lipschitz properties and the fact that $h_i(\cdot)$ satisfies input constraints, we can obtain the following inequality:

$$\begin{aligned} |\dot{e}(t)| &\leq C_x |x_a(t) - x_b(t)| + \sum_{i=1}^m M_{g_i} C_{h_i} |\check{x}_a(0) - \check{x}_b(0)| \\ &\quad + \sum_{i=1}^m u_i^{max} C_{u_i} |x_a(t) - x_b(t)|. \end{aligned} \quad (6.18)$$

Using that $|\tilde{x}_a(0) - \tilde{x}_b(0)| \leq \theta_a + \theta_b + \theta_{ab}$ and defining $L_1 = C_x + \sum_{i=1}^m u_i^{max} C_{u_i}$ and $L_2 = (\theta_a + \theta_b + \theta_{ab}) \sum_{i=1}^m M_{g_i} C_{h_i}$, we obtain $|\dot{e}(t)| \leq L_1|e(t)| + L_2$. Integrating $|\dot{e}(t)|$ with initial condition $|e(0)| \leq \theta_{ab}$, we can obtain $|e(t)| \leq (\theta_{ab} + \frac{L_2}{L_1})e^{L_1 t} - \frac{L_2}{L_1}$ which proves Proposition 6.1.

The following proposition provides sufficient conditions that ensure that $h(\cdot)$ can achieve closed-loop stability of the nominal system in the presence of bounded measurement and communication noise.

Proposition 6.2. *Consider the closed-loop nominal sampled trajectory $x_h(t)$ of the system of Eq. 6.2 as defined in Definition 6.3. Let $\Delta, \epsilon_s, \theta_x > 0$ and $0 < \rho_s < \rho_n < \rho$ satisfy:*

$$\begin{aligned} & \left(L_x + \sum_{i=1}^m u_i^{max} L_{u_i} \right) (f_E(0, 0, \theta_x, \Delta) + M\Delta) \\ & + \theta_x \sum_{i=1}^m C_{g_i} C_{h_i} - \alpha_2(\alpha_1^{-1}(\rho_s)) \leq -\epsilon_s/\Delta. \end{aligned} \quad (6.19)$$

where f_E is defined in Proposition 6.1. For any k , if $x_h(t_k) \in \Omega_{\rho_n}/\Omega_{\rho_s}$, then

$$V(x_h(t_{k+1})) \leq V(x_h(t_k)) - \epsilon_s \quad (6.20)$$

and $V(x_h(t)) \leq V(x_h(t_k))$ for $t \in [t_k, t_{k+1})$. Also, if $\rho_{min} \leq \rho_n$ where $\rho_{min} = \max\{V(x_h(t+\Delta)) : V(x_h(t)) \leq \rho_s\}$ and $x_h(t_0) \in \Omega_{\rho_n}$, then we also have $V(x_h(t_k)) \leq \max\{V(x_h(t_0)) - k\epsilon_s, \rho_{min}\}$ and $V(x_h(t)) \leq \max\{V(x_h(t_k)), \rho_{min}\}$ for $t \in [t_k, t_{k+1})$.

Proof 6.2. Following Definition 6.3, the time derivative of the Lyapunov function along the nominal sampled trajectory $x_h(t)$ of the system of Eq. 6.2 for $t \in [t_k, t_{k+1})$

is given by $\dot{V}(x_h(t)) = \frac{\partial V(x_h(t))}{\partial x} \dot{x}_h(t)$. Adding/subtracting

$$\frac{\partial V(x_{h,2}(t_k))}{\partial x} \left(f(x_{h,2}(t_k)) + \sum_{i=1}^m g_i(x_{h,2}(t_k)) h_i(x_{h,2}(t_k)) \right) \quad (6.21)$$

to/from the expression describing $\dot{V}(x_h(t))$, and then adding/subtracting

$$\frac{\partial V(x_h(t))}{\partial x} \sum_{i=1}^m g_i(x_h(t)) h_i(x_{h,2}(t_k)) \quad (6.22)$$

to/from the resulting inequality, we can obtain the following inequality by the conditions of Eqs. 6.4 and 6.6:

$$\begin{aligned} \dot{V}(x_h(t)) &\leq \left(L_x + \sum_{i=1}^m u_i^{max} L_{u_i} \right) |x_h(t) - x_{h,2}(t_k)| \\ &\quad + \sum_{i=1}^m C_{g_i} C_{h_i} |\check{x}_h(t_k) - x_{h,2}(t_k)| - \alpha_2 (\alpha_1^{-1}(\rho_s)) \end{aligned} \quad (6.23)$$

for all $x_{h,2}(t_k) \in \Omega_{\rho_n}/\Omega_{\rho_s}$. Using the triangular inequality, we obtain $|x_h(t) - x_{h,2}(t_k)| \leq |x_h(t) - x_{h,2}(t)| + |x_{h,2}(t) - x_{h,2}(t_k)|$ for $t \in [t_k, t_{k+1})$. Taking into account the condition of Eq. 6.5, the continuity of $x_{h,2}(t)$, the fact that $|\check{x}_h(t_k) - x_{h,2}(t_k)| \leq \theta_x$, and applying Proposition 6.1, we obtain from Eq. 6.23 the following bound on the time derivative of the Lyapunov function for $t \in [t_k, t_{k+1})$, for all initial states $x_h(t_k) \in \Omega_{\rho_n}/\Omega_{\rho_s}$:

$$\begin{aligned} \dot{V}(x_h(t)) &\leq \theta_x \sum_{i=1}^m C_{g_i} C_{h_i} - \alpha_2 (\alpha_1^{-1}(\rho_s)) \\ &\quad + \left(L_x + \sum_{i=1}^m u_i^{max} L_{u_i} \right) (f_E(0, 0, \theta_x, \Delta) + M\Delta). \end{aligned} \quad (6.24)$$

If the condition of Eq. 6.19 is satisfied, then $\dot{V}(x_h(t)) \leq -\epsilon_s/\Delta$. Integrating this

bound on $t \in [t_k, t_{k+1})$, we obtain that $V(x_h(t_{k+1})) \leq V(x_h(t_k)) - \epsilon_s$ and $V(x_h(t)) \leq V(x_h(t_k))$. Applying this result recursively, it is easy to verify that $V(x_h(t_k)) \leq \max\{V(x_h(t_0)) - k\epsilon_s, \rho_{min}\}$ and $V(x_h(t)) \leq \max\{V(x_h(t_k)), \rho_{min}\}$.

Proposition 6.2 ensures that if the nominal system under the control $h(x)$ implemented in a sample-and-hold fashion starts in Ω_{ρ_n} , then it is ultimately bounded in $\Omega_{\rho_{min}}$.

Proposition 6.3. *Consider the systems*

$$\begin{aligned}\dot{x}_a(t) &= f(x_a(t)) + \sum_{\substack{i=1 \\ m, i \neq j}}^m g_i(x_a(t))u_i^c(t) \\ \dot{x}_b(t) &= f(x_b(t)) + \sum_{i=1}^m g_i(x_b(t))\check{u}_i^{c-1}(t) + g_j(x_b(t))u_j^c(t)\end{aligned}$$

where $\check{u}_i^{c-1}(t) = u_i^{c-1}(t) + n_{u_i}$ with initial states $x_b(t_0) = x_a(t_0) + n_x^j \in \Omega_\rho$, $x_a(t_0) \in \Omega_{\rho_n}$, $|n_x^j| \leq \theta_x^j$ and $|n_{u_i}| \leq \theta_{u_i}$. There exists a function $f_{X,j}(\cdot, \cdot)$ such that

$$|x_a(t) - x_b(t)| \leq f_{X,j}(\theta_x^j, t - t_0) \quad (6.25)$$

for all $x_a(t), x_b(t) \in \Omega_\rho$, and $u_i^c(t), u_i^{c-1} \in U_i$ and $|u_i^c(t) - \check{u}_i^{c-1}(t)| \leq \Delta u_i$, $i = 1, \dots, m$ and $f_{X,j}(\tau) = \left(\frac{C_{2,j}}{C_{1,j}} + \theta_x^j\right) e^{C_{1,j}(\tau)} - \frac{C_{2,j}}{C_{1,j}}$ with $C_{2,j}$ and $C_{1,j}$ are positive constants.

Proof 6.3. Let $e(t) = x_a(t) - x_b(t)$. The derivative of $e(t)$ can be calculated as $\dot{e}(t) = \dot{x}_a(t) - \dot{x}_b(t)$. Adding/subtracting $\sum_{i=1}^{m, i \neq j} g_i(x_a(t))\check{u}_i^{c-1}(t)$ to/from the expression of $e(t)$, and then using the fact $\check{u}_i^{c-1}(t) \leq u_i^{max} + \theta_{u_i}$ and the conditions defined in Eq. 6.6, we obtain the following inequality:

$$|\dot{e}(t)| \leq \left(C_x + u_j^{max} C_{u_j} + \sum_{i=1}^{m, i \neq j} (u_i^{max} + \theta_{u_i}) C_{u_i} \right) |e(t)| + \sum_{i=1}^{m, i \neq j} M_{g,i} \Delta u_i$$

Defining $C_{1,j} = C_x + u_j^{max}C_{u_j} + \sum_{i=1, i \neq j}^m (u_i^{max} + \theta_{u_i})C_{u_i}$ and $C_{2,j} = \sum_{i=1, i \neq j}^m M_{g_i} \Delta u_i$, from the above inequality, we have $|\dot{e}(t)| \leq C_{1,j}|e(t)| + C_{2,j}$. Since the initial condition, $e(t_0)$, satisfies $|e(t_0)| \leq \theta_x^j$ (recall $x_b(t_0) = x_a(t_0) + n_x^j$ where $|n_x^j| \leq \theta_x^j$), we can obtain $|e(t)| \leq \left(\frac{C_{2,j}}{C_{1,j}} + \theta_x^j \right) e^{C_{1,j}(t-t_0)} - \frac{C_{2,j}}{C_{1,j}}$. This proves Proposition 6.3.

Proposition 6.3 bounds the difference between the nominal state trajectory under the optimized control inputs and the predicted nominal state trajectory generated in each LMPC optimization problem.

Proposition 6.4. *Consider the systems*

$$\begin{aligned}\dot{x}_a(t) &= f(x_a(t)) + \sum_{i=1}^m g_i(x_a(t))u_i(t) + k(x_a(t))w(t) \\ \dot{x}_b(t) &= f(x_b(t)) + \sum_{i=1}^m g_i(x_b(t))u_i(t)\end{aligned}$$

with initial states $x_b(t_k) = x_a(t_k) + n \in \Omega_\rho$, $x_a(t_k) \in \Omega_\rho$, and $|n| \leq \theta_x$. There exists a function $f_W(\cdot, \cdot)$ such that

$$|x_a(t) - x_b(t)| \leq f_W(\theta_x, t - t_k), \quad (6.26)$$

for all $x_a(t), x_b(t) \in \Omega_\rho$ and all $w(t) \in W$ with $f_W(\theta_x, \tau) = \left(\theta_x + \frac{\Gamma_2}{\Gamma_1} \right) e^{\Gamma_1 \tau} - \frac{\Gamma_2}{\Gamma_1}$ where Γ_1, Γ_2 are positive real numbers.

Proof 6.4. Define $e(t) = x_a(t) - x_b(t)$, then $\dot{e}(t) = \dot{x}_a(t) - \dot{x}_b(t)$. Using the condition of Eq. 6.6, we obtain the following inequality:

$$|\dot{e}(t)| \leq \left(C_x + \sum_{i=1}^m u_i^{max} C_{u_i} \right) |e(t)| + M_w \theta. \quad (6.27)$$

Defining $\Gamma_1 = C_x + \sum_{i=1}^m u_i^{\max} C_{u_i}$ and $\Gamma_2 = M_w \theta$, and accounting for that $|e(t_k)| \leq \theta_x$, we obtain $|e(t)| \leq \left(\theta_x + \frac{\Gamma_2}{\Gamma_1} \right) e^{\Gamma_1(t-t_k)} - \frac{\Gamma_2}{\Gamma_1}$. This proves Proposition 6.4.

Proposition 6.4 provides an upper bound on the deviation of the state trajectory obtained using the nominal model, from the actual state trajectory when the same control actions are applied. Proposition 6.5 bounds the difference between the magnitudes of the Lyapunov function of two states in Ω_ρ .

Proposition 6.5 (c.f. [60]). *Consider the Lyapunov function $V(\cdot)$ of the system of Eq. 6.2. There exists a quadratic function $f_V(\cdot)$ such that $V(x) \leq V(x') + f_V(|x - x'|)$ for all $x, x' \in \Omega_\rho$.*

In Theorem 6.1 below, we provide sufficient conditions under which the DMPC of Eqs. 6.9-6.10 and 6.12-6.13 guarantees that the state of the closed-loop system is ultimately bounded in a region that contains the origin. To simplify the proof of Theorem 6.1, we define new functions $f_H(\tau)$ and $f_X(\tau)$ based on f_E and $f_{X,i}$ ($i = 1, \dots, m$), respectively, as follows:

$$\begin{aligned} f_H(\tau) &= \sum_{i=2}^m \left(\frac{1}{m} L_x + M_{g_i} C_{h_i} + u_i^{\max} L_{u_i} \right) \\ &\quad \left(\frac{1}{L_1} f_E(\theta_x^i + \theta_x^1, 0, 0, \tau) - \frac{L_2 \tau + \theta_x^i + \theta_x^1}{L_1} \right), \\ f_X(\tau) &= \left(\frac{1}{m} L_x + L_{u_1} u_1^{\max} \right) \left(\frac{1}{C_{1,1}} f_{X,1}(0, \tau) - \frac{C_{2,1}}{C_{1,1}} \tau \right) \\ &\quad + \sum_{i=2}^m \left(\frac{1}{m} L_x + L_{u_i} u_i^{\max} \right) \\ &\quad \left(\frac{1}{C_{1,i}} f_{X,i}(\theta_x^i + \theta_x^1, \tau) - \frac{C_{2,i}}{C_{1,i}} \tau - \frac{\theta_x^i + \theta_x^1}{C_{1,i}} \right). \end{aligned}$$

It is easy to verify that $f_H(\tau)$ and $f_X(\tau)$ are strictly increasing and convex functions of their arguments.

Theorem 6.1. Consider the system of Eq. 6.2 in closed-loop with the DMPC design of Eqs. 6.9-6.10 and 6.12-6.13 based on the controller $h(x)$ that satisfies the conditions of Eq. 6.4 with class \mathcal{K} functions $\alpha_i(\cdot)$, $i = 1, 2$. If there exist $\Delta > 0$, $\epsilon_s > 0$, $\theta_x > 0$, $\rho > \rho_n > \rho_{\min} > 0$, $\rho > \rho_n > \rho_s > 0$ and $N \geq T \geq 1$ that satisfy the conditions of Eqs. 6.19 and the following inequality:

$$f_X(T\Delta) + f_V(f_W(\theta_x, T\Delta)) + f_V(f_W(\theta_x, 0))f_H(T\Delta) + \sum_{i=1}^m C_{g,i}\Delta u_i(T-1)\Delta - T\epsilon_s < 0, \quad (6.28)$$

and if the initial state of the closed-loop system $x(t_0) \in \Omega_{\rho_n}$, then $x(t)$ is ultimately bounded in $\Omega_{\rho_b} \subseteq \Omega_{\rho_n}$ where

$$\rho_b = \rho_{\min} + f_V(f_W(\theta_x, 0))u_i(T-1)\Delta + \sum_{i=1}^m C_{g,i}\Delta + f_H(T\Delta) + f_V(f_W(\theta_x, T\Delta)) + f_X(T\Delta).$$

Proof 6.5. We first consider two consecutive time instants in which both fast and slowly sampled states are available: t_k and t_{k+T} ($k = 0, T, 2T, \dots$). We will prove that the Lyapunov function of the system is decreasing from t_k to t_{k+T} . In the following, we denote the trajectory of the nominal system of Eq. 6.2 under the DMPC of Eqs. 6.9-6.10 and 6.12-6.13 starting from $\tilde{x}^1(t_k)$ (which is the state received by LMPC 1 at t_k) as \tilde{x} , and we also denote the predicted nominal system trajectory in the evaluation of the LMPC of Eq. 6.9 at the final iteration as \tilde{x}^j with $j = 1, \dots, m$. It should be mentioned that the initial condition for the nominal sampled trajectory \tilde{x} under the implementation of u_i^* can be $\tilde{x}(t_k) = x_h^i(0|t_k)$ for any $i = 1, \dots, m$. Without loss of generality, we assume that $\tilde{x}(t_k) = \tilde{x}^1(t_k) = x_h^1(0|t_k)$; use of any $i = 2, \dots, m$ in $\tilde{x}(t_k) = x_h^i(0|t_k)$ would simply require an appropriate modification in the definitions of $f_X(\cdot)$ and $f_H(\cdot)$.

The derivative of the Lyapunov function of the nominal system of Eq. 6.2 under

the DMPC of Eqs. 6.9-6.10 and 6.12-6.13 from t_k to t_{k+T} can be expressed as follows:

$$\dot{V}(\tilde{x}(\tau)) = \frac{\partial V(\tilde{x}(\tau))}{\partial x} \left(f(\tilde{x}(\tau)) + \sum_{i=1}^m g_i(\tilde{x}(\tau)) u_i^*(\tau) \right) \quad (6.29)$$

where $\tilde{x}(t_k) = \tilde{x}^1(t_k) = x_h^1(0|t_k)$ and $u_i^*(\tau)$ is the actual input applied to the system and defined as follows:

$$u_i^*(\tau) = \begin{cases} u_i^{*,f}(\tau|t_k), & \tau \in [0, \Delta) \\ u_i^{*,l}(\tau|t_l), & \tau \in [0, \Delta), l = k+1, \dots, k+T-1. \end{cases}$$

Combining Eq. 6.29 and the inequality constraints of Eq. 6.9g ($i = 1, \dots, m$), and adding/subtracting

$$\frac{\partial V(x_h^1(\tau|t_k))}{\partial x} \left(f(x_h^1(\tau|t_k)) + \sum_{i=1}^m g_i(x_h^1(\tau|t_k)) u_{h,i}^1(\tau|t_k) \right) \quad (6.30)$$

to/from the righthand side of the resulting inequality, we can obtain the following inequality for all $\tau \in [0, T\Delta]$ by taking into account the conditions of Eq. 6.6:

$$\begin{aligned} \dot{V}(\tilde{x}(\tau)) &\leq \dot{V}(x_h^1(\tau|t_k)) + \sum_{i=1}^m C_{g_i} \left(u_i^*(\tau) - u_i^{*,f}(\tau|t_k) \right) \\ &+ \left(\frac{1}{m} L_x + L_{u_1} u_1^{*,f}(\tau|t_k) \right) |\tilde{x}(\tau) - \tilde{x}^1(\tau)| + \dots \\ &+ \left(\frac{1}{m} L_x + L_{u_m} u_m^{*,f}(\tau|t_k) \right) |\tilde{x}(\tau) - \tilde{x}^m(\tau)| \\ &+ \left(\frac{1}{m} L_x + u_2^{max} L_{u_2} \right) |x_h^2(\tau|t_k) - x_h^1(\tau|t_k)| + \dots \\ &+ \left(\frac{1}{m} L_x + u_m^{max} L_{u_m} \right) |x_h^m(\tau|t_k) - x_h^1(\tau|t_k)| \\ &+ M_{g_2} C_{h_2} |x_h^2(\tau|t_k) - x_h^1(\tau|t_k)| + \dots \\ &+ M_{g_m} C_{h_m} |x_h^m(\tau|t_k) - x_h^1(\tau|t_k)| \end{aligned} \quad (6.31)$$

Applying Propositions 6.3 and 6.1 to the inequality of Eq. 6.31, and then integrating the resulting inequality from $\tau = 0$ to $\tau = T\Delta$ and taking into account that $\tilde{x}(t_k) = x_h^1(0|t_k)$, the constraints of Eqs. 6.9d and 6.12e and the definitions of $f_X(\cdot)$, $f_H(\cdot)$ and $u^*(\tau)$, the following inequality can be obtained:

$$V(\tilde{x}(t_{k+T})) \leq V(x_h^1(T\Delta|t_k)) + f_X(T\Delta) + f_H(T\Delta) + \sum_{i=1}^m C_{g,i}\Delta u_i(T-1)\Delta. \quad (6.32)$$

Since $V(x_h^1(T\Delta|t_k)) \leq \max\{V(x_h^1(0|t_k)) - T\epsilon_s, \rho_{min}\}$ from Proposition 6.2, $\tilde{x}(t_k) = x_h^1(0|t_k)$ and $|V(\tilde{x}(t_k)) - V(x(t_k))| \leq f_V(f_W(\theta_x, 0))$ and $|V(\tilde{x}(t_{k+T})) - V(x(t_{k+T}))| \leq f_V(f_W(\theta_x, T\Delta))$ from Propositions 6.4 and 6.5, we can obtain the following inequality from Eq. 6.32:

$$\begin{aligned} V(x(t_{k+T})) \leq & \max\{V(x(t_k)) - T\epsilon_s, \rho_{min}\} + f_X(T\Delta) + f_H(T\Delta) + f_V(f_W(\theta_x, T\Delta)) \\ & + f_V(f_W(\theta_x, 0)) + \sum_{i=1}^m C_{g,i}\Delta u_i(T-1)\Delta. \end{aligned} \quad (6.33)$$

If there exist $\Delta > 0$, $\epsilon_s > 0$, $\theta_x > 0$, $\rho > \rho_n > \rho_{min} > 0$, $\rho > \rho_n > \rho_s > 0$ and $N \geq T \geq 1$ that satisfy the conditions of Eqs. 6.19 and Eq. 6.28, then there exists $\epsilon_w > 0$ such that the following inequality holds

$$V(x(t_{k+T})) \leq \max\{V(x(t_k)) - \epsilon_w, \rho_b\} \quad (6.34)$$

which implies that if $x(t_k) \in \Omega_{\rho_n}/\Omega_{\rho_b}$, then $V(x(t_{k+T})) < V(x(t_k))$, and if $x(t_k) \in \Omega_{\rho_b}$, then $V(x(t_{k+T})) \leq \rho_b$.

Because the upper bound on the difference between the Lyapunov function of the actual trajectory x and the nominal trajectory \tilde{x} (see Eq. 6.34) is a strictly increasing

function of T , the inequality of Eq. 6.34 also implies that:

$$V(x(t)) \leq \max\{V(x(t_k)) - \epsilon_w, \rho_b\}, \quad \forall t \in [t_k, t_{k+T}]. \quad (6.35)$$

Using the inequality of Eq. 6.35 recursively, it can be proved that if $x(t_0) \in \Omega_{\rho_n}$, then the closed-loop trajectories of the system of Eq. 6.2 under the proposed DMPC design stay in Ω_{ρ_n} for all times (i.e., $x(t) \in \Omega_{\rho_n}$ for all t). Moreover, if $x(t_0) \in \Omega_{\rho_n}$, the closed-loop trajectories of the system of Eq. 6.2 under the proposed iterative DMPC design satisfy $\limsup_{t \rightarrow \infty} V(x(t)) \leq \rho_b$. This proves Theorem 6.1.

In addition to the stability result of Theorem 6.1, we note that because the closed-loop states of the system of Eq. 6.2 under the proposed DMPC scheme are guaranteed to be bounded in a compact set containing the origin and the manipulated inputs are bounded for all times (this follows from the practical stability of the closed-loop system), the cost along the closed-loop system trajectory over finite time (which only depends on the absolute values of the magnitude of the system states and the manipulated inputs) is also bounded. We also note that in the context of linear systems and noise-free measurements and communication, the distributed optimization problem of Eq. 6.9 is convex. Furthermore, if the inputs of the distributed controllers are defined as convex combinations of their current and previous solutions as described in Eq. 6.14, as the iteration number c increases, the optimal cost given by the distributed optimization problem of Eq. 6.9 converges to its corresponding centralized optimal value. This property is summarized in the following Corollary 6.1.

Corollary 6.1. *Consider a class of linear time-invariant systems:*

$$\dot{x}(t) = Ax(t) + Bu(t) \quad (6.36)$$

with

$$\dot{x}_i = A_{ii}x_i + \sum_{j \neq i} A_{ij}x_j + B_i u_i(t) \quad (6.37)$$

where A , B , A_{ii} , A_{ij} and B_i are constant matrices with appropriate dimensions. If we define the inputs of the distributed controllers at iteration c as in Eq. 6.14, then at a sampling time t_k , as the iteration number $c \rightarrow \infty$, the optimal cost of the distributed optimization problem of Eq. 6.9 converges to the optimal cost of the corresponding centralized control system. If $x(0) \in \Omega_\rho$ and the corresponding centralized MPC asymptotically stabilizes the origin of the closed-loop system, the DMPC of Eq. 6.9 also asymptotically stabilizes the origin of the closed-loop system and the closed-loop performance of the DMPC converges to the one given by the centralized control system.

Proof 6.6. In this proof, we focus on a simplified case: 1) a linear system composed of two subsystems, and 2) full state feedback, x , is available every sampling time. We first prove that, at each sampling time, the optimal cost of the distributed optimization problem of Eq. 6.9 converges to the optimal cost of the corresponding centralized control system as the iteration number increases, and then prove that if the corresponding centralized MPC asymptotically stabilizes the origin of the closed-loop system, then the DMPC of Eq. 6.9 also asymptotically stabilizes the origin of the closed-loop system. This proof can be extended in a straightforward manner to include general linear systems with measurements available every T ($T \leq N$) sampling times.

For a linear system, it is easy to verify that the constraints of Eqs. 6.9a-6.9f are convex. We will focus on the proof of the convexity of the constraint of Eq. 6.9g. Specifically, using a quadratic Lyapunov function $V(x) = x^T P x$ where P is a positive

definite symmetric matrix, the constraint of Eq. 6.9g takes the following form:

$$\begin{aligned}
& \left(\frac{1}{2} \tilde{x}^j(\tau)^T A^T + u_j(\tau)^T B_j^T \right) P \tilde{x}^j(\tau) + \tilde{x}^j(\tau)^T P \left(\frac{1}{2} A \tilde{x}^j(\tau) + B_j u_j(\tau) \right) \\
& \leq \left(\frac{1}{2} x_h^j(\tau|t_k)^T A^T + u_{h,j}^j(\tau|t_k)^T B_j^T \right) P \tilde{x}_h^j(\tau|t_k) \\
& \quad + x_h^j(\tau|t_k)^T P \left(\frac{1}{2} A x_h^j(\tau|t_k) + B_j u_{h,j}^j(\tau|t_k) \right)
\end{aligned} \tag{6.38}$$

where $j = 1, 2$, $\tau \in [0, \Delta]$ and \tilde{x}^j is the predicted trajectory of the nominal system with u_j computed by the LMPC of Eq. 6.9 and the other input is received from the other controller. The right hand side of Eq. 6.38 has no dependence on u_j or \tilde{x}^j and can be considered as a constant. If we take into account that the input trajectories are piece-wise constant and that $\tilde{x}^j(\tau) = e^{A\tau} \tilde{x}^j(0) + \int_0^\tau e^{A(\tau-s)} B u(s) ds$, for $\tau \in [0, \Delta]$, we can obtain that:

$$\tilde{x}^j(\tau) = C^j(t_k, \tau) + D^j(t_k, \tau) u_j \tag{6.39}$$

where $C^j(t_k, \tau)$ and $D^j(t_k, \tau)$ are matrices that depend only on τ . As it can be seen from Eq. 6.39, u_j appears linearly. Taking into account Eq. 6.39 and the fact that the right hand side of Eq. 6.38 can be considered as a constant, we can re-write Eq. 6.38 in a quadratic form with respect to u_j as follows:

$$u_j^T E^j(t_k, \tau) u_j + F^j(t_k, \tau) u_j \leq G^j(t_k, \tau) \tag{6.40}$$

where $E^j(t_k, \tau)$, $F^j(t_k, \tau)$ and $G^j(t_k, \tau)$ are matrices that depend only on τ . This proves that the constraint of Eq. 6.38 is convex. Therefore, the optimization problem of Eq. 6.9 for the linear system with two subsystems is convex. If the inputs of the distributed controllers at each iteration c are defined as in Eq. 6.14, then the convergence of the cost given by the distributed optimization problem to the corresponding centralized control system can be proved following similar strategies used in [3, 92] for

a specific sampling time t_k . If $x(0) \in \Omega_\rho$ and the centralized MPC can asymptotically stabilize the origin of the closed-loop system, using the above arguments recursively for each sampling time, if $c \rightarrow \infty$ for each sampling time, it follows that the DMPC also asymptotically stabilizes the origin of the closed-loop system and the closed-loop cost converges to the one given by the centralized control system.

Remark 6.4. *Referring to the open-loop nature of the estimator of Eq. 6.11, it is important to note that it does not pose any restrictions on the open-loop stability of the processes in which the proposed multirate DMPC method can be applied. The reason is that this estimator is used to provide “short-term” (within the slow sampling period upper bound) estimates of plant states which are used in the fast sampling-time DMPCs applied in the various subsystems; therefore, if the upper bound on the slow sampling time is sufficiently small as required by Theorem 1, the stability of the closed-loop system under the proposed multirate DMPC scheme is guaranteed.*

Remark 6.5. *Even though the conditions of Theorem 6.1 are conservative in nature in order to guarantee closed-loop stability, they do provide insight into the relationship between the various variables characterizing the controller, process and measurement sampling components of the closed-loop system and can be used to properly tune the overall control system. The degree of conservativeness of the conditions of Theorem 1 can be assessed in practice via closed-loop simulations.*

Remark 6.6. *Note that if all the distributed controllers have access to the whole system state vector measurements at each slow sampling instant, the controllers do not have to communicate and can make their calculation in a decentralized fashion without loss of the closed-loop stability because of the design of the stability constraints. The communication and iteration of the distributed controllers, however, can improve the overall closed-loop system performance significantly. It is also important to note that*

the DMPC system operating at the slow sampling time can utilize alternative communication strategies between the distributed controllers like, for example, sequential communication or local (nearest-neighbor) communication, provided appropriate conditions are satisfied that ensure stability of the closed-loop system in each case. Furthermore, ideas from the quasi-decentralized control framework for multi-unit plants developed in [93] where suitable models are used in each controller to estimate state variables of the other subsystems, can be adopted in the proposed DMPC framework. Finally, we note that if measurements of some of the state variables are not available, networked state estimation schemes [94] may be used within the proposed multirate DMPC framework.

6.3 Application to a chemical process

The process considered in this study is a three vessel, reactor-separator system consisting of two continuously stirred tank reactors (CSTRs) and a flash tank separator. The reactions $A \rightarrow B$ and $A \rightarrow C$ (referred to as 1 and 2, respectively) take place in the two CSTRs before the effluent from CSTR 2 is fed to a flash tank. The detailed description and modeling of the process can be found in [15]. The process is numerically simulated using a standard Euler integration method. Process noise was added to simulate disturbances/model uncertainty and it is generated as autocorrelated noise of the form $w_k = \phi w_{k-1} + \xi_k$ where $k = 0, 1, \dots$ is the discrete time step of 0.001 *hr*, ξ_k is generated by a normally distributed random variable with standard deviation σ_p , and ϕ is the autocorrelation factor and w_k is bounded by θ_p , that is $|w_k| \leq \theta_p$. Table 6.1 contains the parameters used in generating the process noise. The process is divided into three subsystems corresponding to the first CSTR, the second CSTR and the separator, respectively. For the three subsystems, we will refer

Table 6.1: Disturbance parameters.

	σ_p	ϕ	θ_p		σ_p	ϕ	θ_p
C_{A1}	0.1	0.7	0.09	C_{A2}	0.1	0.7	0.09
C_{B1}	0.02	0.7	0.01	C_{B2}	0.1	0.7	0.03
C_{C1}	0.02	0.7	0.01	C_{C2}	0.1	0.7	0.01
T_1	10	0.7	1.17	T_2	10	0.7	1.35
C_{A3}	0.1	0.7	0.09	C_{B3}	0.1	0.7	0.02
C_{C3}	0.02	0.7	0.01	T_3	10	0.7	1.35

Table 6.2: Steady-state values for x_s .

C_{A1s}	3.31 $[\frac{kmol}{m^3}]$	C_{A2s}	2.75 $[\frac{kmol}{m^3}]$
C_{B1s}	0.17 $[\frac{kmol}{m^3}]$	C_{B2s}	0.45 $[\frac{kmol}{m^3}]$
C_{C1s}	0.04 $[\frac{kmol}{m^3}]$	C_{C2s}	0.11 $[\frac{kmol}{m^3}]$
T_{1s}	369.53 [K]	T_{2s}	435.25 [K]
C_{A3s}	2.88 $[\frac{kmol}{m^3}]$	C_{B3s}	0.50 $[\frac{kmol}{m^3}]$
C_{C3s}	0.12 $[\frac{kmol}{m^3}]$	T_{3s}	435.25 [K]

to them as subsystem 1, subsystem 2 and subsystem 3, respectively. The state of subsystem 1 is defined as the deviations of the temperature and species concentrations in the first CSTR from their desired steady-state; that is, $x_1^T = [x_{f,1}^T, x_{s,1}^T]$ where $x_{f,1} = T_1 - T_{1s}$ and $x_{s,1}^T = [C_{A1} - C_{A1s} \ C_{B1} - C_{B1s} \ C_{C1} - C_{C1s}]$ denote fast sampled and slowly sampled measurements of subsystem 1, respectively. Due to the simplicity of temperature measurement at each sampling time, we denote the temperature as the fast sampled measurement of each subsystem. The states of subsystems 2 and 3 are defined similarly; they are $x_2^T = [T_2 - T_{2s} \ C_{A2} - C_{A2s} \ C_{B2} - C_{B2s} \ C_{C2} - C_{C2s}]$ and $x_3^T = [T_3 - T_{3s} \ C_{A3} - C_{A3s} \ C_{B3} - C_{B3s} \ C_{C3} - C_{C3s}]$. The values of the desired steady state are shown in Table 6.2. Accordingly, the state of the whole process is defined as a combination of the states of the three subsystems; that is, $x^T = [x_1^T \ x_2^T \ x_3^T]$.

The process has one unstable and two stable steady states. The control objective is to regulate the process at the unstable steady-state x_s corresponding to the operating

point defined by $Q_{1s} = 0 \text{ KJ/hr}$, $Q_{2s} = 0 \text{ KJ/hr}$ and $Q_{3s} = 0 \text{ KJ/hr}$, respectively. Each of the tanks has an external heat input which is the control input associated with each subsystem, that is, $u_1 = Q_1 - Q_{1s}$, $u_2 = Q_2 - Q_{2s}$ and $u_3 = Q_3 - Q_{3s}$. The inputs are subject to constraints as follows: $|u_1| \leq 5 \times 10^4 \text{ KJ/hr}$, $|u_2| \leq 1.5 \times 10^5 \text{ KJ/hr}$, and $|u_3| \leq 2 \times 10^5 \text{ KJ/hr}$. Three distributed MPC controllers (controller 1, controller 2 and controller 3) will be designed to manipulate each one of the three inputs in the three subsystems, respectively. The process model (see [15]) belongs to the following class of nonlinear systems:

$$\dot{x}(t) = f(x(t)) + \sum_{i=1}^3 g_i(x(t))u_i(t) + w(x(t))$$

where the explicit expressions of f , g_i ($i = 1, 2, 3$), are omitted for brevity. We assume that $x_{f,1}$, $x_{f,2}$, $x_{f,3}$ are measured and sent to controller 1, controller 2 and controller 3, respectively, at synchronous time instants $t_l = l\Delta$, $l = 0, 1, \dots$, with $\Delta = 0.01 \text{ hr} = 36 \text{ sec}$ while we assume that each controller receives $x_{s,i}$ every $T = 4$ sampling times. The three subsystems exchange their states at $t_k = kT\Delta$, $k = 0, 1, \dots$; that is, the full system state x is sent to all the controllers every $T = 4$ sampling times. In the simulations, we consider a quadratic Lyapunov function $V(x) = x^T P x$ with $P = \text{diag}([20 \ 10^3 \ 10^3 \ 10^3 \ 20 \ 10^3 \ 10^3 \ 10^3 \ 20 \ 10^3 \ 10^3 \ 10^3])$. We design the Lyapunov-based controller $h(x)$ following the continuous bounded control law [58, 18] as follows:

$$h(x) = -p(x)(L_G V)^T \tag{6.41}$$

where

$$p(x) = \begin{cases} \frac{L_f V + \sqrt{(L_f V)^2 + (u^{\max} |L_G V^T|)^4}}{|L_G V^T|^2 [1 + \sqrt{1 + (u^{\max} |L_G V^T|)^2}]}, & L_G V \neq 0 \\ 0, & L_G V = 0 \end{cases}$$

with $L_f V = \frac{\partial V}{\partial x} f(x)$ and $L_G V = \frac{\partial V}{\partial x} G(x)$ where $G = [g_1 \ g_2 \ g_3]$ being the Lie derivatives of the scalar function V with respect to the vector fields f and G , respectively. To estimate the stability region Ω_ρ , extensive simulations were carried out to get an estimate of the region of the closed-loop system under Lyapunov-based control $h(x)$ where the time-derivative of the Lyapunov function is negative, and then Ω_ρ is defined as a level set of the Lyapunov function $V(x)$ embedded within this region.

Based on the Lyapunov-based controller $h(x)$ and $V(x)$, we design the three LMPCs following Eqs. 6.9-6.10 and 6.12-6.13 and refer to them as LMPC 1, LMPC 2 and LMPC 3. For each LMPC, we also design a state observer following Eq. 6.11. In the design of the LMPC controllers, the weighting matrices are chosen to be $Q_c = \text{diag}([20 \ 10^3 \ 10^3 \ 10^3 \ 20 \ 10^3 \ 10^3 \ 10^3 \ 20 \ 10^3 \ 10^3 \ 10^3])$, $R_1 = R_2 = R_3 = 10^{-6}$. The prediction horizon for the optimization problem is $N = 5$ with a sampling time of $\Delta = 0.01 \text{ hr}$. In the simulations, we put a maximum iteration number c_{\max} on the DMPC evaluation and the maximum iteration number is chosen to be $c_{\max} = 2$. Also, we set Δu_i as 10% percent of u_i^{\max} ($i = 1, 2, 3$). The optimization problems are solved by the open source interior point optimizer Ipopt [97]. The initial condition which is utilized to carry out simulations is $x(0)^T = [360.69 \ 3.19 \ 0.15 \ 0.03 \ 430.91 \ 2.76 \ 0.34 \ 0.08 \ 430.42 \ 2.79 \ 0.38 \ 0.08]$. We set the bound on the measurement noise to be 1% of the instantaneous value of the signal measured by sensors. The communication channel noise is generated using gaussian random variables with variances σ_n and σ_u bounded by θ_n and θ_u for state values and control inputs, respectively. These values are shown in Table 6.3.

We first carried out simulations to illustrate that the proposed multirate DMPC achieves practical closed-loop stability. Figure 6.2 shows the temperature and concentration trajectories of the process under the DMPC design of Eqs. 6.9-6.10 and 6.12-

Table 6.3: Communication noise parameters.

	σ_n	θ_n		σ_n	θ_n
C_{A1}	1	0.033	C_{A2}	1	0.027
C_{B1}	1	0.001	C_{B2}	1	0.004
C_{C1}	1	0.001	C_{C2}	1	0.001
T_1	10	3.695	T_2	10	4.352
	σ_n	θ_n		σ_u	θ_u
C_{A3}	1	0.028	u_1	10	7.39
C_{B3}	1	0.005	u_2	30	22.17
C_{C3}	1	0.001	u_3	40	29.56
T_3	10	4.352			

6.13, respectively. As it can be seen from the figure, the proposed DMPC system can steer the system state to a neighborhood of the desired steady-state. It should be emphasized that the inequalities of Eqs 6.19 and 6.28 have been confirmed through simulations.

We also carried out a set of simulations to demonstrate the optimality of the closed-loop performance of the proposed multirate DMPC compared with different control schemes. Specifically, we compared the proposed multirate DMPC with five different control schemes from a performance point of view for the case in which there is no communication and measurement noise. The five control schemes considered are as follows: (1) the proposed DMPC design of Eqs. 6.9-6.10 and 6.12-6.13; (2) a DMPC design with LMPCs formulated as in Eq. 6.9 which are only evaluated at time instants in which full system states are available and the inputs are implemented in open-loop fashion between two full system state measurements (in this case, the additional fast sampled measurements are not used to improve the closed-loop performance); (3) the proposed DMPC design but without communication between the distributed controllers and each controller estimating the full system states and the actions of the other controllers based on the process model and $h(x)$ (in this case,

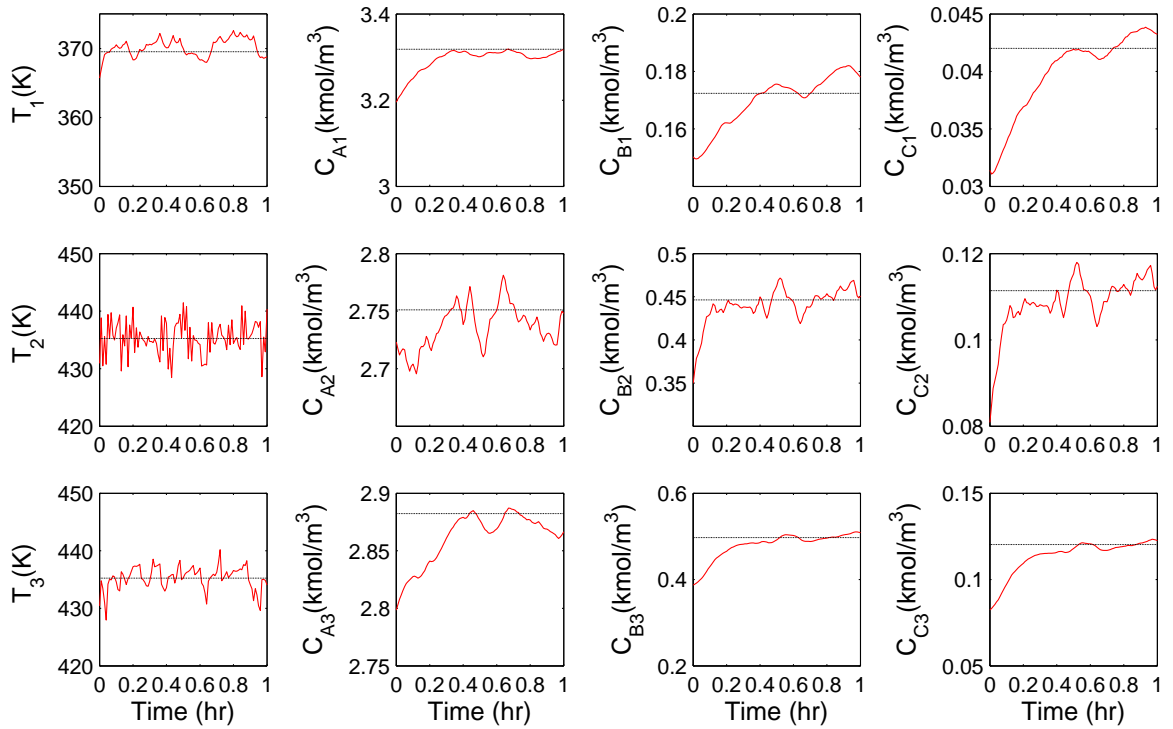


Figure 6.2: State trajectories of the process under the DMPC design of Eqs. 6.9-6.10 and 6.12-6.13 with noise.

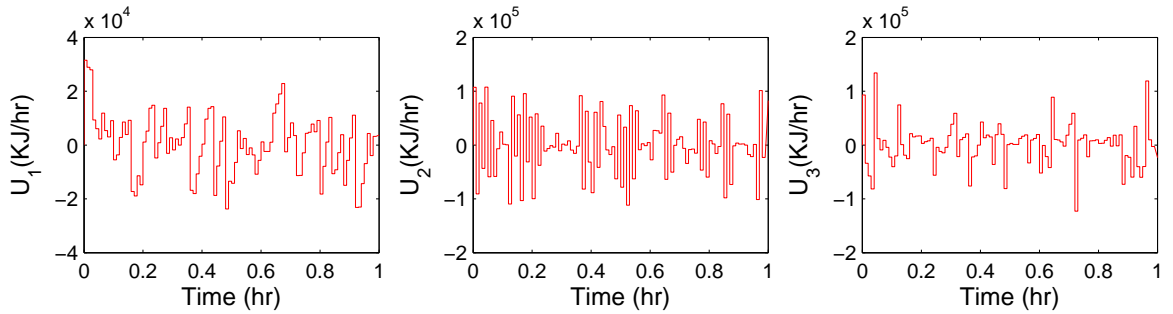


Figure 6.3: Manipulated input trajectories under the DMPC design of Eqs. 6.9-6.10 and 6.12-6.13 with noise.

a distributed LMPC in the DMPC design takes advantage of both fast and slowly sampled measurements of its own local subsystem but does not receive any input or state information from the other subsystems); (4) the DMPC design as in (2) but without communication between the distributed controllers and each controller estimating the full system states and actions of the other controllers based on the process model and $h(x)$; (5) $h(x)$ applied in sample-and-hold; (6) the centralized LMPC [79]. We perform these simulations under different initial conditions and different process noise/disturbances. To carry out this comparison, we have computed the total cost of each simulation based on the index of the following form:

$$J = \sum_{i=0}^M \left[x(t_i)^T Q_c x(t_i) + \sum_{j=1}^3 u_j(t_i)^T R_{c_j} u_j(t_i) \right]$$

where $t_0 = 0$ is the initial time of the simulations and $t_M = 1 \text{ hr}$ is the end of the simulations. Table 6.4 shows the total cost computed for 10 different closed-loop simulations under the six different control schemes. From Table 6.4, we see that the centralized LMPC gives the best performance and the proposed DMPC design gives the second best performance in all the simulations. Also, Table 6.4 demonstrates that when there is communication between controllers or there is MPC implementation when there is only partial state information in each controller (fast sampled state), the closed-loop performance is improved. It should be mentioned that the Lyapunov-based controller is a feasible solution to the DMPC problem; however, the DMPC solution can substantially improve closed-loop performance while it inherits closed-loop stability from the Lyapunov-based controller. All of the DMPC designs yield improvement in performance compared to the Lyapunov-based controller.

In the final set of simulations, we demonstrated that the proposed multirate DMPC has a reduced computational complexity with respect to a corresponding

Table 6.4: Total performance cost comparison along the closed-loop system trajectories in 10 different runs under: (1) the proposed multirate DMPC design; (2) a DMPC design with LMPCs formulated as in Eq. 6.9 evaluated only at time instants in which full system states are available and the inputs are implemented in open-loop fashion between two full system state measurements; (3) the proposed DMPC design but without communication between the distributed controllers and each controller estimating the full system states and the actions of the other controllers based on the process model and $h(x)$; (4) the DMPC design as in (2) but without communication between the distributed controllers and each controller estimating the full system states and actions of the other controllers based on the process model and $h(x)$; (5) $h(x)$ applied in sample-and-hold; (6) the centralized LMPC [79].

(1)	(2)	(3)	(4)	(5)	(6)
43963	633589	72200	812903	1116578	27057
21512	606628	28079	743874	1095819	7370
23041	604148	27407	706319	1084445	15112
24681	613289	30211	720131	1104045	8838
31440	618649	36290	723598	1106508	18654
21775	654268	25950	859380	1079984	15287
28553	667143	34209	879852	1109976	13168
28974	659250	34565	865643	1109363	13424
28228	672756	33949	891549	1110884	12991
23929	668499	29688	887300	1106623	11903

centralized scheme. Specifically, we compared the evaluation time of the centralized LMPC [79] with the one of the proposed DMPC design in the case that there is no noise in communication or measurements. We consider the case where each controller evaluates the input trajectories every $T = 4$ sampling times (both in the centralized and the distributed architectures) and evaluate the computational time of the LMPC optimization problems for 2500 independent closed-loop simulation runs. We consider only the sampling times in which controllers have access to full system states including fast and slowly sampled states. We found that the mean evaluation time of the centralized LMPC is 0.267 *sec* and the mean evaluation time of the DMPC is 0.235 *sec* which is the maximum time among the three distributed controllers (LMPC 1: 0.215 *sec*, LMPC 2: 0.235 *sec* and LMPC 3: 0.206 *sec*). From this set of simulations, we see that the proposed DMPC design leads to about 12% reduction in the controller evaluation time.

6.4 Conclusions

In this chapter, we designed a DMPC system using multirate sampling for large-scale nonlinear uncertain systems composed of several coupled subsystems. In the proposed control architecture, the controllers were designed via LMPC techniques taking into account bounded measurement and communication noise and process disturbances. Sufficient conditions under which the state of the closed-loop system is ultimately bounded in an invariant region containing the origin were derived. Finally, the applicability and performance of the proposed DMPC scheme were demonstrated through a nonlinear chemical process example.

Chapter 7

Distributed Model Predictive Control of Switched Nonlinear Systems with Scheduled Mode Transitions

Due to changes in raw materials (feedstock), energy sources, product specifications and market demands, control of switched nonlinear systems with scheduled mode transitions has received considerable attention in the context of chemical process control applications. From a stability analysis point of view, switched systems are well studied using multiple Lyapunov function (MLF) [5] and dwell time [44] concepts (see also [56, 57] for results and references in this area). From a controller design standpoint, in order to achieve closed-loop stability, mode transition situations should be carefully accounted for in the control problem formulation and solution. In this direction, control of switched systems has been addressed using approaches based

on Lyapunov functions (e.g., [21, 27, 31, 45, 101]) as well as optimal control theory (e.g., [5, 4, 30]). Furthermore, in order to achieve scheduled mode transitions in an optimal setting and accommodate input and state constraints, model predictive control (MPC) framework can be employed to design control systems that can achieve these objectives (see, for example [8, 73, 53, 52] for results on MPC of hybrid systems). As the number of manipulated inputs increases, as it is the case in the context of large-scale chemical plants, the evaluation time of centralized MPC may increase significantly. This may impede the ability of centralized MPC to carry out real-time calculations within the limits imposed by process dynamics and operating conditions. These control action evaluation problems may become more acute when additional constraints are imposed on the MPC as it is the case in the context of switched systems in order to properly force the closed-loop system state to follow a trajectory that meets the desired switching (operating) process schedule. Furthermore, there are cooperative DMPC schemes where each distributed controller optimizes the control actions for its actuators by minimizing a “global” cost accounting for the entire plant state and set of inputs [87, 19]; however, at this point, there is no work on the DMPC of switched or hybrid systems.

In this chapter, we present a framework for the design of distributed model predictive control systems for a broad class of switched nonlinear systems for which the mode transitions take place according to a prescribed switching schedule. Under appropriate stabilizability assumptions on the existence of a set of feedback controllers that can stabilize the closed-loop switched, nonlinear system, we design a Lyapunov-based iterative DMPC scheme with appropriate stability constraints that achieves stability of the switched closed-loop system and tracking of the prescribed switching policy. In terms of DMPC feasibility, the stability constraints make sure that at the moment of mode switching, the closed-loop system state is at the stability region of

the new mode while the value of the Lyapunov function of the new mode (at the moment of entering the new mode) is smaller compared to the value of this Lyapunov function at the last time that the closed-loop system had switched into that mode. The proposed DMPC scheme is applied to a nonlinear chemical process network with scheduled mode transitions and its performance and computational efficiency properties in comparison to centralized MPC are evaluated through simulations.

7.1 Preliminaries

7.1.1 Notation and class of switched nonlinear systems

The notation $|\cdot|$ is used to denote the Euclidean norm of a vector, while we use $|\cdot|_Q$ to denote the square of a weighted Euclidean norm, i.e., $|x|_Q = x^T Q x$ for all $x \in R^n$. A continuous function $\alpha : [0, a) \rightarrow [0, \bar{a})$ is said to belong to class \mathcal{K} if it is strictly increasing and satisfies $\alpha(0) = 0$. The symbol Ω_r is used to denote the set $\Omega_r := \{x \in R^{n_x} : V(x) \leq r\}$ where V is a continuous differentiable, positive definite scalar function, and the operator ‘/’ denotes set subtraction, that is, $A/B := \{x \in R^{n_x} : x \in A, x \notin B\}$. The symbol $diag(v)$ denotes a matrix whose diagonal elements are the elements of vector v and all the other elements are zeros. T denotes matrix transpose operation.

We consider switched nonlinear systems which are composed of p modes (i.e., finite-number of switching modes) described by the following state-space model:

$$\dot{x}(t) = f_{\sigma(t)}(x) + \sum_{i=1}^m g_{i_{\sigma(t)}}(x) u_{i_{\sigma(t)}}(t) \quad (7.1)$$

where $x(t) \in R^{n_x}$ denotes the vector of state variables of the system and $u_{i_{\sigma(t)}}(t) \in$

$R^{m_{u_i}}$ ($i = 1, \dots, m$) is the i^{th} set of control (manipulated) inputs affecting the σ mode. $\sigma : [0, \infty) \rightarrow \mathcal{I}$ denotes the switching signal which is assumed to be a piecewise continuous from the right function of time, i.e., $\sigma(t_k) = \lim_{t \rightarrow t_k^+} \sigma(t)$ for all k , implying that only a finite number of switches is allowed over any finite interval of time. The switching signal takes its values in a finite index set $\mathcal{I} = \{1, 2, \dots, p\}$. The vector function $f_{\sigma(t)}(x)$ and the matrix function $g_{i_{\sigma(t)}}(x)$ have dimension $(n_x \times 1)$ and $(n_x \times m_{u_i})$ respectively. The m sets of inputs are restricted to be in m nonempty convex sets $U_{i_{\sigma(t)}} \subseteq R^{m_{u_i}}$, $i = 1, \dots, m$, which are defined as $U_{i_{\sigma(t)}} := \{u_{i_{\sigma(t)}} \in R^{m_{u_i}} : |u_{i_{\sigma(t)}}| \leq u_{i_{\sigma(t)}}^{\max}\}$ where $u_{i_{\sigma(t)}}^{\max}$, $i = 1, \dots, m$, are the magnitudes of the input constraints. We will design m controllers to compute the m sets of control inputs $u_{i_{\sigma(t)}}$, $i = 1, \dots, m$, respectively. We will refer to the controller computing $u_{i_{\sigma(t)}}$ as controller i at mode $\sigma(t)$.

Throughout the rest of this manuscript, $t_{k_r^{in}}$ and $t_{k_r^{out}}$ denote the time when, for the r^{th} time, the system of Eq. 7.1 has switched in and out of the k^{th} mode, respectively, i.e., $\sigma(t_{k_r^{in}}^+) = \sigma(t_{k_r^{out}}^-) = k$. So, for $t_{k_r^{in}} \leq t < t_{k_r^{out}}$, the system of Eq. 7.1 is represented by $\dot{x} = f_k(x) + \sum_{i=1}^m g_{i_k}(x)u_{i_k}$.

We assume that the vector function f_k , and the matrix functions g_{i_k} , $i = 1, \dots, m$ ($k \in \mathcal{I}$) are locally Lipschitz vector and matrix functions, respectively, and that the origin is an equilibrium point of the unforced system (i.e., system of Eq. 7.1 with $u_{i_k}(t) = 0$, $i = 1, \dots, m$, for all t , $k \in \mathcal{I}$) which implies that $f_k(0) = 0$, $\forall k \in \mathcal{I}$. We further assume that during the system operation at mode k for r^{th} time, i.e., $t_{k_r^{in}} \leq t < t_{k_r^{out}}$, the system state measurements are available and sampled at synchronous time instants $t_q = t_{k_r^{in}} + q\Delta_{k_r}$, $q = 0, 1, 2, \dots, N_{k_r}$ where Δ_{k_r} is the sampling time. Without loss of generality, we assume that N_{k_r} is a positive integer.

7.1.2 Stabilizability assumptions on nonlinear switched system

Consider the system of Eq. 7.1, for a fixed $\sigma(t) = k$ for some $k \in \mathcal{I}$. We assume that there exists a feedback controller $h_k(x) = [h_{1_k}^T(x) \cdots h_{m_k}^T(x)]^T$ with $u_{i_k} = h_{i_k}(x)$, $i = 1, \dots, m$, which renders the origin of the closed-loop system at mode k asymptotically stable while satisfying the input constraints for all the states x inside a given stability region. Using converse Lyapunov theorems [18, 59], this assumption implies that there exist class \mathcal{K} functions $\alpha_{l_k}(\cdot)$, $l = 1, 2, 3, 4$ and a continuously differentiable Lyapunov function $V_k(x)$ for the closed-loop system, that satisfy the following inequalities:

$$\begin{aligned}
 \alpha_{1_k}(|x|) &\leq V_k(x) \leq \alpha_{2_k}(|x|) \\
 \frac{\partial V_k(x)}{\partial x} (f_k(x) + \sum_{i=1}^m g_{i_k}(x) h_{i_k}(x)) &\leq -\alpha_{3_k}(|x|) \\
 \left| \frac{\partial V_k(x)}{\partial x} \right| &\leq \alpha_{4_k}(|x|) \\
 h_{i_k}(x) &\in U_{i_k}, \quad i = 1, \dots, m
 \end{aligned} \tag{7.2}$$

for all $x \in D_k \subseteq R^{n_x}$ where D_k is an open neighborhood of the origin. We denote the region $\Omega_{\bar{\rho}_k} \subseteq D_k$ as the stability region of the closed-loop system at mode k under the controller $h_k(x)$. Using the smoothness assumed for the f_k and g_{i_k} , and taking into account that the manipulated inputs u_{i_k} , $i = 1, \dots, m$, are bounded, there exists a positive constant M_k such that

$$\left| f_k(x) + \sum_{i=1}^m g_{i_k}(x) u_{i_k} \right| \leq M_k \tag{7.3}$$

for all $x \in \Omega_{\bar{\rho}_k}$, $u_{i_k} \in U_{i_k}$, $i = 1, \dots, m$, and $k \in \mathcal{I}$. In addition, by the continuous differentiable property of the Lyapunov function $V_k(x)$ and the smoothness of f_k and

g_{i_k} , there exist positive constants L_{x_k} , $L_{u_{i_k}}$ and $C_{g_{i_k}}$ such that

$$\begin{aligned} \left| \frac{\partial V_k}{\partial x} f_k(x) - \frac{\partial V_k}{\partial x} f_k(x') \right| &\leq L_{x_k} |x - x'| \\ \left| \frac{\partial V_k}{\partial x} g_{i_k}(x) - \frac{\partial V_k}{\partial x} g_{i_k}(x') \right| &\leq L_{u_{i_k}} |x - x'|, \quad i = 1, \dots, m \\ \left| \frac{\partial V_k}{\partial x} g_{i_k}(x) \right| &\leq C_{g_{i_k}}, \quad i = 1, \dots, m \end{aligned} \quad (7.4)$$

for all $x, x' \in \Omega_{\tilde{\rho}_k}$, $u_{i_k} \in U_{i_k}$, $i = 1, \dots, m$, and $k \in \mathcal{I}$.

7.1.3 Stability properties of $h_k(x)$

In this subsection, we address the stability properties of the controller $h_k(x)$. Proposition 7.1 addresses the closed-loop stability properties of the controller $h_k(x)$ while Proposition 7.2 provides sufficient conditions to force the closed-loop system state under implementation of the Lyapunov-based controller in a sample-and-hold fashion to enter the corresponding stability region of the subsequent mode once the system switches to that mode.

We define the following sampled trajectory when the controller $h_k(x)$ is applied in a sample-and-hold fashion at mode k for $t_{k_r^{in}} \leq \tau < t_{k_r^{out}}$ as follows

$$\dot{\hat{x}}(\tau) = f_k(\hat{x}(\tau)) + \sum_{i=1}^m g_{i_k}(\hat{x}(\tau)) h_{i_k}(\hat{x}(t_l)), \quad l = 0, 1, \dots, N_{k_r} - 1, \quad \hat{x}(t_0) = x(t_{k_r^{in}}) \quad (7.5)$$

where $t_0 = t_{k_r^{in}}$.

Proposition 7.1 below ensures that if the closed-loop system at mode k controlled by $h_k(x)$ implemented in a sample-and-hold fashion and with open-loop state estimation (initial state) starts in $\Omega_{\tilde{\rho}_k}$ and stays in mode k for all times, then it is ultimately bounded in $\Omega_{\rho_{\min_k}}$. It characterizes the closed-loop stability region corresponding to

each mode.

Proposition 7.1 (c.f. [19]). *Consider the closed-loop system of Eq. 7.5 and assume it operates at mode k for all times. Let $\Delta_k, \epsilon_{s_k} > 0$ and $\tilde{\rho}_k > \rho_{s_k} > 0$ satisfy:*

$$-\alpha_{3_k}(\alpha_{2_k}^{-1}(\rho_{s_k})) + L'_{x_k} M_k \Delta_k \leq -\epsilon_{s_k} / \Delta_k. \quad (7.6)$$

Then, if $\hat{x}(t_0) \in \Omega_{\tilde{\rho}_k}$ and $\rho_{\min_k} < \tilde{\rho}_k$ where $\rho_{\min_k} = \max\{V_k(\hat{x}(t + \Delta_{k_r})) : V_k(\hat{x}(t)) \leq \rho_{s_k}\}$, $\forall \Delta_{k_r} \in (0, \Delta_k]$ the following inequality holds: $V_k(\hat{x}(t)) \leq V_k(\hat{x}(t_q))$, $\forall t \in [t_q, t_{q+1})$ ($q = 0, 1, \dots$) and $V_k(\hat{x}(t_q)) \leq \max\{V_k(\hat{x}(t_0)) - q\epsilon_{s_k}, \rho_{\min_k}\}$. Since $V_k(\cdot)$ is a continuous function, $V_k(\hat{x}) \leq \rho_{\min_k}$ implies $|\hat{x}| \leq d_k$ where d_k is a positive constant and therefore, $\limsup_{t \rightarrow \infty} |\hat{x}(t)| \leq d_k$.

For each mode $k \in \mathcal{I}$, we assume there exist a set of initial conditions $\Omega_{\tilde{\rho}_k}$, which is estimated as the level set of the Lyapunov function at mode k ($V_k(\cdot)$) and a positive real number ρ_k^* such that under implementation of the Lyapunov-based controller $h_k(\cdot)$ in a sample-and-hold fashion, the state of Eq. 7.5 satisfies

$$\dot{V}_k(\hat{x}(\tau)) \leq -\rho_k^* V_k(\hat{x}(\tau)), \hat{x}(\tau) \in \Omega_{\tilde{\rho}_k / \rho_{s_k}}, t_{k_r}^{in} \leq \tau < t_{k_r}^{out} \quad (7.7)$$

Proposition 7.2. *Consider the closed-loop sampled trajectory $\hat{x}(t)$ defined in Eq. 7.5. Given that $t_{k_r}^{in} \leq t < t_{k_r}^{out} = t_{f_w}^{in}$, and $\hat{x}(t_{k_r}^{in}) \in \Omega_{\tilde{\rho}_k}$, if there exist $\tilde{\rho}_k > 0$, $\rho_k^* > 0$, $N_{k_r} > 0$ and $\Delta_{k_r} > 0 \forall k \in \mathcal{I}$ such that*

$$\alpha_{2_f}(\alpha_{1_k}^{-1}(\tilde{\rho}_k e^{-\rho_k^* N_{k_r} \Delta_{k_r}})) \leq \tilde{\rho}_f, \quad (7.8)$$

then $\hat{x}(t_{f_w}^{in}) \in \Omega_{\tilde{\rho}_f}$.

Proof 7.1. It can be obtained from Eq. 7.7 that

$$V_k(\hat{x}(t_{k_r^{out}})) \leq V_k(\hat{x}(t_{k_r^{in}}))e^{-\rho_k^* N_{k_r} \Delta_{k_r}} \quad (7.9)$$

Since $\hat{x}(t_{k_r^{in}}) \in \Omega_{\tilde{\rho}_k}$, we have

$$V_k(\hat{x}(t_{k_r^{out}})) \leq \tilde{\rho}_k e^{-\rho_k^* N_{k_r} \Delta_{k_r}} \quad (7.10)$$

From Eq. 7.2 we can obtain $|\hat{x}(t_{k_r^{out}})| \leq \alpha_{1_k}^{-1}(\tilde{\rho}_k e^{-\rho_k^* N_{k_r} \Delta_{k_r}})$. If Eq. 7.8 is satisfied, using Eq. 7.2 for the Lyapunov-based controller at mode f , it can be concluded that $V_f(\hat{x}(t_{f_w^{in}})) \leq \tilde{\rho}_f$ which implies that $\hat{x}(t_{f_w^{in}}) \in \Omega_{\tilde{\rho}_f}$.

Assumption 7.1. Consider the closed-loop system state trajectory of Eq. 7.5 and assume that $\hat{x}(t_{k_r^{in}}) \in \Omega_{\tilde{\rho}_k}$. Suppose, after switching out from mode k for r^{th} time, the system switches to mode f for w^{th} time, i.e., $t_{k_r^{out}} = t_{f_w^{in}}$. We assume that there exists $\epsilon^* > 0$ such that the closed-loop system state of Eq. 7.5 satisfies the following MLF constraint

$$V_f(\hat{x}(t_{f_w^{in}})) \leq \begin{cases} V_f(\hat{x}(t_{f_{w-1}^{in}})) - \epsilon^*, & w > 1, V_f(\hat{x}(t_{f_{w-1}^{in}})) > \rho_{\min_f} \\ \rho_{\min_f} & , w > 1, V_f(\hat{x}(t_{f_{w-1}^{in}})) \leq \rho_{\min_f} \\ \tilde{\rho}_f & , w = 1 \end{cases} \quad (7.11)$$

where ρ_{\min_f} is defined in Proposition 7.1 below, $V_f(\hat{x}(t_{f_{w-1}^{in}}))$ is the value of the Lyapunov function of mode f when the system switches into mode f for $(w-1)^{\text{th}}$ time and $V_f(\hat{x}(t_{f_w^{in}}))$ is the value of the Lyapunov function of mode f when the system switches into mode f for w^{th} time.

Assumption 7.1 implies that there exists a Lyapunov-based controller correspond-

ing to each switching mode that meets the prescribed switching policy and at each mode the value of the Lyapunov function of the corresponding mode decreases to a certain level to ensure that when the system switches out of this mode to enter the subsequent mode, the closed-loop system state enters the stability region of the corresponding switching mode and the Lyapunov-based controllers of all the modes satisfy the MLF constraint [5].

Remark 7.1. *It should be emphasized that the stability region $\Omega_{\tilde{\rho}_k}$ characterizes the set of initial conditions starting from where, the closed-loop system state enters the corresponding stability region of the subsequent mode to proceed at the time of the switch. From a feasibility point of view, the Lyapunov-based controller satisfying Assumption 7.1 yields a feasible solution to the prescribed switching policy. It should be emphasized that the purpose of the MPC formulation in this chapter (centralized or distributed) is to take advantage of this feasible solution to improve closed-loop performance.*

7.1.4 Centralized MPC of switched systems

In this section, we briefly review the formulation of the centralized MPC for switched systems proposed in [73]. For initialization purposes we assume that $x(t_{1_i^n}) \in \Omega_{\tilde{\rho}_1}$. We assume that the system upon exiting from the mode k for the r^{th} time enters mode f for the w^{th} time (i.e., $t_{f_i^w} = t_{k_r^{out}} < \infty$). Specifically, the centralized MPC at mode k is formulated as follows:

$$\min_{u_{1_k}, \dots, u_{m_k} \in S(\Delta_{k_r})} \int_0^{\tilde{T}} [|\tilde{x}(\tau)|_{Q_{c_k}} + \sum_{i=1}^m |u_{i_k}(\tau)|_{R_{ci_k}}] d\tau \quad (7.12a)$$

$$\text{s.t. } \dot{\tilde{x}}(\tau) = f_k(\tilde{x}(\tau)) + \sum_{i=1}^m g_{i_k}(\tilde{x}(\tau))u_{i_k} \quad (7.12b)$$

$$u_{i_k}(\tau) \in U_{i_k}, \quad i = 1, \dots, m \quad (7.12c)$$

$$\tilde{x}(0) = x(t_q) \quad (7.12d)$$

$$\frac{\partial V_k(x(t_q))}{\partial x} g_{i_k}(x(t_q))u_{i_k}(0) \leq \frac{\partial V_k(x(t_q))}{\partial x} g_{i_k}(x(t_q))h_{i_k}(x(t_q)), \quad i = 1, \dots, m \quad (7.12e)$$

$$V_f(\tilde{x}(t_{f_w}^{in})) \leq \begin{cases} V_f(x(t_{f_{w-1}}^{in})) - \epsilon^*, & w > 1, \quad V_f(x(t_{f_{w-1}}^{in})) > \rho_{min_f} \\ \rho_{min_f} & , \quad w > 1, \quad V_f(x(t_{f_{w-1}}^{in})) \leq \rho_{min_f} \\ \tilde{\rho}_f & , \quad w = 1 \end{cases} \quad (7.12f)$$

where \tilde{x} is the predicted state trajectory of the closed-loop system, $S(\Delta_{k_r})$ is the family of piece-wise continuous functions over $[0, \tilde{T}]$, Q_{c_k} and R_{ci_k} , $i = 1, \dots, m$, are positive definite weight matrices and \tilde{T} is the time interval corresponding to prediction horizon and

$$\tilde{T} = \begin{cases} t_{k_r^{out}} - t_q, & \text{if } t_{k_r^{out}} < \infty \\ T_{design}, & \text{if } t_{k_r^{out}} = \infty \end{cases} \quad (7.13)$$

where $0 < T_{design} < \infty$ is a design parameter. The transition constraint of Eq.7.12f ensures that if this mode is switched out and then switched back in, then $V_k(x(t_{k_r+1}^{in})) < V_k(x(t_{k_r}^{in}))$. In general $V_k(x(t_{k_r}^{in})) < V_k(x(t_{k_r-1}^{in})) < \dots < \tilde{\rho}_k$. In other words, this constraint enforces the MLF stability condition in the switched system.

Remark 7.2. *It should be emphasized that the centralized MPC of Eq. 7.12 is not implemented in the context of conventional receding horizon scheme. Based on the prescribed switching schedule policy, at each time interval that the system is supposed to operate in a specific mode, it uses a prediction horizon from the current time until*

the time that the system is supposed to be switched out from that mode. Furthermore, if the system is supposed to operate in a single mode for a specific time, it uses a fixed horizon T_{design} based on Eq. 7.13.

The manipulated inputs of the centralized control design of Eq. 7.12 at mode k are defined as follows:

$$u_{i_k}(t) = u_{i_k}^*(t - t_q | t_q), \quad i = 1, \dots, m, \quad \forall t \in [t_q, t_{q+1}). \quad (7.14)$$

A potential drawback of the centralized MPC framework is that its computational burden significantly increases as the number of manipulated inputs and constraints grow, motivating the development of DMPC algorithms for switched systems.

7.2 DMPC of switched nonlinear systems

In this section, we propose an iterative Lyapunov-based DMPC scheme for switched nonlinear systems given a prescribed switching sequence (see also [39, 35]). We assume that there exists a Lyapunov-based controller for each of the switched system modes which satisfies Eqs. 7.2 and 7.7. The controller design problem seeks to enforce appropriate Lyapunov-based stability constraint in the DMPC formulation to achieve practical stability in the closed-loop switched system. From a control design perspective, DMPC forces the system state to evolve at each switching mode such that at the time of switching into the next mode, the closed-loop system state is within the stability region of the new mode. One of the difficulties in the implementation of distributed MPC in switched systems is the enforcement of the MLF constraint (Eq. 7.12f) from a feasibility point of view; however, in this chapter, we take advantage of the specified properties of the Lyapunov-based controller (Eqs. 7.2

and 7.7) to provide a feasible solution to the optimization problem of the DMPC for switched systems. Specifically, the implementation strategy of DMPC of switched nonlinear systems can be described as follows:

1. At sampling time t_q all of the distributed controllers receive the state measurements $x(t_q)$ through sensors.
2. At each iteration $c < c_{max}$
 - 2.1 All of the distributed controllers exchange their latest optimal input trajectories.
 - 2.2 Each MPC evaluates its own future input trajectory based on $x(t_q)$ and the latest received input trajectories of all the other MPCs.
 - 2.3 Using the computed input trajectories of all DMPCs the constraint of Eq. 7.12f is checked. If this constraint is satisfied go to step 2.5; otherwise, go to step 2.4.
 - 2.4 Provide the distributed MPCs a new initial guess by slightly perturbing the latest feasible optimal solution (if $c = 1$, this solution is $h(x(t_q))$; for $c > 1$, it is the solution obtained at iteration $c - 1$) and re-calculate the input trajectories of the DMPCs. If the new input trajectories satisfy the constraint of Eq. 7.12f, go to step 2.5; otherwise, re-calculate the input trajectories of the DMPCs by slightly perturbing the latest initial guess and check if the constraint of Eq. 7.12f is satisfied. If a new DMPC solution that satisfies the constraint of Eq. 7.12f can not be found after a set number of evaluations, if $c = 1$, use $h(x(t_q))$ as a solution, else, keep the solution obtained at iteration $c - 1$. Go to step 2.5.
 - 2.5 Set $c \leftarrow c + 1$ and return to step 2.1.

3. After a number of iterations/evaluations that depend on the sampling time, pick the input trajectories which yield the minimum cost function and satisfy the constraint of Eq. 7.12f over the iterations.
4. Each MPC controller sends the first step input value of its optimal input trajectory to its actuators.

At each sampling time and at first iteration, the Lyapunov-based controller of the corresponding mode is a feasible solution for the optimization problem of each distributed MPC of Eq. 7.15 and also for the centralized MPC problem of Eq. 7.12; this is consequence of Assumption 7.1 which imposes the existence of a feasible control input trajectory for the centralized control problem for the switched systems and also because $h(x(t_q))$ is a feasible solution for the DMPCs.

According to this implementation strategy, the DMPC formulation of MPC j at iteration c is as follows:

$$\min_{u_{j_k} \in S(\Delta_{k\tau})} \int_0^{\tilde{T}} [|\tilde{x}^j(\tau)|_{Q_{c_k}} + \sum_{i=1}^m |u_{i_k}(\tau)|_{R_{c_i_k}}] d\tau \quad (7.15a)$$

$$\text{s.t. } \dot{\tilde{x}}^j(\tau) = f_k(\tilde{x}^j(\tau)) + \sum_{i=1}^m g_{i_k}(\tilde{x}^j(\tau))u_{i_k} \quad (7.15b)$$

$$u_{i_k}(\tau) = u_{i_k}^{*,c-1}(\tau|t_q), \quad i \neq j \quad (7.15c)$$

$$u_{j_k}(\tau) \in U_{j_k} \quad (7.15d)$$

$$\tilde{x}^j(0) = x(t_q) \quad (7.15e)$$

$$\frac{\partial V_k(x(t_q))}{\partial x} g_{j_k}(x(t_q))u_{j_k}(0) \leq \frac{\partial V_k(x(t_q))}{\partial x} g_{j_k}(x(t_q))h_{j_k}(x(t_q)) \quad (7.15f)$$

$$V_f(\tilde{x}^j(t_{f_w^{in}})) \leq \begin{cases} V_f(x(t_{f_{w-1}^{in}})) - \epsilon^*, & w > 1, V_f(x(t_{f_{w-1}^{in}})) > \rho_{min_f} \\ \rho_{min_f} & , w > 1, V_f(x(t_{f_{w-1}^{in}})) \leq \rho_{min_f} \\ \tilde{\rho}_f & , w = 1 \end{cases} \quad (7.15g)$$

where $u_{i_k}^{*,c-1}(\tau|t_q)$ are the optimal control input trajectories from MPC i ($i = 1, \dots, m, i \neq j$) and \tilde{x}^j is the predicted system state trajectory while MPC j uses the optimal control input trajectories of the rest of the controllers from iteration $c - 1$. The constraint of Eq. 7.15f enforces that the amount of reduction in the value of the Lyapunov function by applying the control inputs of the distributed MPCs is at least at the level achieved by the Lyapunov-based controller when it is applied in a sample and hold fashion. $S(\Delta_{k_r})$ is the family of piece-wise continuous functions over $[0, \tilde{T}]$. \tilde{T} is the time interval corresponding to the prediction horizon which is chosen according to Eq. 7.13. The transition constraint of Eq.7.15g ensures that if the f mode is switched out and then switched back in for the w^{th} time, then $V_f(x(t_{f_w^{in}})) < V_f(x(t_{f_{w-1}^{in}}))$. In other words, this constraint enforces the MLF stability constraint in the switched system. If previously, the closed-loop system state entered the final invariant set $\Omega_{\rho_{min_f}}$, it will stay there. If it is the first time that the system switched to mode f , the closed-loop system state is restricted to the set $\Omega_{\tilde{\rho}_f}$.

It should be emphasized that at the first iteration ($c = 1$), $h(x(t_q))$ is a feasible solution to the DMPC and each MPC assumes that the rest of the MPCs apply the Lyapunov-based controller at the current mode. The manipulated inputs of the proposed control design of Eq. 7.15 at mode k are defined as follows:

$$u_{i_k}(t) = u_{i_k}^*(t - t_q|t_q), \quad i = 1, \dots, m, \quad \forall t \in [t_q, t_{q+1}). \quad (7.16)$$

Remark 7.3. Referring to the implementation of the DMPC of Eq. 7.15 with the

objective of ensuring that the computed optimal solution satisfies the transition constraint of the centralized MPC of Eq. 7.12f at each sampling time, we can take advantage of a sequential implementation strategy at the cost of increasing the computational time of the DMPC calculation because in this case the computational time at each sampling time will be the sum of the computational times of all DMPCs involved in the sequential implementation. In the sequential architecture, if we evaluate MPCs in an increasing order and pass optimal solutions to the adjacent controller, $(h_1(x(t_q)), \dots, h_m(x(t_q)))$ is a feasible control input used for MPC 1, $(u_1^*(t_q), h_2(x(t_q)), \dots, h_m(x(t_q)))$ is a feasible control input used for MPC 2 where $u_1^*(t_q)$ is the optimal manipulated input obtained by MPC 1 at sampling time t_q and so on.

7.3 Stability analysis

The following theorem characterizes the stability properties of the DMPC design of Eq. 7.15.

Theorem 7.1. *Consider the system of Eq. 7.1 in closed-loop under the distributed MPC of Eqs. 7.15-7.16 and assume that there exists Lyapunov-based controllers $h_k(\cdot)$, $\forall k \in \mathcal{I}$ satisfying Eq. 7.2 and Assumption 7.1. Let $0 < T_{design} < \infty$ be a design parameter, \tilde{T} satisfy Eq. 7.13 and $t_{k_r^{in}} \leq t < t_{k_r^{out}} = t_{f_w^{in}}$ for some $f, k \in \mathcal{I}$. Then, given a positive real number d^{max} , if there exist $\Delta_k, \epsilon_{s_k} > 0$, $\tilde{\rho}_k > \rho_{s_k} > 0$ and $\epsilon_{w_k} > 0$ ($\forall k \in \mathcal{I}$) such that Eqs. 7.6 and 7.8 are satisfied and $\Delta_{k_r} \in (0, \Delta^*]$ where $\Delta^* = \min_{k \in \mathcal{I}} \Delta_k$, then $x(t)$ is bounded and $\limsup_{t \rightarrow \infty} |x(t)| \leq d_{max}$.*

Proof 7.2. First we prove that the optimization problem of Eq. 7.15 is feasible at all times and then we proceed with the closed-loop stability analysis. Since the

Lyapunov-based controller through implementation in a sample-and-hold fashion satisfies the MLF constraint of Eq. 7.12f and at the end of each switching mode it constraints the system state to enter the stability region of the subsequent mode, it follows that at each iteration $h_{j_k}(\cdot)$ is a feasible solution for the optimization problem of Eq. 7.15.

Given the radius of the ball around the origin, d^{max} , the values of ρ_{min_k} and Δ_k $\forall k \in \mathcal{K}$ are computed based on Propositions 7.2 and 7.1. Then, for the purpose of DMPC implementation, a value of $\Delta_{k_r} \in (0, \Delta^*]$ is chosen where $\Delta^* = \min_{k \in \mathcal{I}} \Delta_k$ and $t_{k_r^{out}} - t_{k_r^{in}} = l_{k_r} \Delta_{k_r}$ for some integer $l_{k_r} > 0$ (note that given any two positive real numbers $t_{k_r^{out}} - t_{k_r^{in}}$ and Δ^* , one can always find a positive real number $\Delta_{k_r} \leq \Delta^*$ such that $t_{k_r^{out}} - t_{k_r^{in}} = l_{k_r} \Delta_{k_r}$ for some integer $l_{k_r} > 0$).

Part 1: First consider the case when the switching is infinite. Let t be such that $t_{k_r^{in}} \leq t < t_{k_r^{out}}$ and $t_{f_w^{in}} = t_{k_r^{out}} < \infty$. Consider the active mode k . If $V_k(x) > \rho_{min_k}$, the continued feasibility of the constraint of Eq.7.15f implies that $V_k(x(t_{k_r^{out}})) < V_k(x(t_{k_r^{in}}))$. The transition constraint of Eq.7.15g ensures that if this mode is switched out and then switched back in, then $V_k(x(t_{k_r+1}^{in})) < V_k(x(t_{k_r^{in}}))$. In general $V_k(x(t_{k_r^{in}})) < V_k(x(t_{k_r-1}^{in})) < \dots < \tilde{\rho}_k$. Under the feasibility of the constraints of Eqs.7.15f and 7.15g for all future times, the value of $V_k(x)$ continues to decrease. If the mode of this Lyapunov function is not active, there exists at least some $z \in \mathcal{I}$ such that mode z is active and Lyapunov function V_z continues to decrease until the time that $V_z \leq \rho_{min_z}$ (this happens because there is a finite number of modes, even if the number of switches may be infinite). From this point onwards, Propositions 7.1 ensures that V_z continues to be less than or equal to ρ_{min_z} . Due to continuity of Lyapunov functions, there exists d^{max} such that $\limsup_{t \rightarrow \infty} |x(t)| \leq d^{max}$.

Part 2: For the case of a finite switching sequence, consider a t such that $t_{k_r^{in}} \leq t < t_{k_r^{out}} = \infty$. Following a similar argument, $V_k(x(t_{k_r^{in}})) < V_k(x(t_{k_{r-1}^{in}})) < \dots < \tilde{\rho}_k$. At the time of the switch to mode k , therefore, $x(t_{k_r^{in}}) \in \Omega_{\tilde{\rho}_k}$. From this point onwards, the DMPC is applied without any switching constraint, i.e., the constraint of Eq.7.15g is removed. Since the DMPC at mode k is stabilizing, it follows that $\limsup_{t \rightarrow \infty} |x(t)| \leq d^{max}$. This completes the proof of Theorem 7.1.

Remark 7.4. *The purpose of Theorem 7.1, is to clarify under appropriate assumptions which include I) existence of Lyapunov-based controllers corresponding to each mode that can asymptotically stabilize the closed-loop system at that switching mode, II) satisfaction of the prescribed switching schedule by the Lyapunov-based controllers, and III) picking appropriate finite prediction horizon according to Eq. 7.13, that the closed-loop system state under the DMPC of Eq. 7.15 is bounded in a final invariant set.*

7.4 Distributed optimization considerations

In this section, we address the question of convergence of the solution of the distributed MPC to the one of the centralized MPC. It should be emphasized that for general nonlinear systems it is not possible to prove convergence of the iterations of the distributed MPC to the optimal centralized MPC cost at each sampling time due to the way the Lyapunov-based constraint of the centralized MPC is broken down into constraints imposed on the individual MPCs. However, under appropriate assumptions which include linear model, quadratic Lyapunov functions corresponding to each mode and an appropriate update rule in the DMPC iterations, it can be shown that the MPC optimization problem is convex and under a sufficiently large number of iterations, the optimal value of the objective function under the DMPC converges

to the optimal value of the corresponding centralized MPC at each sampling time.

Specifically, we consider a class of switched, linear time-invariant systems with a state-space description of the form at mode $k \in \mathcal{I}$:

$$\dot{x}(t) = A_k x(t) + \sum_{i=1}^m B_{i_k} u_{i_k}(t) \quad (7.17)$$

where A_k and B_{i_k} ($i = 1, \dots, m$) are constant matrices with appropriate dimensions. We assume, in accordance with Assumption 7.1, that there exist a set of quadratic Lyapunov functions $V_k = x^T P_k x$, $\forall k \in \mathcal{I}$, where P_k , are positive definite matrices, and a set of explicit feedback controllers $u_{i_k} = K_{i_k} x$, where K_{i_k} is a constant coefficient matrix, meet the prescribed switching schedule defined in subsection 7.1.1. We also assume that the input used as the initial guess in the optimization problem of MPC at iteration $c + 1$ is computed according to the following expression

$$u_{j_k}^c(\tau|t_k) = (1 - \tilde{w}_{j_k}) u_{j_k}^{c-1}(\tau|t_k) + \tilde{w}_{j_k} u_{j_k}^{*,c}(\tau|t_k) \quad (7.18)$$

where $\sum_{j=1}^m \tilde{w}_{j_k} = 1$ with $0 < \tilde{w}_{j_k} < 1$, $u_{j_k}^{*,c}$ is the optimal solution of controller j ($j = 1, \dots, m$) at iteration c and $u_{j_k}^{c-1}$ is the input trajectory assumed by the rest of controllers for controller j at iteration c and mode k .

Corollary 7.1. *Consider the switched, linear system of Eq. 7.17, assume that the conditions of Assumption 7.1 hold with $V_k = x^T P_k x$ and $u_{i_k} = K_{i_k} x$ and let the input to the optimization problem of MPC i of Eq. 7.15 at mode k (using $V_k = x^T P_k x$, $h_{i_k} = K_{i_k} x$ where $i = 1, \dots, m$ and the linear model of Eq. 7.17) at iteration c be defined according to Eq. 7.15. Let also $x(t_q) \in \Omega_{\tilde{p}_k}$. Then, if the iteration number $c \rightarrow \infty$, the optimal cost of the distributed optimization problem of Eqs. 7.15-7.18, at sampling time t_q converges to the optimal cost of the corresponding centralized MPC.*

Furthermore, if the corresponding centralized MPC asymptotically stabilizes the origin of the closed-loop system, the DMPC of Eq. 7.15 also asymptotically stabilizes the origin of the closed-loop system and the closed-loop cost of the DMPC converges to the one given by the centralized control system.

Proof 7.3. We first prove that the optimization problems for both the centralized and the distributed MPC are convex. Specifically, the optimization problem for the centralized MPC of Eq. 7.12 with $V_k = x^T P_k x$ and $h_{i_k}(x) = K_{i_k} x$ at sampling time t_q takes the following form:

$$\min_{u_{1_k}, \dots, u_{m_k} \in S(\Delta_{k_r})} \int_0^{\tilde{T}} [|\tilde{x}(\tau)|_{Q_{c_k}} + \sum_{i=1}^m |u_{i_k}(\tau)|_{R_{c_{i_k}}}] d\tau \quad (7.19a)$$

$$\text{s.t. } \dot{\tilde{x}}(\tau) = A_k \tilde{x}(\tau) + \sum_{i=1}^m B_{i_k} u_{i_k} \quad (7.19b)$$

$$u_{i_k}(\tau) \in U_{i_k}, \quad i = 1, \dots, m \quad (7.19c)$$

$$\tilde{x}(0) = x(t_q) \quad (7.19d)$$

$$\frac{\partial V_k(x(t_q))}{\partial x} B_{i_k} u_{i_k}(0) \leq \frac{\partial V_k(x(t_q))}{\partial x} B_i K_{i_k} x(t_q), \quad i = 1, \dots, m \quad (7.19e)$$

$$V_f(\tilde{x}(t_{f_w^{in}})) \leq \begin{cases} V_f(x(t_{f_{w-1}^{in}})) - \epsilon^*, & w > 1, \quad V_f(x(t_{f_{w-1}^{in}})) > \rho_{min_f} \\ \rho_{min_f} & , \quad w > 1, \quad V_f(x(t_{f_{w-1}^{in}})) \leq \rho_{min_f} \\ \tilde{\rho}_f & , \quad w = 1 \end{cases} \quad (7.19f)$$

Specifically, the constraint of Eq. 7.19e takes the following form:

$$\begin{aligned} & (u_{i_k}(0)^T B_{i_k}^T P_k x(t_q) + x(t_q)^T P_k B_{i_k} u_{i_k}(0)) \\ & \leq ((K_{i_k} x(t_q))^T B_{i_k}^T P_k x(t_q) + x(t_q)^T P_k B_{i_k} K_{i_k} x(t_q)) \end{aligned} \quad (7.20)$$

which is linear in terms of u_{i_k} ($i = 1, \dots, m$). If we take into account that the input trajectories are piece-wise constant and that

$$\tilde{x}(\tau) = e^{A\tau}\tilde{x}(t_q) + \int_0^\tau e^{A(\tau-s)} \sum_{i=1}^m (B_{i_k} u_{i_k}(s)) ds, \tau \in [0, \tilde{T}] \quad (7.21)$$

and quadratic Lyapunov functions are used, it can be verified that all the constraints are convex in terms of the control inputs. Since U_{i_k} is also convex for $i = 1, \dots, m$, it can be concluded that the switched centralized MPC optimization problem of Eq. 7.19 is convex. Since the centralized MPC optimization problem for switched linear systems is convex and it has been initialized by a feasible solution $h_{i_k}(x(t_q)) = K_{i_k}x(t_q)$ under Assumption 7.1 and the fact that $x(t_q) \in \Omega_{\tilde{\rho}_k}$, it has a unique optimal solution $u_k^* = (u_{1_k}^*, \dots, u_{m_k}^*)$ which yields $J(u_k^*)$ at sampling time t_q , where $J(\cdot)$ is the quadratic cost function of the optimization problem (See Eq. 7.19a). Following a similar argument, it can be proved that the DMPC optimization problem of MPC j ($j = 1, \dots, m$) at mode k is also convex. Next, we prove that the optimal inputs and the cost of the distributed MPC converge to the ones of the centralized MPC at a fixed sampling time as $c \rightarrow \infty$. The proof follows similar arguments to the proofs presented in [3, 92]. Defining $u_k^c = (u_{1_k}^c, \dots, u_{m_k}^c)$ and the cost function by $J(u_k^c)$ at iteration c and mode k where the update rule is defined in Eq. 7.18 while considering the fact that

$$u_k^{c+1} = \tilde{w}_{1_k}(u_{1_k}^{*,c+1}, u_{2_k}^c, \dots, u_{m_k}^c) + \dots + \tilde{w}_{m_k}(u_{1_k}^c, \dots, u_{(m-1)_k}^c, u_{m_k}^{*,c+1}) \quad (7.22)$$

we can obtain

$$\begin{aligned}
J(u_k^{c+1}) &= J(\tilde{w}_{1_k}(u_{1_k}^{*,c+1}, u_{2_k}^c, \dots, u_{m_k}^c) + \dots + \tilde{w}_{m_k}(u_{1_k}^c, \dots, u_{(m-1)_k}^c, u_{m_k}^{*,c+1})) \\
&< \tilde{w}_{1_k} J(u_{1_k}^{*,c+1}, u_{2_k}^c, \dots, u_{m_k}^c) + \dots + \tilde{w}_{m_k} J(u_{1_k}^c, \dots, u_{(m-1)_k}^c, u_{m_k}^{*,c+1}) \\
&\leq \tilde{w}_{1_k} J(u_{1_k}^c, u_{2_k}^c, \dots, u_{m_k}^c) + \dots + \tilde{w}_{m_k} J(u_{1_k}^c, \dots, u_{(m-1)_k}^c, u_{m_k}^c) \\
&= J(u_k^c)
\end{aligned} \tag{7.23}$$

where the first inequality is the result of strict convexity of the cost function $J(\cdot)$ and the second one arises from optimality of the control inputs $u_{i_k}^{*,c}$ at iteration c where $i = 1, \dots, m$. So, through iterations over a fixed sampling time, the value of the cost function decreases. Since the cost function is positive definite and strictly convex and it is bounded from above by the value achieved by the Lyapunov-based controller, we can conclude that the value of the cost function converges to some value \bar{J} as $c \rightarrow \infty$. Since the cost function $J(\cdot)$ is strictly convex and the level sets of the cost function are compact, there is a limit point $\tilde{u}_k = (\tilde{u}_{1_k}, \dots, \tilde{u}_{m_k})$ where $\bar{J} = J(\tilde{u}_k)$. We choose an index set $Z \subset \{0, 1, 2, \dots\}$ such that the sequence $\{u_k^z\}_{z \in Z}$ converges to \tilde{u}_k . Furthermore, all iterations u_k^z are in the intersection of $U_{1_k} \times U_{2_k} \times \dots \times U_{m_k}$, where \times denotes cartesian product, and the level set $J \leq J(u_k^0)$. Thus, $\lim_{z \in Z, z \rightarrow \infty} J(u_k^z) = \bar{J}$. Note that the optimal solution u_k^* of the centralized problem of Eq. 7.19 is also a feasible solution to the DMPC problem. Subsequently, we prove that if $c \rightarrow \infty$, then $\tilde{u}_k \rightarrow u_k^*$. Using contradiction, assume $\tilde{u}_k \neq u_k^*$. Since $J(\cdot)$ is a strict convex function we can write

$$\nabla J(\tilde{u}_k)^T (u_k^* - \tilde{u}_k) \leq J(u_k^*) - J(\tilde{u}_k) \equiv \Delta J(u_k) < 0 \tag{7.24}$$

From Eq. 7.24 and using contradiction, if we define

$$\Delta \tilde{u}_i^{*T} = (\mathbf{0}, \dots, \mathbf{0}, (u_{i_k}^* - \tilde{u}_{i_k})^T, \mathbf{0}) \tag{7.25}$$

where $\mathbf{0}$ are vector columns of zeros with appropriate dimensions, it can be easily shown that the following equation is satisfied for at least one i where $i = 1, \dots, m$

$$\nabla J(\tilde{u}_k)^T \Delta \tilde{u}_i^* \leq \frac{\Delta J(u_k)}{m} < 0 \quad (7.26)$$

Suppose it holds for $i = 1$. Using Taylor's expansion around \tilde{u}_k for $\epsilon_k \in (0, 1)$, $\delta_k \in (0, \epsilon)$, $c \rightarrow \infty$ and taking advantage of Eq. 7.26, we can write

$$\begin{aligned} J(\tilde{u}_{1_k} + \epsilon_k(u_{1_k}^* - \tilde{u}_{1_k}), \tilde{u}_{2_k}, \dots, \tilde{u}_{m_k}) &= J(\tilde{u}_k) + \epsilon_k \nabla J(\tilde{u}_k)^T \Delta \tilde{u}_1^* \\ &\quad + \frac{1}{2} \epsilon_k^2 \Delta \tilde{u}_1^{*T} \nabla^2 J(\tilde{u}_{1_k} + \epsilon_k(u_{1_k}^* - \tilde{u}_{1_k}), \tilde{u}_{2_k}, \\ &\quad \dots, \tilde{u}_{m_k}) \Delta \tilde{u}_1^* \\ &\leq J(\tilde{u}_k) + \frac{\epsilon_k}{m} \Delta J(u_k) + \varsigma_k \epsilon_k^2 \\ &< J(\tilde{u}_k) \end{aligned} \quad (7.27)$$

if ϵ_k is small enough such that $\frac{\epsilon_k}{m} \Delta J(u_k) + \varsigma_k \epsilon_k^2$ is negative (this is always possible since $\Delta J(u_k) < 0$) and ς_k is independent of c and ϵ_k . Since the iterative algorithms converges to $J(\tilde{u}_k)$ we can write

$$J(\tilde{u}_k) = \lim_{c \rightarrow \infty} J(u_{1_k}^{*,c}, u_{2_k}^c, \dots, u_{m_k}^c) \quad (7.28)$$

Also, from optimality of $u_{1_k}^{*,c}$, if $c \rightarrow \infty$, we can obtain

$$\lim_{c \rightarrow \infty} J(u_{1_k}^{*,c}, u_{2_k}^c, \dots, u_{m_k}^c) \leq J(\tilde{u}_{1_k} + \epsilon_k(u_{1_k}^* - \tilde{u}_{1_k}), \tilde{u}_{2_k}, \dots, \tilde{u}_{m_k}) \quad (7.29)$$

It should be emphasized that for $c \rightarrow \infty$, $u_{i_k}^c \rightarrow \tilde{u}_{i_k}$ where $i = 1, \dots, m$. Considering

Eqs. 7.27-7.29, we can obtain

$$\begin{aligned}
J(\tilde{u}_k) &= \lim_{c \rightarrow \infty} J(u_{1_k}^{*,c}, u_{2_k}^c, \dots, u_{m_k}^c) \\
&\leq J(\tilde{u}_{1_k} + \epsilon_k(u_{1_k}^* - \tilde{u}_{1_k}), \tilde{u}_{2_k}, \dots, \tilde{u}_{m_k}) \\
&< \tilde{J}(\tilde{u}_k)
\end{aligned} \tag{7.30}$$

Therefore, $J(\tilde{u}_k) < J(\tilde{u}_k)$ which is a contradiction. Therefore, the assumption $\tilde{u}_k \neq u_k^*$ was not true. It can be concluded that $\tilde{u}_k = u_k^*$ when $c \rightarrow \infty$ and $J(\tilde{u}_k) = J(u_k^*)$. If $x(t_q) \in \Omega_{\tilde{\rho}_k}$ and the centralized MPC can asymptotically stabilize the origin of the closed-loop system, using the above arguments recursively for each sampling time, if $c \rightarrow \infty$ for each sampling time, it follows that the DMPC also asymptotically stabilizes the origin of the closed-loop system and the closed-loop cost converges to the one given by the centralized control system.

7.5 Application to a chemical process network

The process considered in this study is a three vessel, reactor-separator system consisting of two continuously stirred tank reactors (CSTRs) and a flash tank separator shown in Figure 7.1 [15]. The operation schedule requires switching between two available inlet streams consisting of pure reactant at different flow rates, concentrations and temperatures. At mode $\sigma = \{1, 2\}$ a feed stream to the first CSTR F_{10_σ} contains the reactant A which is converted into the desired product B . The effluent of the first CSTR along with additional fresh feed F_{20_σ} makes up the inlet to the second CSTR. The reactions $A \rightarrow B$ and $A \rightarrow C$ (referred to as 1 and 2, respectively; C is an undesired product) take place in the two CSTRs in series before the effluent from CSTR 2 is fed to a flash tank. The overhead vapor from the flash tank is condensed

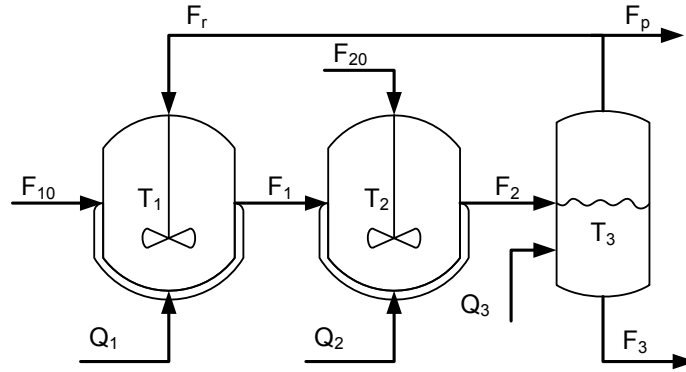


Figure 7.1: Two CSTRs and a flash tank with recycle stream.

and recycled to the first CSTR, and the bottom product stream is removed. A small portion of the overhead is purged before being recycled to the first CSTR. All the three vessels are assumed to have static holdup. The dynamic equations describing the behavior of the system at mode σ , obtained through material and energy balances under standard modeling assumptions, can be found in [15]. Each of the tanks has an external heat input/removal actuator. The model of the flash tank separator is derived under the assumption that the relative volatility for each of the species remains constant within the operating temperature range of the flash tank. This assumption allows calculating the mass fractions in the overhead based upon the mass fractions in the liquid portion of the vessel. It has also been assumed that there is a negligible amount of reaction taking place in the separator. The process model (system of non-linear ordinary differential equations) is numerically simulated using standard Euler integration method.

This process is divided into three subsystems corresponding to the first CSTR, the second CSTR and the separator, respectively. For the three subsystems, we will refer to them as subsystem 1, subsystem 2 and subsystem 3, respectively. The state of subsystem 1 is defined as the deviations of the temperature and species concentrations in the first CSTR from the desired, operating steady-state; that is,

$x_1^T = [T_1 - T_{1s_\sigma} \ C_{A1} - C_{A1s_\sigma} \ C_{B1} - C_{B1s_\sigma} \ C_{C1} - C_{Cs_\sigma}]^T$ for the system at mode σ . Similarly, we define the state of subsystems 2 and 3. Accordingly, the state of the whole process is defined as a combination of the states of the three subsystems; that is, $x^T = [x_1^T \ x_2^T \ x_3^T]$.

The process has one unstable and two stable steady states. The control objective is to regulate the process at the unstable steady-state x_{s_2} corresponding to the operating point defined by $Q_{1s} = Q_{2s} = Q_{3s} = 0 \frac{KJ}{hr}$ (which are the same for both process operating modes), respectively. The values of the operating steady-states corresponding to each mode are shown in Tables 7.1 and 7.2. Each of the tanks has an external heat input which is the control input associated with each subsystem, that is, $u_{1\sigma} = Q_1 - Q_{1s}$, $u_{2\sigma} = Q_2 - Q_{2s}$ and $u_{3\sigma} = Q_3 - Q_{3s}$ for $\sigma = 1, 2$. For mode 1 the inputs are subject to constraints as follows: $|u_{11}| \leq 1.5 \times 10^5 \text{ KJ/hr}$, $|u_{21}| \leq 1.5 \times 10^5 \text{ KJ/hr}$, and $|u_{31}| \leq 2 \times 10^5 \text{ KJ/hr}$ while in mode 2 $|u_{12}| \leq 10^5 \text{ KJ/hr}$, $|u_{22}| \leq 10^5 \text{ KJ/hr}$, and $|u_{32}| \leq 1.33 \times 10^5 \text{ KJ/hr}$. Three distributed MPC controllers (controller 1, controller 2 and controller 3) will be designed to manipulate each one of the three inputs in the three subsystems, respectively. Furthermore, we assume that the system state, x , is available at synchronous time instants $t_q = q\Delta$, $q = 0, 1, \dots$, with $\Delta = 0.001 \text{ hr} = 3.6 \text{ sec}$ to all the controllers. The process model belongs to the following class of nonlinear systems:

$$\dot{x}(t) = f_\sigma(x(t)) + \sum_{i=1}^3 g_{i\sigma}(x(t))u_{i\sigma}(t)$$

where the explicit expressions of f_σ , $g_{i\sigma}$ ($i = 1, 2, 3$ and $\sigma = \{1, 2\}$), are omitted for brevity.

In the simulations, we consider a quadratic Lyapunov function $V_\sigma(x) = x^T P_\sigma x$ with $P_1 = \text{diag}([10 \ 10^3 \ 10^3 \ 10^3 \ 20 \ 10^3 \ 10^3 \ 10^3 \ 10 \ 10^3 \ 10^3 \ 10^3])$ and $P_2 = \text{diag}([10 \ 10^3$

Table 7.1: Steady-state values for x_{s_1} .

C_{A1s_1}	$3.31 \left[\frac{\text{kmol}}{\text{m}^3} \right]$	C_{A2s_1}	$2.75 \left[\frac{\text{kmol}}{\text{m}^3} \right]$	C_{A3s_1}	$2.88 \left[\frac{\text{kmol}}{\text{m}^3} \right]$
C_{B1s_1}	$0.17 \left[\frac{\text{kmol}}{\text{m}^3} \right]$	C_{B2s_1}	$0.45 \left[\frac{\text{kmol}}{\text{m}^3} \right]$	C_{B3s_1}	$0.50 \left[\frac{\text{kmol}}{\text{m}^3} \right]$
C_{C1s_1}	$0.04 \left[\frac{\text{kmol}}{\text{m}^3} \right]$	C_{C2s_1}	$0.11 \left[\frac{\text{kmol}}{\text{m}^3} \right]$	C_{C3s_1}	$0.12 \left[\frac{\text{kmol}}{\text{m}^3} \right]$
T_{1s_1}	$369.53 [K]$	T_{2s_1}	$435.25 [K]$	T_{3s_1}	$435.25 [K]$

Table 7.2: Steady-state values for x_{s_2} .

C_{A1s_2}	$3.32 \left[\frac{\text{kmol}}{\text{m}^3} \right]$	C_{A2s_2}	$2.69 \left[\frac{\text{kmol}}{\text{m}^3} \right]$	C_{A3s_2}	$2.91 \left[\frac{\text{kmol}}{\text{m}^3} \right]$
C_{B1s_2}	$0.34 \left[\frac{\text{kmol}}{\text{m}^3} \right]$	C_{B2s_2}	$0.70 \left[\frac{\text{kmol}}{\text{m}^3} \right]$	C_{B3s_2}	$0.85 \left[\frac{\text{kmol}}{\text{m}^3} \right]$
C_{C1s_2}	$0.08 \left[\frac{\text{kmol}}{\text{m}^3} \right]$	C_{C2s_2}	$0.17 \left[\frac{\text{kmol}}{\text{m}^3} \right]$	C_{C3s_2}	$0.20 \left[\frac{\text{kmol}}{\text{m}^3} \right]$
T_{1s_2}	$370.98 [K]$	T_{2s_2}	$429.65 [K]$	T_{3s_2}	$429.64 [K]$

$10^3 \ 10^3 \ 10 \ 10^3 \ 10^3 \ 10^3 \ 10 \ 10^3 \ 10^3 \ 10^3$). We design the Lyapunov-based controller $h_\sigma(x)$ following the continuous bounded control law design [58, 18] as follows:

$$u_\sigma = [u_{1\sigma} \ u_{3\sigma} \ u_{3\sigma}]^T = h_\sigma(x) = -p_\sigma(x)(L_{G_\sigma} V_\sigma)^T \quad (7.31)$$

where

$$p_\sigma(x) = \begin{cases} \frac{L_{f_\sigma} V_\sigma + \sqrt{(L_{f_\sigma} V_\sigma)^2 + (u^{\max} |L_{G_\sigma} V_\sigma^T|)^4}}{|L_{G_\sigma} V_\sigma^T|^2 [1 + \sqrt{1 + (u^{\max} |L_{G_\sigma} V_\sigma^T|)^2}]}, & L_{G_\sigma} V_\sigma \neq 0 \\ 0, & L_{G_\sigma} V_\sigma = 0 \end{cases}$$

with $L_{f_\sigma} V_\sigma = \frac{\partial V_\sigma}{\partial x} f_\sigma(x)$ and $L_{G_\sigma} V_\sigma = \frac{\partial V_\sigma}{\partial x} G_\sigma(x)$ where $G_\sigma = [g_{1\sigma} \ g_{2\sigma} \ g_{3\sigma}]$ being the Lie derivatives of the scalar function V_σ with respect to f_σ and G_σ , respectively. To estimate the stability region $\Omega_{\tilde{\rho}_\sigma}$, extensive simulations were carried out to get an estimate of the region of the closed-loop system under Lyapunov-based control $h_\sigma(x)$ where the time-derivative of the Lyapunov function is negative, and then $\Omega_{\tilde{\rho}_\sigma}$ is defined as a level set of the Lyapunov function $V_\sigma(x)$ embedded within this region.

To carry out the closed-loop performance evaluation, we have computed the total cost of each simulation based on an index of the following form:

$$J = \sum_{i=0}^M \left[x(t_i)^T Q_{c_\sigma} x(t_i) + \sum_{j=1}^3 u_{j_\sigma}(t_i)^T R_{c_{j_\sigma}} u_{j_\sigma}(t_i) \right] \quad (7.32)$$

where $t_0 = 0$ is the initial time of the simulations, $t_M = 0.1 \text{ hr}$ is the end time of the simulations and $t_{i+1} = t_i + \Delta$ for $i = 0, 1, \dots$. In the design of the controllers, the weighting matrices are chosen to be $Q_{c_1} = Q_{c_2} = \text{diag}([10 \ 10^3 \ 10^3 \ 10^3 \ 20 \ 10^3 \ 10^3 \ 10^3 \ 10 \ 10^3 \ 10^3 \ 10^3])$ and $R_{1_1} = R_{2_1} = R_{3_1} = R_{1_2} = R_{2_2} = R_{3_2} = 10^{-8}$. We set the number of iterations between controllers $c_{max} = 2$. The simulations were carried out using Java programming language in a Pentium 3.20 GHz computer. The optimization problems in MPC were solved using the open-source interior point optimizer Ipopt.

We first carried out simulations to illustrate that the Lyapunov-based controller and the centralized MPC scheme achieve practical closed-loop stability in each mode of operation, respectively. Figures 7.2 and 7.3 show the Lyapunov function trajectory in the closed-loop system under the Lyapunov-based controller implemented in a sample-and-hold-fashion and the centralized MPC scheme at mode one and two, respectively. As it can be seen from these two figures, both control schemes at each mode achieve practical closed-loop stability, while the centralized MPC requests more aggressive moves to steer the closed-loop system state to the origin. From a closed-loop performance point of view, the centralized MPC outperforms the Lyapunov-based controller by 30% at mode one and 28% at mode two, respectively.

As a scheduling policy, we assume that at time $t = 0.004 \text{ hr}$, the process switches from mode 1 to mode 2. It should be emphasized that after the system enters mode 2, it stays there until the end of the simulation time ($t_f = 0.1 \text{ hr}$), and the MPC/DMPC of mode 2 is used. Figure 7.4 compares the Lyapunov function trajectory of the closed-loop system under the Lyapunov-based controller implemented in a sample-and-hold fashion, the centralized MPC of Eq. 7.12 and the DMPC of Eq. 7.15 for a given

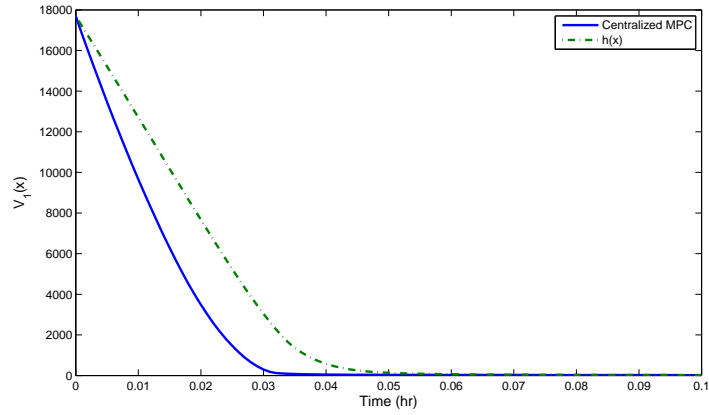


Figure 7.2: Lyapunov function trajectory of the closed-loop system under the implementation of the Lyapunov-based controller (dashed-dotted line) in a sample-and-hold fashion and of the centralized MPC (solid line) at mode one.

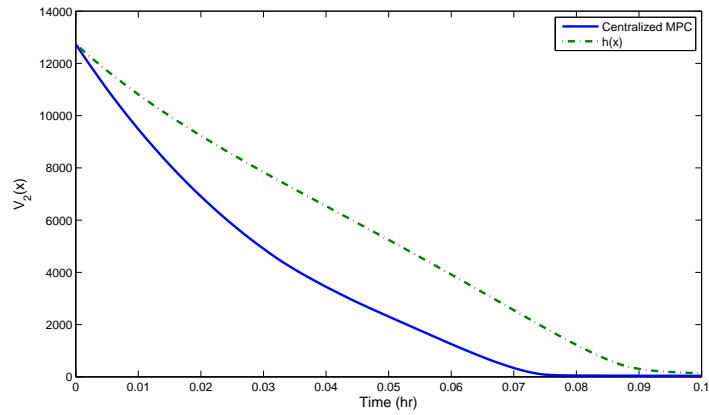


Figure 7.3: Lyapunov function trajectory of the closed-loop system under the implementation of the Lyapunov-based controller (dashed-dotted line) in a sample-and-hold fashion and of the centralized MPC (solid line) at mode two.

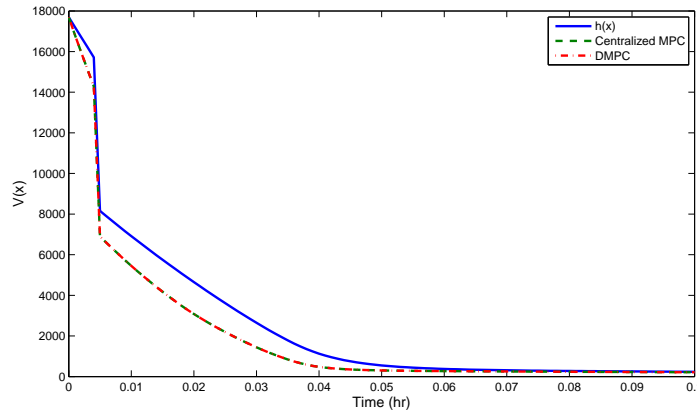


Figure 7.4: Lyapunov function trajectory of the closed-loop system under the implementation of the Lyapunov-based controller (solid line) in a sample-and-hold fashion, centralized MPC of Eq. 7.12 (*) and DMPC of Eq. 7.15 (dashed-dotted line) for the given switching policy; the line composed of the (*) and the dashed-dotted line overlap. From $t = 0$ to 0.004 hr , the lines show $V_1(x)$ and from $t = 0.004 \text{ hr}$ to 0.1 hr , the lines show $V_2(x)$.

switching policy, respectively. It illustrates that the Lyapunov-based controller can meet the given schedule by steering the closed-loop system state to the stability region of mode 2 at the time of the switch. So, for the given switching policy, the Lyapunov-based controller provides a feasible solution. Figure 7.4 shows the Lyapunov function trajectory of the closed-loop system under the implementation of the centralized MPC scheme subject to the switching constraint. As it can be seen from Figure 7.4, the MPC (both centralized and distributed) design enforces the appropriate constraint to steer the closed-loop system state at mode 1 to the stability region of mode 2 at the time of the switch. In Figure 7.4, the Lyapunov function is computed for each mode, independently. It should be emphasized that the MPC designs require more aggressive control actions to enter the stability region of mode 2 and subsequently stabilizing the plant compared to the Lyapunov-based controller, which yields improvement in terms of closed-loop performance.

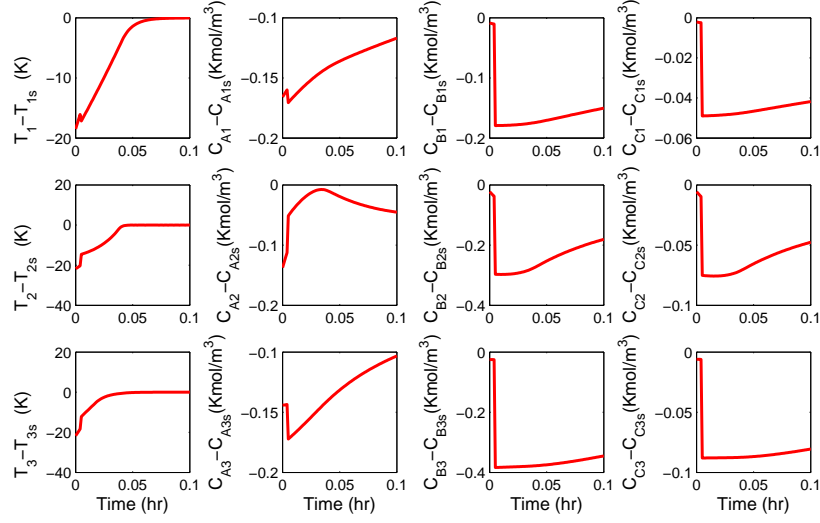


Figure 7.5: State trajectories of the closed-loop system under the implementation of the DMPC system of Eq. 7.15.

Figures 7.5 and 7.6 depict the state and manipulated inputs in the closed-loop system under the DMPC design of Eq. 7.15 subject to the same switching schedule, respectively. Figure 7.5 shows the deviation of the state trajectories from their corresponding steady-state values at each mode. As it can be seen in these figures, the proposed DMPC design enforces the appropriate constraints to steer the closed-loop system state to the stability region of mode two at the time of the switch and subsequently, achieves practical closed-loop stability. From a closed-loop performance point of view based on Eq. 7.32, the centralized MPC formulation of Eq. 7.12 yields 236447.02 in cost function value J while the DMPC design of Eq. 7.15 yields 236446.87. Therefore, the DMPC achieves nearly the centralized MPC closed-loop performance.

Finally, we compare centralized MPC and DMPC from a control action evaluation time point of view. We set the horizon of MPC to $N = 30$. We compute the average evaluation time of the MPC formulation at mode 1 (40 times) which includes the switching constraint and the MPC after we switch to mode 2 (960 times) in both

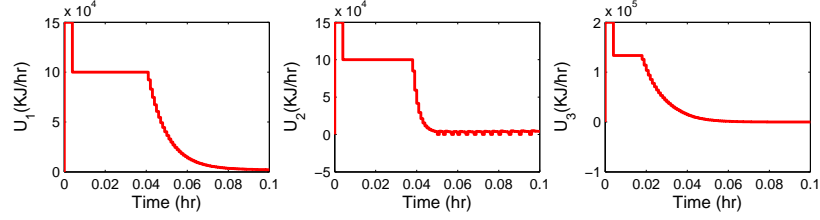


Figure 7.6: Manipulated input trajectories computed by the DMPC of Eq. 7.15.

centralized and DMPC formulations. For the DMPC design, we add the simulation time of two iterations and since the three controllers optimize in parallel, we consider the maximum time of the computational time of the distributed controllers as the computational time of the DMPC. The result indicates that for mode 1 there is an almost 36 % improvement ($\max\{104.18, 38.27, 164.29\}$ seconds vs. 259.50 seconds) and for mode 2 there is an almost 39 % improvement ($\max\{31.70, 32.99, 37.68\}$ seconds vs. 63.41 seconds) in computational time when we utilize the DMPC framework compared to the centralized MPC while the closed-loop performance remains nearly the same.

7.6 Conclusions

This chapter focused on the design of DMPC systems for a class of switched nonlinear systems subject to a prescribed switching policy. Under appropriate stabilizability assumptions, the proposed DMPC systems ensure closed-loop stability and satisfaction of the switching policy. Convergence of the DMPC optimal solution to the corresponding centralized MPC optimum was established for the linear case. A chemical process network example was used to demonstrate the proposed DMPC design method.

Chapter 8

Conclusions and Future Research

Directions

This dissertation presented Lyapunov-based economic and distributed model predictive control (MPC) schemes for nonlinear systems and demonstrated their applicability and effectiveness using various chemical process examples.

8.1 Summary

Specifically, Chapter 2 developed Lyapunov-based economic model predictive control (LEMPC) designs which are capable of optimizing closed-loop performance with respect to general economic considerations for nonlinear systems. First, we considered nonlinear systems with synchronous measurement sampling and uncertain variables, and designed an LEMPC via Lyapunov-based techniques. The proposed LEMPC design has two different operation modes. The first operation mode corresponds to the period in which the cost function should be optimized; and in this operation mode, the LEMPC maintains the closed-loop system state within the stability region and

optimizes the cost function to its maximum extent. The second operation mode corresponds to operation in which the system is driven by the LEMPC to an appropriate steady-state. Subsequently, we extended the results to nonlinear systems subject to asynchronous and delayed measurements and uncertain variables. In both LEMPC designs, suitable constraints were incorporated to guarantee that the closed-loop system state is always bounded in the stability region and is ultimately bounded in small regions containing the origin. The theoretical results were illustrated through a chemical process example.

In Chapter 3, we designed an estimator-based economic MPC (EMPC) for the class of full-state feedback linearizable nonlinear systems. A high-gain observer is used to estimate the nonlinear system state using output measurements and a Lyapunov-based approach is adopted to design the EMPC that uses the observer state estimates. It was proved, using singular perturbation arguments, that the closed-loop system is practically stable provided the observer gain is sufficiently large. A chemical process example was used to demonstrate the ability of the state estimation-based economic MPC to achieve time-varying process operation that leads to a superior cost performance metric compared to steady-state operation using the same amount of reactant material.

Chapter 4 focused on the design of LEMPC algorithms for a class of nonlinear systems which are capable of optimizing closed-loop performance with respect to a general objective function that may directly address economic considerations. Under appropriate stabilizability assumptions, the proposed LEMPC designs very often dictate time-varying operation to optimize an economic (typically non-quadratic) cost function in contrast to conventional Lyapunov-based MPC (LMPC) designs which typically include a quadratic objective function and regulate a process at a steady-

state. The proposed LEMPC algorithms took advantage of the solution of auxiliary LMPC problems at different sampling times to incorporate appropriate economic cost and control action-based constraints in the LEMPC formulations and ensure improved performance, measured by the desired economic cost, with respect to conventional LMPC. A chemical process example was used to demonstrate the proposed LEMPC algorithms.

In Chapter 5, we proposed a DMPC design for nonlinear systems taking into account explicitly communication disruptions (i.e., data losses and channel noise) between the distributed controllers. In the proposed DMPC architecture, one of the distributed controllers is responsible for ensuring closed-loop stability while the rest of the distributed controllers communicate and cooperate with the stabilizing controller to further improve the closed-loop performance. To determine if the data transmitted through the communication channel is reliable or not, feasibility problems were incorporated in the DMPC design and based on the result of these feasibility problems, the transmitted information was accepted or rejected by the stabilizing MPC. In order to ensure the stability of the closed-loop system under communication disruptions, each distributed controller utilized a stability constraint which is based on a suitable Lyapunov-based controller. The proposed DMPC system possesses an explicit characterization of the closed-loop system stability region and guarantees that the closed-loop system is ultimately bounded in an invariant set which contains the origin. The theoretical results were demonstrated through a nonlinear chemical process example.

In Chapter 6, we designed a DMPC system using multirate sampling for large-scale nonlinear uncertain systems composed of several coupled subsystems. In the proposed control architecture, the controllers were designed via LMPC techniques

taking into account bounded measurement and communication noise and process disturbances. Sufficient conditions under which the state of the closed-loop system is ultimately bounded in an invariant region containing the origin were derived. Finally, the applicability and performance of the proposed DMPC scheme were demonstrated through a nonlinear chemical process example.

Chapter 7 focused on the design of DMPC systems for a class of switched nonlinear systems subject to a prescribed switching policy. Under appropriate stabilizability assumptions, the proposed DMPC systems ensure closed-loop stability and satisfaction of the switching policy. Convergence of the DMPC optimal solution to the corresponding centralized MPC optimum was established for the linear case. A chemical process network example was used to demonstrate the proposed DMPC design method.

8.2 Future Research Work

Based on previous chapters, the research work in this dissertation can be extended in the broad areas of economic and distributed control of nonlinear systems. Specifically, some of the main directions for future research directions include:

- Cooperative and distributed control using networks
- Monitoring and reconfiguration of cooperative, distributed control systems
- Distributed state estimation
- Economic MPC of singularly perturbed systems

In the first direction, the research efforts will focus on the development of networked cooperative, distributed control schemes for nonlinear systems. Specifically,

the following topics will be considered. First, the multirate distributed MPC scheme developed in Chapter 6 will be extended to take into account asynchronous and delayed measurements. This extension is rather direct from a theory standpoint but it is very important from an application point of view. The model of the system is utilized to estimate the current state (which will be used in the design of the distributed MPC controllers) when delays are involved and design the controllers to use last evaluated input trajectories when measurements are not available at a time due to asynchronous samplings. A Lyapunov-based stability constraint will also be incorporated to each distributed controller to ensure the closed-loop stability. Moreover, network traffic and field interference may cause data package dropouts and data transmission delays. In order to deal with such kind delays and data losses in the communication, not only the distributed controllers needs to be carefully designed, but the network topology should be also carefully designed at the same time. It needs to scan the most common used network protocols in field and based on their properties, knowledge from topology and game theory will be applied in the design of the network topology for the distributed control system. At the same time, the distributed controllers will be designed to cooperate to achieve the closed-loop stability and improve the closed-loop performance. Furthermore, multirate distributed control system with output feedback will also be considered. For a distributed controller in a large-scale control system, it may not have access to all the measurements and the state measurement of the process may be not available. In the design of the distributed controllers, we need to take into account that different controllers may have access to different parts of measurements. There are different approaches to address this problem. One approach is to design a different observer for each controller, and an alternative is to design a centralized observer and the observer sends the observed state to all the distributed controllers. Both the approaches can be considered in the future research and they

will be compared extensively from performance and computational complexity points of view.

In the second direction, future research will address the design of systems to monitor cooperative, distributed control systems and the design of strategies to reconfigure the control systems. From the point of view of monitoring, the coupling and interaction between cooperative, distributed control systems make the design of such systems and residuals and their evaluation more challenging than in conventional control systems based on centralized architectures. The occurrence of asynchronous behavior and delays in the measurement sampling further complicates the design of the monitoring systems. In the context of cooperative, distributed control, the problem of designing systems which can detect and isolate the presence of actuator/sensor/controller failures has received no attention. We plan to investigate an approach that unites model-based and data-based approaches for the design of monitoring systems. The information available through the model structure will be used to aid the task of building model-based and data-based monitoring systems. The overall reliability of the plant is strongly dependent on the phenomenon of fault propagation where the occurrence of an actuator/process fault in some part of the plant puts the system in a working mode in which other faults are more likely to happen elsewhere, thus increasing the likelihood of a plant-wide failure. Compared to centralized control systems, monitoring of cooperative, distributed control systems has received little attention. In a cooperative, distributed control system, if an actuator fault occurs, it is possible to carry out fault handling in some cases without activating a backup control loop. This is because the function of the actuator may be possible to be complemented by the other remaining actuators with acceptable loss of overall closed-loop performance. The future research focuses on deriving the conditions under which actuator fault handling can be carried out without backup control

loops and studying how the remaining cooperative, distributed controllers should be reconfigured.

In the third direction, future research will focus on the development of distributed state estimation methods for nonlinear systems. Traditionally, state estimation for control system design purpose is usually studied within a centralized framework in which only one centralized observer is designed to estimate all the unknown system states. However, for large-scale systems, it may not be feasible to design a centralized state observer to estimate the system states based on available output measurements. This is because that: 1) the computational complexity of a centralized observer increases significantly with the increase of the number of unknown states, and 2) the difficulties in the management of the model used in the observer increase when the number of states and equations involved in the model increase. In the control, especially distributed control of large-scale nonlinear systems, distributed state estimation based on sensor networks is of great importance, however, little attention has been given to this problem in the literature. In the design of distributed state estimation systems, it needs to take into account the observability and stability of the system, and the computational complexity of the observers. Future research would focus on studying the problem of distributed state estimation based on the concept of moving horizon estimation. This approach has the following advantages: 1) the observer is optimal because a well-designed optimization problem must be solved online at each sampling time; 2) the convergence of the distributed state observers can be guaranteed in a deterministic fashion; and 3) different constraints on the system states and inputs can be taken into account, which is common in receding horizon approaches in control and estimation.

Recently, we studied MPC of nonlinear singularly perturbed systems in the context of fast-slow MPC design. Please refer to [9, 13, 11, 14, 12] for a detailed description of the proposed control schemes. In the forth direction, economic optimization aspects of two time scale nonlinear systems as well as closed-loop stability analysis can be addressed by taking advantage of the proposed methods in Chapters 2, 3 and 4 and the singular perturbation framework.

Bibliography

- [1] D. Angeli, R. Amrit, and J. B. Rawlings. On average performance and stability of economic model predictive control. *IEEE Transactions on Automatic Control*, in press.
- [2] T. Backx, O. Bosgra, and W. Marquardt. Integration of model predictive control and optimization of processes : enabling technology for market driven process operation. In *Proceedings of the IFAC Symposium on Advanced Control of Chemical Processes*, pages 249–260, Pisa, Italy, 2000.
- [3] D. P. Bertsekas and J. N. Tsitsiklis. *Parallel and Distributed Computation*. Athena Scinetific, Belmont, Massachusetts, 1997.
- [4] F. Borrelli, M. Baotic, A. Bemporad, and M. Morari. Dynamic programming for constrained optimal control of discrete-time linear hybrid systems. *Automatica*, 41:1709–1721, 2005.
- [5] M. S. Branicky. Multiple Lyapunov functions and other analysis tools for switched and hybrid systems. *IEEE Transactions on Automatic Control*, 43:475–482, 1998.
- [6] C. Brosilow, G. Q. Zhao, and K. C. Rao. A linear programming approach to constrained multivariable control. In *Proceedings of the American Control Conference*, pages 667–674, San Diego, California, 1984.
- [7] E. Camponogara, D. Jia, B. H. Krogh, and S. Talukdar. Distributed model predictive control. *IEEE Control Systems Magazine*, 22:44–52, 2002.
- [8] C. Cassandras and R. Mookherjee. Receding horizon optimal control for some stochastic hybrid systems. In *Proceedings of 41th IEEE Conference on Decision and Control*, pages 2162–2167, Maui, Hawaii, 2003.
- [9] X. Chen, M. Heidarinejad, J. Liu, and P. D. Christofides. Composite fast-slow MPC design for nonlinear singularly perturbed systems. *AIChE Journal*, 58:1802–1811, 2012.

- [10] X. Chen, M. Heidarinejad, J. Liu, and P. D. Christofides. Distributed economic MPC: Application to a nonlinear chemical process network. *Journal of Process Control*, 22:689–699, 2012.
- [11] X. Chen, M. Heidarinejad, J. Liu, and P. D. Christofides. Composite fast-slow mpc design for nonlinear singularly perturbed systems: Stability analysis. In *Proceedings of the American Control Conference*, Montreal, Canada, in press, 2012.
- [12] X. Chen, M. Heidarinejad, J. Liu, and P. D. Christofides. Composite fast-slow MPC design for nonlinear singularly perturbed systems: Near-optimality and process network application. submitted to the 51th IEEE Conference on Decision and Control, 2012.
- [13] X. Chen, M. Heidarinejad, J. Liu, D. Muñoz de la Peña, and P. D. Christofides. Model predictive control of nonlinear singularly perturbed systems: Application to a large-scale process network. *Journal of Process Control*, 21:1296–1305, 2011.
- [14] X. Chen, M. Heidarinejad, J. Liu, D. Muñoz de la Peña, and P. D. Christofides. Model predictive control of nonlinear singularly perturbed systems: Application to a reactor-separator process network. In *Proceedings of 50th IEEE Conference on Decision and Control and European Control Conference*, pages 8125–8132, Orlando, Florida, 2011.
- [15] D. Chilin, J. Liu, D. Muñoz de la Peña, P. D. Christofides, and J. F. Davis. Detection, isolation and handling of actuator faults in distributed model predictive control systems. *Journal of Process Control*, 20:1059–1075, 2010.
- [16] P. D. Christofides. Robust output feedback control of nonlinear singularly perturbed systems. *Automatica*, 36:45–52, 2000.
- [17] P. D. Christofides, J. F. Davis, N. H. El-Farra, D. Clark, K. R. D. Harris, and J. N. Gipson. Smart plant operations: Vision, progress and challenges. *AIChE Journal*, 53:2734–2741, 2007.
- [18] P. D. Christofides and N. H. El-Farra. *Control of Nonlinear and Hybrid Process Systems: Designs for Uncertainty, Constraints and Time-Delays*. Springer-Verlag, Berlin, Germany, 2005.
- [19] P. D. Christofides, J. Liu, and D. Muñoz de la Peña. *Networked and Distributed Predictive Control: Methods and Nonlinear Process Network Applications*. Advances in Industrial Control Series. Springer-Verlag, London, England, 2011.
- [20] T. M. Cover, J. A. Thomas, and J. Wiley. *Elements of Information Theory*. Wiley, New York, 1991.

- [21] J. Daafouz, P. Riedinger, and C. Iung. Stability analysis and control synthesis for switched systems: a switched Lyapunov function approach. *IEEE Transactions on Automatic Control*, 47:1883–1887, 2002.
- [22] M. T. de Gouvea and D. Odloak. One-layer real time optimization of LPG production in the FCC unit: procedure, advantages and disadvantages. *Computers & Chemical Engineering*, 22:191–198, 1998.
- [23] D. Muñoz de la Peña and P. D. Christofides. Output feedback control of nonlinear systems subject to sensor data losses. *Systems & Control Letters*, 57:631–642, 2008.
- [24] M. Diehl, R. Amrit, and J. B. Rawlings. A Lyapunov function for economic optimizing model predictive control. *IEEE Transactions on Automatic Control*, 56:703–707, 2011.
- [25] W. B. Dunbar. Distributed receding horizon control of dynamically coupled nonlinear systems. *IEEE Transactions on Automatic Control*, 52:1249–1263, 2007.
- [26] N. H. El-Farra and P. D. Christofides. Bounded robust control of constrained multivariable nonlinear processes. *Chemical Engineering Science*, 58:3025–3047, 2003.
- [27] N. H. El-Farra and P. D. Christofides. Coordinating feedback and switching for control of hybrid nonlinear processes. *AIChE Journal*, 49:2079–2098, 2003.
- [28] S. Engell. Feedback control for optimal process operation. *Journal of Process Control*, 17:203–219, 2007.
- [29] C. E. García, D. M. Prett, and M. Morari. Model predictive control: Theory and practice—A survey. *Automatica*, 25:335–348, 1989.
- [30] D. Gorges, M. Izak, and S. Liu. Optimal control and scheduling of switched systems. *IEEE Transactions on Automatic Control*, 56:135–140, 2011.
- [31] T. T. Han, S. S. Ge, and T. H. Lee. Adaptive neural control for a class of switched nonlinear systems. *Systems & Control Letters*, 58:109–118, 2009.
- [32] M. Heidarinejad, J. Liu, and P. D. Christofides. Economic model predictive control using lyapunov techniques: Handling asynchronous, delayed measurements and distributed implementation. In *Proceedings of 50th IEEE Conference on Decision and Control and European Control Conference*, pages 4646–4653, Orlando, Florida, 2011.

- [33] M. Heidarinejad, J. Liu, and P. D. Christofides. Lyapunov-based economic model predictive control of nonlinear systems. In *Proceedings of 2011 American Control Conference*, pages 5195–5200, San Francisco, California, 2011.
- [34] M. Heidarinejad, J. Liu, and P. D. Christofides. Economic model predictive control of nonlinear process systems using Lyapunov techniques. *AIChE Journal*, 58:855–870, 2012.
- [35] M. Heidarinejad, J. Liu, and P. D. Christofides. Distributed model predictive control of switched nonlinear systems with scheduled mode transitions. In *Proceedings of the American Control Conference*, Montreal, Canada, in press, 2012.
- [36] M. Heidarinejad, J. Liu, and P. D. Christofides. Algorithms for improved finite-time performance of lyapunov-based economic model predictive control of nonlinear systems. *Chemical Engineering Science*, submitted for publication, 2012.
- [37] M. Heidarinejad, J. Liu, and P. D. Christofides. State estimation-based economic model predictive control of nonlinear systems. *Systems & Control Letters*, submitted for publication, 2012.
- [38] M. Heidarinejad, J. Liu, and P. D. Christofides. State estimation-based economic model predictive control of nonlinear systems. submitted to the 51th IEEE Conference on Decision and Control, 2012.
- [39] M. Heidarinejad, J. Liu, and P. D. Christofides. Distributed model predictive control of switched nonlinear systems with scheduled mode transitions. *IEEE Transactions on Automatic Control*, under revision, 2012.
- [40] M. Heidarinejad, J. Liu, D. Muñoz de la Peña, and P. D. Christofides. Handling communication disruptions in distributed model predictive control of nonlinear systems. In *Proceedings of 9th International Symposium on Dynamics and Control of Process Systems*, pages 282–287, Leuven, Belgium, 2010.
- [41] M. Heidarinejad, J. Liu, D. Muñoz de la Peña, J. F. Davis, and P. D. Christofides. Handling communication disruptions in distributed model predictive control of nonlinear systems. *Journal of Process Control*, 21:173–181, 2011.
- [42] M. Heidarinejad, J. Liu, D. Muñoz de la Peña, J. F. Davis, and P. D. Christofides. Multirate distributed model predictive control of nonlinear systems. In *Proceedings of the American Control Conference*, pages 5181–5188, San Francisco, California, 2011.

- [43] M. Heidarinejad, J. Liu, D. Muñoz de la Peña, J. F. Davis, and P. D. Christofides. Multirate lyapunov-based distributed model predictive control of nonlinear uncertain systems. *Journal of Process Control*, 21:1231–1242, 2011.
- [44] J. P. Hespanha and A. S. Morse. Stability of switched systems with average dwell-time. In *Proceedings of the 38th IEEE Conference on Decision and Control*, pages 2655–2660, Phoenix, Arizona, 1999.
- [45] J. P. Hespanha and A. S. Morse. Switching between stabilizing controllers. *Automatica*, 38:1905–1917, 2002.
- [46] T. G. Hovgaard, L. F. S. Larsen, and J. B. Jørgensen. Robust economic MPC for a power management scenario with uncertainties. In *Proceedings of 50th IEEE Conference on Decision and Control and European Control Conference*, pages 1515–1520, Orlando, Florida, 2011.
- [47] R. Huang, E. Harinath, and L. T. Biegler. Lyapunov stability of economically oriented NMPC for cyclic processes. *Journal of Process Control*, 21:501–509, 2011.
- [48] J. V. Kadam and W. Marquardt. Integration of economical optimization and control for intentionally transient process operation. In *Assessment and Future Directions of Nonlinear Model Predictive Control, Lecture Notes in Control and Information Science Series*, volume 358, pages 419–434, 2007.
- [49] T. Keviczky, F. Borrelli, and G. J. Balas. Decentralized receding horizon control for large scale dynamically decoupled systems. *Automatica*, 42:2105–2115, 2006.
- [50] H. K. Khalil and F. Esfandiari. Semiglobal stabilization of a class of nonlinear systems using output feedback. *IEEE Transactions on Automatic Control*, 38:1412–1415, 1993.
- [51] P. Kokotovic and M. Arcak. Constructive nonlinear control: a historical perspective. *Automatica*, 37:637–662, 2001.
- [52] M. Lazar and W. Heemels. Predictive control of hybrid systems: Input-to-state stability results for sub-optimal solutions. *Automatica*, 45:180–185, 2009.
- [53] M. Lazar, W. Heemels, S. Weiland, and A. Bemporad. Stabilizing model predictive control of hybrid systems. *IEEE Transactions on Automatic Control*, 51:1813–1818, 2006.
- [54] C. Lee and J. Bailey. Modification of consecutive-competitive reaction selectivity by periodic operation. *Industrial and Engineering Chemistry Process Design and Development*, 19:160–166, 1980.

- [55] J. Lee and D. Angeli. Cooperative distributed model predictive control for linear plants subject to convex economic objectives. In *Proceedings of 50th IEEE Conference on Decision and Control and European Control Conference*, pages 3434–3439, Orlando, Florida, 2011.
- [56] D. Liberzon. *Switching in Systems and Control*. Springer, Boston, MA, 2003.
- [57] H. Lin and P. J. Antsaklis. Stability and stabilizability of switched linear systems: a survey of recent results. *IEEE Transactions on Automatic Control*, 54:308–322, 2009.
- [58] Y. Lin and E. D. Sontag. A universal formula for stabilization with bounded controls. *Systems & Control Letters*, 16:393–397, 1991.
- [59] Y. Lin, E. D. Sontag, and Y. Wang. A smooth converse Lyapunov theorem for robust stability. *SIAM Journal on Control and Optimization*, 34:124–160, 1996.
- [60] J. Liu, X. Chen, D. Muñoz de la Peña, and P. D. Christofides. Sequential and iterative architectures for distributed model predictive control of nonlinear process systems. *AIChE Journal*, 56:2137–2149, 2010.
- [61] J. Liu, D. Muñoz de la Peña, and P. D. Christofides. Distributed model predictive control of nonlinear process systems. *AIChE Journal*, 55:1171–1184, 2009.
- [62] J. Liu, D. Muñoz de la Peña, and P. D. Christofides. Distributed model predictive control of nonlinear systems subject to asynchronous and delayed measurements. *Automatica*, 46:52–61, 2010.
- [63] J. Liu, D. Muñoz de la Peña, P. D. Christofides, and J. F. Davis. Lyapunov-based model predictive control of nonlinear systems subject to time-varying measurement delays. *International Journal of Adaptive Control and Signal Processing*, 23:788–807, 2009.
- [64] J. Liu, D. Muñoz de la Peña, B. J. Ohran, P. D. Christofides, and J. F. Davis. A two-tier control architecture for nonlinear process systems with continuous/asynchronous feedback. *International Journal of Control*, 83:257–272, 2010.
- [65] J. Ma, J. Qin, T. Salsbury, and P. Xu. Demand reduction in building energy systems based on economic model predictive control. *Chemical Engineering Science*, 67:92–100, 2012.
- [66] J. M. Maestre, D. Muñoz de la Peña, and E. F. Camacho. A distributed MPC scheme with low communication requirements. In *Proceedings of 2009 American Control Conference*, pages 2797–2802, Saint Louis, Missouri, 2009.

- [67] L. Magni and R. Scattolini. Stabilizing decentralized model predictive control of nonlinear systems. *Automatica*, 42:1231–1236, 2006.
- [68] N. A. Mahmoud and H. K. Khalil. Asymptotic regulation of minimum phase nonlinear systems using output feedback. *IEEE Transactions on Automatic Control*, 41:1402–1412, 1996.
- [69] J. P. Maree and L. Imsland. On combining economical performance with control performance in NMPC. In *Proceedings of the 18th IFAC World Congress*, volume 18, pages 5501–5506, Milan, Italy, 2011.
- [70] T. E. Marlin and A. N. Hrymak. Real-time operations optimization of continuous processes. In *AIChE Symposium Series on CPC V*, volume 93, pages 156–164, 1997.
- [71] J. L. Massera. Contributions to stability theory. *The Annals of Mathematics*, 64:182–206, 1956.
- [72] D. Q. Mayne, J. B. Rawlings, C. V. Rao, and P. O. M. Scokaert. Constrained model predictive control: Stability and optimality. *Automatica*, 36:789–814, 2000.
- [73] P. Mhaskar, N. H. El-Farra, and P. D. Christofides. Predictive control of switched nonlinear systems with scheduled mode transitions. *IEEE Transactions on Automatic Control*, 50:1670–1680, 2005.
- [74] P. Mhaskar, N. H. El-Farra, and P. D. Christofides. Stabilization of nonlinear systems with state and control constraints using Lyapunov-based predictive control. *Systems & Control Letters*, 55:650–659, 2006.
- [75] P. Mhaskar, A. Gani, and P. D. Christofides. Fault-tolerant control of nonlinear processes: Performance-based reconfiguration and robustness. *International Journal of Robust and Nonlinear Control*, 16:91–111, 2006.
- [76] L. A. Montestruque and P. J. Antsaklis. On the model-based control of networked systems. *Automatica*, 39:1837–1843, 2003.
- [77] L. A. Montestruque and P. J. Antsaklis. Stability of model-based networked control systems with time-varying transmission times. *IEEE Transactions on Automatic Control*, 49:1562–1572, 2004.
- [78] A. M. Morshedi, C. R. Cutler, and T. A. Skrovanek. Optimal solution of dynamic matrix control with linear programming techniques. In *Proceedings of the American Control Conference*, pages 199–208, Boston, Massachusetts, 1985.

- [79] D. Muñoz de la Peña and P. D. Christofides. Lyapunov-based model predictive control of nonlinear systems subject to data losses. *IEEE Transactions on Automatic Control*, 53:2076–2089, 2008.
- [80] K. R. Muske. Steady-state target optimization in linear model predictive control. In *Proceedings of the American Control Conference*, pages 3597–3601, Albuquerque, New Mexico, 1997.
- [81] D. Nešić and A. R. Teel. Input-to-state stability of networked control systems. *Automatica*, 40:2121–2128, 2004.
- [82] P. Neumann. Communication in industrial automation: What is going on? *Control Engineering Practice*, 15:1332–1347, 2007.
- [83] C. R. Porfírio and D. Odloak. Optimizing model predictive control of an industrial distillation column. *Control Engineering Practice*, 19:1137–1146, 2011.
- [84] J. G. Proakis and M. Salehi. *Digital communications*. McGraw-hill, New York, 2001.
- [85] J. B. Rawlings. Tutorial overview of model predictive control. *IEEE Control Systems Magazine*, 20:38 – 52, 2000.
- [86] J. B. Rawlings and R. Amrit. Optimizing process economic performance using model predictive control. In L. Magni, D. M. Raimondo, and F. Allgöwer, editors, *Nonlinear Model Predictive Control, Lecture Notes in Control and Information Science Series*, volume 384, pages 119–138, Springer, Berlin, 2009.
- [87] J. B. Rawlings and B. T. Stewart. Coordinating multiple optimization-based controllers: New opportunities and challenges. *Journal of Process Control*, 18:839–845, 2008.
- [88] A. Richards and J. P. How. Robust distributed model predictive control. *International Journal of Control*, 80:1517–1531, 2007.
- [89] R. Scattolini. Architectures for distributed and hierarchical model predictive control - A review. *Journal of Process Control*, 19:723–731, 2009.
- [90] D. Sincic and J. Bailey. Analytical optimization and sensitivity analysis of forced periodic chemical processes. *Chemical Engineering Science*, 35:1153–1161, 1980.
- [91] S. S. Stankovic, D. M. Stipanovic, and D. D. Siljak. Decentralized dynamic output feedback for robust stabilization of a class of nonlinear interconnected systems. *Automatica*, 43:861–867, 2007.

- [92] B. T. Stewart, A. N. Venkat, J. B. Rawlings, S. J. Wright, and G. Pannocchia. Cooperative distributed model predictive control. *Systems & Control Letters*, 59:460–469, 2010.
- [93] Y. Sun and N. H. El-Farra. Quasi-decentralized model-based networked control of process systems. *Computers & Chemical Engineering*, 32:2016–2029, 2008.
- [94] Y. Sun and N. H. El-Farra. A quasi-decentralized approach for networked state estimation and control of process systems. *Industrial and Engineering Chemistry Research*, 49:7957–7971, 2010.
- [95] M. Tabbara, D. Nešić, and A. R. Teel. Stability of wireless and wireline networked control systems. *IEEE Transactions on Automatic Control*, 52:1615–1630, 2007.
- [96] A. N. Venkat, J. B. Rawlings, and S. J. Wright. Stability and optimality of distributed model predictive control. In *Proceedings of the 44th IEEE Conference on Decision and Control, and the European Control Conference ECC 2005*, pages 6680–6685, Seville, Spain, 2005.
- [97] A. Wächter and L. T. Biegler. On the implementation of an interior-point filter line-search algorithm for large-scale nonlinear programming. *Mathematical Programming*, 106:25–57, 2006.
- [98] N. Watanabe, H. Kurimoto, M. Matsubara, and K. Onogi. Periodic control of continuous stirred tank reactors—II: cases of a nonisothermal single reactor. *Chemical Engineering Science*, 37:745–752, 1982.
- [99] N. Watanabe, K. Onogi, and M. Matsubara. Periodic control of continuous stirred tank reactors—I: The Pi criterion and its applications to isothermal cases. *Chemical Engineering Science*, 36:809–818, 1981.
- [100] D. Wei, I. K. Craig, and M. Bauer. Multivariate economic performance assessment of an MPC controlled electric arc furnace. *ISA Transactions*, 46:429–436, 2007.
- [101] H. Yang, V. Cocquempot, and B. Jiang. On stabilization of switched nonlinear systems with unstable modes. *Systems & Control Letters*, 58:703–708, 2009.
- [102] E. B. Ydstie. New vistas for process control: Integrating physics and communication networks. *AIChE Journal*, 48:422–426, 2002.
- [103] C. Yousfi and R. Tournier. Steady state optimization inside model predictive control. In *Proceedings of the American Control Conference*, pages 1866–1870, Boston, Massachusetts, 1991.

- [104] A. C. Zanin, M. T. de Gouvea, and D. Odloak. Integrating real-time optimization into the model predictive controller of the FCC system. *Control Engineering Practice*, 10:819–831, 2002.
- [105] X. Zhu, W. Hong, and S. Wang. Implementation of advanced control for a heat-integrated distillation column system. In *Proceedings of the 30th Annual Conference of IEEE Industrial Electronics Society*, pages 2006–2011, Busan, Korea, 2004.